RECLAMATION

Managing Water in the West

Technical Report No. SRH-2008-7

Two-Dimensional Numerical Model Study of Sediment Movement at the Robles Diversion Dam on the Ventura River, California

U.S. Department of the Interior
Bureau of Reclamation
Technical Service Center
Denver, Colorado

April, 2008

Mission Statements

The mission of the Department of the Interior is to protect and provide access to our Nation's natural and cultural heritage and honor our trust responsibilities to Indian Tribes and our commitments to island communities.

The mission of the Bureau of Reclamation is to manage, develop, and protect water and related resources in an environmentally and economically sound manner in the interest of the American public.

Cover Photo: Looking upstream at the Robles Diversion Dam.

Technical Report No. SRH-2008-7

Two-Dimensional Numerical Model Study of Sediment Movement at the Robles Diversion Dam on the Ventura River, California

Report Prepared by:

Yong G. Lai, Ph.D., Hydraulic Engineer
Sedimentation and River Hydraulics Group, Technical Service Center

Blair P. Greimann, P.E., Ph.D., Hydraulic Engineer
Sedimentation and River Hydraulics Group, Technical Service Center

Report Peer Reviewed by:

Robert Hilldale, Hydraulic Engineer
Sedimentation and River Hydraulics Group, Technical Service Center

U.S. Department of the Interior
Bureau of Reclamation
Technical Service Center
Denver, Colorado

April, 2008

Acknowledgements

Technical assistance, discussion, and review by Robert Hilldale (Technical Service Center, Bureau of Reclamation) considerably improved the study and the report. Great appreciation is expressed to them for their efforts.

Table of Contents

Index of Figures

Page

Index of Tables

Page

Executive Summary

Summary

This report presents the results of a Bureau of Reclamation numerical model study of the proposed high flow bypass (HFB) spillway for Robles Diversion Dam. Robles Diversion Dam is located on the Ventura River approximately 14 river miles from the ocean. A two-dimensional flow and sediment transport model (SRH-2D) was used to determine the interaction of flows and bed load sediments near the facility following decommissioning and removal of Matilija Dam located about two river miles upstream. The HFB spillway was proposed to enhance sediment movement through the diversion pool thereby reducing the impacts of elevated bed load levels resulting from the upstream dam removal.

Major Findings

Three diversion gate scenarios were modeled, similar to the physical model tests: Existing Condition, Right High Flow Bypass (RHFB), and Left High Flow Bypass (LHFB). Layouts of the three scenarios are illustrated in Figure E. 1.

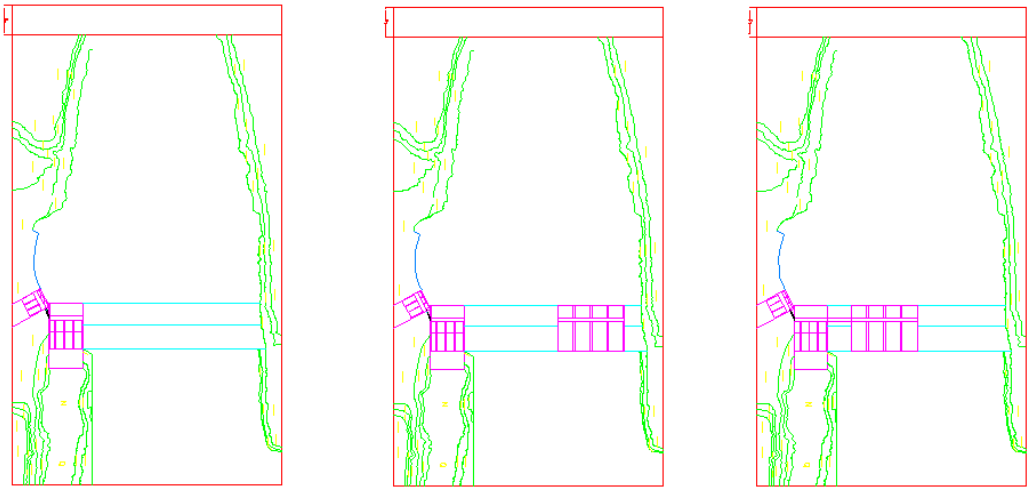

(a) Existing Condition (b) LHFB (c) RHFB

Figure E. 1 Layout of three diversion gate scenarios

Numerical modeling was carried out under both the physical model condition and the prototype field condition scenarios. Major findings based on the model results may be summarized as follows:

Physical Model Scenario

Numerical modeling of physical model cases presented in Chapter 5.0 show the following:

(1) Results from both the numerical and physical models are in agreement with each other. This on one hand provides confidence in the numerical model, and on the other hand points to the reliability of the results from both models.

(2) With the existing radial gates, excessive deposition would occur upstream of the Robles weir. Specifically, the sediment delta would reach the diversion canal gates under both the 6,000 cfs and 14,000 cfs hydrographs. The thickness of the delta is high enough that there is a high likelihood of bedload sediments being transported into the canal.

(3) With the high flow bypass (HFB) gates added, the model results show that it is less likely that the bedload sediments would enter the diversion canal.

(4) The total amount of sediment depositions upstream of the weir is tabulated in Table 10 for all simulated physical model cases. It shows that more than 85% of the incoming sediments would be trapped upstream of the weir under the 6,000 cfs hydrograph with or without the HFB gates. The benefit of the HFB gates exists only for flows higher than 6,000 cfs. For example, with the 14,000 cfs hydrograph, about 70% of the input sediments are deposited upstream of the weir for the existing condition scenario while the percentage is reduced to about 53% if the HFB gates are operated. It is interesting to note that the delta deposition remains constant when the flow is increased from 6,000 cfs hydrograph to 14,000 cfs hydrograph.

(5) No appreciable difference is observed between the left and right HFB options in terms of the ability to move the sediment.

(6) The final bed topography near the existing and diversion canal gates may be altered through the sluicing ability of the existing radial gates. But not enough study has been carried out to derive a quantitative scheme for sluicing.

Field Scenario

The physical model test cases are limited in several aspects. The 14,000 cfs hydrograph used in the lab is not the same as the 1998 hydrograph in the field

which had a peak of more than 20,000 cfs. Also, the total sediments added for the 14,000 cfs hydrograph may not be high enough, as the computed input based on the transport capacity is more than 10 yd^3. Coupled with the potential effects of the limited size of the test box and the scalability, there is a need to model the field cases which would eliminate most of the limitations mentioned above. Major findings from both the physical and numerical models are summarized as follows:

(1) Major conclusions derived from the physical model cases remain valid when the filed model results are examined except for changes in some quantities.

(2) The field model results were calibrated with the available flow data. A qualitative comparison of the simulated mobile-bed results with field observations under the existing condition scenario showed that the model results were reasonable. The total amount of predicted sediment deposition upstream of the weir was in agreement with the field observation; and the predicted bed form and flow pattern after a major flood were plausible.

(3) The flow discharge of 1,000 cfs may be taken as the threshold below which no appreciable sediment movement and deposition would occur near the Robles Diversion Dam.

(4) For all modeled scenarios, sediments would be accumulated behind the Robles Diversion Dam (Weir) quickly. The overall deposition pattern was largely determined during the rising limb of the hydrograph. Only minor deposition and bed form adjustments would occur shortly after the flow peak.

(5) After dam removal, more sediment is expected to accumulate upstream of the Robles Diversion Dam for the existing condition scenario. The estimated deposition depth (with voids) and volume (without voids) are tabulated in Table 11 under the existing condition scenario.

(6) Model results showed that the existing radial gates alone are not capable of efficiently moving the additional sediments added after dam removal. Sediment deposition in front of the canal gates would be so high that there is a high likelihood the bedload sediments would be transported into the diversion canal if a flood similar to 1998 (about 15-year flood) would occur.

(7) If the high flow bypass (HFB) radial gates are in place, the total sediment deposition between RM 14.1098 and Robles Diversion Dam would be reduced by approximately 50% and 40% for the 1991 and 1998 hydrographs, respectively. HFB gates are capable of moving sediments efficiently once the dam is removed and there is less likelihood for the bedload sediments to enter the diversion canal.

(8) Numerical model results showed that the right HFB appeared to have an advantage over the left HFB. Firstly, the average total deposition depth near the weir was lower for the right HFB case: 2.5 ft for the right HFB versus 3.0 ft for the left HFB for the 1991 hydrograph and 5.0 ft versus 6.5 ft for the 1998 hydrograph. Secondly, the total sediment volume deposited between RM 14.1098 and Robles Diversion Dam is also lower for the right HFB. Finally, more deposition occurred in front of the canal diversion gates for the left HFB scenario.

Recommendations

The numerical model results are in qualitative and quantitative agreement with the physical model results and field observations. The existing radial gates at Robles Diversion are not capable of efficiently moving the additional sediments added after dam removal. The HFB gates are capable of moving sediments efficiently once the dam is removed and there is less likelihood for the bedload sediments to enter the diversion canal.

1.0 Project Background

Robles diversion dam is located on the Ventura River near Ventura, California at approximately river mile (RM) 14.16 (figure 1). The diversion supplies water to Lake Casitas by canal. The normal maximum diversion is approximately 500 ft^3/s. The existing diversion dam is a low rock weir with a gated spillway, canal diversion headworks and a fish pass located on the right abutment. The diversion weir has a hydraulic height of 13 feet. The fish passage was constructed in 2002 to allow southern California steelhead (Oncorhynhus mykiss), a listed species, to migrate upstream of the diversion dam. Matilija Dam is a 160 ft high (originally 190 ft high) concrete arch dam located about 2 miles upstream of Robles diversion dam on Matilija Creek. Decommissioning and removal of Matilija Dam is proposed to address a dam safety risk and re-establish access for endangered steelhead to the upper reaches of Matilija Creek. The storage behind the dam has been significantly reduced by deposition of coarse sediment (Greimann, 2006). The proposed removal of Matilija Dam is expected to result in increased sediment transport to the Ventura River for many years. The focus of this study is the hydraulic design of a new high flow bypass (HFB) spillway for Robles diversion dam. The HFB will improve the movement of bed load sediments past the diversion structure. This report covers numerical modeling of the diversion facility conducted at the Bureau of Reclamation's Technical Service Center (TSC) in Denver, Colorado. The numerical model study provided design support to the Army Corps of Engineers, Los Angles District, the principle designer for the project.

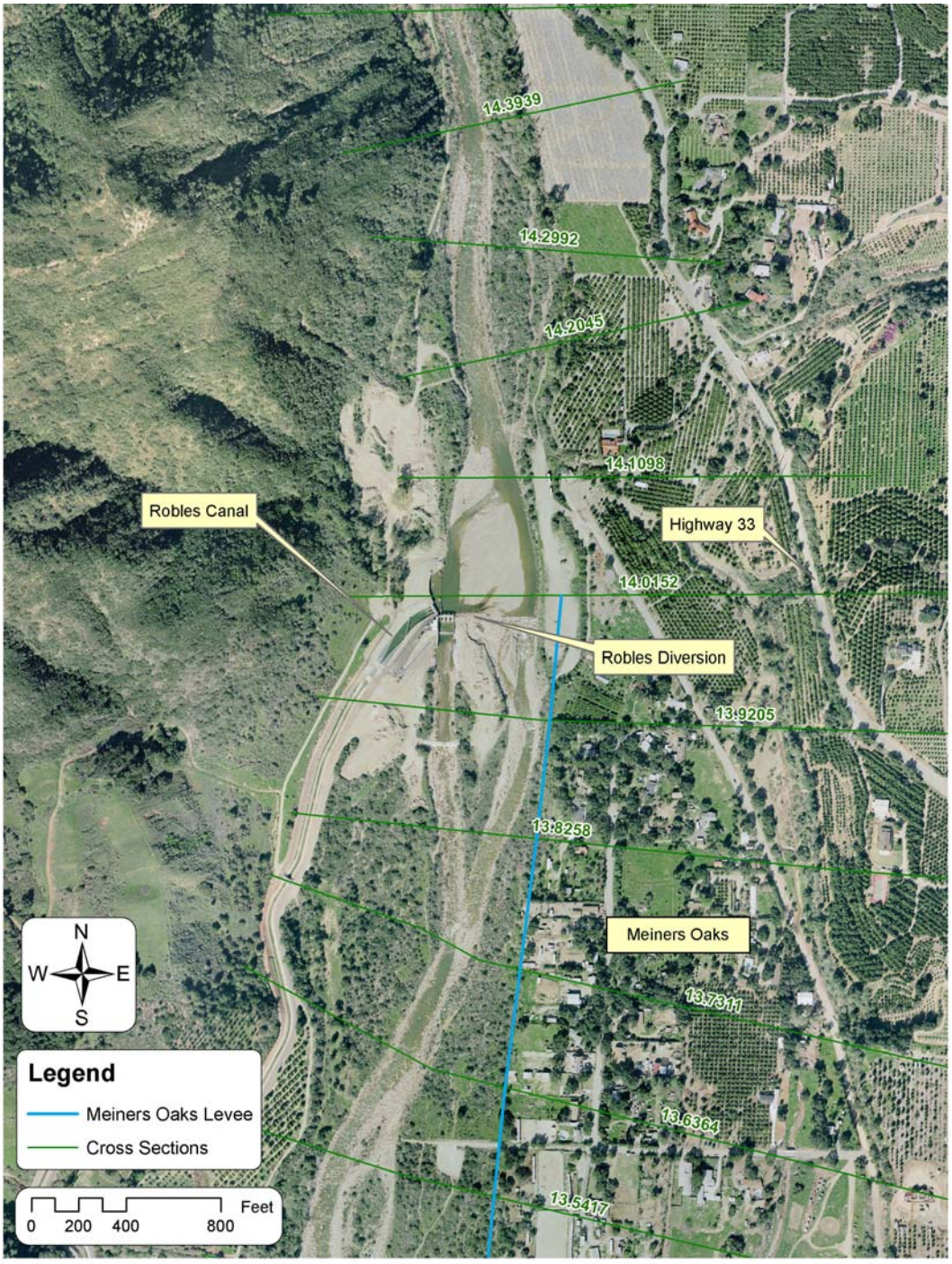

Figure 1. Aerial view of Robles Diversion taken in 2005.

2.0 Numerical Model Study Benefits

The numerical model study was carried out to assist, complement, and extend the physical model results as documented in Mefford et al. (2008). Combined results

from physical and numerical models provide relatively complete data that helps develop an informed design and selection of alternatives. Anticipated specific benefits of the numerical modeling for the current project are as follows:

(1) The physical model includes only a small section of the river with the upstream boundary located at a meander bend. Conditions at the upstream inlet of the physical model may be obtained by the numerical model.

(2) The discharge and sediment input are limited for the physical model. The numerical model has the capability to simulate higher flows once verified at the lower flows.

(3) Issues of the upstream fish migration at the Robles diversion are hard to be resolved with the physical model due to limited modeling of the downstream reach. The numerical model includes a much longer river reach and the data provide information about fish migration issues.

(4) The scale issue of sediment modeling is well known for the physical model. The numerical model provides a check on the scale effect.

3.0 Field Data

Data related to the physical model tests are presented in the physical model sections of the report, and they are not repeated. This Chapter focuses on the field data used for the current 2D numerical modeling.

3.1 Topographic and Bathymetric Data

The current study uses SRH-2D, which is a two-dimensional (2D) depth-averaged hydraulic and sediment transport model. SRH-2D simulates water surface elevation, flow velocity, and channel bed change in an unsteady manner for a specified flow hydrograph, sediment load, and other input parameters. The topographic and bathymetric data are needed for the numerical modeling. The model results can only be as detailed and accurate as the bathymetric data used.

In this study, LiDAR data collected in March, 2005 were used to represent the topography of the river section to be modeled. The survey data were imported into the SMS software for mesh generation. A perspective view of the topography near the Robles Diversion Dam is shown in Figure 2.

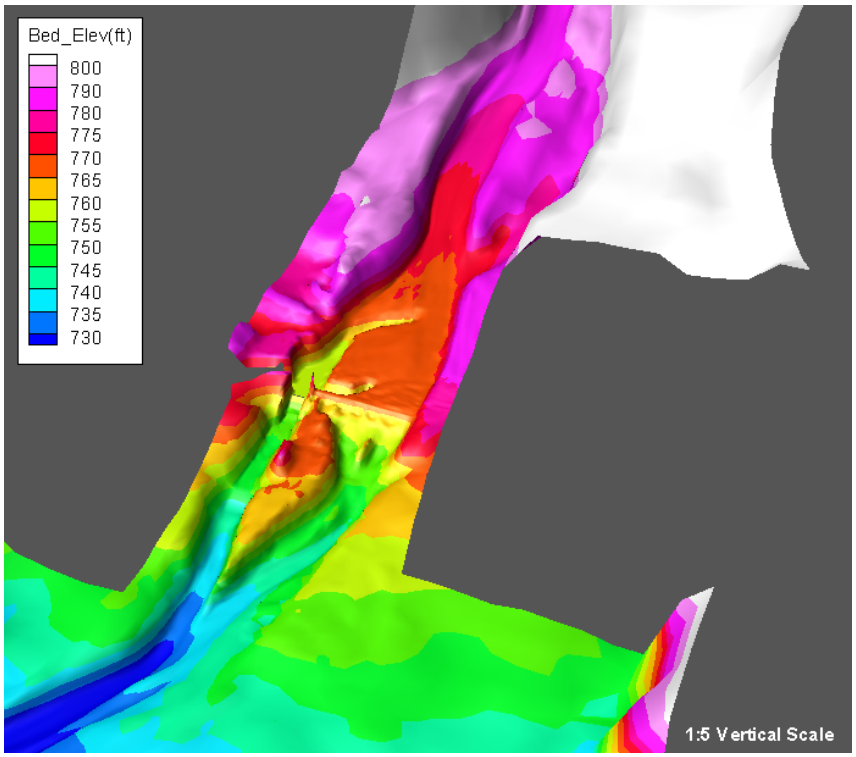

Figure 2. Topography near the Robles Diversion Dam based on the LiDAR data in March 2005

3.2 Hydrologic Data

The hydrologic data have been discussed in great detail in previous studies (Greimann, 2004 and 2006). In the current study, the flood frequency analysis reported by Greimann (2004) (Table 22) was followed. The peak flows downstream of the confluence with N. Fork Matilija Creek were used and they are listed in Table 1. The water surface elevations shown in Table 1 are the elevations at cross section RM 12.7841; as obtained by the one-dimensional (1D) model results reported by Greimann (2006).

Table 1. Peak flows downstream of the confluence with N. Fork Matilija Creek and the water elevation at RM 12.7841

Return Period (yr)	2	5	10	20	50	100	500
Flow (cfs)	3,250	7,580	15,000	18,800	24,000	27,100	35,200
Water surface elevation(ft)	660.7	662.2	663.7	664.2	664.8	665.2	665.9

Further, specific flood events were selected for the sediment routing study. Two flow events were chosen: the 1991 flood and the 1998 flood. The flow hydrographs for the two events are shown in Figure 3. About 200 hours of the hydrograph were modeled. The 1991 hydrograph had a peak of 6,065 cfs at time 78.3 hour and represented the 3 to 4 year flood. The 1998 hydrograph had a peak of 20,240 cfs at time 59.8 hour which corresponded approximately to the 15 year flood.

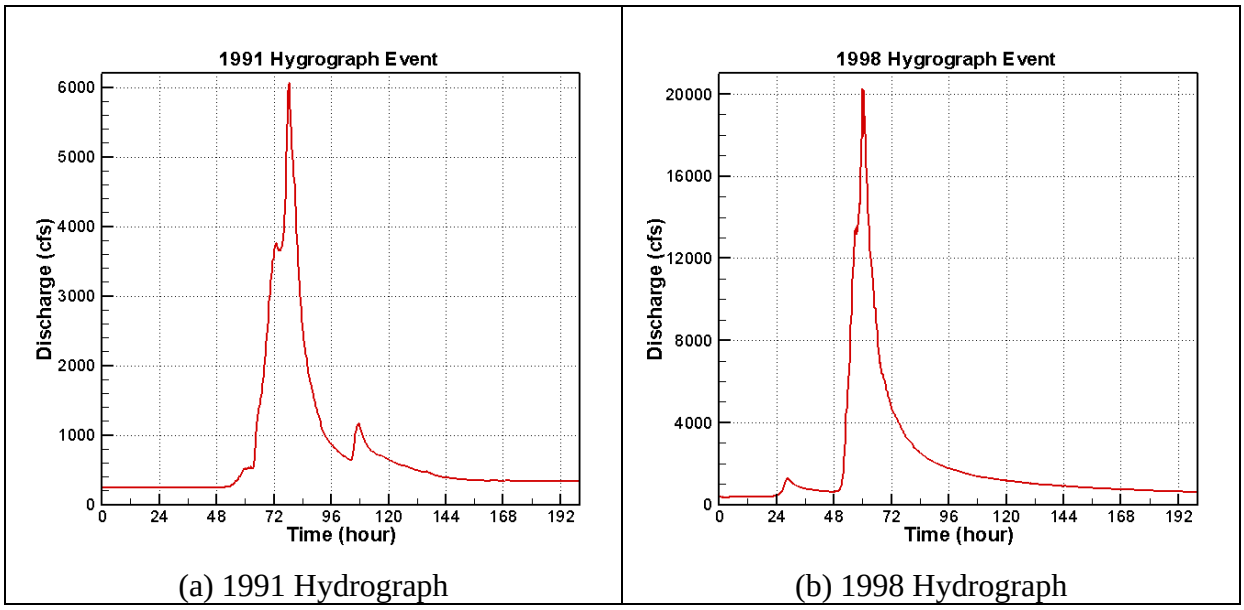

(a) 1991 Hydrograph (b) 1998 Hydrograph

Figure 3. The 1991 and 1998 hydrographs used for the sediment modeling

3.3 Sediment Data

Input data required for the numerical modeling include the sediment load (input) at the upstream boundary and the sediment gradations of the bed material, in addition to the flow hydrograph and topography/bathymetry.

The cross section RM 14.8674 was chosen as the upstream boundary of the 2D numerical model. The sediment input at this location was obtained using results of the SRH-1D (formerly GSTAR-1D) model. The input rates of each sediment size class were computed by SRH-1D and used as input boundary conditions. Two scenarios were modeled, before and after the removal of Matilija Dam. The before-dam removal scenario represented the existing conditions with the Matilija Dam in place; and the after-dam removal scenario represented the case of removing the Matilija Dam.

The total sediment load at RM 14.8674 is shown in Figure 4 for the two dam removal scenarios and two different flood events. The total amount of sediments moving through the cross section RM 14.8674 over the 200 hour period is compared in Table 2.

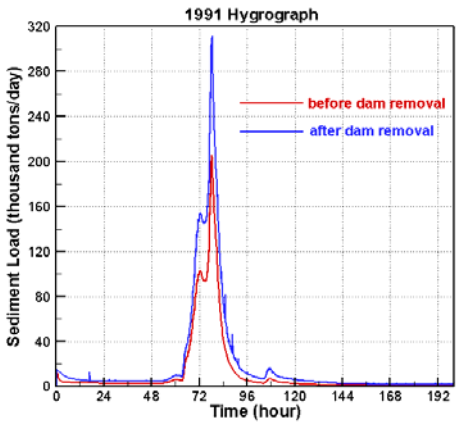

(a) 1991 Hydrograph

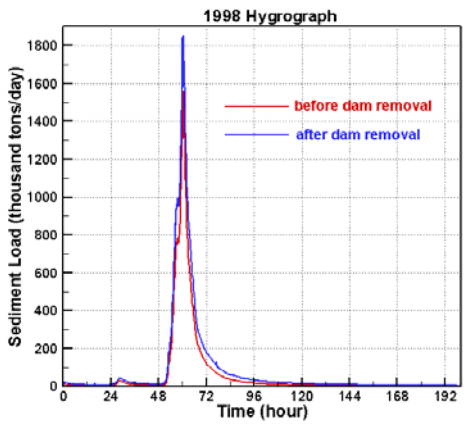

(b) 1998 Hydrograph

Figure 4. Total sediment load (input) at RM 14.8674 computed from the SRH-1D model

Table 2. Total sediment volume (yd^3) moving through RM 14.8674 over the 200-hour period (volume is without voids)

	Before dam removal	After dam removal
1991 Hydrograph	**43,930**	**72,130**
1998 Hydrograph	**233,650**	**318,490**

Limited bed material gradation measurements were available as discussed in the reports of Greimann (2004, 2006). Bed gradation data near RM 14.4, about 0.4 miles upstream of the Robles Diversion Dam, were used for the current numerical modeling study. These surveyed gradation data were applied to the entire solution domain. The cumulative size distribution of the bed materials is shown in Figure 5. It is seen that sediments upstream of the Robles Diversion Dam are quite coarse having a medium diameter of 154 mm.

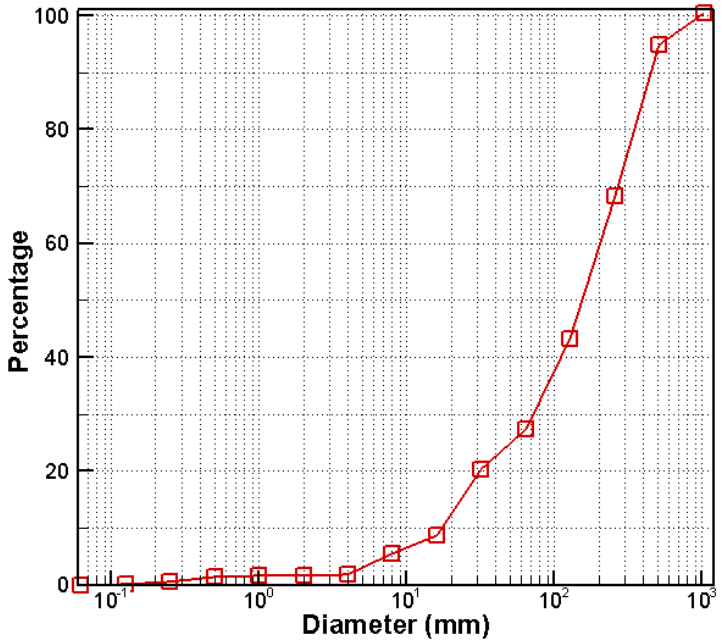

Figure 5. Size distribution of the bed materials at a location about 0.4 mile upstream of the Robles Diversion Dam (d_{50} is about 154 mm)

4.0 Methods of Analysis

4.1. SRH-2D model

Sedimentation and River Hydraulics – Two-Dimensional model (SRH-2D) is used for this study. The model is a 2D depth-averaged hydraulic and sediment transport model for river systems, and is a product of research and development at the Bureau of Reclamation. SRH-2D is based on SRH-W (Lai, 2006) for its flow modeling capability, while its sediment module is based on the Reclamation's latest sediment modeling concept (Greimann et al. 2007). SRH-2D is chosen for several reasons. First, there are not many mature 2D mobile-bed models readily available. Second, the hydraulic flow capability is based on SRH-W which is a mature and flexible tool. Its robustness and accuracy have been demonstrated by many Reclamation project applications. Detailed technical information and application cases may be obtained from the following Reclamation website: http://www.usbr.gov/pmts/sediment/. Third, one of the project team members, Dr. Yong G. Lai, is the lead developer of SRH-2D and SRH-W. Expert knowledge of a numerical model is critical for the success of the modeling and interpretation of the numerical results.

One of the major features of SRH-2D is the adoption of the arbitrarily shaped element method of Lai et al. (2003) for geometry representation. This allows use of the unstructured hybrid mesh for river modeling which has been shown to be flexible and has led to increased accuracy and efficiency.

Major capabilities of SRH-2D are listed below:

- 2D depth-averaged solution of the dynamic wave equations for flow hydraulics;
- An implicit solution scheme for solution robustness and efficiency;
- Unstructured or structured meshes with arbitrary mesh cell shapes may be used. In most applications, a combination of quadrilateral and triangular meshes works the best;
- Steady or unsteady flows;
- All flow regimes can be avaluated: subcritical, supercritical, or transcritical flows;
- Unsteady, non-equilibrium, and non-uniform modeling of the sediment transport;
- Multi-size sediment transports, with bed sorting and armoring;
- Effects of gravity and secondary flows; and
- Non-cohesive or cohesive sediments.

SRH-2D is a two-dimensional (2D) model, and it is particularly useful for problems where 2D effects are important. Examples include flows with in-stream structures such as weirs, diversion dams, release gates, coffer dams, etc.; bends and point bars; perched rivers; and multi-channel systems. 2D models may also be needed if some hydraulic characteristics are important such as flow recirculation and eddy patterns, lateral variations, flow overtopping banks and levees, differential flow shears on river banks, and interaction between the main channel, vegetated areas and floodplains. Some of the scenarios listed above may be modeled in 1D, but additional empirical models are used and extra calibration must be carried out with unknown accuracy.

Similar to any numerical model, uncertainty is inherent in SRH-2D due to assumptions made by the model and uncertainties in user-supplied input data. Specific assumptions and the associated uncertainties are discussed in Section 7 of the report.

4.2. Modeling Scenarios

The 2D numerical model study consisted of three categories of simulations: (1) simulation of the physical model scenarios; (2) calibration study using flows in the field; and (3) simulation of the field scenarios.

Simulation of the physical model scenarios was carried out for two purposes: to verify and validate the mobile-bed sediment model and to investigate various cases under different conditions. Cross check of results between the physical and numerical model results may provide further confidence in using the model data to develop the recommended measures.

Calibration study of the field flows was conducted for developing and testing the numerical model for the field cases so that the appropriateness of the developed model may be assessed and the flow resistance of the model may be calibrated. The study lends credence to the validity of the numerical model. Additionally, the numerical model provided the necessary flow data for designing and conducting the physical model study.

The numerical model simulated the field scenarios and represented the the mobile-bed conditions present at the site. The numerical model covered a much larger reach of the river than the physical model, which eliminated sensitivity of the results to the inlet conditions. In addition, the results of the numerical model eliminated the complication of the scale effects in the physical model. Comparison of the physical model scale and the field prototype scale may shed further light on the recommended measures for the project.

A number of simulation cases were developed and performed within each category. Table 3 is a list of all simulation cases which may be used as a summary and a reference.

Table 3. List of model simulation cases and associated conditions

Model Category	Scenario Description	Case Name	Flow Hydrograph	Case Description
Physical Model Simulation	Flow Calibration	PM-FLOW-1	6,000 cfs	
		PM-FLOW-2	6,000 cfs	
	Sediment: Existing	PM-SED-EX-91	1991	
		PM-SED-EX-98	1998	
	Sediment: RHFB	PM-SED-RHFB-91	1991	
		PM-SED-RHFB-98	1998	
	Sediment: LHFB	PM-SED-LHFB-91	1991	
		PM-SED-LHFB-98	1998	
Field Scale Simulation	Flow Calibration & Application	FD-CA-2005	12,400 cfs	2005 Flood
		FD-CA-100Year	27,100 cfs	100-Yr Flood
		FD-AP-24K	24,000 cfs	
		FD-AP-15K	15,000 cfs	
		FD-AP-6K	6,000 cfs	
	Sediment; Existing	FD-EX-1991-1	1991	before-dam
		FD-EX-1991-2	1991	after-dam
		FD-EX-1998-1	1998	before-dam
		FD-EX-1998-2	1998	after-dam
	Sediment: RHFB	FD-RHFB-1991	1991	after-dam
		FD-RHFB-1998	1998	after-dam
	Sediment: LHFB	FD-LHFB-1991	1991	after-dam
		FD-LHFB-1998	1998	after-dam

4.3. Numerical Model Details

2D modeling, in general, includes the following steps:

(1) Selection of the solution domain;
(2) Mesh generation for the solution domain;
(3) Zonal representation of bed properties such as flow roughness and sediment gradation;
(4) Model development and calibration; and
(5) Model applications.

The first three steps are discussed in this section.

4.3.1. Solution Domain and Mesh Generation

A 2D analysis begins by defining a solution domain and then generating a mesh that covers the domain. The solution domain of the field cases for the present analysis was based on the objectives of the project, the available data, and the limit of the computing power. This process largely relied on the past experience of applying the model to other similar rivers. The final solution domain for the present study is shown in Figure 6, and it has the following characteristics:

- Downstream boundary: It is located about 1.2 miles downstream of the Robles Diversion Dam, at the cross-section RM 12.7841, with a relatively straight section.
- Upstream boundary: It is located about 0.9 miles upstream of the Robles Diversion Dam, at the cross-section RM 14.8674, with a relatively straight channel.
- Lateral extent: It is wide enough laterally that the domain would fully contain the 500-year flood; based on the results of the 1D numerical modeling (Greimann, 2004).
- The total length of the river reach modeled is about 2.1 miles.

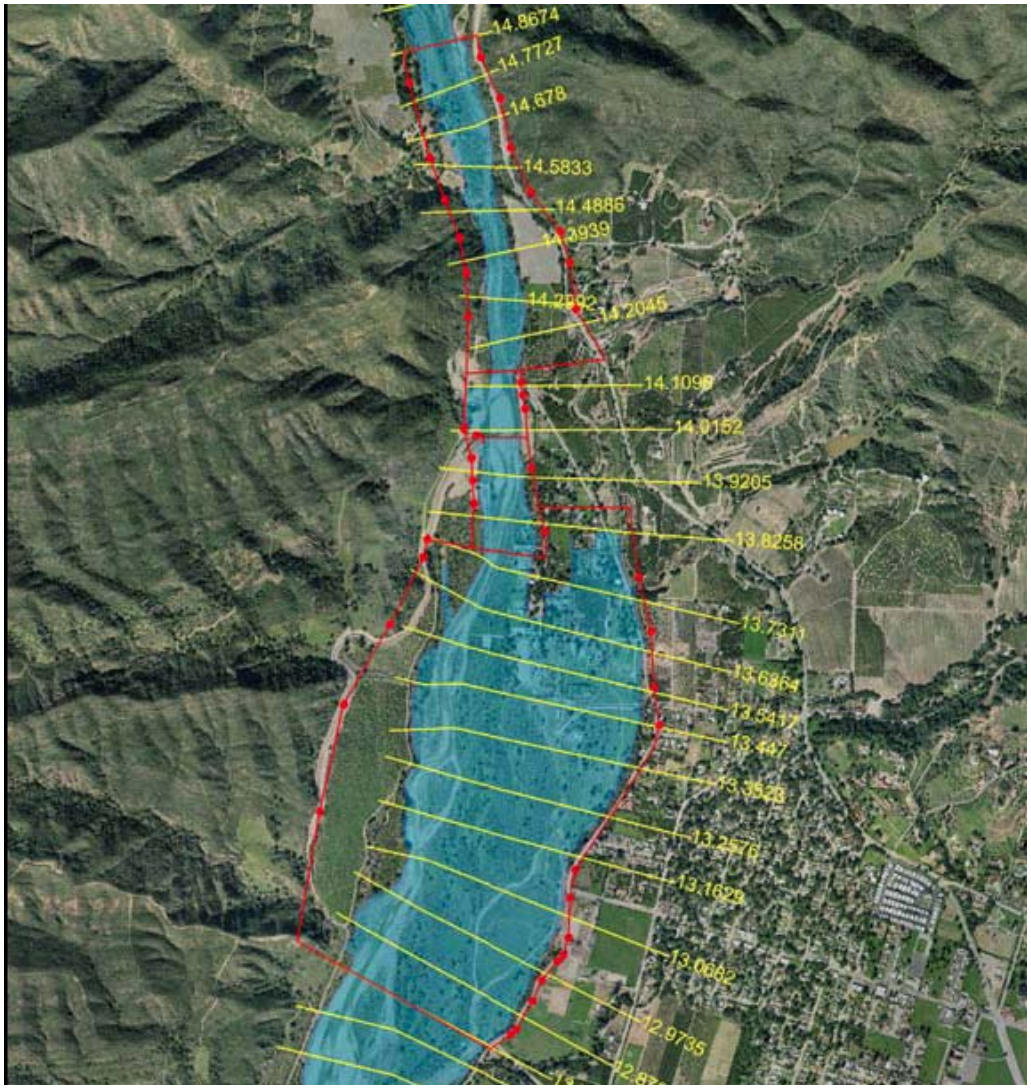

Figure 6. Solution domain (red) of the 2D numerical model for the field simulation

A 2D mesh was generated using the Surface water Modeling System software (SMS). The following website link provides more information for the software: www.ems-i.com. Additionally, the SRH-W manual (Lai, 2006) may be consulted for discussion on how the SRH-2D model interacts with SMS. Different meshes were generated for each scenario and they are discussed. In reference to the following discussion, the mesh used for the calibration study of field flows is shown in Figure 7. A total of about 10,000 hybrid quadrilateral and triangular mesh cells were used to represent the solution domain. The topography/bathymetry of the solution domain represented by the mesh is shown in Figure 8. Note that the bathymetry was based on the March 2005 LiDAR survey as discussed in Chapter 3.0.

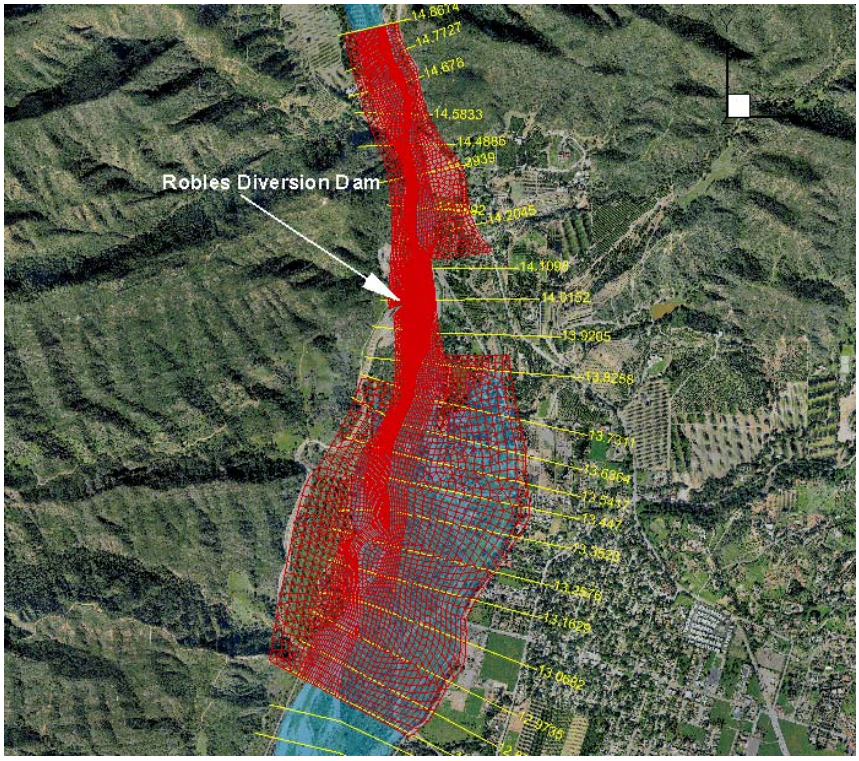

Figure 7. Mesh generated for the calibration study of field flows discussed in Chapter 5.0

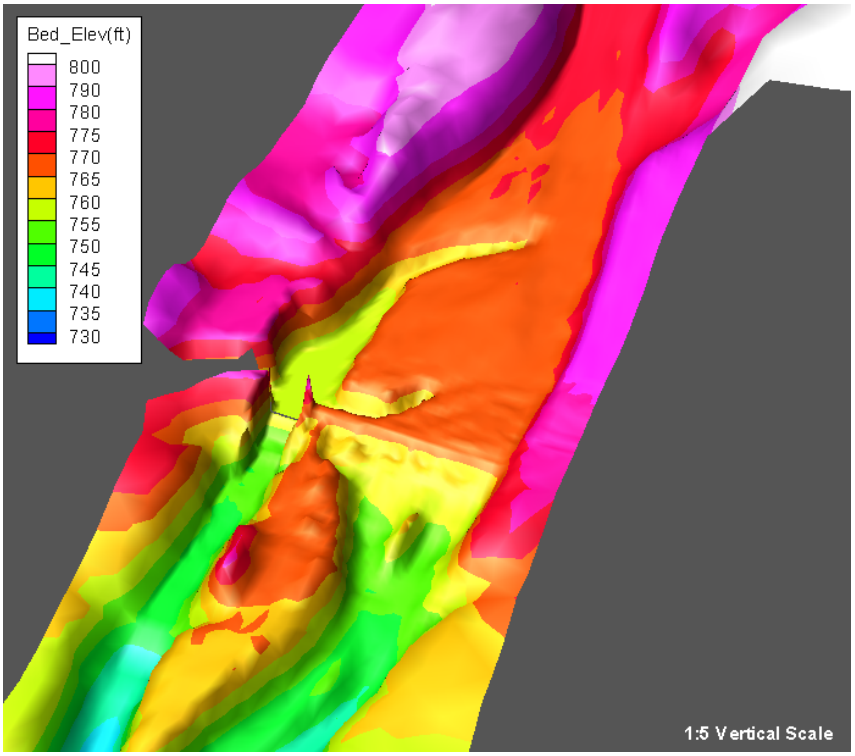

Figure 8. 3D perspective view of the topography for the existing condition scenario based on March 2005 LiDAR survey data

4.3.2. Representation of Flow Roughness and Bed Gradation

Flow resistance was calculated with the Manning's roughness equation in which the Manning's coefficient (n) was used as one of the model inputs. Major bed properties include the Manning's coefficient and the bed gradation. The bed properties may be spatially distributed over the solution domain. The zonal representation approach was used: the solution domain was partitioned into a number of bed-property zones and each zone was assigned different properties of the roughness and bed gradation.

In this study, the solution domain was divided into three bed-property zones based on the aerial photo: main channel, light vegetation, and heavy vegetation. The zonal partition is shown in Figure 9. Each zone is assigned a different Manning's coefficient n. Based on the report of Greimann (2006) (p.67), the previous 1D model study used the Manning's roughness coefficient of 0.04 for the main channel, and 0.08 for the floodplain. In general, 2D models use smaller roughness coefficients than the 1D model, as some energy losses are taken into account by the 2D model. In this study, the main channel has n =0.035, light vegetation has n =0.045, and heavy vegetation n =0.075. These initial values were confirmed to give good results during the calibration study reported in Chapter 5.0, and they were used unchanged for all field simulations reported.

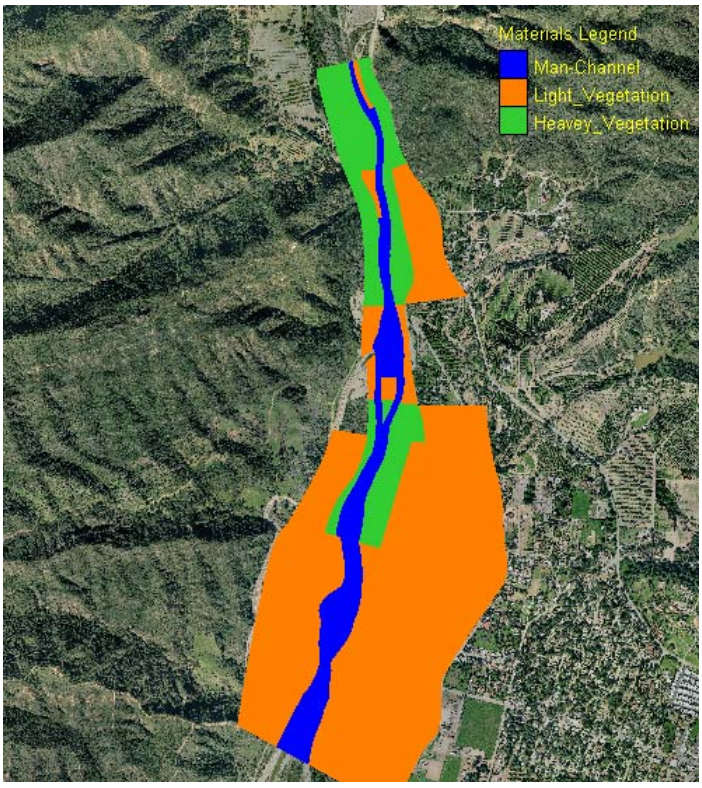

Figure 9. Three zones were used to represent the bed properties on the solution domain: the main channel, light vegetation and heavy vegetation

4.4. Sedimentation Analysis Method

The mobile-bed sediment analysis was carried out with SRH-2D. The flow modeling capability is well documented by Lai (2006); but the sediment module is not. Readers may consult a few recent papers for details (e.g., Greimann et al. 2007; Lai and Greimann 2007; Lai and Greimann 2008a,). In the following, a brief description of the sediment analysis methodology and the related modeling parameters is provided.

4.4.1. Sediment Transport Equations

Sediment transport in a mobile-bed river depends on many input variables such as topographic and bathymetric features, flow hydraulics, bed gradation, and upstream sediment supply. The bed gradation changes from its initial state as sediment particles are eroded from or deposited on the bed, which in turn changes flow hydraulics and fractional sediment transport rates.

In general, a water column and a river bed may be divided into four separate vertical layers, from a computational point of view:

- Suspended Load Layer: a top layer in the water column where sediment particles are in suspension and are transported as suspended load (including wash load);
- Bed Load Layer: a layer near the bed where sediment particles roll, slide, or saltate. Particles are transported as bed load;
- Active Layer: a layer on the top surface of the bed where sediment exchange occurs between the sediment load above and the bed underneath;
- Subsurface Layers: one or several bed layers, which have not been mobilized by flow and are underneath the active layer.

In this project, transport of the bed material load is considered. That is, the combined suspended load and bed load, but without the wash load, is simulated. The wash load refers to those fine sediments that are transported from the upstream boundary to the downstream exit without interaction with the bed sediments. Wash load is ignored as it does not contribute to the bed morphological changes.

Furthermore, the general modeling approach of the non-uniform and non-equilibrium sediment transport is adopted. Non-uniform transport refers to the representation of sediments with multiple sediment size classes and transport of each size class is tracked separately. The non-uniform approach may be compared with the alternative of the uniform transport method in which all sediments are represented by one size class (d_{50} is usually used). The non-uniform approach is closer to field conditions and is the choice if sediment sorting and other related features are of interest. Non-equilibrium transport refers to the use of the full sediment transport equation in which the sediment concentration does not equal

the sediment transport capacity. This is in contrast to the commonly used Exner equation, an equilibrium model, which assumes instant exchange between the transported loads and the bed materials. With the non-equilibrium method, the sediment concentration is allowed to vary in response to local flow features such as convection and dispersion, local transport capacity, and local bed gradation.

With the non-uniform non-equilibrium approach, sediments are divided into a number of size classes and each sediment size class (*k*) obeys the following transport equation derived from mass conservation:

$$\frac{\partial hC}{\partial t} + \frac{\partial \cos(\alpha) V_t hC}{\partial x} + \frac{\partial \sin(\alpha) V_t hC}{\partial y} = S_E \qquad (1)$$

where C is the depth-averaged sediment concentration, *h* is water depth, *t* is time, *x* and *y* are two horizontal Cartesian coordinates, respectively, V_t is the depth-averaged total sediment velocity, α is the angle of sediment transport direction relative to the *x*-axis, and S_E is the sediment exchange term between the total sediment load and the active layer. Specific models for a number of variables in the above equation will not be discussed and may be found in Greimann et al. (2007). It is sufficient to point out that the angle of sediment transport direction is not the same as the water flow. Instead, the angle depends on whether or not the size class is suspended load, bed load, or mixed load, and the impacts of secondary flows and gravity are also included.

The sediment exchange term is discussed next. For the non-cohesive sediments, the exchange term may be expressed as:

$$S_E = \frac{1}{L_{tot}} (q_{tot}^* - V_t hC) \qquad (2)$$

where q_{tot}^* is the equilibrium transport capacity for the total load, and L_{tot} is the adaptation length of the total load and is calculated as:

$$L_{tot} = (1 - f) L_b + f \zeta V_t h / \omega_s \qquad (3)$$

where *f* is the fraction of the suspended sediments in the total load, ζ is the parameter for the rate of suspended load exchange, L_b is the bed load adaptation length, and ω_s is the particle fall velocity. The bed load adaptation length characterizes the distance for sediments to adjust from the non-equilibrium state to the equilibrium state, and is related to scales of sediment transport, bedform, and geometry. In this study, a constant L_b was specified. The suspended sediment coefficient, ζ, equals 1.0 for net erosion and 0.25 for net deposition.

The Parker (1990) sediment transport equation was used in this project and is suitable for rivers composed of gravel and mixed sand and gravel beds. The transport equation for sediment size class *k* may be expressed as:

$$\frac{q_{t,k}^{*} g(s-1)}{(\tau_b / \rho)^{1.5}} = p_{ak} G(\phi_k); \qquad \phi_k = \frac{\theta_k}{\theta_r}\left(\frac{d_k}{d_{50}}\right)^{\alpha} \tag{4}$$

In the above, $q_{t,k}^{*}$ is the volumetric sediment transport rate per unit width, p_{ak} is the volumetric fraction of sediment size class *k* on the bed surface, $s = \rho_S / \rho - 1$, ρ and ρ_S are the water and sediment density, respectively, g is the gravitational acceleration, τ_b is bed shear stress, $\theta_k = \tau_b / [\rho g(s-1)d_k]$ is Shield's parameter of sediment size class *k*; θ_r is the reference Shield's parameter, d_k is diameter of sediment size class *k*, and d_{50} is the median diameter of the sediment mixture in bed. The function in the transport equation was fit to the field data by Parker (1990) and is expressed as:

$$G = \begin{cases} 11.933(1 - 0.853/\phi)^{4.5}, & \phi > 1.59 \\ .00218 \exp[14.2(\phi - 1) - 9.28(\phi - 1)^2], & 1.0 \le \phi \le 1.59 \\ .00218\,\phi^{14.2}, & \phi < 1.0 \end{cases}$$

Two parameters must be defined by a user to apply the Parker equation: θ_r and α. The parameter θ_r is a reference value above which sediment is mobilized and α is the exposure (or hiding) factor to account for reduction in critical shear stress for larger particles and increase in critical shear stress for smaller particles. In this project, θ_r =0.055 and α =0.65 were used.

Dynamics of the bed sediments and the bed interaction with the sediment load were also simulated, and details may be found in Greimann et al. (2008).

4.4.2. Boundary Conditions and Other Input Data

At the upstream boundary, conditions include the flow discharge and the sediment supply rate (load) for each size class. In this study, a constant flow discharge or a time series flow hydrograph was imposed as discussed in Chapter 3.0. The upstream sediment supply was obtained from the SRH-1D simulation results as discussed in Chapter 3.0 for the filed scenarios and was estimated from the total sediment added for the physical model cases.

At the downstream boundary, the water surface elevation (stage) was specified. A rating curve was generated at the downstream boundary based on the SRH-1D model results and was tabulated in Table 1.

Ten sediment size classes, as shown in Table 4, were used to represent the sediments on the river bed and at the inlet. The bed gradation has been presented in Figure 5 and it was used throughout the solution domain. Note that size class 10 was used to represent the non-erodible bed such as the radial gates and at spillways. Each size class will be transported and modeled individually.

Table 4. Size ranges of each sediment size class

Sediment Size Class	Size Range (mm)
1	0.0064 to 0.0625
2	0.0625 to 0.25
3	0.25 to 1
4	1 to 4
5	4 to 16
6	16 to 64
7	64 to 256
8	256 to 1028
9	1028 to 4096
10	Non-erodible

5.0 Physical Model Scenarios

5.1. Discussion of Physical Model Scenarios

Different physical model scenarios have been discussed and results are presented in the physical model results portion of the report. Only information relevant to the numerical simulation is summarized and discussed next.

Three test scenarios were performed in the physical model: Existing Condition, Right High Flow Bypass (RHFB), and Left High Flow Bypass (LHFB). The existing condition has the existing radial gates and the diversion canal gates in operation. With the RHFB and LHFB, the new high flow bypass radial gates are added to the existing condition. Layouts of the three scenarios are illustrated in Figure 10.

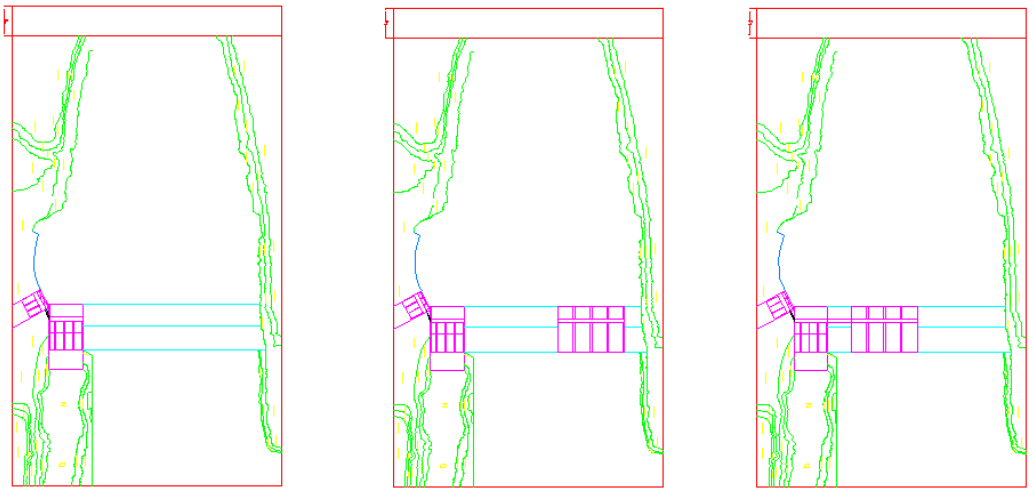

(a) Existing Condition (b) LHFB (c) RHFB

Figure 10. Layouts of three physical model scenarios (looking upstream)

The flow capacities of the existing gates, the diversion canal gates, and the new high flow bypass gates are about 3.3538 cfs, 0.2795 cfs, and 6.149 cfs, respectively. These correspond to 6,000 cfs, 500 cfs, and 11,000c cfs, respectively, in the prototype field scale.

For each scenario, two flow hydrographs were tested: 1991 hydrograph and 1998 hydrograph. The 1991 hydrograph has a peak flow of about 6,000 cfs in the prototype scale and 1998 hydrograph has a peak of 14,000 cfs in the prototype scale. The actual peak of the 1998 flood was more than 20,000 cfs and the smaller value of 14,000 cfs was used for the physical model due to the limit of sediment feed at the laboratory. The two hydrographs in the physical model scale, along

with the sediment input rate at the model inlet, are shown in Figure 11 and Figure 12. Only the total sediment input was recorded during the physical model test: an average of about 3.5 yd^3 and 6.85 yd^3 for the 1991 and 1998 hydrographs, respectively. In the numerical modeling, the curves of the total sediment rates in Figure 11 and Figure 12 were determined as follows. The numerical model was first run assuming that the sediment transport rate at the inlet equaled the sediment capacity. Integration of the resultant curve gave the total amount of sediments into the test box. In general, however, the calculated input volume would not equal the actual one used. The sediment rating curve was then scaled up or down so that the total sediment input volume would be the same as the recorded volume used during the test. It is interesting to point out that the total input volume based on the transport capacity was approximately the value of 3.5 yd^3 for the 1991 hydrograph case while it was about 11.5 yd^3 for the 1998 hydrograph case.

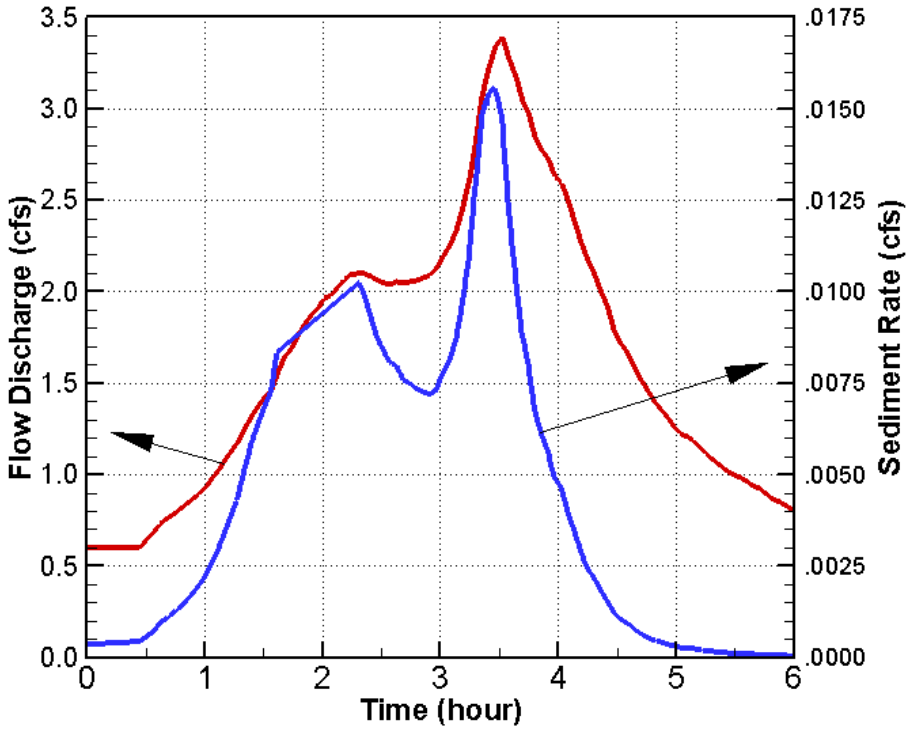

Figure 11. Flow hydrograph and total sediment load at the inlet with the 1991 hydrograph

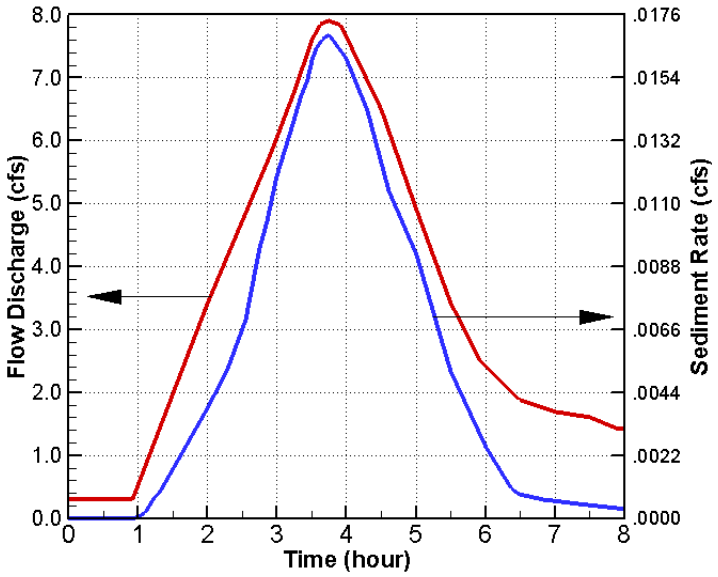

Figure 12. Flow hydrograph and total sediment load at the inlet with the 1998 hydrograph

A sediment mixture with medium diameter d_{50}=1.75 mm was used for the physical model test. It was used as the initial bed and it was also used as the sediment feed at the inlet. The gradation sample analysis provided the cumulative size distribution as plotted in Figure 13. For the numerical modeling, the sediment mixture was divided into seven size classes listed in Table 5. The bed upstream of the weir was initially filled with the sediments while the test section downstream of the weir was non-erodible.

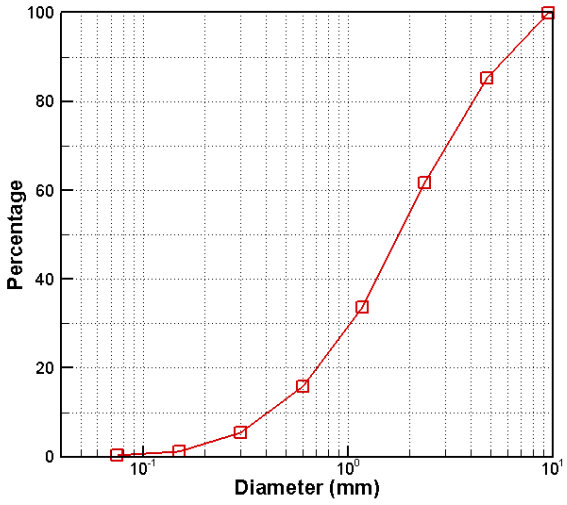

Figure 13. Size distribution of the base sediment mixture used for the physical model test (d_{50}=1.75 mm)

Table 5. The lower (d_low) and upper (d_upp) diameter of each sediment size class used for the numerical modeling of the physical model scenarios

Size ID	1	2	3	4	5	6	7
d_low(mm)	0.0625	0.15	0.30	0.60	1.18	2.36	4.75
d_upp(mm)	0.15	0.30	0.60	1.18	2.36	4.75	9.5

5.2. Calibration Using the Measured Flow Data

With SRH-2D, the major flow calibration parameter is the Manning's roughness coefficient. In the physical model, flow velocity measurements were made under a constant flow discharge of 3.3538 cfs (6,000 cfs at the prototype field scale) under several gate scenarios. The data were used to calibrate the Manning's coefficient and then used to verify the numerical model. The final calibrated Manning's coefficient for the physical model scenarios was 0.026 which was a constant uniformly distributed over the solution domain.

The RHFB scenario was set up for the flow measurement in the laboratory. The layout of the flow case is shown in Figure 14. In this setting, the existing gate, the diversion canal gates, and the RHFB gates were all in place. The solution domain was the same as the test box. The mesh generated for the numerical modeling, along with the bathymetry represented by the mesh, is displayed in Figure 15. A perspective view of the bathymetry is shown in Figure 16.

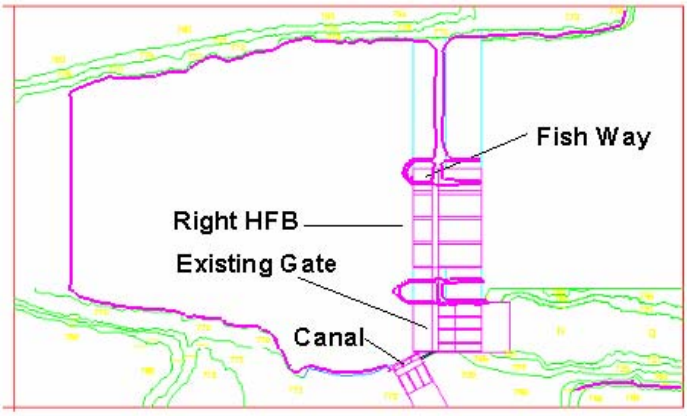

Figure 14. Layout of the right HFB case

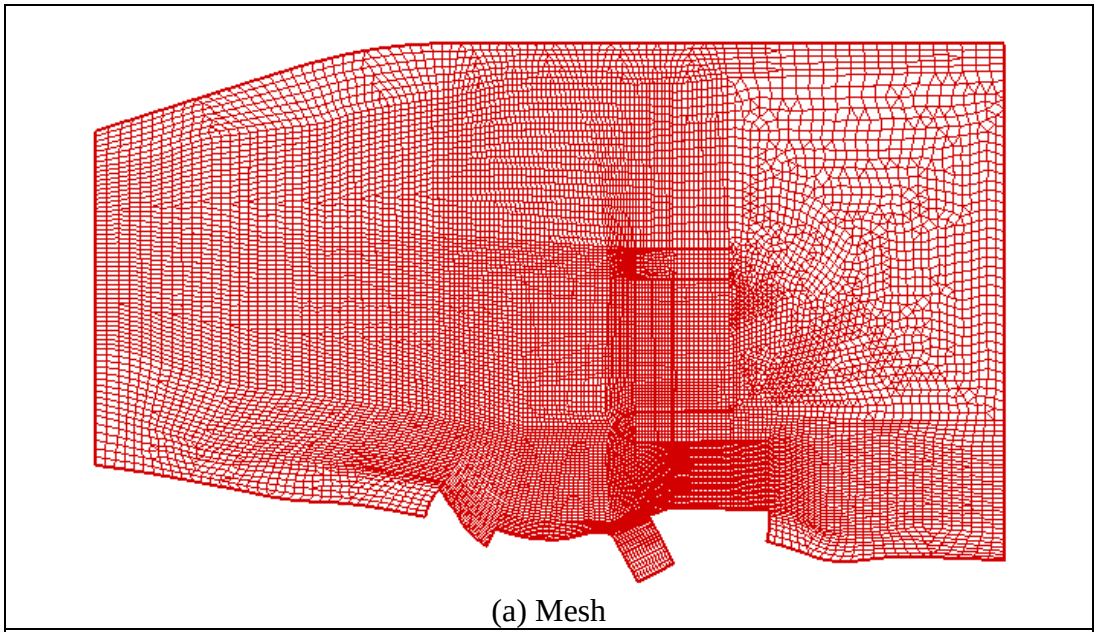

(a) Mesh

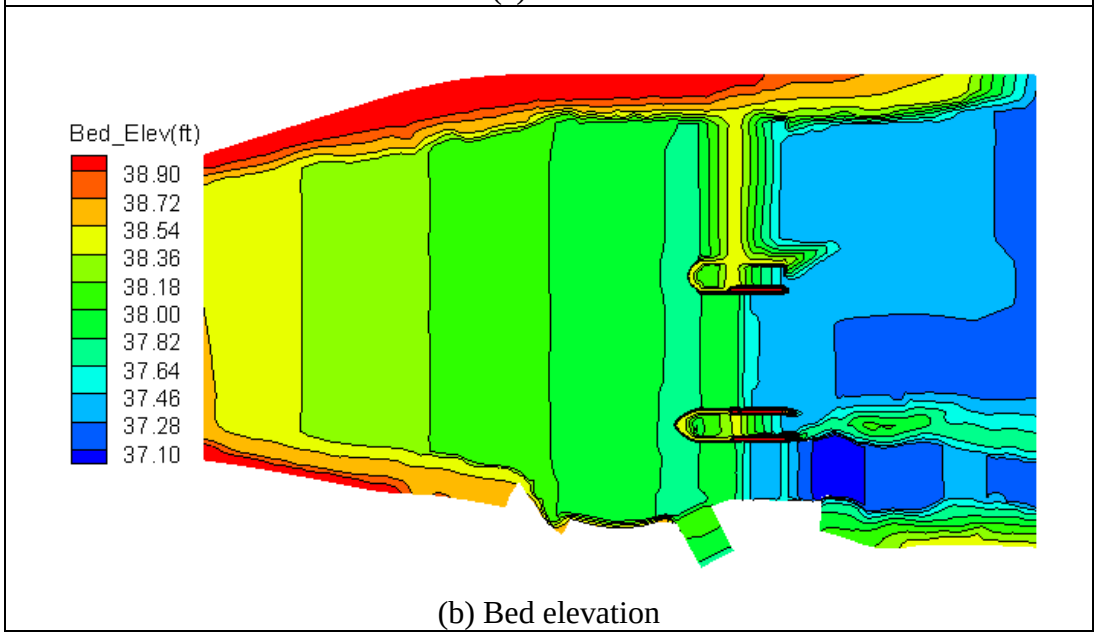

(b) Bed elevation

Figure 15. Mesh and bathymetry of the RHFB numerical model used for the calibration study

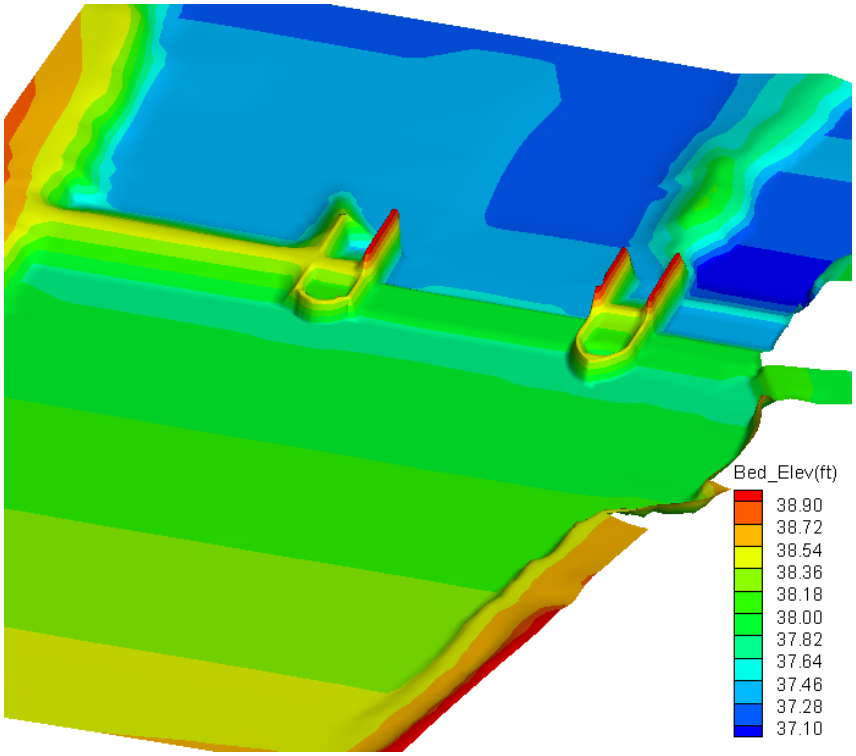

Figure 16. Perspective view of the bathymetry of the RHFB case in the physical model used for the calibration study

Two flow cases were simulated and results were compared with the measurements. The first case was named PM-FLOW-1 for which the existing gates were fully open while the RHFB gates were closed completely. The second case, PM-FLOW-2, reversed the gate operation: the RHFB gates were fully open while the existing gates were closed. The diversion canal gates were fully open for both cases.

A comparison of the measured and computed depth-averaged velocity along several transects is shown in Figure 17 and Figure 18. It is seen that agreement between the measurement and computation is reasonably good. The measured depth-averaged velocity was obtained at the 60% flow depth. Some of the measurement points, particularly at the upstream transects, were not accurate as they were strongly influenced by the delta movement.

The predicted flow streamlines and flow patterns are also shown in the figures. The computed recirculation location, size and shape at the top right corner were in agreement with the observation made during the physical model test.

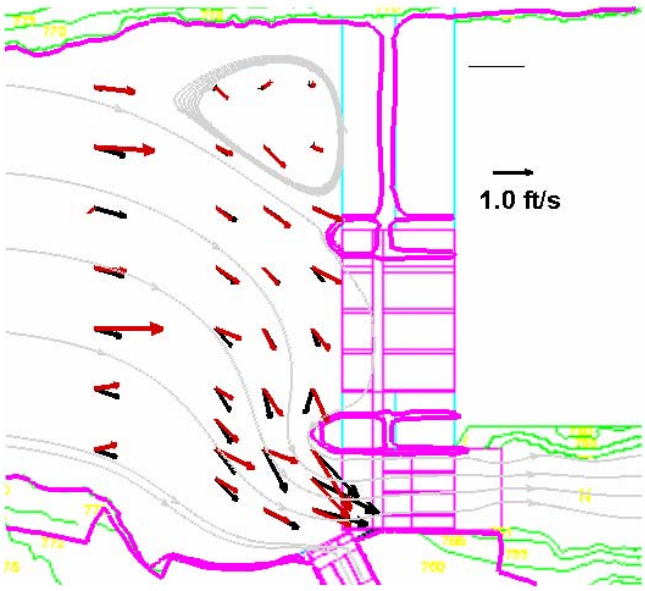

Figure 17. Comparison of measured (red) and computed (black) depth-averaged velocity for case PM-FLOW-1

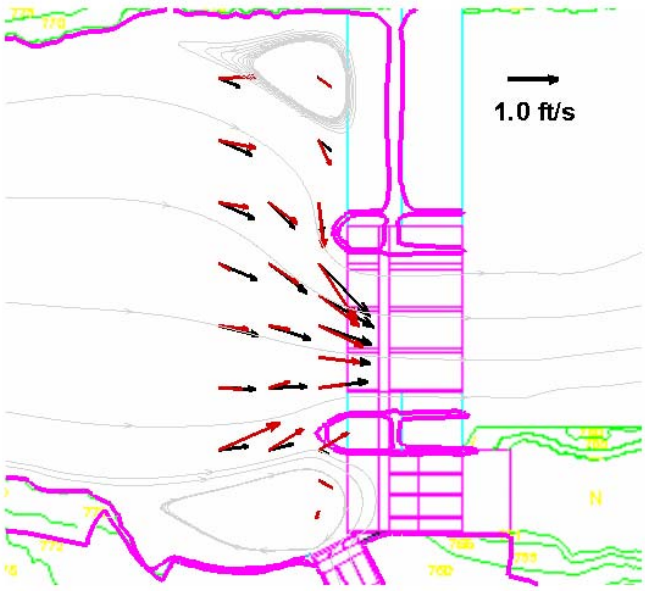

Figure 18. Comparison of measured (red) and computed (black) depth-averaged velocity for case PM-FLOW-2

5.3. Mobile-Bed Simulation with the Existing Condition

The mobile-bed simulation was carried out for the existing condition scenario. The mesh is shown in Figure 19, and the bathymetry of the initial bed is displayed in Figure 20. The mesh has a total of 10,285 combined quadrilateral and triangular cells.

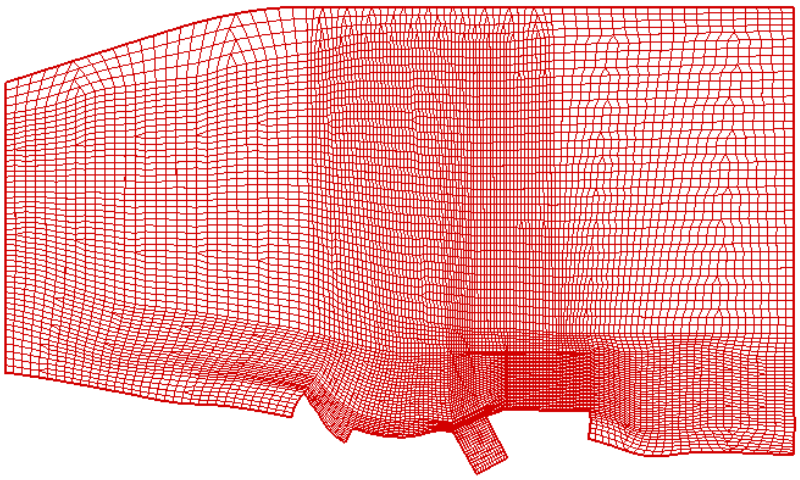

Figure 19. Mesh for the existing condition scenario mobile-bed simulation (physical model)

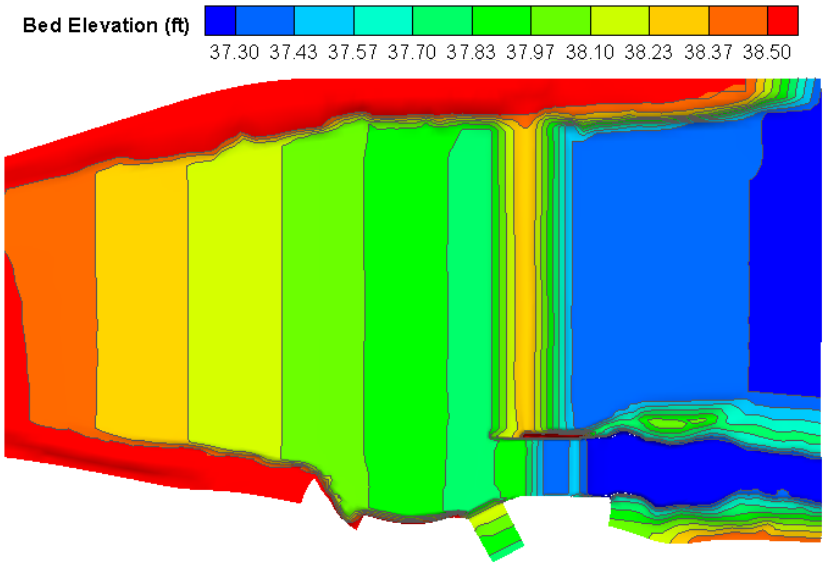

Figure 20. Bed elevation of the existing condition scenario for the mobile-bed simulation (Physical model)

Two unsteady mobile-bed simulations were carried out in the physical model corresponding to the 1991 hydrograph and the 1998 hydrograph (see Figure 11

and Figure 12). They are labeled as PM-SED-EX-91 and PM-SED-EX-98, respectively. The diversion canal gates were open all the time with a flow capacity of 0.2795 cfs (500 cfs in the prototype). Operation of the existing gates followed the operation of the physical model test as closely as possible and the discharge capacity of the gates is shown in Figure 21 which was used for both simulation cases. The existing gates were open to a capacity of 0.2 cfs for the first 1.16 hours; the capacity was jumped to 1.0 cfs for the period of 1.16 to 1.685 hours; and the gates were fully open to 3.35 cfs after 1.685 hours. The gate capacity was reduced down to 1.4 cfs after 5.94 hours.

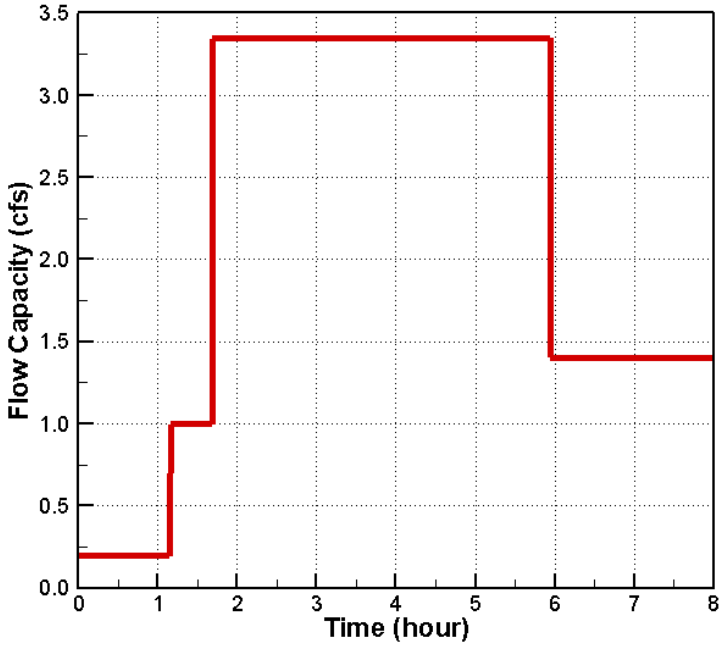

Figure 21. Gate operation curve (flow capacity versus time) of the existing radial gates for the existing condition modeling

For case PM-SED-EX-91 (1991 hydrograph), the final bed topography is compared in Figure 22 at time 6 hours between the simulated results and the physical model results. The simulated bed form evolution in time is plotted in Figure 23.

The simulated final bed form is in qualitative agreement with that of the physical model test. Some discrepancy is observed and is mainly near the existing gate. It may be attributed to the possible difference in the radial gate operation during the falling limb of the hydrograph. In the numerical model, all gates (a total of four) could only be opened or closed at the same time and they were not allowed to operate separately. In the physical model test, each individual gate may be operated to different capacity. In addition, the gate operation during the falling limb was not well documented during the physical model test. Another source of uncertainty is related to the spatial distribution of the input sediments. During the

physical model tests, sediments addition at the inlet was not uniform laterally, but the numerical model assumed a uniform distribution of the sediment concentration across the inlet.

(a) Photo taken at the end of the physical model test

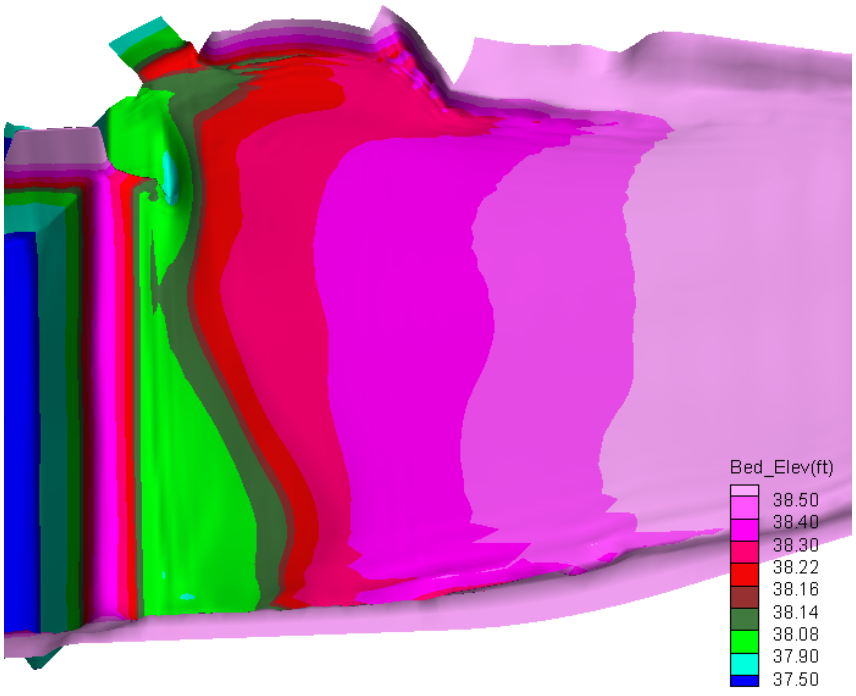

(b) Simulated bed elevation

Figure 22. Comparison of bed topography at the end of the hydrograph (6 hours) between the physical model and the simulation for PM-SED-EX-91

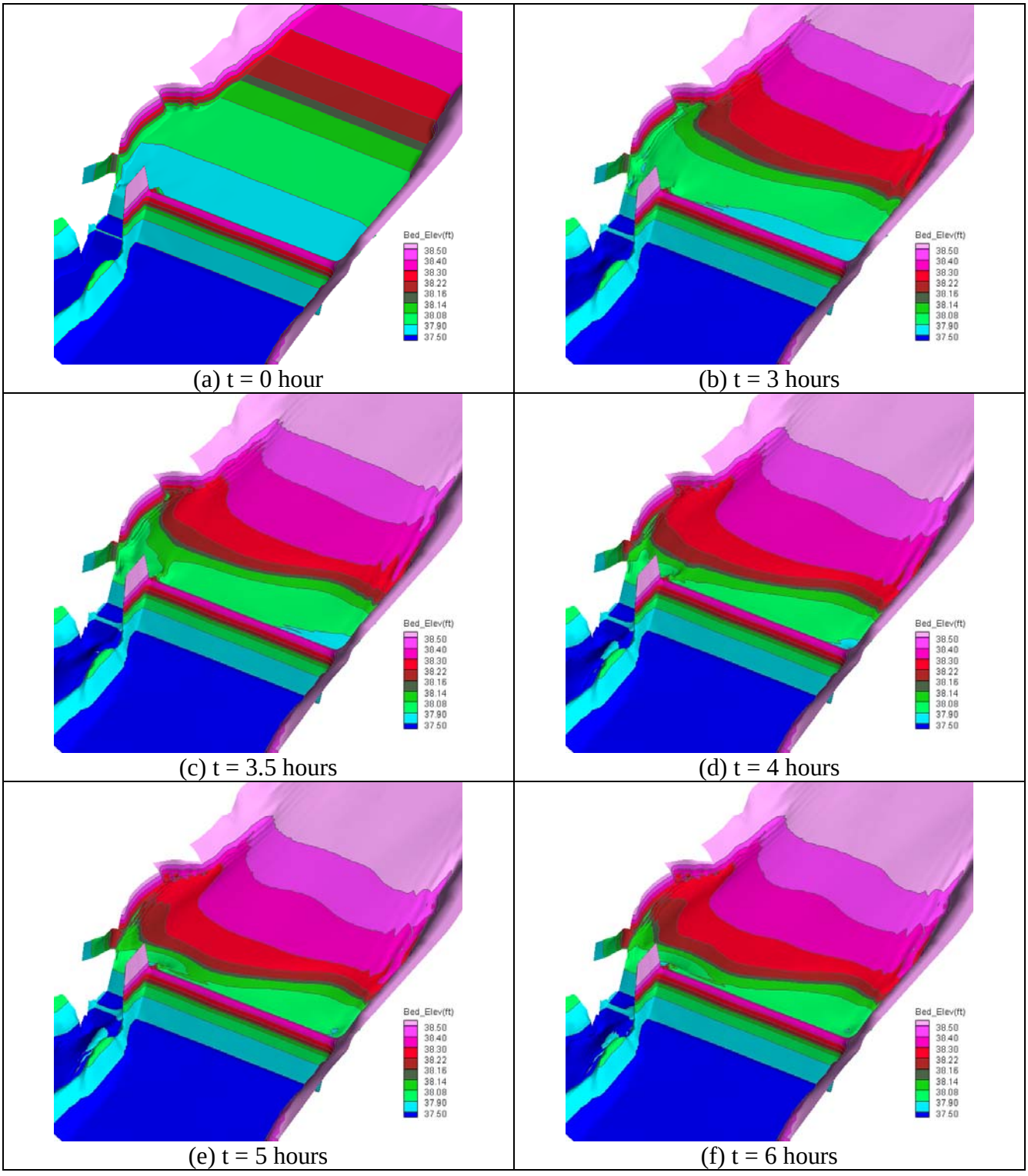

(a) t = 0 hour (b) t = 3 hours

(c) t = 3.5 hours (d) t = 4 hours

(e) t = 5 hours (f) t = 6 hours

Figure 23. Simulated bed form evolution at different times for case PM-SED-EX-91 (1:4 vertical distortion)

For case PM-SED-EX-98 (1998 hydrograph), the bed topography is compared in Figure 24 and Figure 25 at the end of the hydrograph (8 hours) between the simulated and physical model test results. The simulated bed form evolution in time is plotted in Figure 26.

Figure 24 and Figure 25 show that the model results were in qualitative agreement with the physical model results. In the area upstream of the existing gates and the diversion canal gates, greater deposition occurred in the middle while "channel"-type topography appeared on the two sides. The "channel" on the left was more significant in the numerical model as shown in Figure 24 and it was due to sluicing by the existing gates. The sluicing effect can be seen by comparing results of 5.5 hours and 8.0 hours in Figure 26. The right "channel" was less significant near the canal diversion gate (Figure 24) but more significant upstream (Figure 25). The right "channel" was only marginally captured by the numerical model as shown in Figure 25 and this may be attributed to the difference in sediment feeding at the inlet upstream. Much less sediments were added on the right side of the inlet during the physical model tests but uniform constant sediment concentration was assumed in the numerical model. The final bed form may be sensitive to the existing gate operation particularly during the falling limb of the hydrograph, and to a lesser degree, also sensitive to the spatial distribution of the sediment input at the inlet.

High sediment deposition was observed in the middle section of the weir and it was captured by the numerical model as shown in Figure 24.

Model results of the case PM-SED-EX-98 point to the possibility of using the existing radial gates to remove the sediments deposited in front of the existing gates and the diversion canal gates by opening the existing gates as much as possible during the falling limb of the hydrograph. Since the sluicing does not take place for case PM-SED-EX-91, an estimate may be made based on the model results. It is found that a discharge above 1.5 cfs (2,236 cfs in the prototype) is needed for effective sluicing using the existing gates. However, the numerical model assumed that all four gates are open; it is expected that much less flow is needed if only one of the four gates is open for sediment sluicing.

The bed evolution pattern in Figure 23 showed that the delta has reach the canal diversion gates but the delta elevation in front of the gate is still less than the gate sill elevation. Figure 26 clearly showed the risk of bed load sediments transported into the diversion canal during the flood as the delta elevation in front of the canal gates is about the same as the gate sill.

(a) Photo looking towards the gates

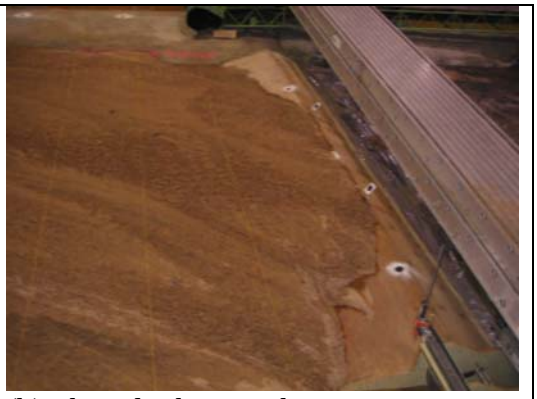

(b) Photo looking at the weir

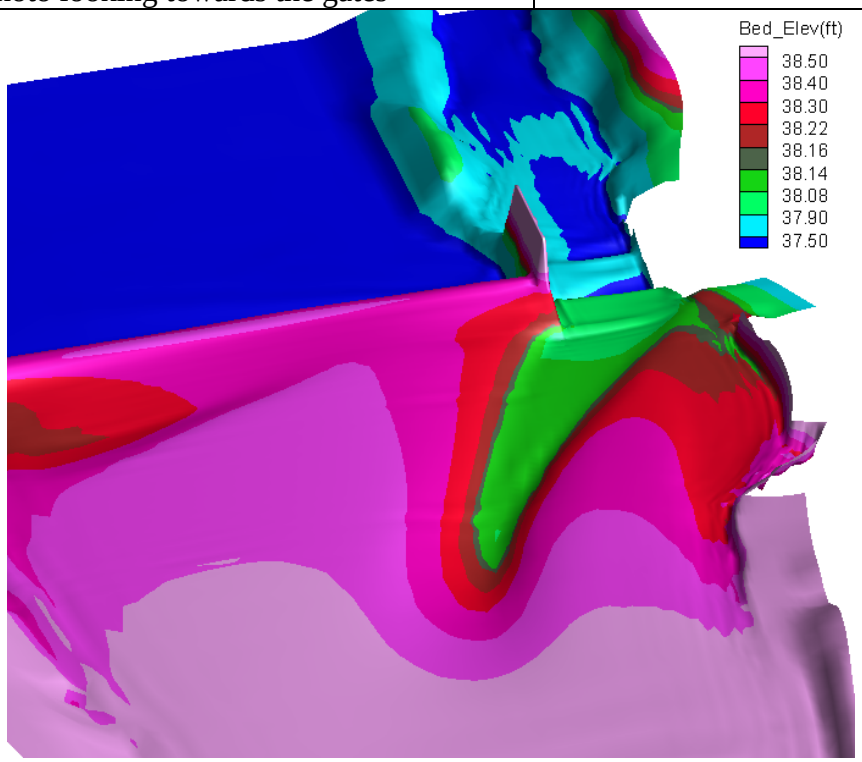

(c) Simulated bed elevation

Figure 24. Comparison of bed topography at time 8 hours between the physical model and the simulation for PM-SED-EX-98

(a) Photo looking upstream and at the right bank

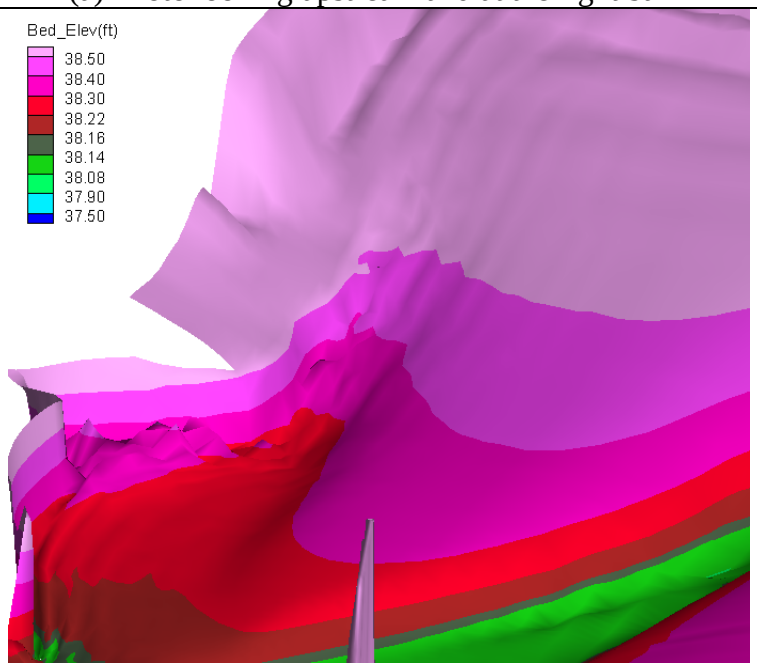

(b) Simulated bed form

Figure 25. Comparison of bed topography near the right bank between the physical and numerical models for PM-SED-EX-98 at the end of the hydrograph (8 hours)

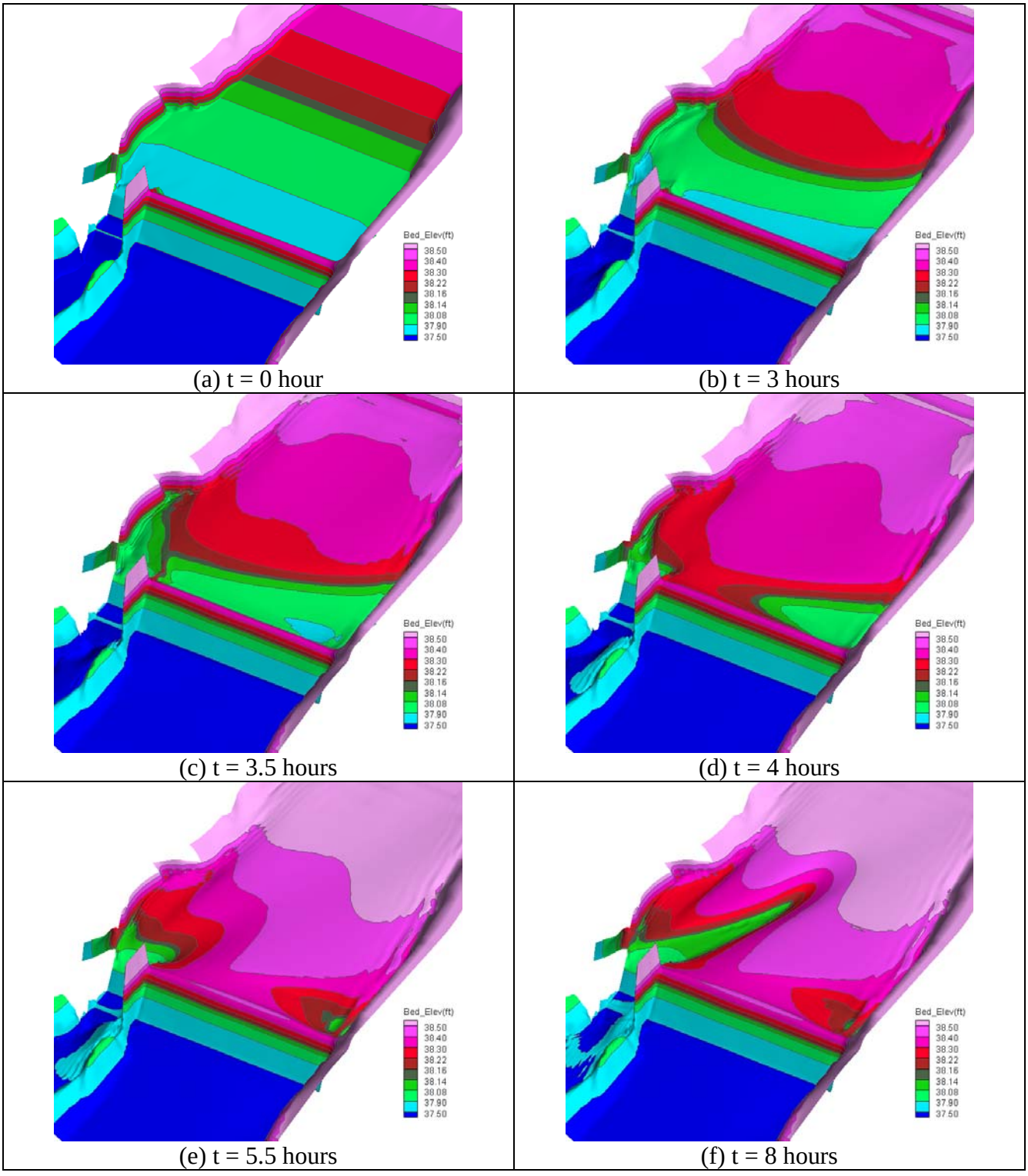

(a) t = 0 hour (b) t = 3 hours

(c) t = 3.5 hours (d) t = 4 hours

(e) t = 5.5 hours (f) t = 8 hours

Figure 26. Simulated bed form evolution with time for case PM-SED-EX-98 (1:4 vertical distortion)

5.4. Mobile-Bed Simulation with the Right HFB

The right high flow bypass (RHFB) scenario was simulated with both the 1991 and 1998 hydrographs, and the two cases are labeled as PM-SED-RHFB-91 and PM-SED-RHFB-98. The mesh generated for the scenario is shown in Figure 27. The bathymetry of the initial bed is displayed in Figure 28. The RHFB mesh has a total of 13,513 combined quadrilateral and triangular cells.

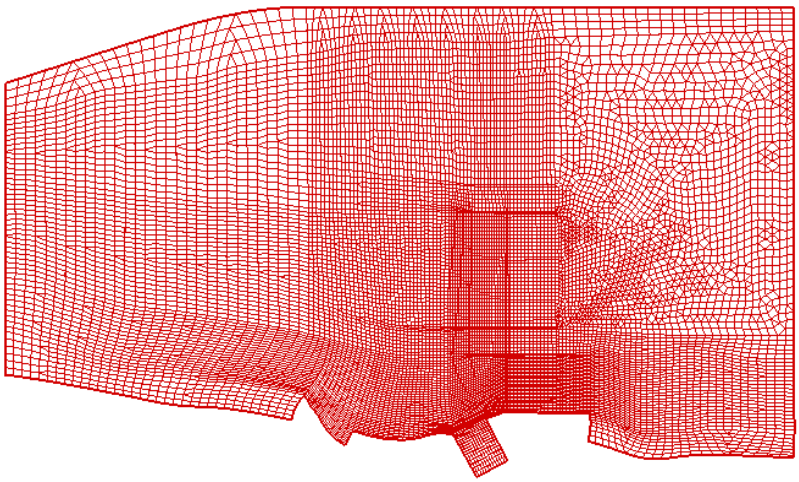

Figure 27. Mesh used for the RHFB scenario for the mobile-bed simulation of the physical model cases

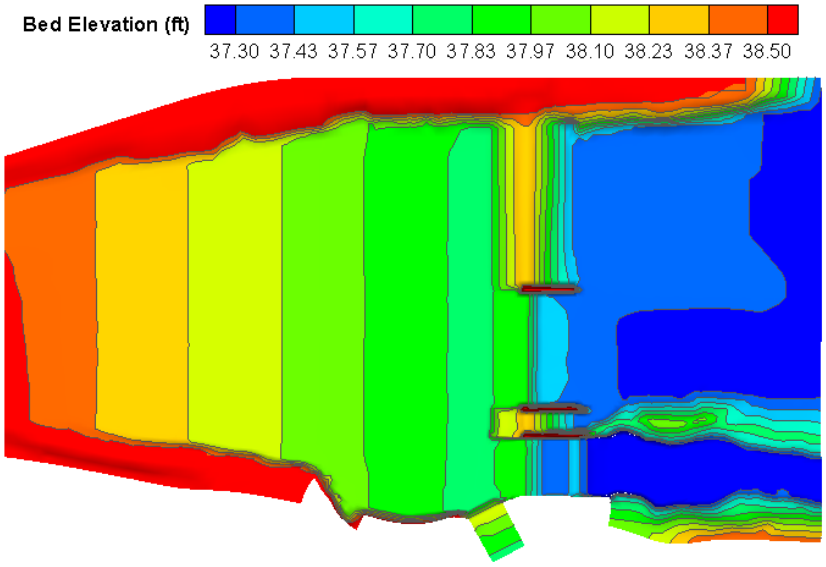

Figure 28. Bed elevation of the RHFB scenario for the mobile-bed simulation of the physical model cases

The gate operation was prescribed as follows. The diversion canal gates were open all the time with a flow capacity of 0.2795 cfs (500 cfs in the prototype). The high flow bypass has four gates and were numbered as 5 to 8 from right to left (looking downstream). The four HFB gates were divided into two groups: 5 and 8 gates as one group and 6 and 7 as another. The two gates within each group were operated the same way but each group may be operated independently. For case PM-SED-RHFB-91 (1991 hydrograph), the existing gates were closed all the time and the flow capacity for gates 5/8 and gates 6/7 were as shown in Figure 29. For case PM-SED-RHFB-98 (1998 hydrograph), gate operation of the existing gates and the HFB gates were specified as in Figure 30. The gate operation used by the numerical models followed the physical model tests as closely as possible. However, the operation during the falling limb of the hydrograph was not documented and there might be unknown differences between the physical model and numerical model.

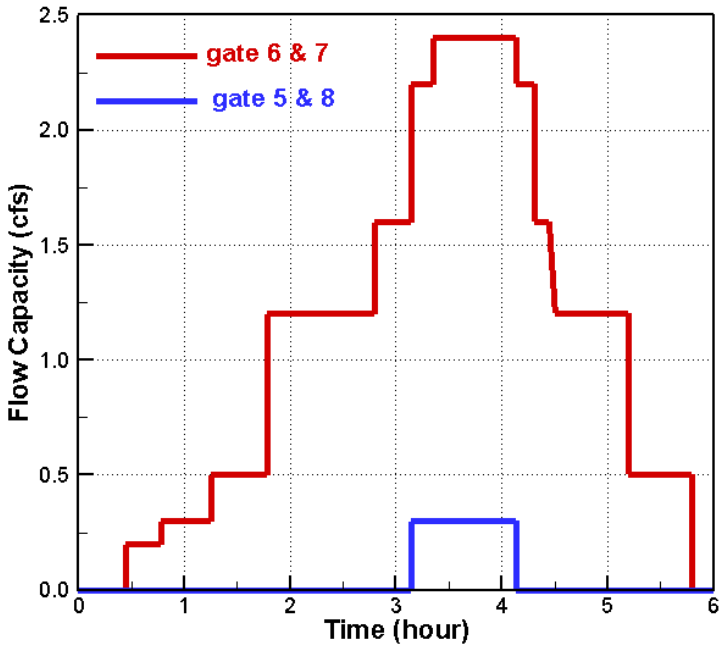

Figure 29. Gate operation capacity of the high flow bypass gates for the right HFB scenario for case PM-SED-RHFB-91 (1991 hydrograph)

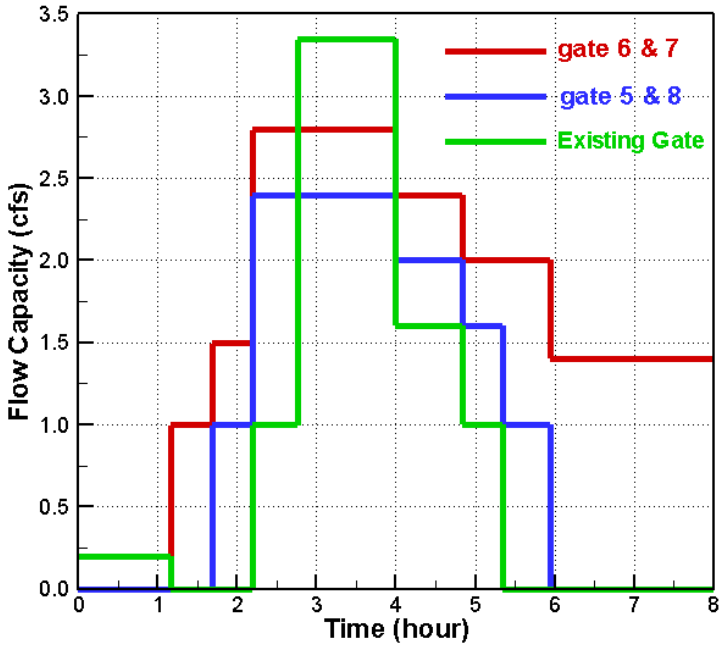

Figure 30. Gate operation capacity of the existing gates and the HFB gates for the right HFB scenario for case PM-SED-RHFB-98 (1998 hydrograph)

For case PM-SED-RHFB-91 (1991 hydrograph), the bed topography between the simulated and physical model results is compared in Figure 31 and Figure 32 at the end of the hydrograph (6 hours). The simulated bed form evolution in time is plotted in Figure 33.

The simulated final bed form is qualitatively in agreement with the physical model test. Particularly, the delta front reached the high flow bypass first for both the numerical and physical models. The main discrepancy was in the area upstream of the exiting gates. As discussed before it may be due to the difference in the gate operation during the falling limb of the hydrograph. The numerical model assumed that the existing gates were completely closed but non-negligible flow leaking was present at the existing gates during the physical model test.

Both models showed that the sediment delta has not reached the diversion canal gates. The result points to a decreased likelihood of bed load sediments being transported into the diversion canal.

(a) Photo taken at the end of the physical model test

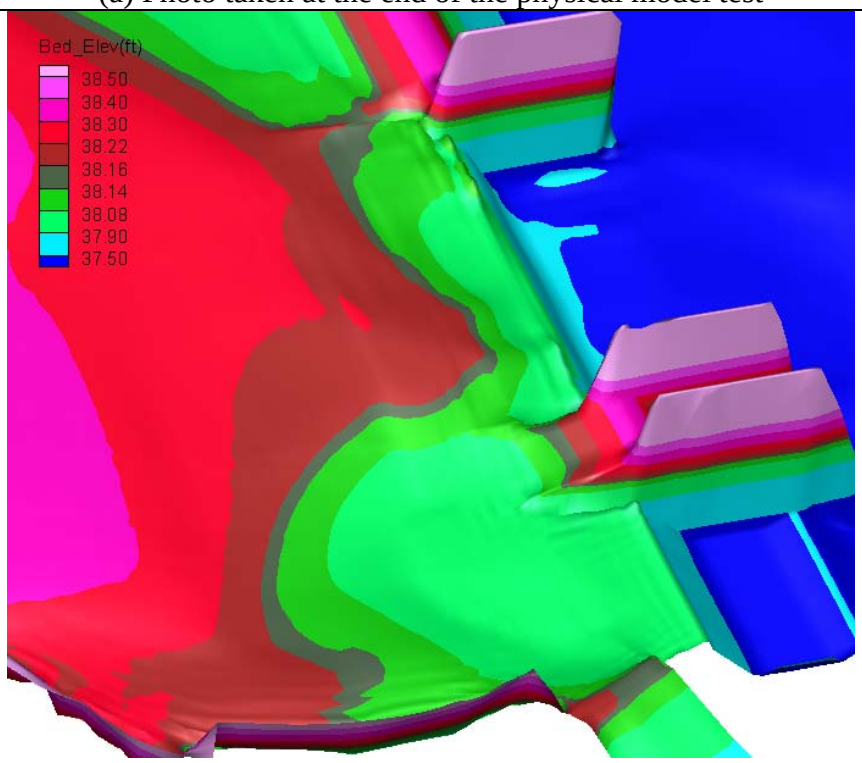

(b) Simulated bed elevation

Figure 31. Comparison of bed topography at the end of the hydrograph (6 hours) between the physical and numerical models for PM-SED-RHFB-91

(a) Photo taken at the end of the physical model test

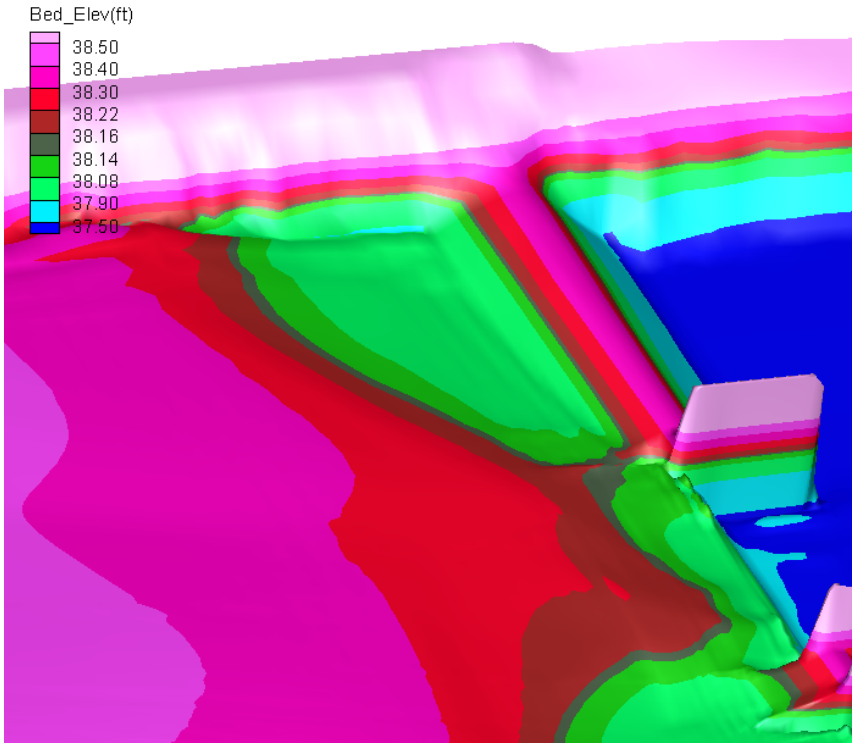

(b) Simulated bed elevation

Figure 32. Comparison of bed topography at the end of the hydrograph (6 hours) between the physical and numerical models PM-SED-RHFB-91

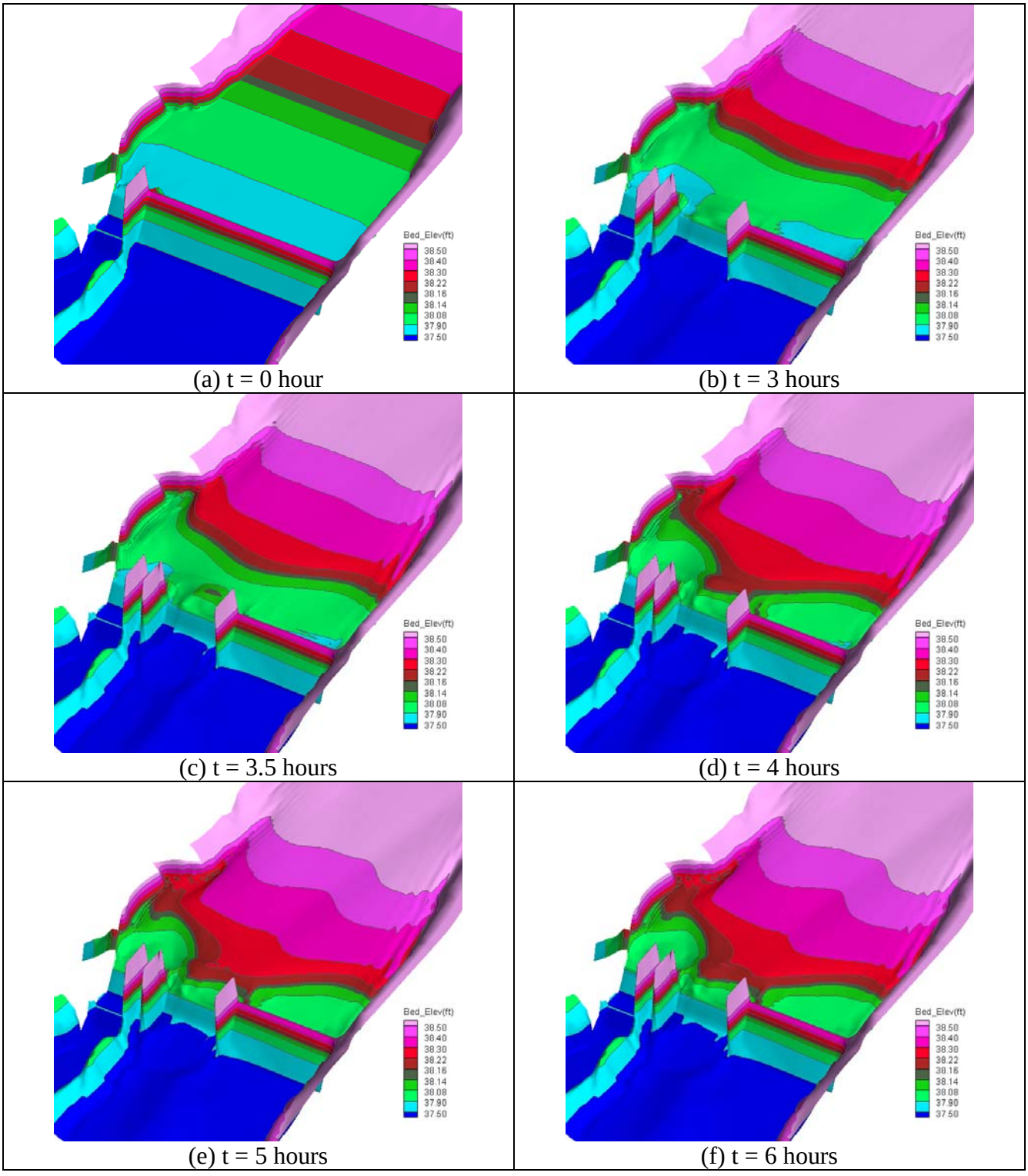

(a) t = 0 hour (b) t = 3 hours

(c) t = 3.5 hours (d) t = 4 hours

(e) t = 5 hours (f) t = 6 hours

Figure 33. Simulated bed form evolution in time for case PM-SED-RHFB-91 (1:4 vertical distortion)

For case PM-SED-RHFB-98 (1998 hydrograph), the bed topography between the physical and numerical model results is compared in Figure 34 at the end of the hydrograph (8 hours). The simulated bed form evolution in time is plotted in Figure 35.

It is seen that the model results were in qualitative agreement with the physical model results. The sediment delta has reached both the high flow bypass gates and the existing gates. However, the elevation of the delta was relatively low in comparison with the sill elevation of the diversion canal. Therefore, it can be concluded that there is much less likely that the bed load sediments will be transported to the diversion canal under the RHFB scenario. Both the PM-SED-RHFB-91 and PM-SED-RHFB-98 cases have much less deposition in front of the canal gates than the existing condition scenario.

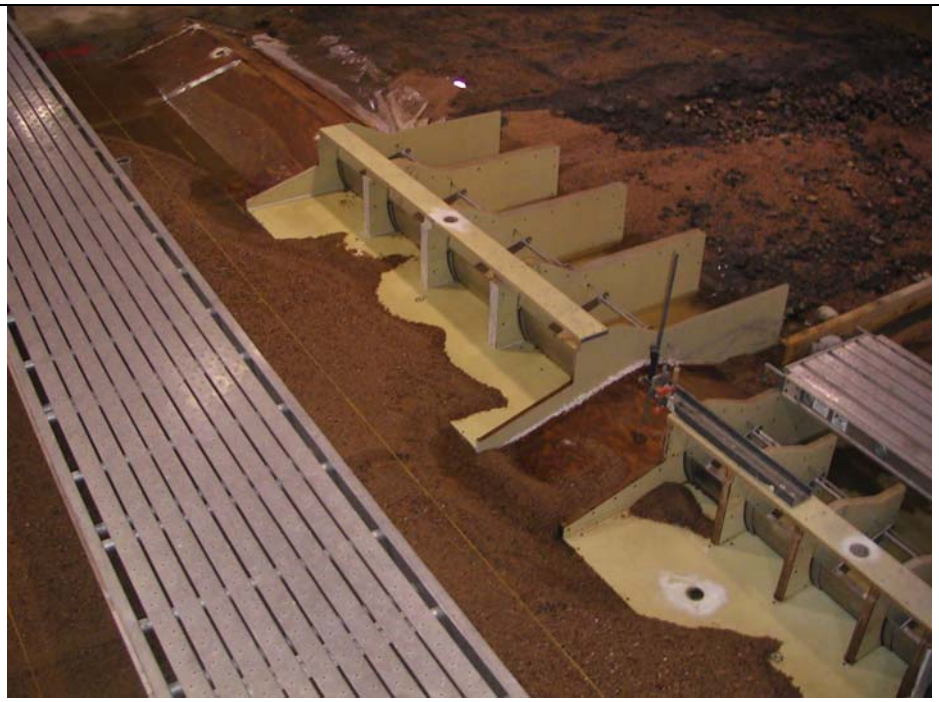

(a) Photo taken at the end of the physical model test

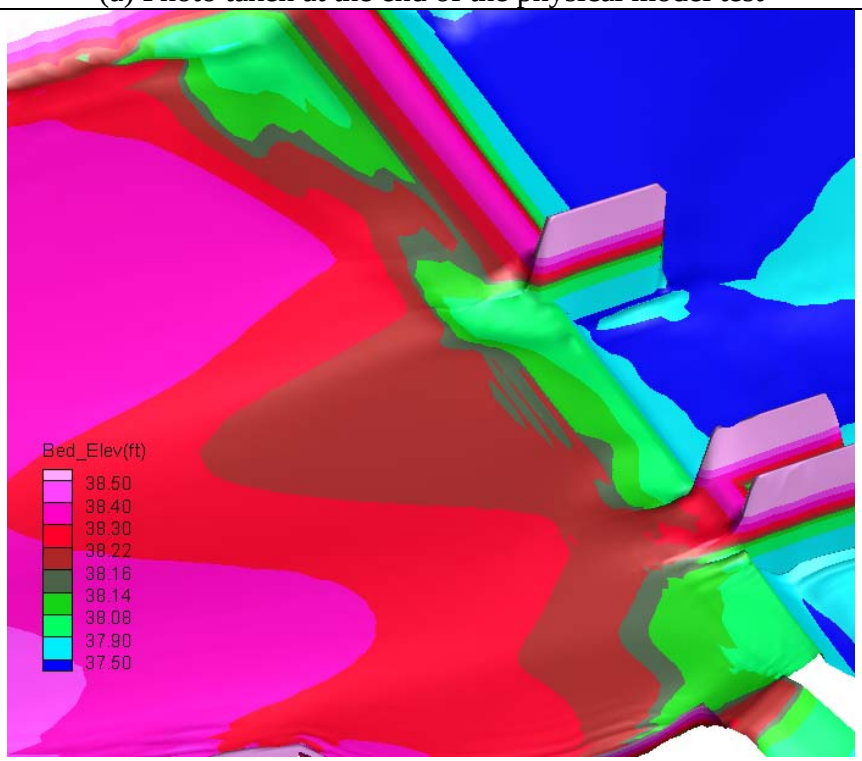

(b) Simulated bed elevation

Figure 34. Comparison of bed topography at the end of the hydrograph (8 hours) between the physical and numerical models for PM-SED-RHFB-98

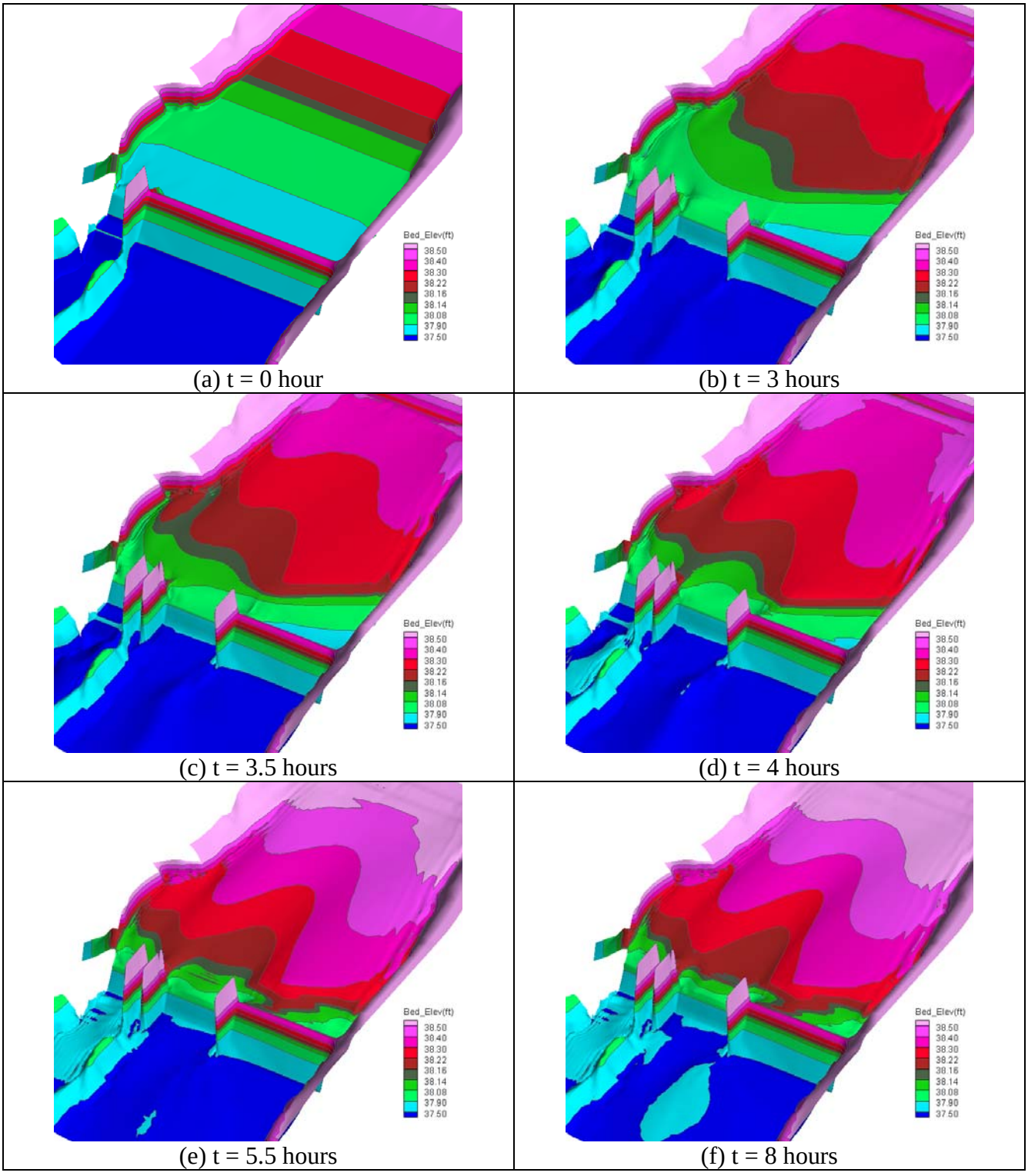

(a) t = 0 hour

(b) t = 3 hours

(c) t = 3.5 hours

(d) t = 4 hours

(e) t = 5.5 hours

(f) t = 8 hours

Figure 35. Simulated bed form evolution in time for case PM-SED-RHFB-98 (1:4 vertical distortion)

5.5. Sediment Results with the Left HFB Gate

The left high flow bypass (LHFB) scenario was simulated with both the 1991 and 1998 hydrographs and results are reported in this section. The mesh generated for the scenario is shown in Figure 36. The bathymetry of the initial bed is displayed in Figure 37. The LHFB mesh has a total of 14,417 combined quadrilateral and triangular cells.

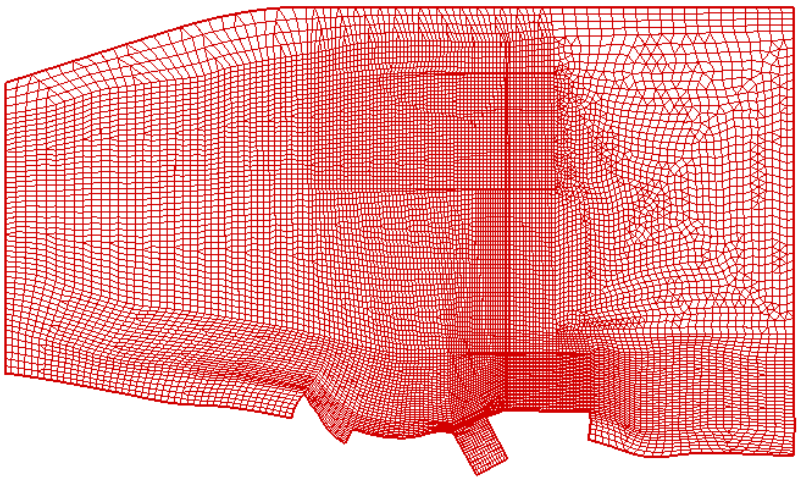

Figure 36. Mesh used for the LHFB scenario mobile-bed simulation of the physical model cases

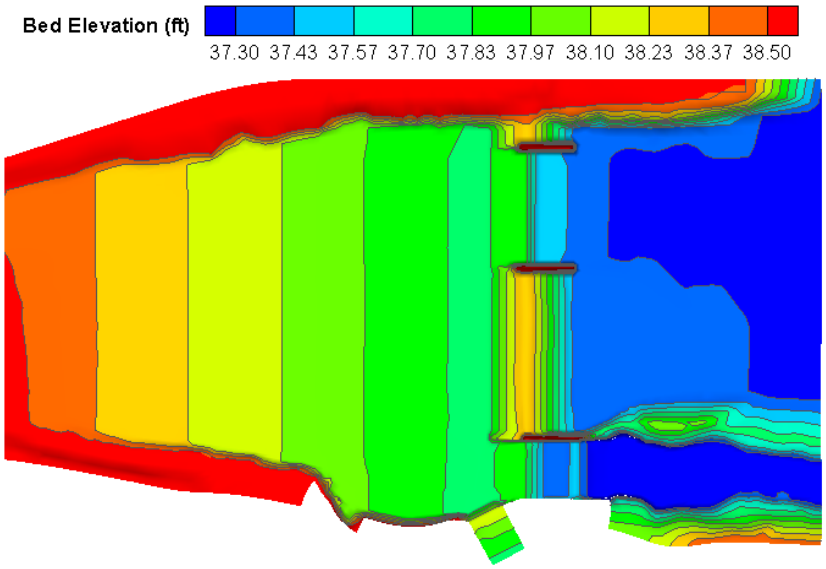

Figure 37. Bed elevation of the LHFB scenario for the mobile-bed simulation of the physical model cases

Two cases were simulated using the 1991 hydrograph and the 1998 hydrograph, and they are labeled as PM-SED-LHFB-91 and PM-SED-LHFB-98, respectively. The diversion canal gates were open all the time with a flow capacity of 0.2795 cfs (500 cfs in the prototype). For case PM-SED-LHFB-91 (1991 hydrograph), the existing gates were always open with a capacity of 0.25 cfs; the flow capacity for gates 5 and 8 and gates 6 and 7 are shown in Figure 38. For case PM-SED-LHFB-98 (1998 hydrograph), gate operation of the existing gates and the HFB gates are specified as in Figure 39. The gate operation used by the numerical model followed the physical model tests as closely as possible; but again, the operation during the falling limb of the hydrograph was not documented and was estimated.

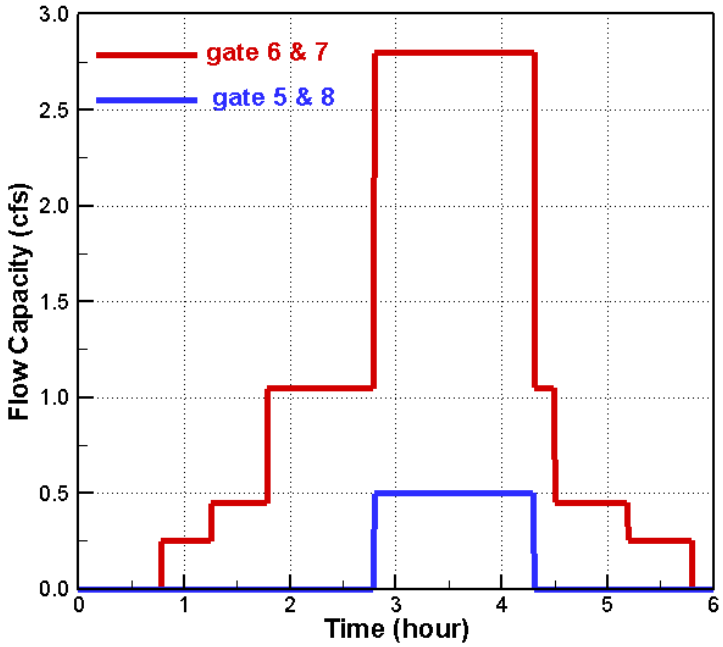

Figure 38. Gate operation capacity of the high flow bypass gates for case PM-SED-LHFB-91 (1991 hydrograph)

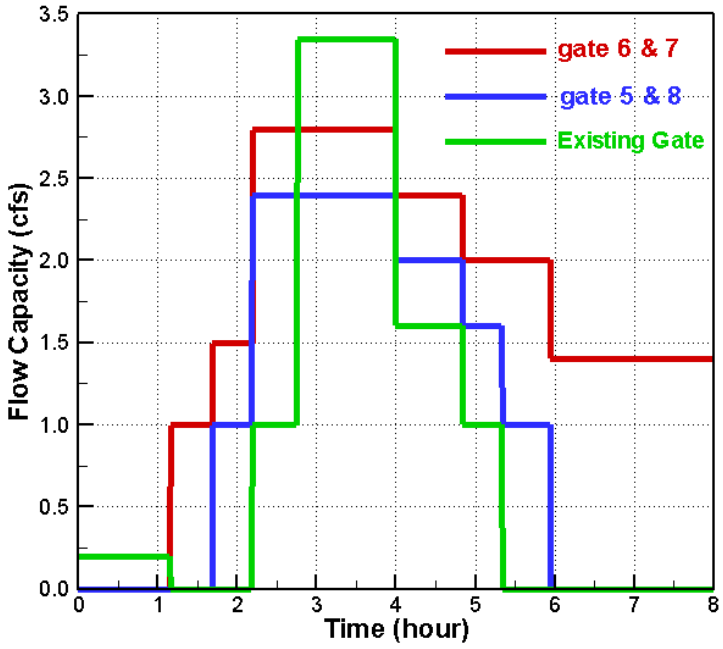

Figure 39. Gate operation capacity of the existing gates and the HFB gates for case PM-SED-LHFB-98 (1998 hydrograph)

For case PM-SED-LHFB-91 (1991 hydrograph), the bed topography between the physical and numerical model results is compared in Figure 40 at the end of the flow hydrograph (6 hours). The simulated bed form evolution in time is plotted in Figure 41.

The simulated final bed form is qualitatively in agreement with the physical model test. Both the numerical and physical models predicted that the delta front reached the high flow bypass on the left bank first, and front shape of the delta was in agreement with each other. It is seen that the delta did not reach the area in front of the diversion canal. The result points to a decreased likelihood of bed load sediments being transported into the canal.

(a) Photo taken at the end of the physical model test

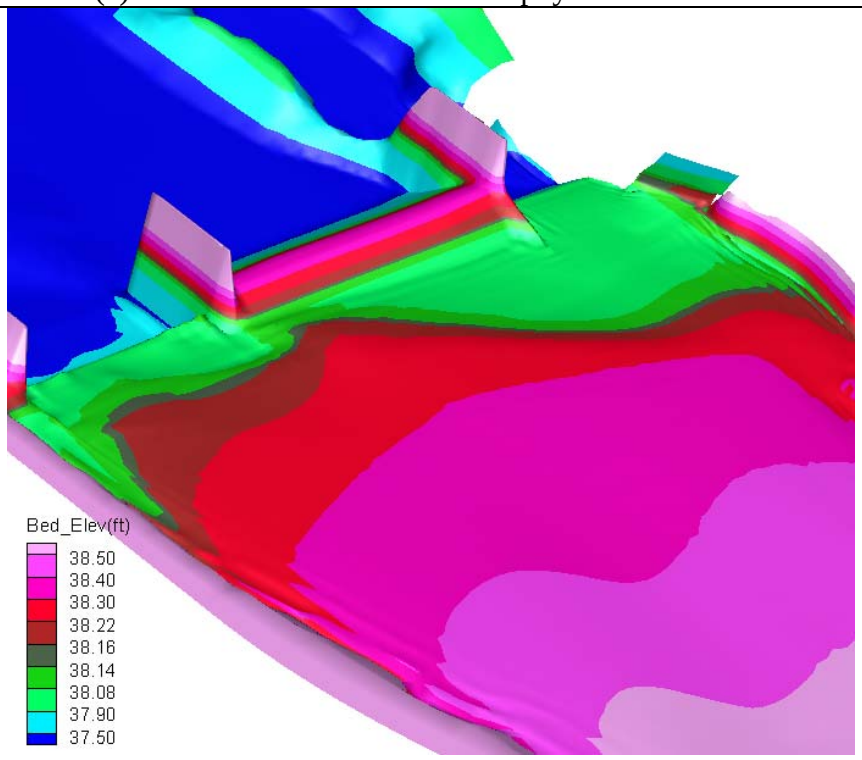

(b) Simulated bed elevation

Figure 40. Comparison of bed topography at the end of the hydrograph (6 hours) between the physical and numerical models for PM-SED-LHFB-91

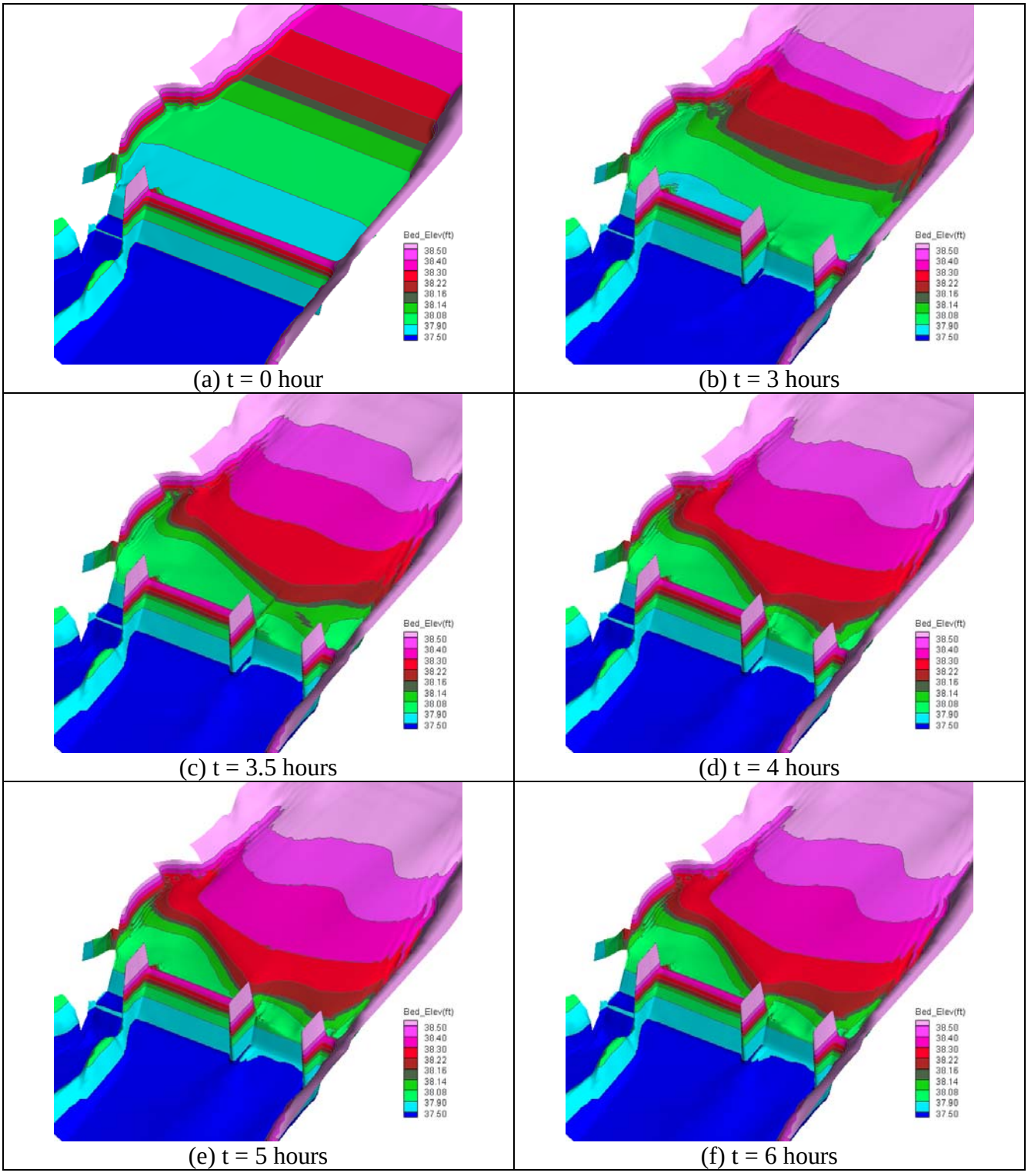

(a) t = 0 hour

(b) t = 3 hours

(c) t = 3.5 hours

(d) t = 4 hours

(e) t = 5 hours

(f) t = 6 hours

Figure 41. Simulated bed evolution in time for case PM-SED-LHFB-91 (1:4 vertical distortion)

For case PM-SED-LHFB-98 (1998 hydrograph), the bed topography between the physical and numerical models is compared in Figure 42 at the end of the flow hydrograph (8 hours). The simulated bed form evolution in time is plotted in Figure 43.

It is seen that the model results were in qualitative agreement with the physical model results. The delta has reached both the high flow bypass gates and the existing gates.

(a) Photo taken at the end of the physical model test

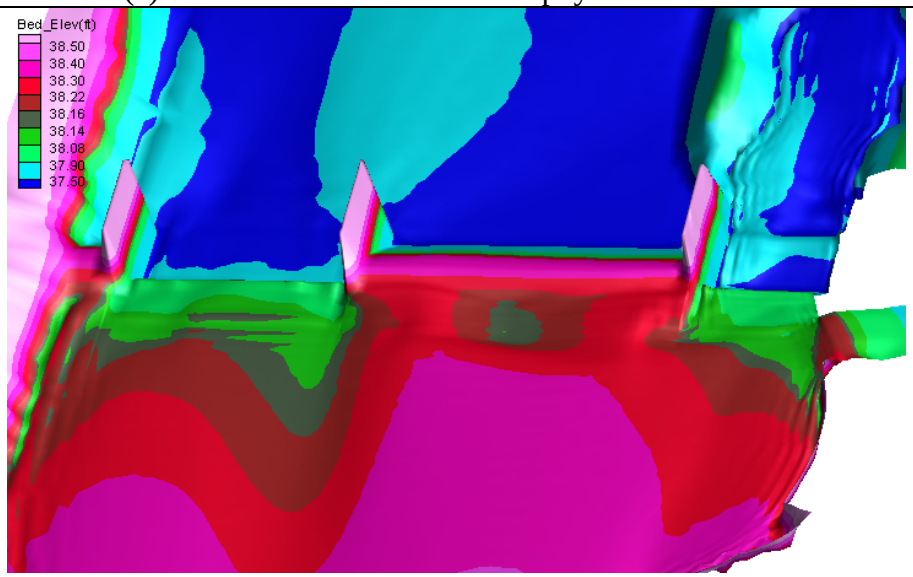

(b) Simulated bed elevation

Figure 42. Comparison of bed topography at the end of hydrograph (8 hours) between the physical and numerical models for PM-SED-LHFB-98

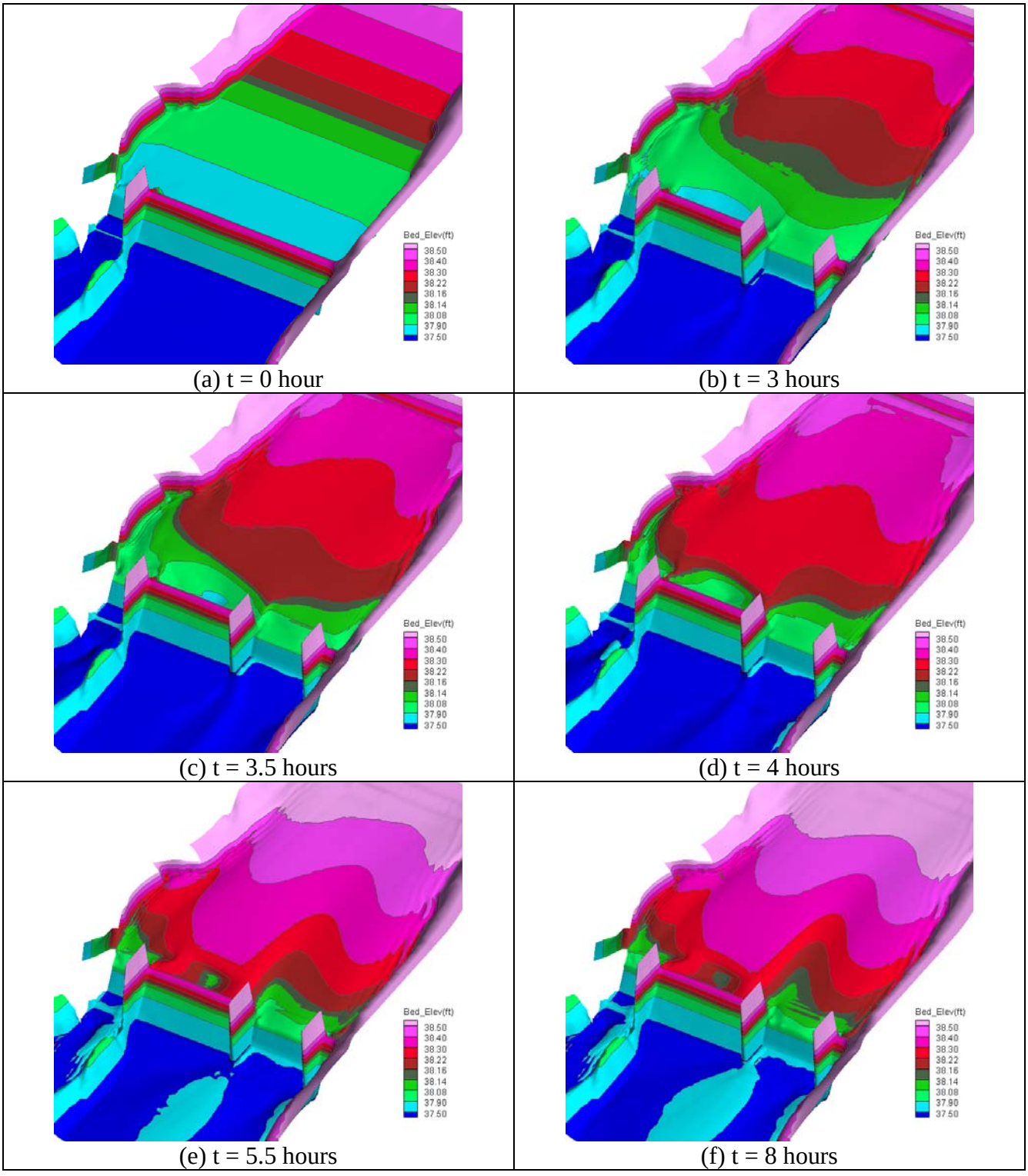

(a) t = 0 hour (b) t = 3 hours

(c) t = 3.5 hours (d) t = 4 hours

(e) t = 5.5 hours (f) t = 8 hours

Figure 43. Simulated bed evolution in time for case PM-SED-LHFB-98 (1:4 vertical distortion)

6.0 Field Model Scenarios

Modeling of field scenarios consisted of two categories: the calibration study with the field flows and the mobile bed simulations. In this Chapter, the calibration results were presented first and the field model results are then discussed.

6.1. Calibration with Field Flow Cases

Two field flow simulations were performed and compared with the available flow data. They served as the calibration study to ensure the adequacy of the numerical model and the selection of the Manning's roughness coefficient. One simulation was carried out for the 12,400 cfs flood which occurred in 2005 (7,400 cfs was from Matilija Creek and 5,000 cfs was from North Fork). High water marks were surveyed in 2005 after the flood and two high water mark survey points were located within the solution domain. The second calibration simulation was carried out for the 100 year flood (27,100 cfs) so that a comparison may be made with the previous 1D models. The results of the two cases are reported below.

6.1.1. 2005 Flood Flow

In 2005 a flood with a peak flow of about 12,400 cfs occurred, and this flow was simulated with the SRH-2D model. A constant flow discharge of 12,400 cfs was imposed at the upstream boundary while the water surface elevation at the downstream boundary, cross-section RM 12.7841, was 663.2 ft based on the 1D model result. Also, the flow through the existing gate at the Robles diversion dam was calculated to be 8,540 cfs if the flow through the gate was assumed to be fully open channel flow (versus pressurized flow). It is known that the design capacity of the existing gates is about 7,000 cfs, and the above open channel gate flow assumption cannot be right. Therefore, special boundary treatment was applied at the gate so that only 7,000 cfs was allowed to pass through the gates. In addition, it was assumed that 500 cfs was diverted into the canal upstream of the gate which leaves 11,900 cfs to be passed downstream.

A comparison of the simulated water surface elevation and surveyed high water marks at two survey points is shown in Table 6. The difference between the simulation and survey is 0.22 ft and 0.36 ft, respectively, for the two survey points. It is seen that the numerical model compares well with the surveyed data.

Table 6. Comparison of simulated and surveyed water elevation at two points

High Water Mark Point	Northing Coordinate (ft)	Easting Coordinate (ft)	Surveyed Elevation (feet)	Simulated Elevation (feet)
#1	1991570.69	6172432.59	724.04	724.26
#2	1991939.71	6172523.82	728.82	729.18

6.1.2. 100 Year Flood

The model was next applied to compute the 100 year flood. A discharge of 27,100 cfs was imposed at the upstream boundary, and a water surface elevation of 665.2 ft, from the 1D model, was applied at the downstream exit boundary. Similarly, 7,000 cfs was passing though the existing gate at the Robles diversion dam and 500 cfs was diverted to the canal. The simulated water surface elevation along the main channel thalweg is compared with the HEC-RAS model in Figure 44. Note that the water surface elevation from the HEC-RAS model is the cross section averaged value.

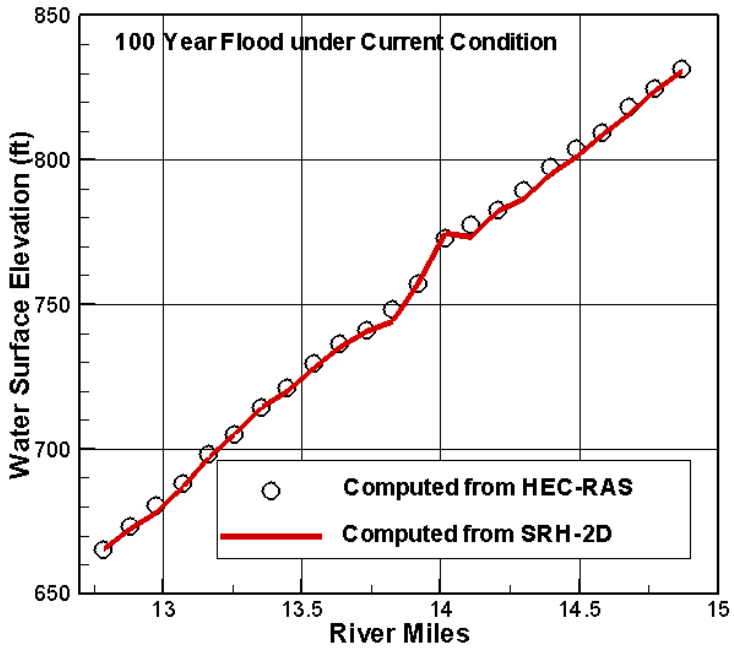

Figure 44. Comparison of the water surface elevation (WSE) from SRH-2D and HEC-RAS; SRH-2D represents the WSE along the channel thalweg, and HRC-RAS is cross section averaged WSE.

6.2. Flow Simulation Results at Other Discharges

Three more flow discharges, 24,000 cfs, 15,000 cfs, and 6,000 cfs, were simulated to provide the flow data for the physical model portion of the project. Major parameters are summarized in Table 7. Note that 500 cfs was diverted to the canal for all three cases.

Table 7. Flow parameters for the three simulations

Discharge (cfs)	24,000	15,000	6,000
WSE at exit (ft)	664.80	663.70	661.65
Flow at the existing gate (cfs)	7,000	7,000	5,381

Simulated results are shown from Figure 45 to Figure 50.

Figure 45 and Figure 47 display the simulated water depth near the Robles diversion dam, Figure 48 and Figure 49 show the predicted water surface elevation at two cross sections: 14.2045 RM and 13.9205 RM, and the velocity distribution is plotted in Figure 50 for three flows. All these results were used to decide the boundary conditions for the physical model study.

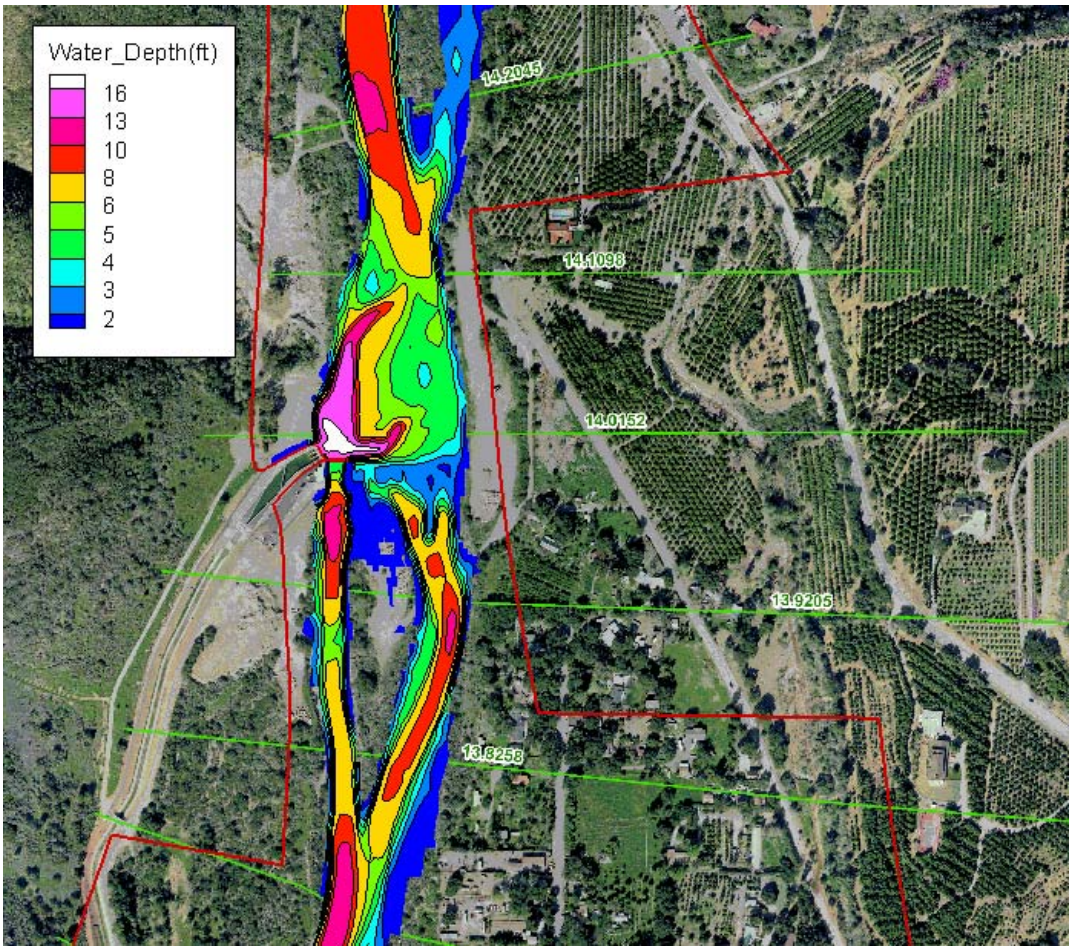

Figure 45. Simulated water depth for the 24,000 cfs flow discharge in the Robles dam area.

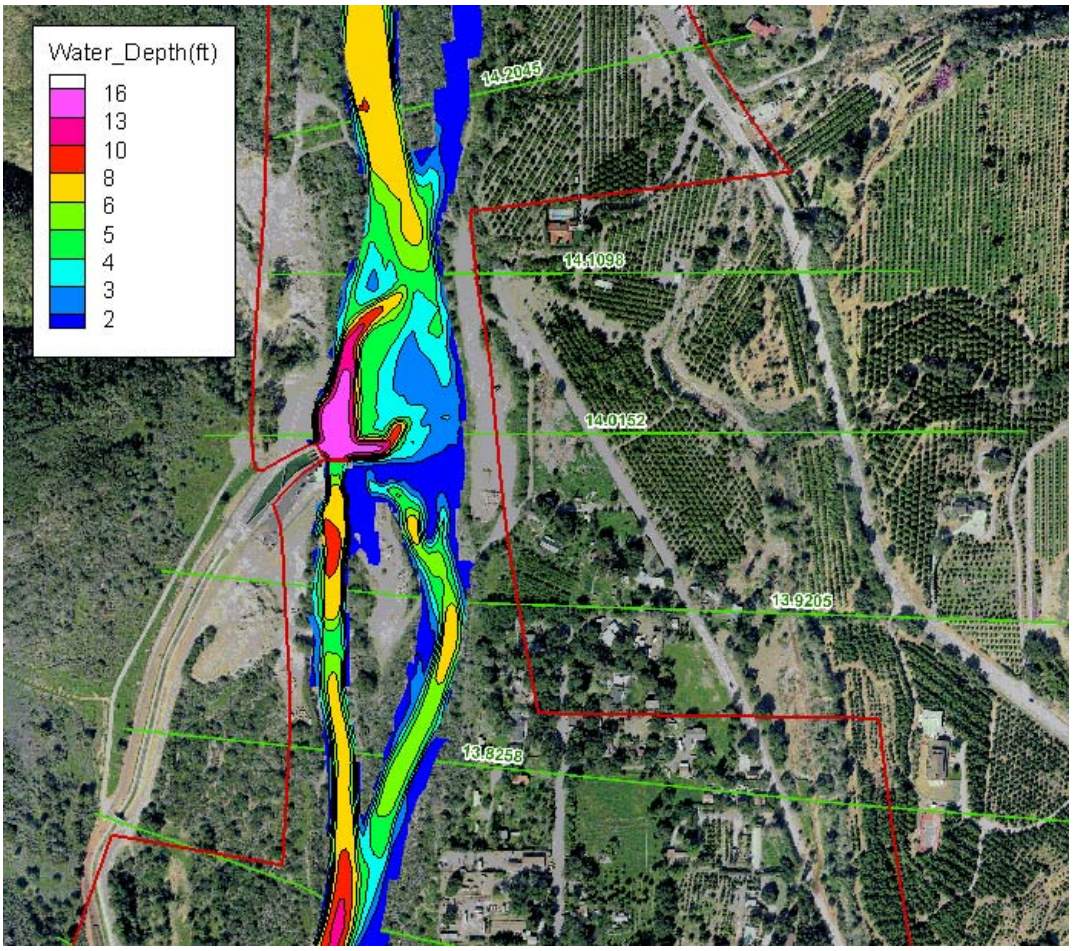

Figure 46. Simulated water depth for the 15,000 cfs flow discharge in the Robles dam area.

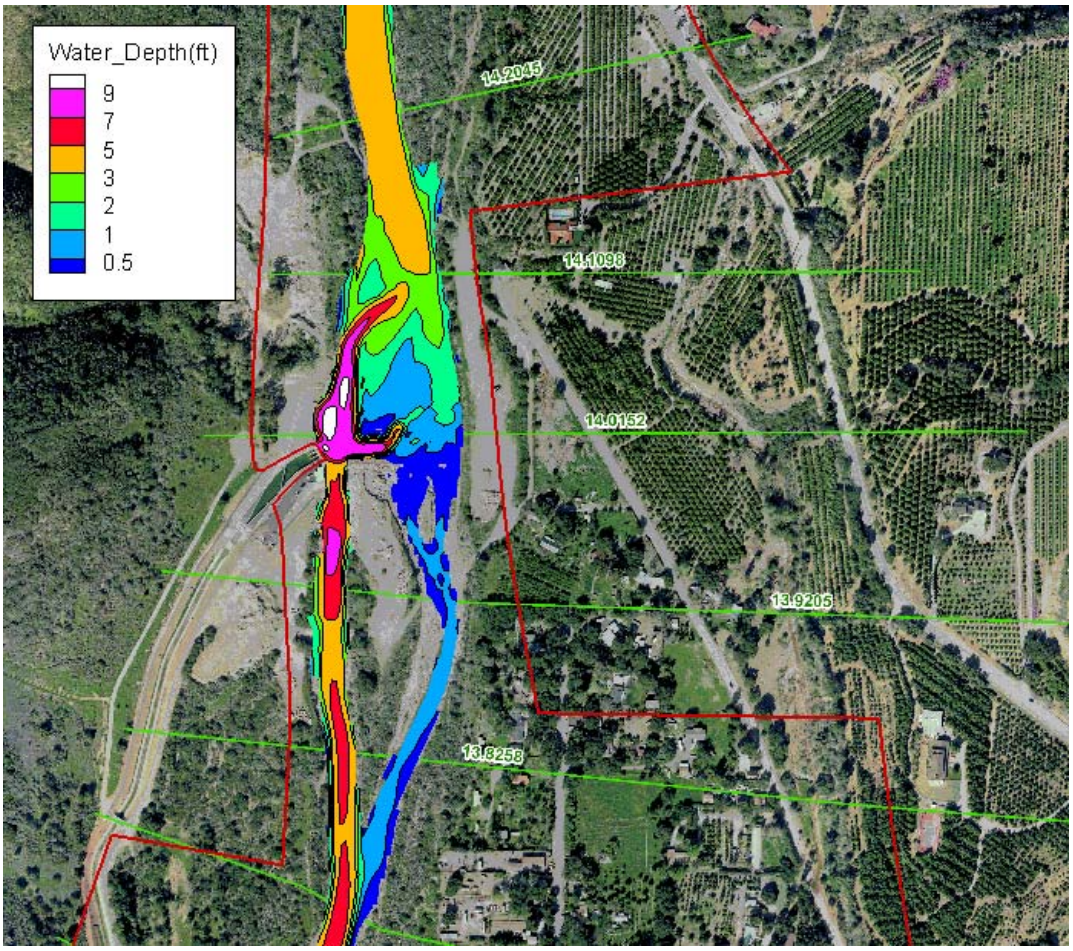

Figure 47. Simulated water depth for the 6,000 cfs flow discharge in the Robles dam area.

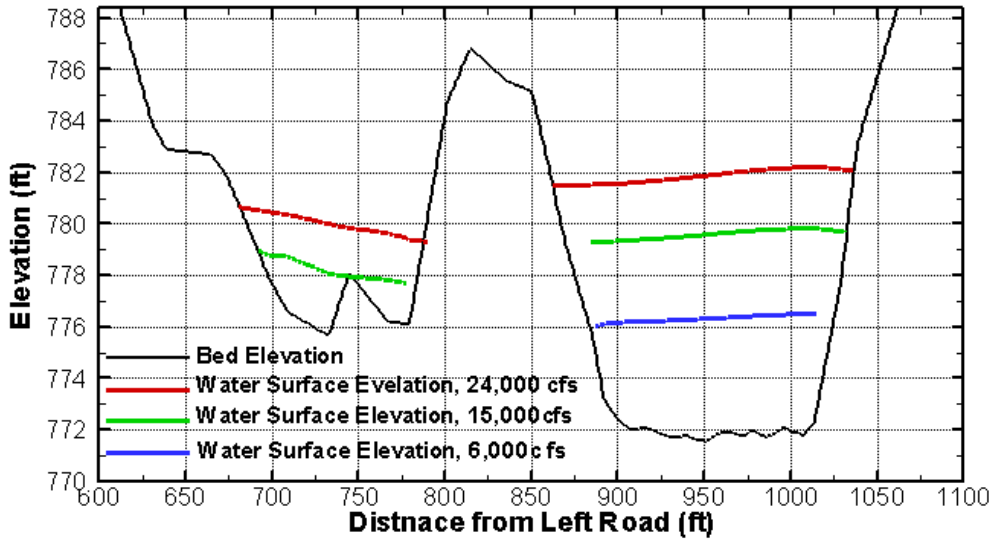

Figure 48. Simulated water surface elevation at cross section 14.2045 for three discharges; Distance is measured from the middle of road on the left side of the river (looking downstream).

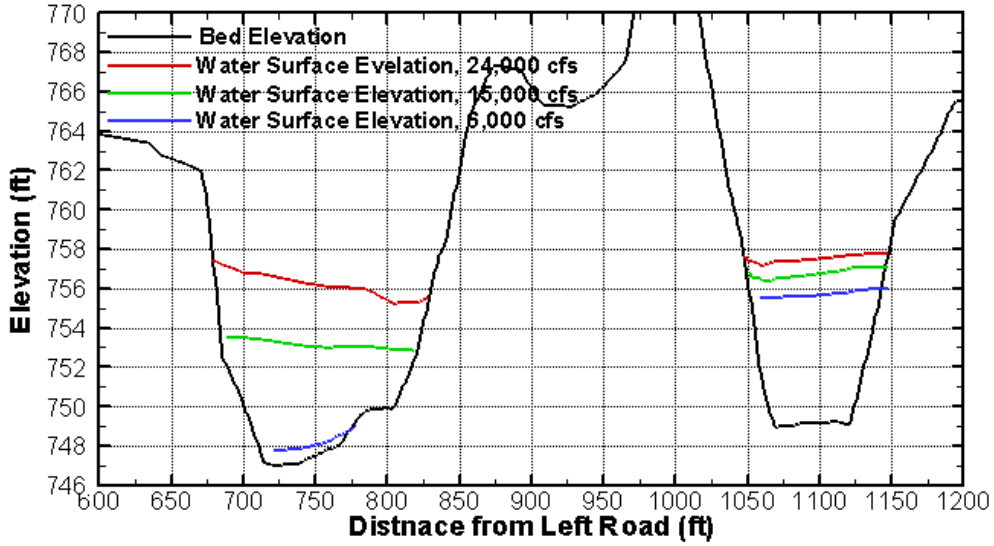

Figure 49. Simulated water surface elevation at cross section 13.9205 for three discharges; Distance is measured from the middle of road on the left side of the river (looking downstream).

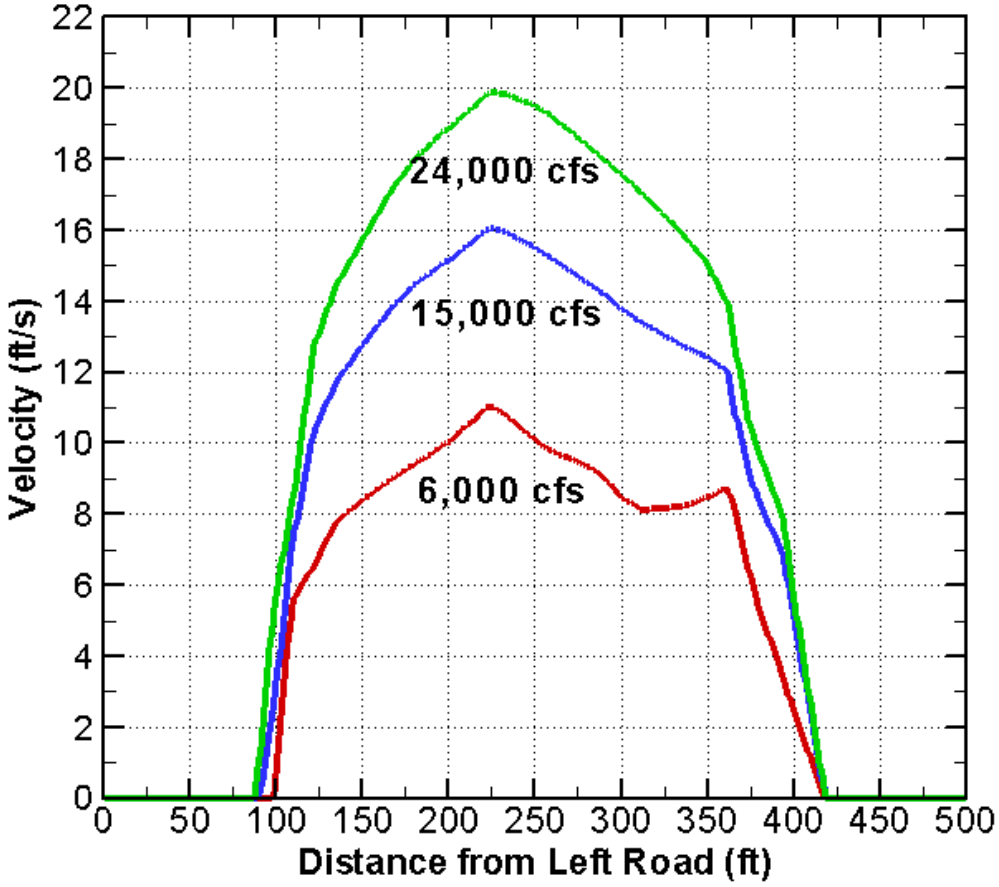

Figure 50. Computed velocity distribution at cross section 14.1089 RM.

6.3. Mobile-Bed Model Inputs

Three topographic scenarios, the existing, the right high flow bypass (RHFB), and the left high flow bypass (LHFB) were modeled. For each scenario, two flow hydrographs, 1991 and 1998 hydrographs as discussed in Chapter 3, were used. There were also two inlet sediment load conditions: before-dam and after-dam removal (see discussion in Chapter 3). Most simulations were carried out for the after-dam removal sediment input and a few used the before-dam removal sediment input.

The topography was based on the March 2005 LiDAR data as discussed in Chapter 3. For the mobile-bed simulations, the bathymetry upstream of the Robles diversion weir was modified through “excavation” since the 2005 survey showed that the dam was almost filled upstream of the weir. This way the simulation

would reveal how the area upstream of the dam would be filled again after excavation.

The excavation was performed as follows. An area between the weir and the cross section RM 14.1098, shown in Figure 51 as a red box, was excavated to create a constant slope. At the face of the weir, approximately 10 feet of material was removed in order to make the elevation equal to 757.8 ft, the sill elevation of the existing radial gate. If the bed elevation at the cross section RM 14.1098 remains the same, a constant slope of about 1.6% was created. The total excavated sediment volume was estimated to be about 20,000 cubic yards excluding the voids and 33,000 cubic yards including the voids. Periodic excavation at the Robles Diversion was performed after a major flood and a record of the sediment removal was tabulated in the report of Greimann (2004) and was reproduced in Table 8.

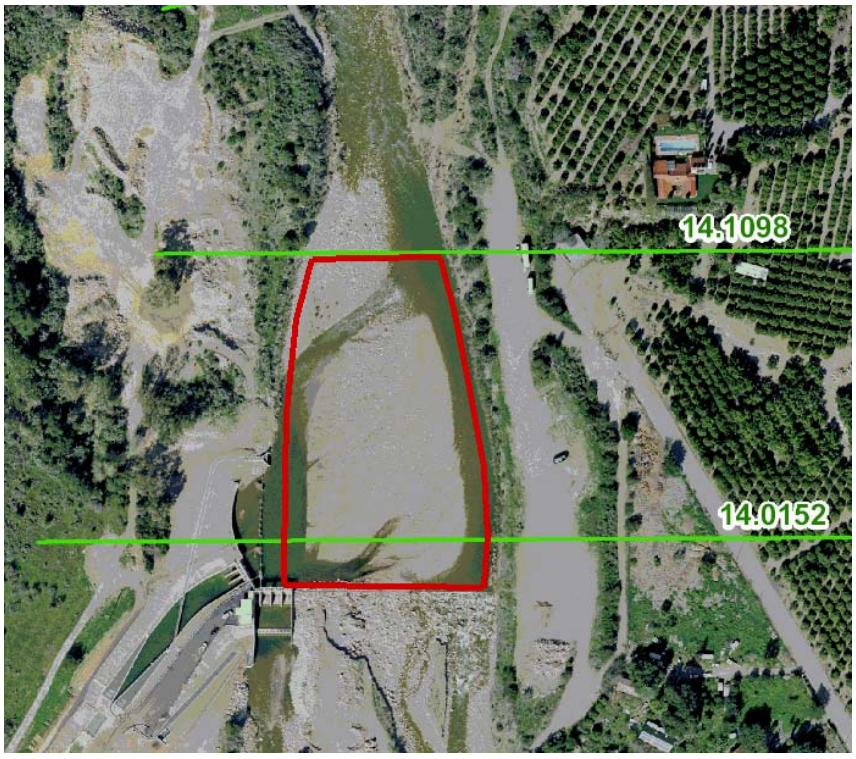

Figure 51. Excavation area, shown in red box, for the mobile-bed simulation

Three topographic scenarios were developed using the excavated bathymetry and they are compared in Figure 52. Some characteristic bed elevations are as follows: the sill elevation at the existing gate is 757.8 ft; the sill elevation of the canal diversion gate is 762.7 ft; the top elevation of the weir is about 767.5 ft; the width of the high flow bypass is 131.25 ft. Note that the geometry did not include the small features added later such as the fish way, etc.

Three corresponding meshes are displayed in Figure 53 and only the portion of the mesh near the Robles dam is shown. The total number of hybrid quadrilateral and triangular mesh cells is 12,184, 13,373, and 14,050 cells, respectively for the existing, RHFB, and LHFB scenarios.

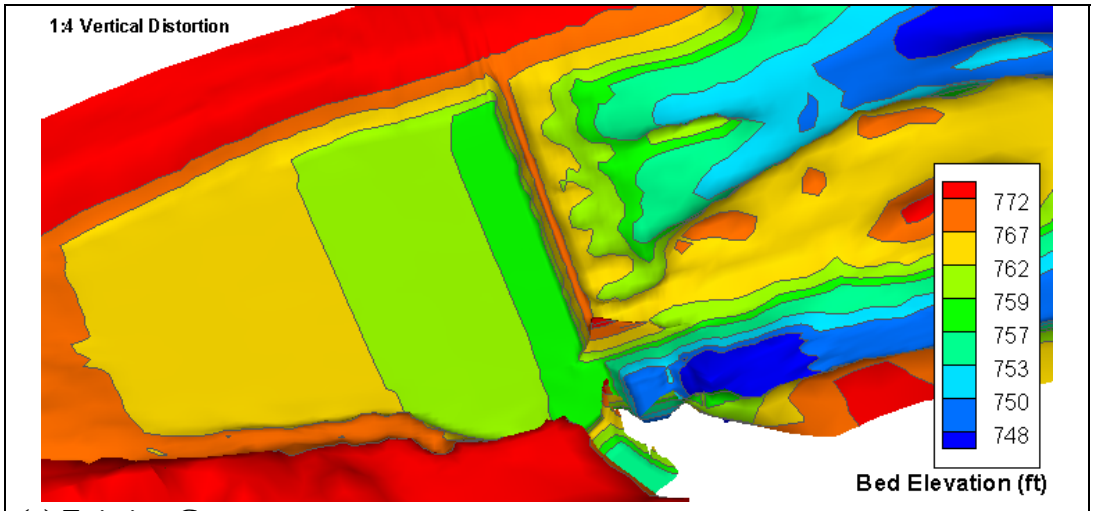

(a) Existing Gate

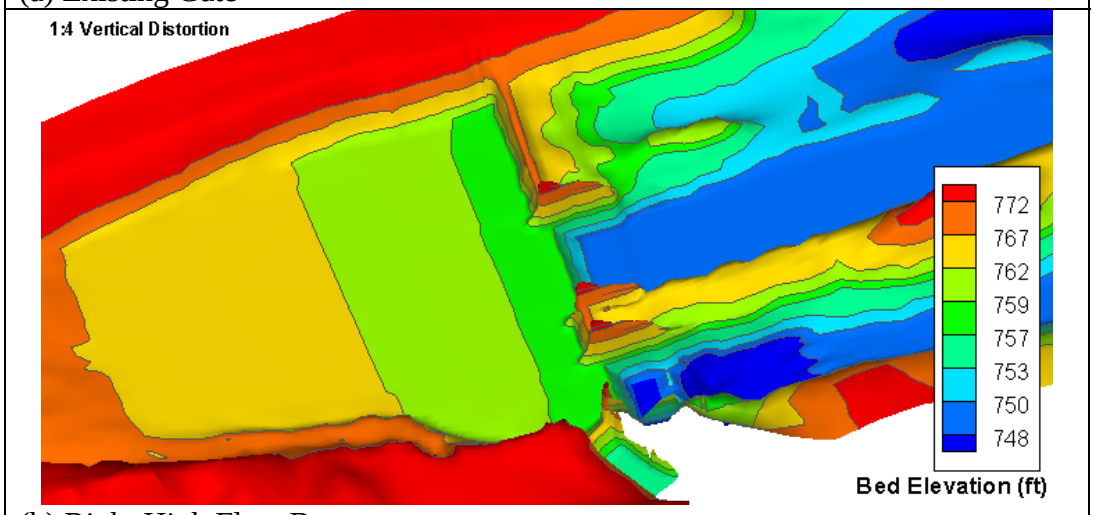

(b) Right High Flow Bypass

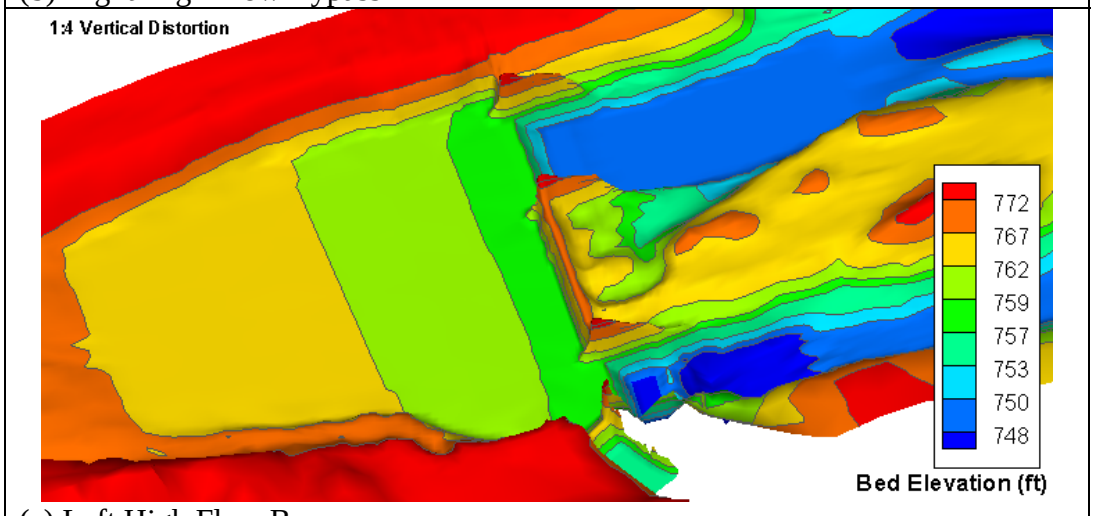

(c) Left High Flow Bypass

Figure 52. Perspective view of the three topographic scenarios

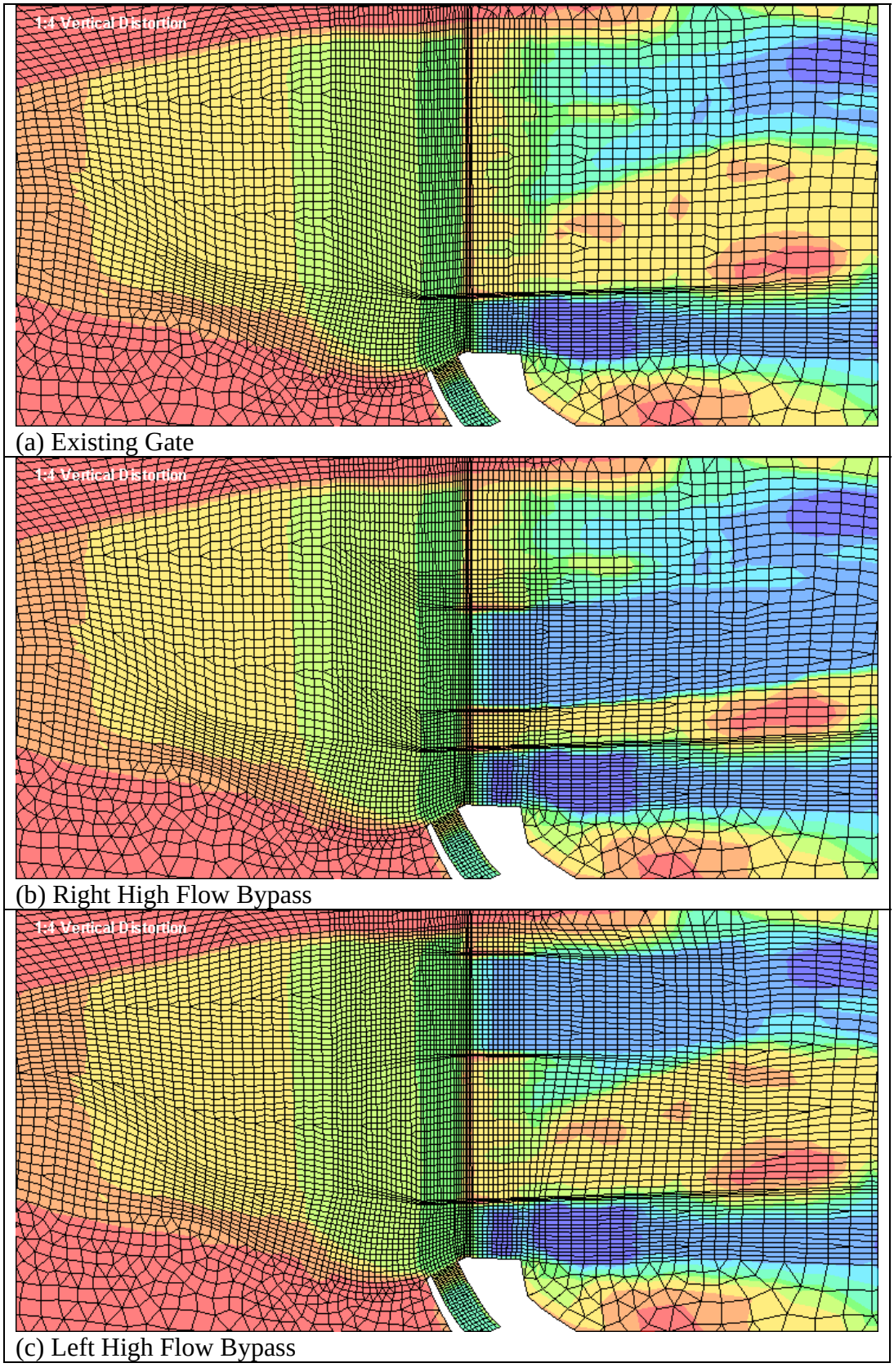

(a) Existing Gate

(b) Right High Flow Bypass

(c) Left High Flow Bypass

Figure 53. Zoom-in view of the meshes for the three topographical scenarios

Gate operation needs to be specified for both the existing radial gates and the new high flow bypass gates (HFB). For the field modeling reported below, gate operation was incorporated by specifying the flow capacity (the maximum discharge allowed) for each gate structure. If the actual flow through the gate structure is below the capacity, regular open channel flow is assumed; but if the flow is above the capacity, it is limited to the capacity and the pressurized flow is assumed. Figure 54 shows the capacity used for the existing gates under the existing condition and the high flow bypass (HFB) scenarios and the capacity for the HFB gates.

Under the existing condition scenario, the operation of the existing gates is different for the two hydrographs. With the 1991 hydrograph, the gates were open to a capacity of 100 cfs for the first 64.5 hours and were fully open (6,000 cfs capacity) afterwards. With the 1998 hydrograph, the existing gates were open to a capacity of 200 cfs for the first 27.5 hours. They were fully open (6,000 cfs capacity) from 27.5 to 80.0 hours. After 80 hours, the gate capacity was gradually reduced. The capacity remained at 300 cfs from 160 to 200 hours. The existing gate capacity for the existing condition scenario is shown in Figure 54.

Under the high flow bypass (HFB) scenarios, the same gate operations were used for the 1991 and 1998 hydrographs. The existing gates were closed except for the period of 55.7 to 65 hours during which the capacity was set at 6,000 cfs. The high flow bypass (HFB) gates started to open at 27 hours with a capacity of 600 cfs. HFB gates were fully open from 52.3 to 91 hours with a capacity of 10,000 cfs and back to 600 cfs capacity from 91 to 200 hours.

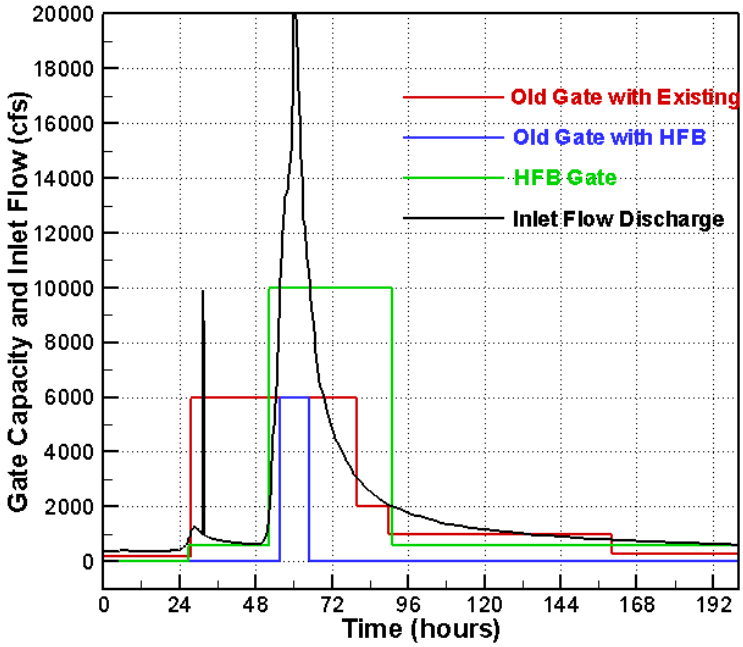

Figure 54. Gate capacity versus time for the existing and HFB gates for the field modeling; the 1998 hydrograph is also shown as a reference

6.4. Qualitative Comparison of Results under the Existing Condition

Numerical model results were examined for the existing condition scenario with the before-dam removal sediment inputs. A comparison of the net deposited depth after 200 hours for the 1991 and 1998 hydrographs is shown in Figure 55. Note that the deposition depth reported in this study refers to the sediment depth including the voids (porosity) while the sediment volume reported is without the voids unless it is explicitly stated otherwise.

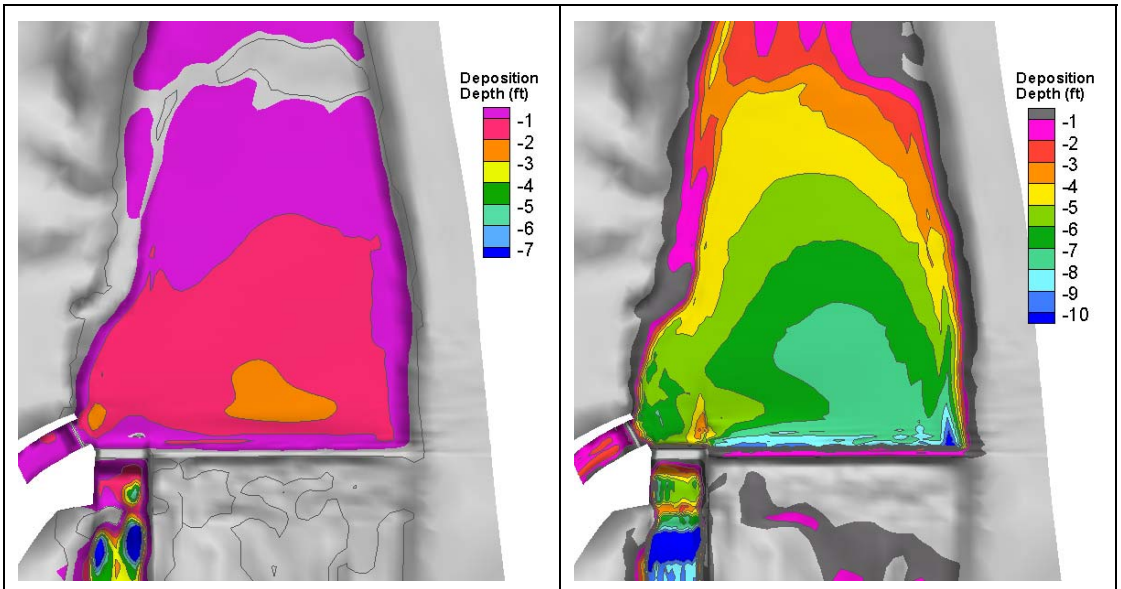

(a) 1991 Hydrograph **(b) 1998 Hydrograph**

Figure 55. A comparison of the deposition depth after 200 hours between the 1991 hydrograph and 1998 hydrograph for the existing condition with the before-dam removal sediment input

The model predicted that the average deposition depth in front of the diversion weir, after 200 hours, was about 2.0 ft and 7.0 ft, respectively, for the 1991 and 1998 hydrographs. It showed that a flood with the magnitude of 1991 hydrograph would not cause serious sedimentation problem at the diversion canal. However, with the 1998 flood, the deposition in front of the canal gates would be high enough that there would be a risk of bedload sediments being transported into the diversion canal.

With the 1991 hydrograph, it was estimated that a total of 34,190 yd^3 of sediments (excluding voids) was moving through the cross section RM 14.1098, and about 4,130 yd^3 of sediments were deposited behind the Robles diversion weir. In contrast, with the 1998 hydrograph, about 205,500 yd^3 of sediments (excluding voids) were moving through RM 14.1098 and about 21,900 yd^3 of sediments were deposited behind the weir.

The model results indicated that a flood similar to the 1998 event (near 15-year flood) would move a majority of the sediments towards the diversion dam and fill the area upstream of the weir almost completely even if excavation had been done before the flood. The result is in agreement with the field observation that significant sediment deposition occurred after each major flood and sediment removal was often necessary. A record of sediment removal from 1966 to 1998 was shown in Table 8 and a total of 419,000 yd^3 of sediments (including the voids) was removed in the period from 1966 to 1998. Each removal was about 46,000 yd^3 (including the voids) on average. The simulation estimated that sediment deposition between the weir and RM 14.1098 (Figure 51) is 21,900 yd^3

without the voids, which is equivalent of 36,500 yd^3 with the voids. This amount is in agreement with the recorded sediment removal of 35,000 yd^3 in 1998. For 1991, the simulated deposition is about 8,300 yd^3 (including the voids) which was much less than the reported removal of 20,000 yd^3 in 1991. Several possibilities might contribute to this discrepancy. For one, the modeling assumed that the gate was fully open during the flood which would maximize the sediment sluicing through the gates. Another possibility may be that the reported removal was the result of accumulated sediment depositions for the period of 1987 to 1991.

Table 8. Record of sediment removal at Robles Diversion Dam

Year	Amount of Sediment Removal (yd^3)
1966	30,000
1969	N/A
1973	50,000
1978	91,000
1980	71,000
1983	57,000
1986	30,000
1991	20,000
1993	N/A
1995	35,000
1998	35,000

The simulated flow velocity and topographic pattern for the 1998 hydrograph and before-dam removal scenario are shown in Figure 56 at the end of the flood (200 hours). The results may be compared with the aerial photo which represents typical flow pattern upstream of the Robles Diversion Dam. It is seen that the predicted flow pattern at low flow after major floods is qualitatively in agreement with the field observation.

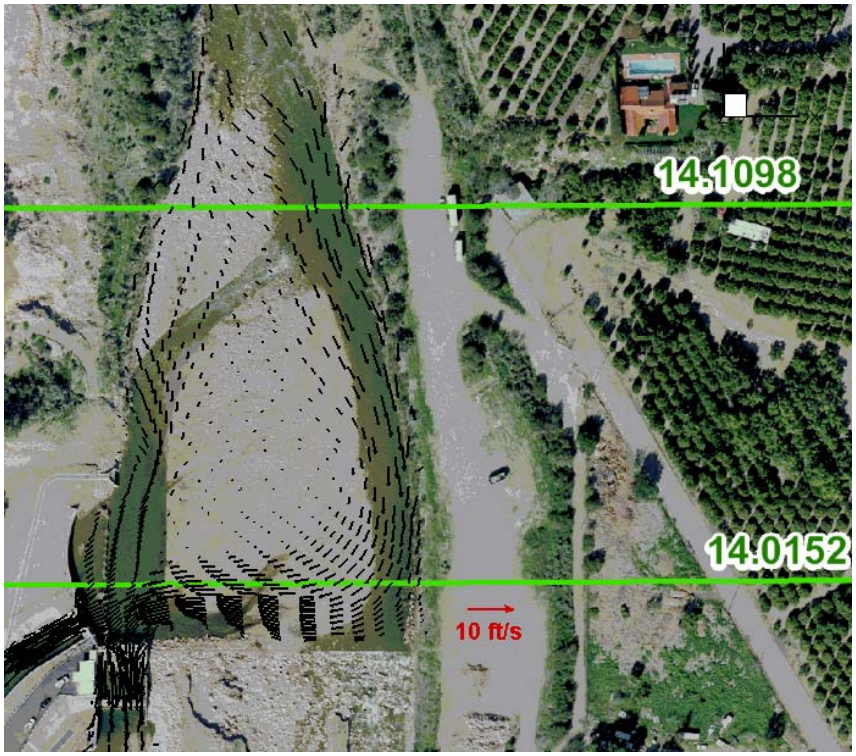

Figure 56. Simulated flow velocity and pattern for the 1998 hydrograph before-dam removal scenario at 200 hours

6.5. Results with the 1991 Hydrograph

The 1991 hydrograph is shown in Figure 3a. It is seen that the flow was relatively low (less than 500 cfs) before hour 60, rose to a maximum of 6,065 cfs at about 78.5 hours, receded below 1,000cfs after 109 hours. Under the after-dam removal scenario (see Figure 4a), the simulated bed elevation evolution in time, along with the net deposited depth, is displayed in Figure 57 and Figure 59 for all three scenarios.

The following observations may be made based on the simulation results:

(1) No appreciable sediment deposition was observed if the flow was less than 1,000 cfs (e.g., the first 65 hours). The sediments may be mobilized only by flows larger than 1,000 cfs.

(2) For all scenarios, sediments were accumulated behind the weir quickly. The overall deposition pattern was largely determined during the rising limb of the hydrograph.

(3) A comparison of the deposition depth after 200 hours between the before- and after-dam removal scenarios is shown in Figure 60 and the simulated bed elevation is in Figure 61. The average deposition depth behind the weir was estimated to be 2.0 ft and 3.5 ft, respectively, for before-dam and after-dam

removal scenarios. The total predicted sediment deposition volume is tabulated in Table 9 for all cases. It is noted that the deposition volume was more than doubled for the existing condition scenario and 1991 hydrograph when the sediment input was changed from before-dam to after-dam. In numerical numbers, about 19,400 yd^3 additional sediments (relative to the before-dam) were added to go through the Robles diversion after the dam removal, and 4,640 yd^3 additional sediments were accumulated between RM 14.1098 and the weir. It indicates that the existing radial gates are not capable of efficiently moving the additional sediments added after dam removal.

(4) If the high flow bypass (HFB) radial gates are in place, the total sediment deposits between RM 14.1098 and the weir would be reduced by approximately 50% (see Table 9) for the 1991 hydrograph and after-dam removal condition. The average deposition depth near the weir is reduced from 3.5 ft to less than 2.5 ft under the right HFB and 3.0 ft for the left HFB, respectively. It may be concluded that the HFB gates are capable of moving sediments efficiently under the after-dam removal condition.

(5) A comparison between the right and left high flow bypass (HFB) is shown in Figure 62. It is seen that the right HFB appeared to have an advantage over the left HFB. Firstly, the total deposited depth near the weir was lower for the right HFB case (2.5 ft for the right HFB versus 3.0 ft for the left HFB). Secondly, the total sediment volume deposited upstream of the weir is also lower for the right HFB (see Table 9). In addition, more deposition occurred in front of the canal diversion gates for the left HFB scenario.

In summary, model results suggested that there would be no sediment issues for the 1991 hydrograph for all cases simulated except for the existing condition scenario with the after-dam removal sediment input. Under the existing condition, a less severe flood such as the 1991 flood may lead to much deposition upstream of the weir after dam removal.

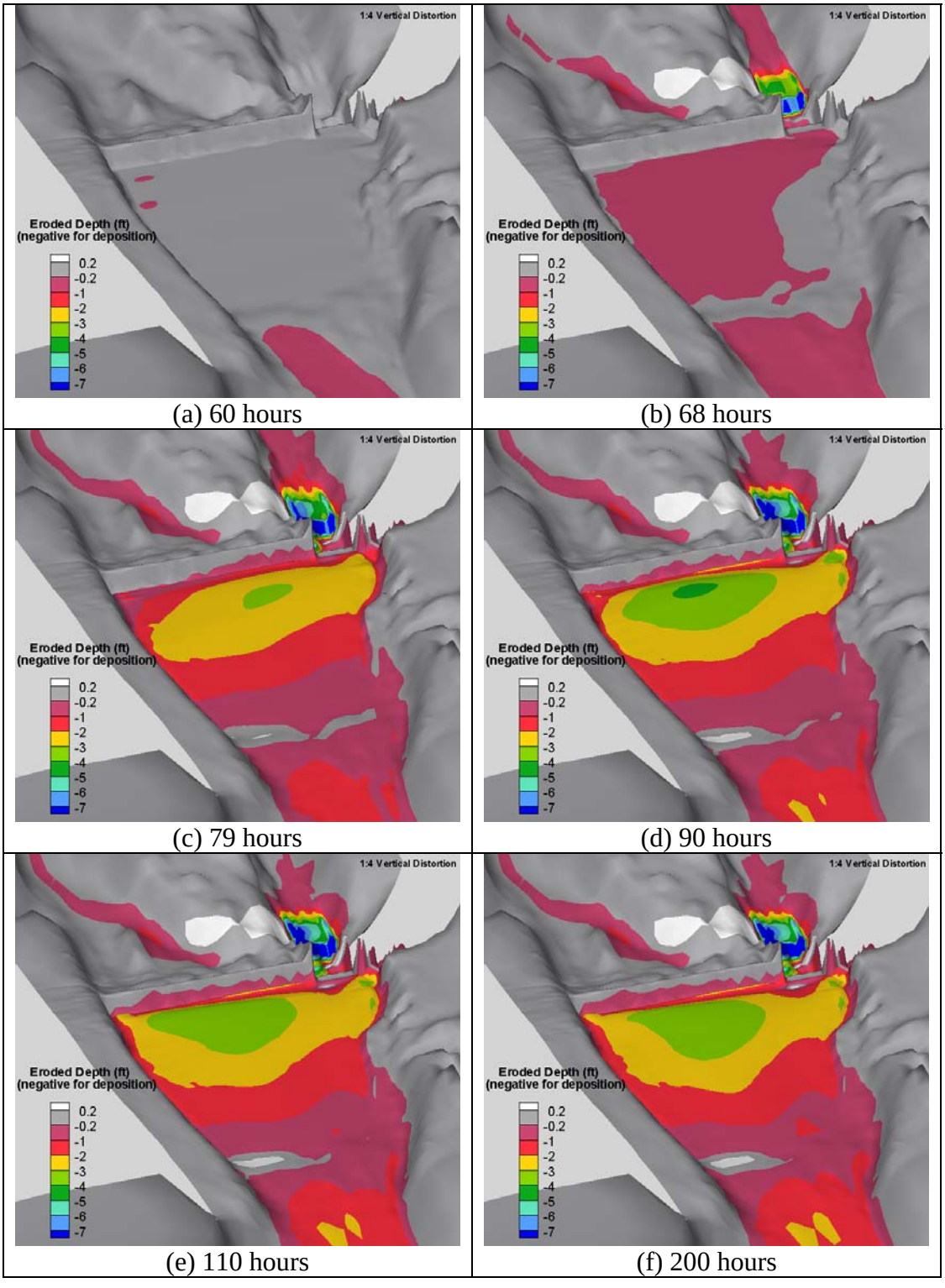

(a) 60 hours (b) 68 hours

(c) 79 hours (d) 90 hours

(e) 110 hours (f) 200 hours

Figure 57. Simulated bed elevation and deposited depth for the existing condition with the 1991 hydrograph and after-dam removal sediment input

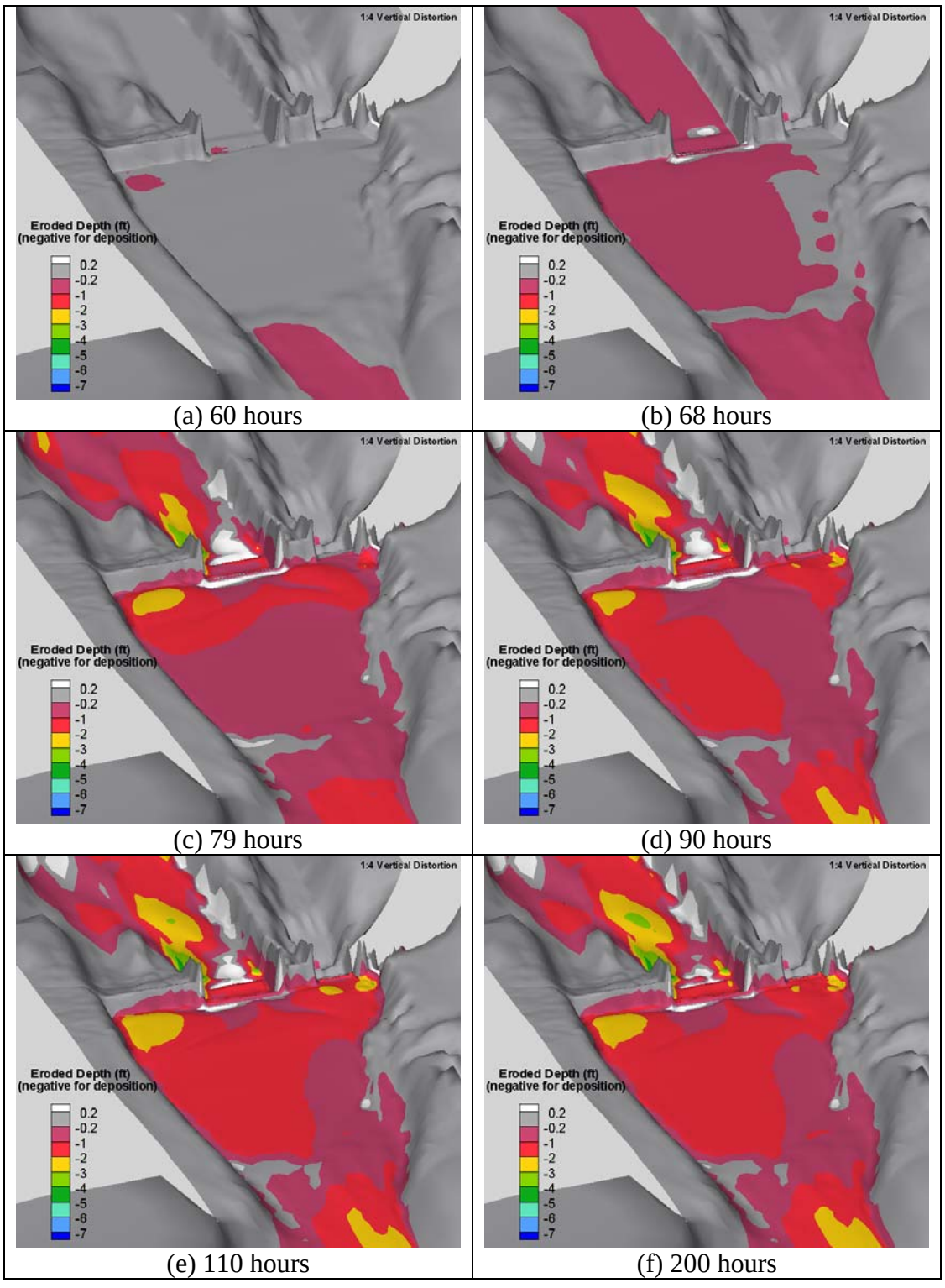

(a) 60 hours (b) 68 hours

(c) 79 hours (d) 90 hours

(e) 110 hours (f) 200 hours

Figure 58. Simulated bed elevation and deposited depth for the RHFB scenario with the 1991 hydrograph and after-dam removal sediment input

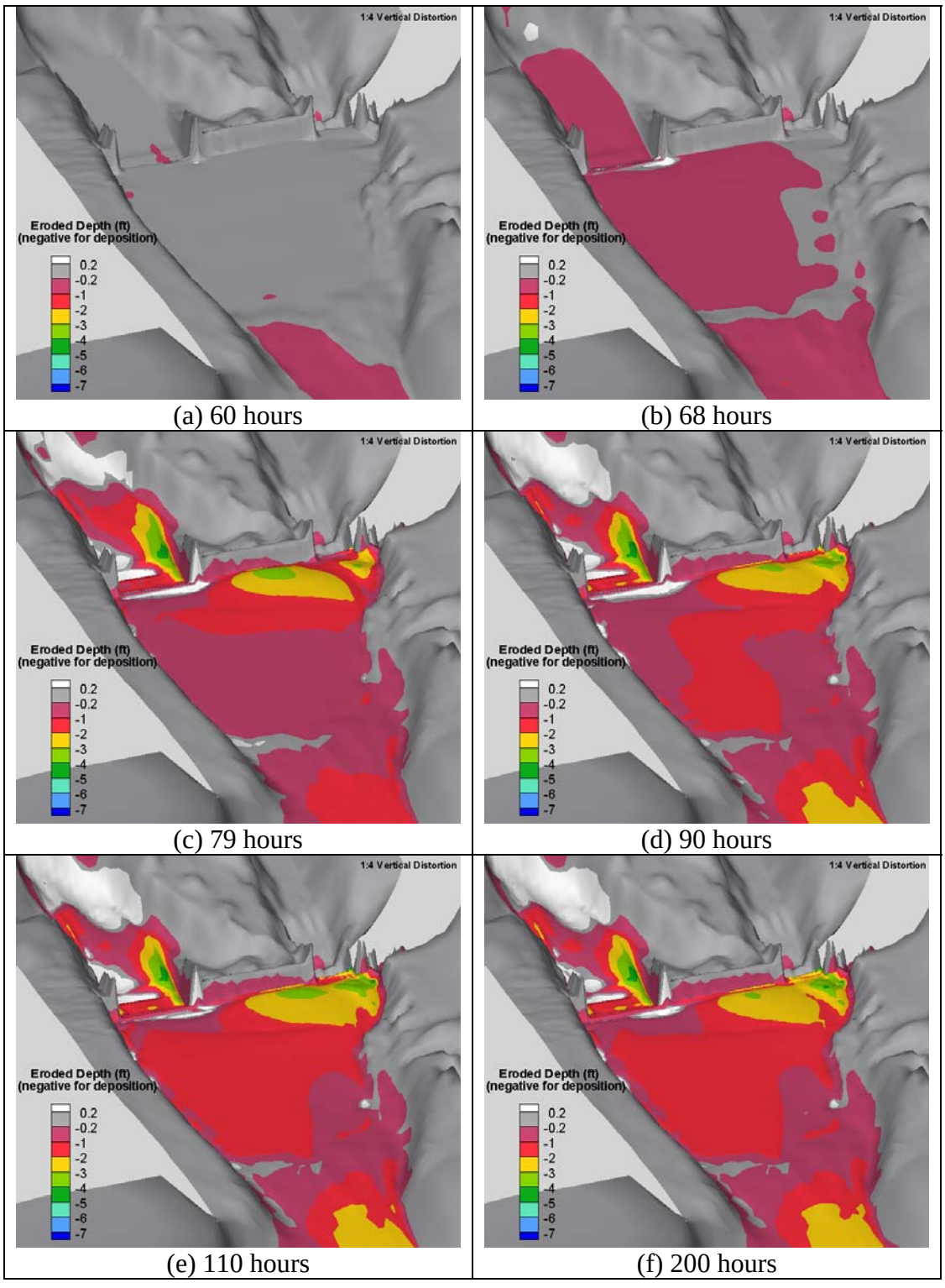

(a) 60 hours (b) 68 hours

(c) 79 hours (d) 90 hours

(e) 110 hours (f) 200 hours

Figure 59. Simulated bed elevation and deposited depth for the LHFB scenario with the 1991 hydrograph and after-dam removal sediment input

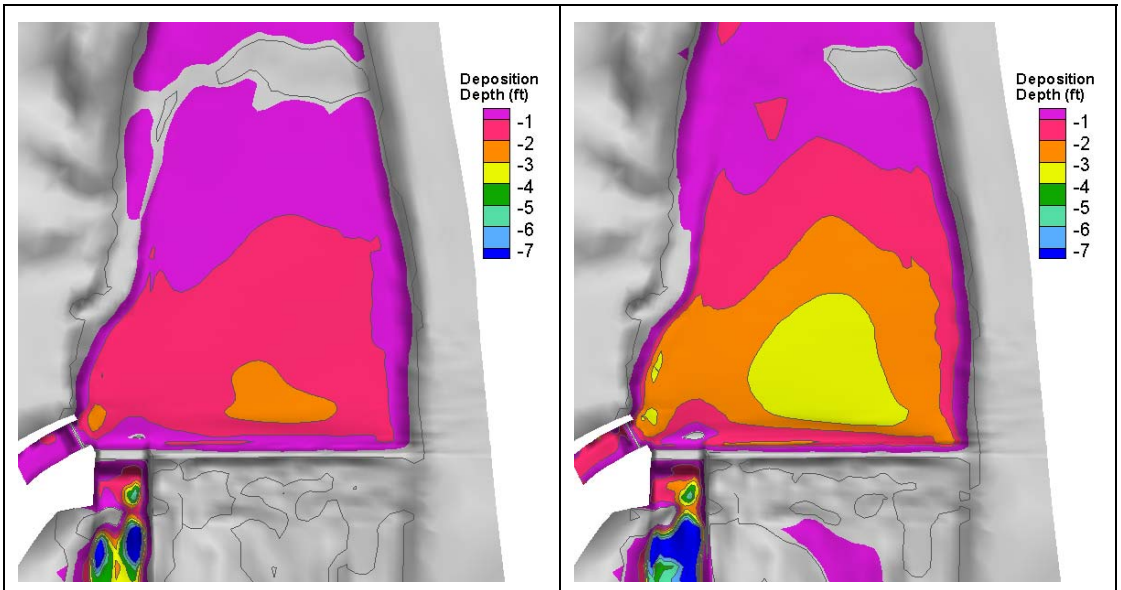

(a) before dam removal **(b) after dam removal**

Figure 60. Comparison of deposition depth between before-dam and after-dam removal for the 1991 hydrograph and existing condition scenario

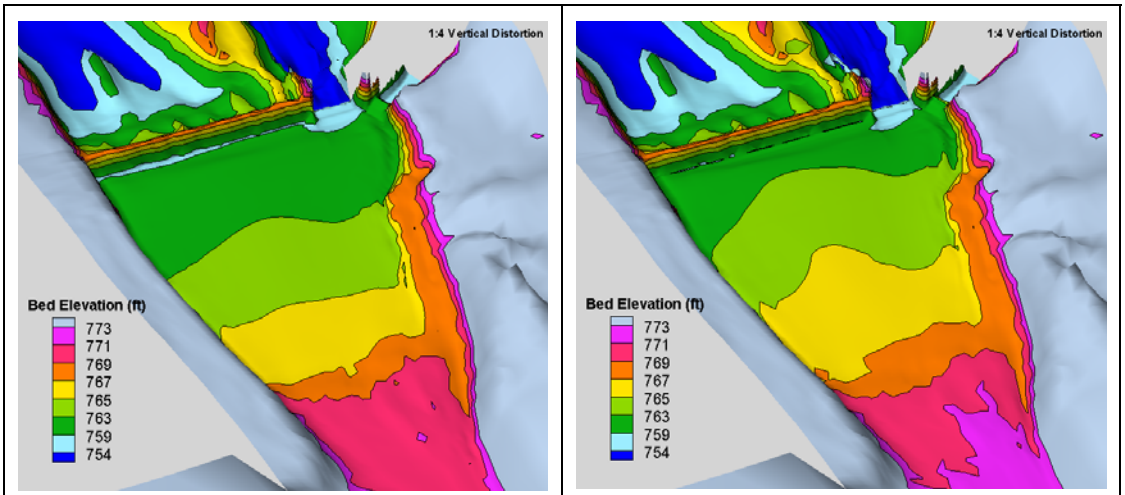

(a) before dam removal **(b) after dam removal**

Figure 61. Comparison of bed elevation between before-dam and after-dam removal for the 1991 hydrograph and existing condition scenario

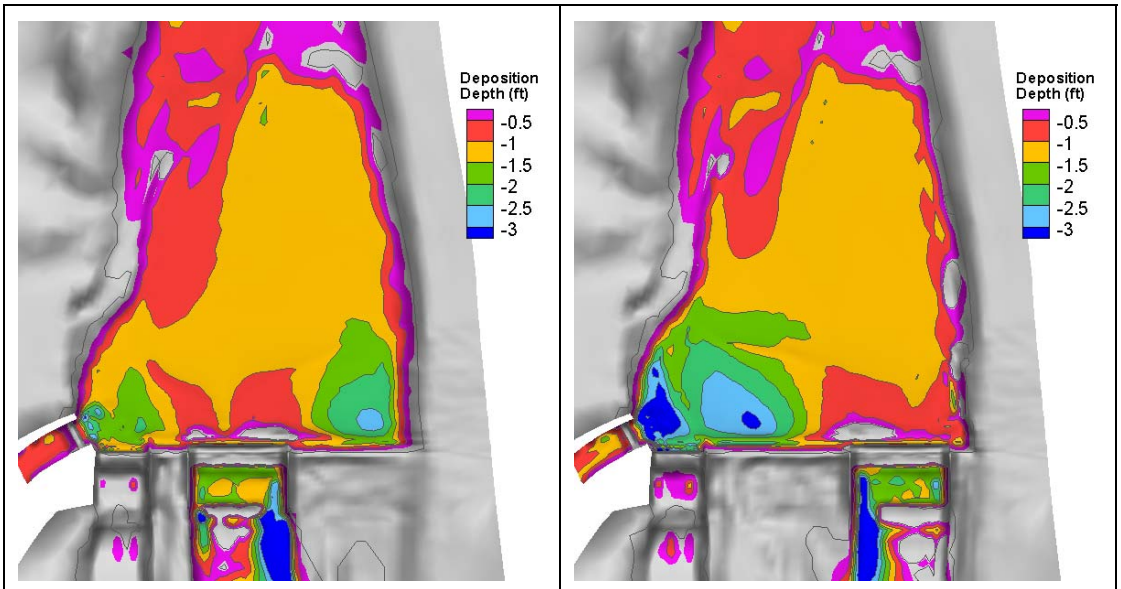

(a) Right HFB **(b) Left HFB**

Figure 62. Comparison of deposition depth between the right and left HFB cases for the 1991 hydrograph and after dam removal

6.6. Results with the 1998 Hydrograph

The 1998 hydrograph had a relatively low flow for the first 50 hours (less than 1,000 cfs). The flow started to increase at 50 hours, reached the peak of 20,240cfs at 59.8 hours, receded below 4,000cfs after 75 hours and below 1,000cfs after 120 hours (see Figure 3b). Comparisons are mostly for the after-dam removal scenarios (see Figure 4b). The simulated bed elevation evolution in time, along with the net deposition depth, is displayed in Figure 63 to Figure 65.

Following observations may be made based on the simulation results:

(1) Similar to the 1991 hydrograph scenario, no appreciable sediment deposition was observed for the first 50 hours due to relatively low flow (less than 1,000 cfs). More deposition occurred for the existing condition scenario at 50 hours. This may be attributed to the fact that the existing gates were opened earlier (see Figure 54) which would promote faster sediment movement towards the diversion weir.

(2) For the existing condition scenario, sediments were accumulated behind the weir quickly, similar to the 1991 hydrograph scenarios. A comparison of the deposition depth between the before- and after-dam scenarios is shown in Figure 66 at 200 hours; the simulated bed elevation is compared in Figure 67. An average deposition depth behind the weir was estimated to be 7.5 ft and 10.5 ft, respectively, for before- and after-dam scenarios. The results indicate that a flood similar to the 1998 event (near 15-year flood) would move a majority of the

sediments towards the diversion dam and fill the area upstream of the weir quickly even if excavation has been done before the flood. Under the existing condition scenario, sediment deposition in front of the canal gates was predicted to be high enough that bedload would be transported into the canal for both before- and after-dam removal scenarios with the 1998 flood.

(3) If the high flow bypass (HFB) radial gates would be in place, the total amount of sediment deposits between RM 14.1098 and the weir would be reduced by about 40% (see Table 9) under the 1998 hydrograph and after-dam removal conditions, in comparison with those of the existing gates. The average deposition depth near the weir is reduced from 10.5 ft to 5.0 ft under the right HFB and 6.5 ft for the left HFB, respectively. The results show that the HFB gates would be able to move sufficient sediments through the gates that there is less likelihood for the bedload to move through the diversion canal.

(4) A comparison between the right and left high flow bypass (HFB) showed that the right HFB case would be preferred to the left HFB. Firstly, the total deposited depth near the weir was lower for the right HFB case (5.0 ft versus 6.5 ft for the left HFB) despite that the total amount of deposited sediment volume between the weir and RM 14.1098 was not much different (Figure 68). This suggests a reduced potential for the bed load sediments transported into the diversion canal directly. The difference may be explained as follows. The flow entering the cross section RM 14.1098 is not uniform laterally; the flow tends towards the left bank due to the channel meander bend upstream. With the HFB placed on the left, the sediments on the left would move through the left HFB directly while those on the right would remain on the right and be stored in front of the weir. If the HFB is placed on the right, the sediments on the left continue to be swept towards the HFB due to the stronger flow on the left; but the sediments on the right are also transported towards the HFB. The combined effect leads to increased sediment transport and reduced deposition. The above explanation is supported by the results shown in Figure 64and Figure 65.

Table 9. Total amount of sediments moving into and stored in the area between RM 14.1098 and the weir based on model (volume excluding voids)

Case Name	Sediment Supply at Inlet	Sediment Volume (yd^3) through RM 14.1098	Sediment Volume (yd^3) stored upstream
FD-EX-1991-1	before-dam	34,190	4,130
FD-EX-1991-2	after-dam	53,600	8,770
FD-RHFB-1991	after-dam	57,530	4,330
FD-LHFB-1991	after-dam	62,340	4,923
FD-EX-1998-1	before-dam	205,500	21,900
FD-EX-1998-2	after-dam	258,400	26,500
FD-RHFB-1998	after-dam	282,500	15,700
FD-LHFB-1998	after-dam	282,500	16,100

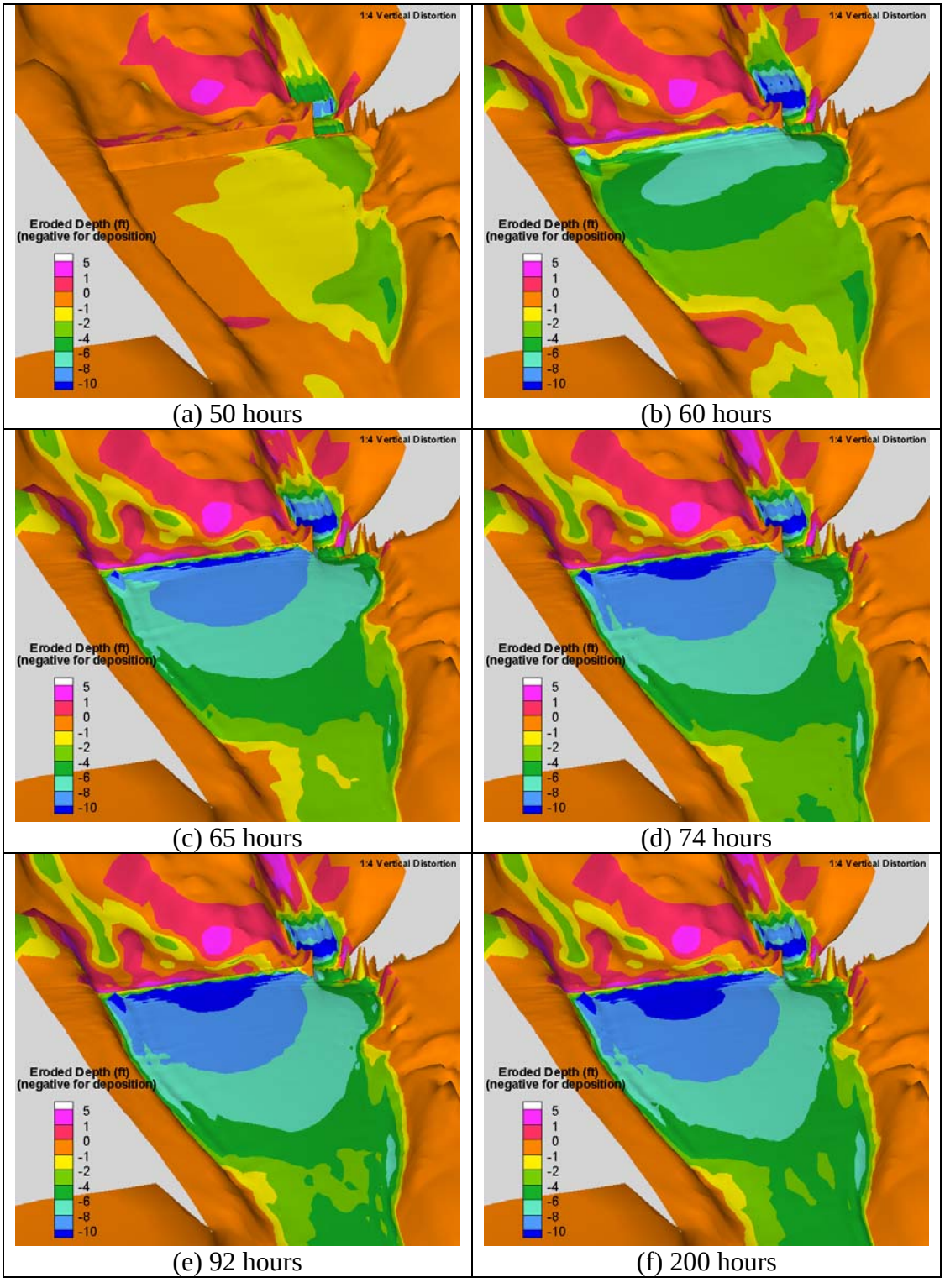

(a) 50 hours (b) 60 hours

(c) 65 hours (d) 74 hours

(e) 92 hours (f) 200 hours

Figure 63. Simulated bed elevation and deposited depth for the existing condition with the 1998 hydrograph and after-dam removal sediment input

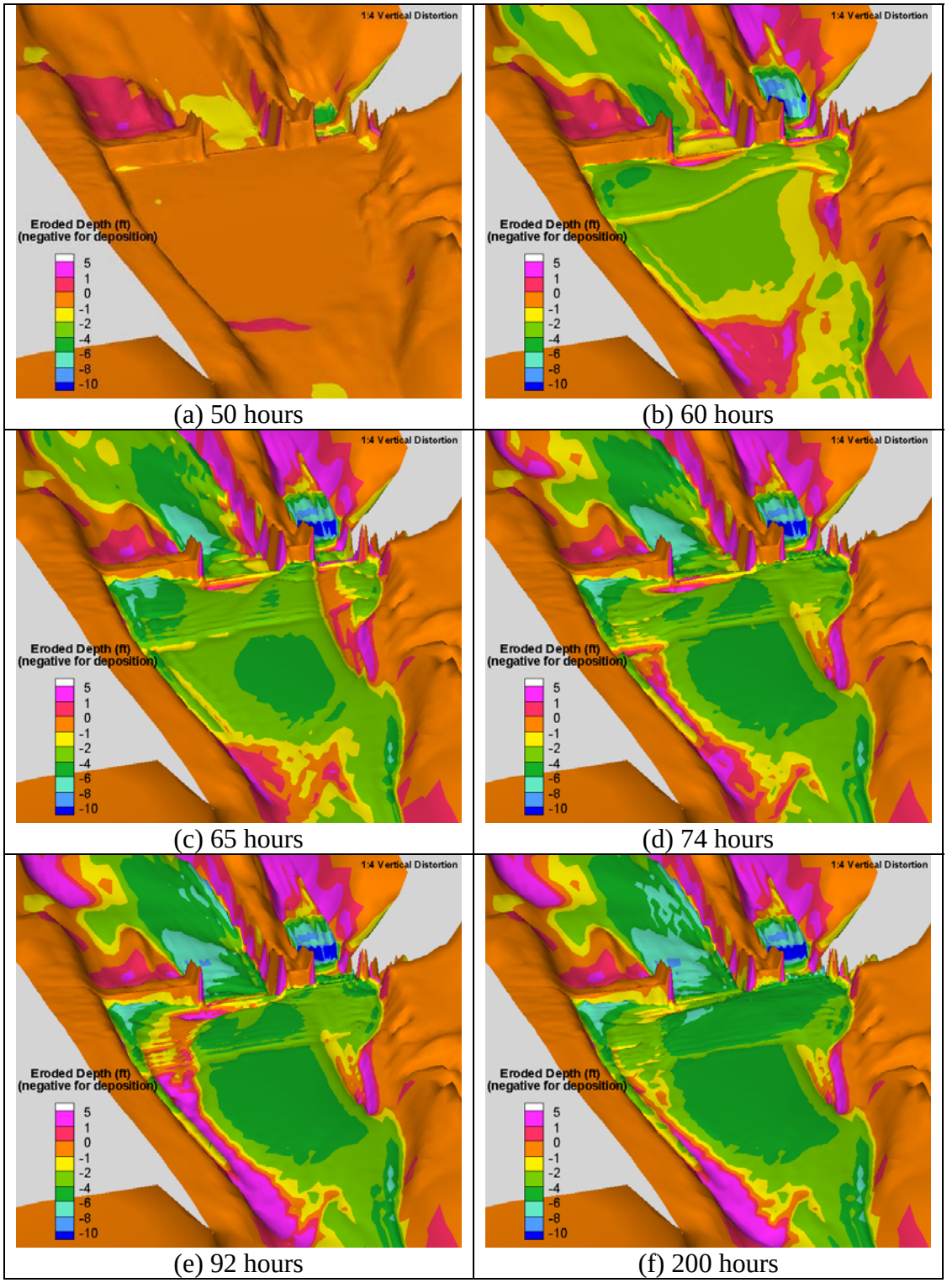

(a) 50 hours (b) 60 hours

(c) 65 hours (d) 74 hours

(e) 92 hours (f) 200 hours

Figure 64. Simulated bed elevation and deposited depth for the RHFB scenario with the 1998 hydrograph and after-dam removal sediment input

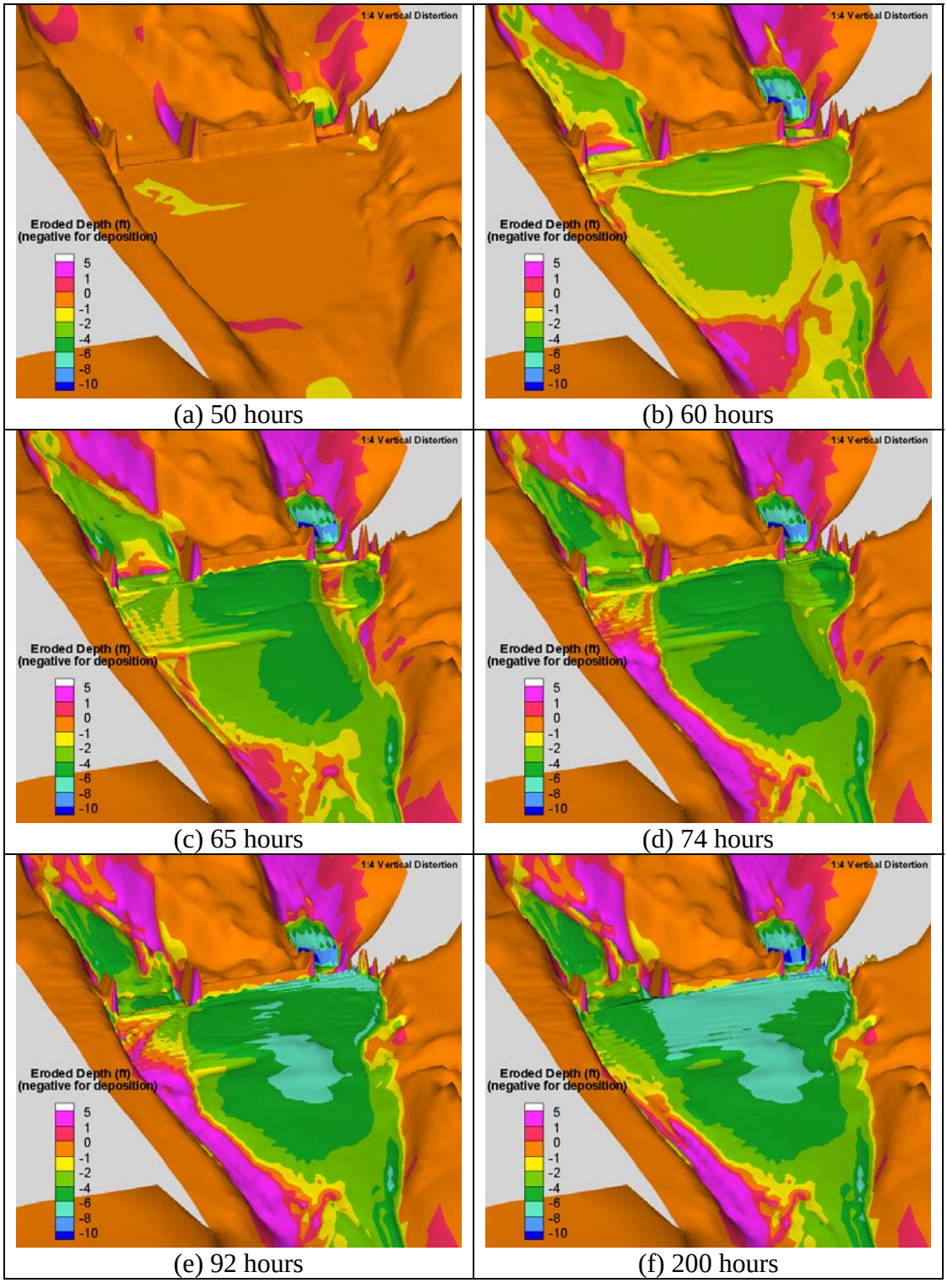

(a) 50 hours (b) 60 hours

(c) 65 hours (d) 74 hours

(e) 92 hours (f) 200 hours

Figure 65. Simulated bed elevation and deposited depth for the LHFB scenario with the 1998 hydrograph and after-dam removal sediment input

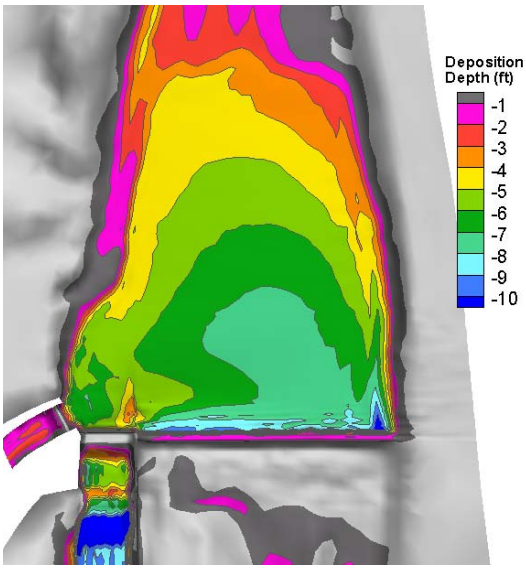

(a) before dam removal

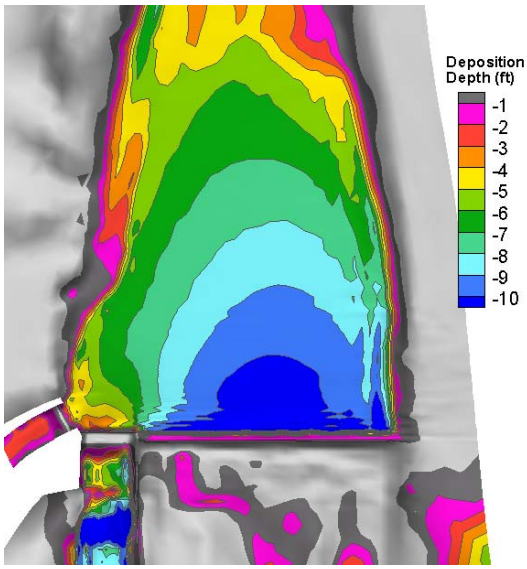

(b) after dam removal

Figure 66. Comparison of deposited depth between before-dam and after-dam removal for the 1998 hydrograph and existing condition scenario

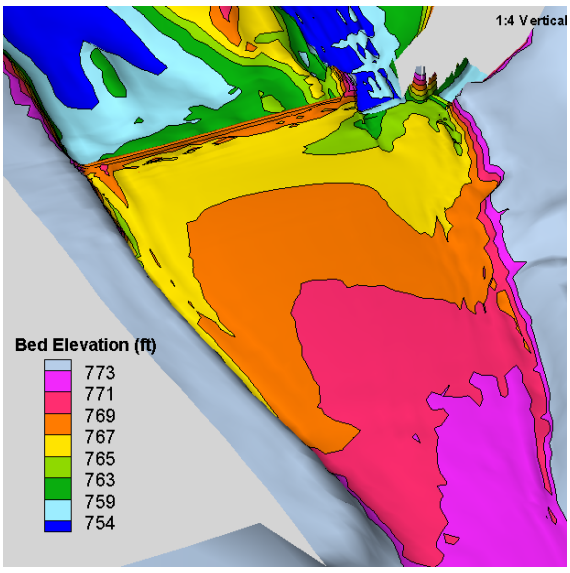

(a) before dam removal

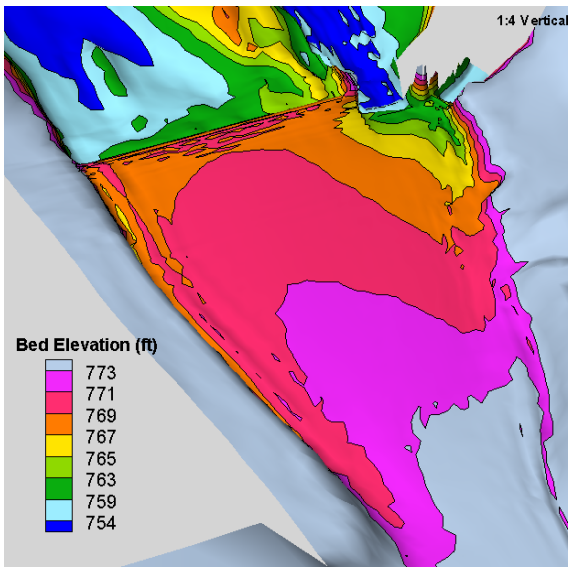

(b) after dam removal

Figure 67. Comparison of bed elevation between before-dam and after-dam removal for the 1998 hydrograph and existing condition scenario

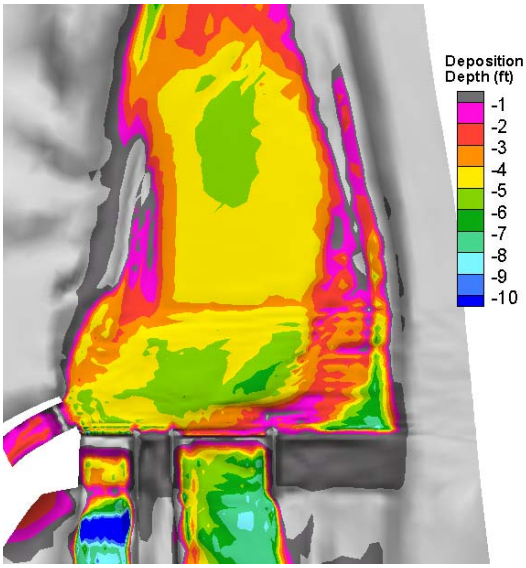

(a) Right HFB

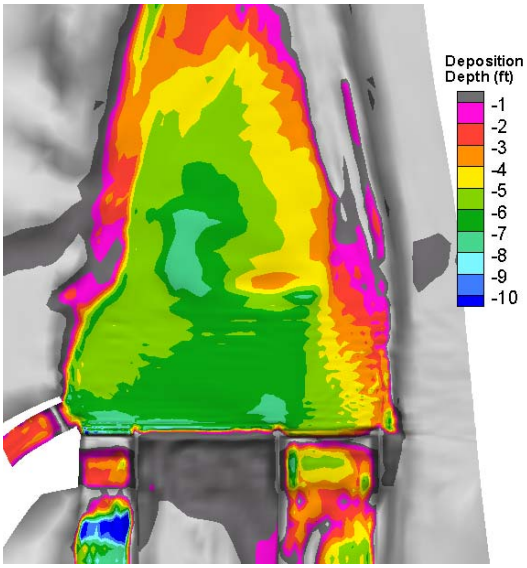

(b) Left HFB

Figure 68. Comparison of deposited depth between the right and left HFB cases for the 1998 hydrograph and after dam removal

7.0 Discussion and Uncertainty

7.1. Discussion and Summary

Numerical modeling of physical model cases presented in Chapter 5.0 shows that the results from both the numerical and physical models are in agreement with each other. This provides confidence in the numerical model and points to the reliability of the results from both models. Major findings, based on the modeling of physical model cases, are:

(1) With the existing radial gates, too much deposition would occur upstream of the Robles weir. Specifically, the sediment delta would reach the diversion canal gates under both the 6,000 cfs and 14,000 cfs hydrographs. The thickness of the delta is high enough that there is a high likelihood of bedload sediments being transported into the canal.

(2) With the high flow bypass (HFB) gates added, the model results show that it is less likely that the bedload sediments would enter the diversion canal.

(3) The total amount of sediment deposition upstream of the weir is tabulated in Table 10 for all simulated physical model cases. It shows that more than 85% of the incoming sediments would be trapped upstream of the weir under the 6,000 cfs hydrograph with or without the HFB gates. The benefit of the HFB gates shows up only for flows higher than 6,000 cfs. For example, with the 14,000 cfs hydrograph, about 70% of the input sediments are deposited upstream of the weir for the existing condition scenario while the percentage is reduced to about 53% if the HFB gates are operated. It is interesting to note that the delta deposition remains constant when the flow is increased from the 6,000 cfs hydrograph to the 14,000 cfs hydrograph.

(4) No appreciable difference is observed between the left and right HFB options in terms of the ability to move the sediment.

(5) The final bed topography near the existing and diversion canal gates may be altered through the sluicing ability of the existing radial gates. But not enough research has been carried out to derive a quantitative scheme for sluicing.

The physical model test cases are limited in several aspects. The 14,000 cfs hydrograph used in the lab is not the same as the 1998 hydrograph in the field which had a peak of more than 20,000 cfs. Also, the total sediments added for the 14,000 cfs hydrograph may not be high enough as the computed input based on the fact that transport capacity is more than 10 yd^3. Coupled with the potential

effects of the limited size of the test box and the scalability, there is a need to model the field cases which would eliminate most of the limitations mentioned above.

Table 10. Cumulative volume (excluding voids) deposited upstream of the weir during the period of test hydrograph

Cases	Total Sediment Volume Input (yd^3)	Volume Deposited Upstream of Weir (yd^3)
PM-SED-EX-91	3.7	3.25
PM-SED-EX-98	5.85	4.03
PM-SED-RHFB-91	3.7	3.24
PM-SED-RHFB-98	5.85	3.08
PM-SED-LHFB-91	3.7	3.10
PM-SED-LHFB-98	5.85	3.22

The numerical model for the field study was calibrated first with the available flow data. Simulation of the 2005 flood allowed the comparison of the simulated water surface elevation with the high water mark survey. The comparison was tabulated in Table 6. The difference between the simulation and survey is 0.22 ft and 0.36 ft, respectively, for the two survey points.

The field model was then used to simulate the 100-year flood and results were compared with the previous inundation study results based on the 1D model. Close agreement was obtained between the two models as far as the water surface elevation is concerned.

The mobile-bed simulation was carried out to study the sediment transport and bed evolution. Qualitative comparison of the simulated results with the field observation under the existing condition scenario showed that the model results were reasonable. The total amount of predicted sediment deposition upstream of the weir was in agreement with the field observation; and the predicted bed form and flow pattern after a major flood were plausible. Simulation of the existing condition scenario and comparison of the model results with the available data and observations gave us confidence about the reliability of the numerical model.

Mobile-bed simulations for all three scenarios - the existing, the right HFB, and left HFB - were carried out with both flow hydrograph and results were examined and compared. Major conclusions may be summarized as follows:

(1) The flow discharge of 1,000 cfs may be taken as the threshold below which no appreciable sediment movement and deposition would occur near the Robles Diversion Dam.

(2) For all modeled scenarios, sediments would be accumulated behind the Robles Diversion Dam (Weir) quickly. The overall deposition pattern was largely determined during the rising limb of the hydrograph. Only minor

deposition and bed form adjustments would occur shortly after the flow peak.

(3) After dam removal, more sediment depositions would be accumulated upstream of the Robles Diversion Dam for the existing condition scenario. The model estimated deposition depth (with voids) and volume (without voids) are tabulated in Table 11 under the existing condition scenario.

Table 11. Average deposition depth (with voids) and total deposition volume (without voids) under the existing condition scenario

Sediment Input Case	Before-Dam Removal 1991 Hydrograph	After-Dam removal 1991 Hydrograph	Before-Dam Removal 1998 Hydrograph	After-Dam Removal 1998 Hydrograph
Deposition Depth (ft)	2.0	3.5	7.5	10.5
Deposition Volume (yd^3)	4,130	8,770	21,900	26,500

(4) Model results showed that the existing radial gates alone are not capable of efficiently moving the additional sediments added after dam removal. Sediment deposition in front of the canal gates would be so high that there is a high likelihood the bedload sediments would be transported into the diversion canal if a flood similar to 1998 (about 15-year flood) would occur.

(5) If high flow bypass (HFB) radial gates are in place, the total sediment deposits between RM 14.1098 and Robles Diversion Dam would be reduced by approximately 50% and 40%, respectively, for the 1991 and 1998 hydrographs. HFB gates are capable of moving sediments efficiently once the dam is removed and there is less likelihood for the bedload sediments to move through the diversion canal.

(6) Model results showed that the right HFB appeared to have an advantage over the left HFB. Firstly, the average total deposition depth near the weir was lower for the right HFB case: 2.5 ft for the right HFB versus 3.0 ft for the left HFB for the 1991 hydrograph and 5.0 ft versus 6.5 ft for the 1998 hydrograph. Secondly, the total sediment volume deposited between RM 14.1098 and Robles Diversion Dam is also lower for the right HFB. Finally, more deposition occurred in front of the canal diversion gates for the left HFB scenario.

7.2. Model Uncertainties and Limitations

The mobile bed modeling performed in this project represents the current state-of-the-art. However, even the most advanced modeling typically cannot exactly predict the complex three-dimensional geomorphic response. Uncertainty is inherent in any numerical modeling due to the assumptions used to develop the model. Assumptions are mostly related to the theoretical development (e.g., the sediment transport equation and bed dynamics) and the method and input data used. Key areas of modeling uncertainty and limitations for this project are listed below:

- 2D modeling was necessary for the present analysis due to lateral (across the river) variations and the local erosion. The 2D model represents a significant improvement over a 1D approach. However, 3D effects are expected near the radial gates. The current 2D model does not take the vertical variation into account, and blockage of the bedload movement by a vertical wall was not modeled. As a result, the model cannot predict the amount of sediments moving through the canal diversion gates accurately. The risk of sediments movement into the diversion canal can only be indirectly assessed by examining the delta location and thickness in front of the canal gates.
- The sediment model was not calibrated or verified with field-measured sediment transport rates due to lack of such data. However, the flow model is calibrated in Section 6.1, and limited qualitative comparisons are discussed in Section 6.4.
- Uncertainties due to the sediment transport mechanics, such as the capacity equation and bed dynamics equations, are well known. The best available information, however, has been used in this project. The Parker (1990) sediment transport equation was used based on our past experience in modeling similar rivers.
- Other uncertainties include the impact of hydraulic flows, the initial bed gradation, etc. But they are deemed less important.

Despite various uncertainties, the current analysis is based on the current state-of-the-art modeling approach. The model has been carefully calibrated and compared with the available data in the laboratory and field. The analysis method chosen is adequate for the estimation of the bed evolution and sediment deposition study.

8.0 References

Greimann, B.P., (2004). *Hydrology, Hydraulics and Sediment Studies of Alternatives for the Matilija Dam Ecosystem Restoration Project, Ventura, CA – Final Report*, Technical Service Center, Bureau of Reclamation, Denver, CO 80225.

Greimann, B. P., (2006). *Hydrology, Hydraulics, and Sediment Studies for the Matilija Dam Ecosystem Restoration Project, Ventura, CA – DRAFT Report*, Technical Service Center, Bureau of Reclamation, Denver, CO 80225.

Greimann, B.P., Lai, Y.G., and Huang, J., (2007). "Two-Dimensional Total Sediment Load Model Equations," to appear in: J. *Hydraulic Engineering, ASCE*.

Lai, Y.G., Weber, L.J., and Patel, V.C. (2003). "Non-hydrostatic three-dimensional method for hydraulic flow simulation - Part I: formulation and verification." *J. Hydraulic Engineering*, 129(3), 196-205.

Lai, Y.G. (2006). *Theory and User Manual for SRH-W 1.1*, Technical Service Center, Bureau of Reclamation, Denver, CO 80225.

Lai, Y.G., and Greimann, B.P. (2007). "Numerical modeling of alternate bar formation downstream of a dike," World Environmental & Water Resources Congress, May 15-19, 2007, Tampa, Florida.

Lai, Y.G., and Greimann, B.P. (2008a). "Predicting contraction scour with a 2D model," World Environmental & Water Resources Congress, May 12-16, 2008, Honolulu, Hawaii.

Lai, Y.G., and Greimann, B.P. (2008b). "Modeling of erosion and deposition at meandering channels," World Environmental & Water Resources Congress, May 12-16, 2008, Honolulu, Hawaii.

Mefford, B., Stowell, H., Heinje, C. (2008). *Robles Diversion Dam High Flow and Sediment Bypass Structure, Ventura, California, Physical Model Study*, Hydraulic Laboratory Report HL-2008-7, Technical Service Center, Bureau of Reclamation, Denver, CO.

Parker, G., (1990). "Surface-Based Bedload Transport Relation for Gravel Rivers," *J. Hydraulic Research*, 28(4):417-436.

RECLAMATION

Managing Water in the West

Hydraulic Laboratory Report HL-2008-7

Robles Diversion Dam
High Flow and Sediment Bypass Structure
Ventura, California

U.S. Department of the Interior
Bureau of Reclamation

September 2008

Hydraulic Laboratory Report HL-2008-7

Robles Diversion Dam
High Flow and Sediment Bypass Structure
Ventura, California

Physical Model Study

Brent Mefford
Hillary Stowell
Chuck Heinje

Mission Statements

The mission of the Department of the Interior is to protect and provide access to our Nation's natural and cultural heritage and honor our trust responsibilities to Indian Tribes and our commitments to island communities.

The mission of the Bureau of Reclamation is to manage, develop, and protect water and related resources in an environmentally and economically sound manner in the interest of the American public.

Acknowledgments

The author would like to thank Mr. Rudy Campbell and Mr Billy Baca for assisting with model design, construction and testing. Mr. Blair Greiman (D86-68540) and Yong Lai (D86-68540) for provided technical support on sediment transport. This report was peer reviewed by Robert Einhellig, (D86-68640).

Hydraulic Laboratory Reports

The Hydraulic Laboratory Report series is produced by the Bureau of Reclamation's Water Resources Research Laboratory (Mail Code D-8560), PO Box 25007, Denver, Colorado 80225-0007. At the time of publication, this report was also made available online at **http://www.usbr.gov/pmts/hydraulics_lab/pubs/HL/HL-2008-7.pdf**

Disclaimer

No warranty is expressed or implied regarding the usefulness or completeness of the information contained in this report. References to commercial products do not imply endorsement by the Bureau of Reclamation and may not be used for advertising or promotional purposes.

Table of Contents

LIST OF FIGURES

LIST OF TABLES

Robles Diversion Dam Physical Model Study

Summary

This report presents the results of a Bureau of Reclamation hydraulic model study of the proposed high flow bypass (HFB) spillway for Robles Diversion Dam. Robles Diversion Dam is located on the Ventura River approximately 14 river miles from the ocean. A 1:20 Froude-scale model of the proposed facility was tested to determine the interaction of flows and bed load sediments near the facility following decommissioning and removal of Matilija Dam located about two river miles upstream. The HFB spillway was proposed to enhance sediment movement through the diversion pool thereby reducing the impacts of elevated bed load levels resulting from the upstream dam removal. A new auxiliary fishway and 1.5 ft dam raise associated with the HFB is also proposed to improve upstream fish passage at the diversion dam during HFB operation.

HFB Spillway Location - Tests of two- and ten-year floods passing through the diversion pool without the HFB spillway showed canal diversions would be significantly impacted by the entrainment of bed sediments into the canal. In contrast, tests of the HFB spillway located near the left bank or adjacent to the right bank service spillway resulted in unimpacted canal diversion during both floods. The tests clearly demonstrated the importance of passing the majority of the flow away from the canal intake during flood flows transporting high bed load. A comparison of sediment deposition in the diversion pool following the two-year flood event (figures 29 and 41) shows a left bank spillway location provides the least sediment deposition near the canal headworks when the service spillway is not operated. A similar response was also noted from the ten-year flood tests. Prior to operating the service spillway the sediment delta progressed down the right bank at a slower rate for the HFB left bank location compared to the near right bank location. The slower initial movement of sediment along the right bank for the left bank HFB option resulted in sediment taking about 3.0 hrs (prototype) longer to reach the service spillway after the service spillway gates were opened compared to the near right bank location. However, no discernable difference of sediment entrainment into the canal was observed between HFB locations. For both locations, high flow releases through the service spillway dominated bed load movement near the canal headworks quickly negating bed sediment differences resulting from HFB spillway location.

Neither spillway location prevented inundation of the right bank fishway exit located well upstream of the dam. The fishway exit was impacted by sediment during all model tests. Also, the HFB spillway at either location will likely not prevent deposition in front of the canal followed by entrainment of bed sediments into the canal if significant sediment deposits are present in the pool area prior to a flood event, during larger floods or significantly longer duration floods than those tested.

Locating the HFB spillway adjacent to the service spillway as shown in figure 60 is recommended. The near right bank location provides for better attraction for fish to the fishways and better access to the HFB facility during flood events.

Service Spillway Performance - The flow pattern entering the left spillway bays was relatively poor. A strong flow contraction occurred off the left wall of bay 4 and to a lesser extent bay 3. Flow velocities measured upstream of the dam show flow approaches the service spillway entrance at a sharp angle. Adding a curved upstream guide wall extending about 21 ft into the diversion pool was found to effectively guide flow into the spillway. The spillway had a discharge capacity of 5,800 ft^3/s at pool elevation 767.1 with the curved guide wall extension on bay 4.

Operation of the service spillway at full diversion pool during periods of high bed load generally increased movement of bed sediments toward the canal headworks and increased the potential for entrainment of bed sediments into the canal. Best results were achieved by using the HFB spillway to pass all spillway flows from about 2,500 ft^3/s up to the capacity of the HFB spillway. Sluicing bed load through the service spillway also resulted in significant deposition of sediment in the downstream spillway channel. Tests of the existing downstream channel during the ten-year flood event resulted in approximately 10 ft of sediment deposited against the baffled apron energy dissipater and sediment completely filling the downstream pools between the rock weirs.

Several modifications to the service spillway and downstream channel were tested to improve downstream flushing of bed sediments and attraction conditions for upstream fish passage. These tests resulted in recommended modifications to the spillway and downstream river channel. The recommended design is shown in figure 60. The major recommendations are:

- The service spillway radial gates should be modified to control flow to elevation 768.5.
- The stilling basin end sill should be raised to elevation 754.25 to prevent the hydraulic jump from sweeping out of the basin at higher pool elevations.
- The channel invert between the baffled apron drop and the downstream end of the fishway entrance structure should be raised to elevation 745.0 and the entrance slots for the fishway raised to about elevation 745.5.
- The channel downstream of the fishway entrance structure should slope up to elevation 750 to provide a pool area at the fishway entrance then slope downward at 1.5 percent to the existing channel, a distance of about 400 ft.

HFB Spillway Hydraulic Performance – Similar to the service spillway, strong flow contractions occurred off the outer spillway walls as flow entered spillway bays 5 and 8. Flow contractions occurred at both spillway locations tested. Entrance conditions to the spillway were improved by adding curved guide walls extended into the diversion pool similar to the wall proposed for the service spillway. Guide walls tested for the near right bank HFB spillway location are shown in figure 49. Guide walls were not included in the left bank HFB tests. However, a similar wall shape could also be applied to a HFB spillway located on the left bank to reduce the flow contractions noted during the tests. For the near right bank HFB location shown, guide walls between bays 4 and 5 were tested as a single pier that improved flow into both bays. With the upstream guide

walls installed the spillway discharge capacity was 9,900 ft^3/s at pool elevation 767.1 (test conducted without sediment transport through the spillway).

Stilling basins of different lengths and with and without endsills were tested. Type 1 basins without endsills are recommended to promote flushing of bed load away from the structure and the HFB fishway entrance, figure 56. Downstream of the HFB stilling basins, a 2.0 percent slope rock ramp provides a transition between the HFB structure, the service spillway channel and the downstream river channel.

Fish Passage – The existing upstream fish passage exit was inundated by sediment deposition in the diversion pool for all test conditions. HFB spillway location and gate operation were ineffective at preventing the sediment delta in the diversion pool from building in front of the fishway exit. Flow into the fishway exit was not modeled, however, flow passing through the fishway with the sediment deposition observed would likely entrain large amounts of sediment resulting in plugging of the fishway. Based on the test results, the fishway exit gates would likely be closed prior to a large flood. Fish would then exit through the canal headworks structure and swim in front of the service spillway entrance to pass upstream. An evaluation of flow velocities upstream of the canal and service spillway found flow velocities are less than about 6 ft/s during single spillway gate operation (figure 50). Operating with multiple service spillway gates open would likely increase sediment deposition in front of the canal diversion and result in widely variable flow velocity in the area. Flow velocities reaching about 15 ft/s were measured upstream of the spillway apron with a fully developed sediment delta passing through the spillway. The downstream entrance to the fishway may also be impacted during large flows by sediment deposition. In all tests sediment deposited against the fishway entrance structure obstructing the fishway entrance gates to varying degrees. For the recommended design, sediment deposits about 3 ft deep covered the area around the fishway entrance following the ten-year flood.

A second fishway was proposed adjacent to the left wall of the HFB spillway to provide fish passage during HFB spillway operation (figure 60). The HFB fishway was designed to operate only during operation of the HFB spillway at diversion pool elevation 768.0. Downstream of the HFB spillway a constructed channel approximately 400 ft long starting at elevation 753.25 and sloping at about 2 percent conveyed flow and sediment downstream away from the diversion structure. The slope of the channel is similar to other reaches of the Ventura River. The downstream channel was sloped from right to left at 0.5 percent to cause flow to gradually contract to a remnant channel downstream of the right bank fishway as spillway flows recede.

Service Spillway Modifications - Increasing the diversion pool elevation by about 1 ft requires several modifications to the existing spillway and fishway. The top of the current service spillway gates is 767.25. A 1-ft pool rise would require the top of the gates be also raised approximately 1 foot.

The model showed the hydraulic jump in the service spillway stilling basin sweeps out of the basin under the higher diversion pool at some gate openings. To hold the jump in the basin, the model endsill was raised 1.5 ft prototype.

Background

Figure 1 - View of Robles Diversion Dam from above the right bank.

Robles diversion dam is located on the Ventura River near Ventura, California at approximately river mile (RM) 14.16 (figure 1). The diversion supplies water to Lake Casitas by canal. The normal maximum diversion is approximately 500 ft^3/s. The existing diversion dam is a low rock weir with a gated spillway, canal diversion headworks and a fish pass located on the right abutment. The diversion weir has a hydraulic height of 13 feet. The fish pass was constructed in 2002 to allow southern California steelhead (*Oncorhynhus mykiss*), a listed species, to migrate upstream of the diversion dam.

Matilija Dam is a 160 ft high (originally 190 ft high) concrete arch dam located about 2 miles upstream of Robles diversion dam on Matilija Creek (figure 2). Decommissioning and removal of Matilija Dam is proposed to address a dam safety risk and re-establish access for endangered steelhead to the upper reaches of Matilija Creek. The storage behind the dam has been significantly reduced by deposition of coarse sediment (USBR, 2002). The proposed removal of Matilija Dam is expected to result in increased sediment transport to the Ventura River for many years. The focus of this study is the hydraulic design of a new high flow bypass (HFB) spillway for Robles diversion dam. The HFB will improve the movement of bed load sediments past the diversion structure. This report covers physical modeling of the diversion facility conducted at the Bureau of Reclamation's Water Resources Research Laboratory (WRRL) in Denver, Colorado. The physical model study provided design support to the Army Corps of Engineers, Los Angles District, the principle designer for the project.

Figure 2 - View of Matilija Dam

Model Objective

The primary objectives of the model study were to evaluate the HFB spillway effectiveness for reducing the impact of future increases in sediment load on canal operation and fish passage. These objectives were pursued through the following study tasks:

For two-year and ten-year return flood events,

- Investigate the position of the HFB structure in relation to flow and bed sediment movement.
- Investigate spillway gate operation in relation to the movement and deposition of bed load sediment within the backwater influence of the diversion dam.
- Evaluate sediment deposition and sluicing near the canal intake structure.
- Investigate hydraulics with respect to fish passage.
- Investigate the impact of increased bed load sediment on operation of the existing fishway.

Study Test Plan

The study test plan was designed to evaluate HFB spillway benefits to project operations by contrasting post-dam removal bed load sediment conditions with and without the HFB spillway. Also, the study was designed to address HFB sediment sluicing performance with respect to spillway location on the dam. HFB locations adjacent to the service spillway (referred to as right-bank) and near the left bank were studied. The performance of each alternative was evaluated for the two-year and ten-year floods.

Physical Model

A 1:20 Froude-scale physical model of the river and diversion dam facility was constructed at the WRRL (figure 3). The model was constructed using NAVD 1988 reference for the prototype. This resulted in a vertical datum increase of 2.25 ft from the original structure design drawings. The extent of the model is shown in figure 4. River stationing referenced in this report is based on stationing established by the Corp of Engineers HEC-RAS flood plain modeling conducted as part of the dam removal project. The model represented the bankfull river channel from 575 ft upstream of the dam crest to 325 ft downstream of the crest. Generally, topography between elevations 750 and 780 ft was modeled. The river channel was modeled from LIDAR topography collected in March 2005. The channel upstream of the diversion dam was modeled with a moveable bed. The channel banks and downstream channel were modeled as non-erodible. The area within the diversion pool upstream of the dam was modeled as a plain bed of constant slope in the streamwise direction. The model topography allowed river flows up to approximately the ten-year flood of 14,000 ft^3/s to be modeled. Downstream of the dam the channel topography within the model was configured to a constructed channel that conveyed river flow from the dam and spillways to the downstream river channel.

Figure 3 – View of 1:20 scale moveable-bed model of Robles diversion Dam.

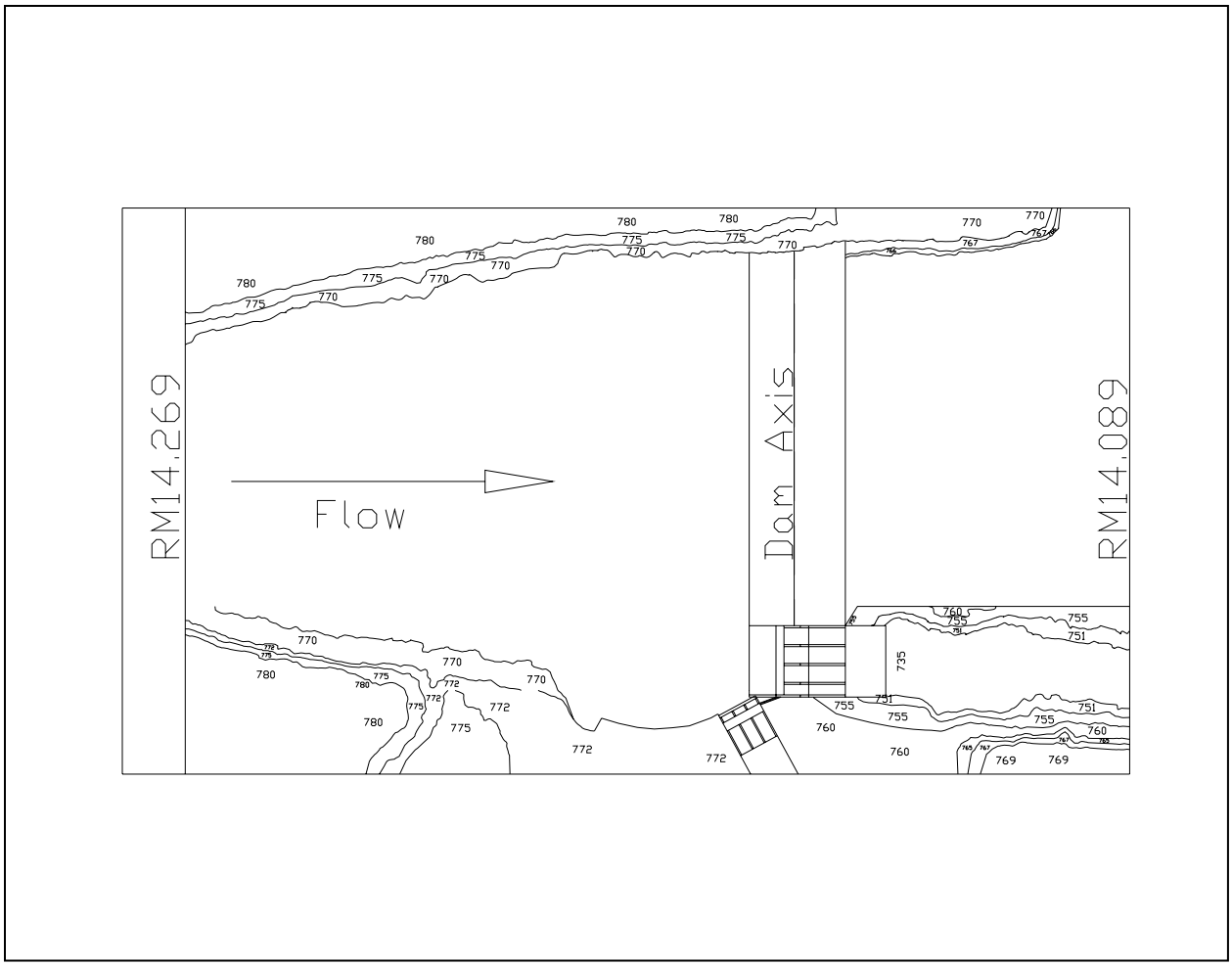

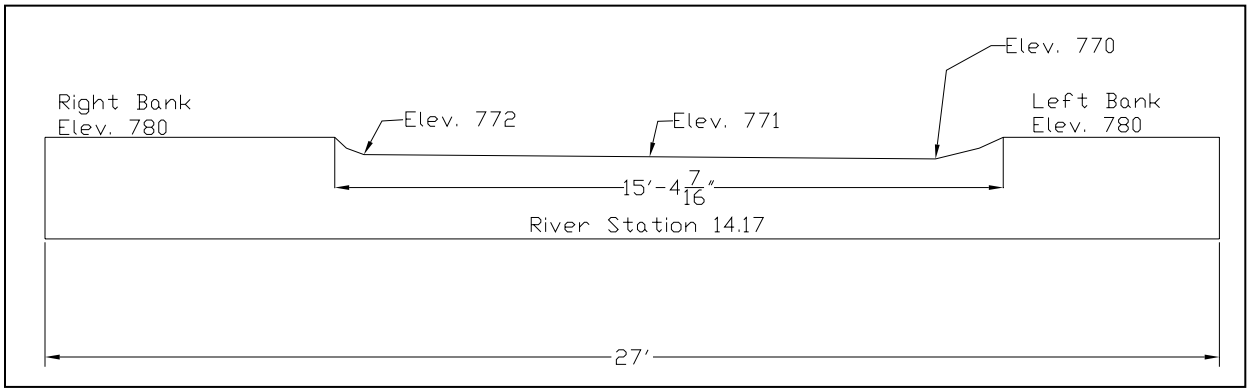

Figure 4 - Plan view of model and section showing model upstream boundary weir.

Model Scaling

Physical model scaling is used to create similitude between model and prototype of major forces controlling the physical processes being studied. Not all forces can be properly scaled simultaneously. Generally, open channel flow problems are modeled based on a Froude scaling relationship. The Froude number relates inertia and gravity forces expressed as, $F_r = v/\sqrt{gd}$ (*v = flow velocity, g = acceleration of gravity and d = flow depth)*. Similitude between model and prototype is achieved when the Froude number in the model and prototype are the same. Using Froude scaling the following relationships apply to the 1:20 geometric scale chosen:

$$L_{p/m} = 20$$

$$V_{p/m} = \sqrt{20} = 4.47$$

$$q_{p/m} = 20^{1.5} = 89$$

$$Q_{p/m} = 20^{2.5} = 1{,}788$$

where: L is length or depth, V is velocity, q is discharge per unit width, Q is discharge and p/m refers to a ratio of prototype to model

Forces not related in the Froude number, such as surface tension and viscosity do not scale by the Froude relationship. The effect on model similitude of distorting these forces must be evaluated separately. Surface tension can normally be neglected unless very shallow flows are anticipated in the model. Viscosity can be neglected when flow in the model and prototype is fully turbulent. The transition between laminar flow (viscous flow) and turbulent flow is defined by a relationship of viscous forces to inertial forces referred to as the Reynolds number, $R_e = Vd_r/\nu$ (V = average velocity, d_r = hydraulic radius and ν = kinematic viscosity). Turbulent flow occurs when the Reynolds number is larger than about 2000. For physical models of natural channels, a Reynolds number threshold of 5000 is often used due to the high variability of flow velocity and depth. Based on Froude scaling, the Reynolds number in the model will be distorted by the Froude scale ratio to the exponent 1.5. The 20:1 geometric scale selected for the model yields a distortion of the model Reynolds number of 89.4. Therefore, model Reynolds numbers are equal to prototype values divided by 89.4. Model Reynolds numbers were determined using HEC-RAS flow modeling to predict average flow velocity and hydraulic depth as a function of river flow near the upstream extent of the model (RM 14.17). For each river flow, prototype Reynolds numbers were calculated and divided by the model distortion factor to determine model values (see table 1). Model Reynolds numbers are greater than 5000 for modeled river flows above 3000 ft^3/s and greater than 2000 for modeled river flows above about 1000 ft^3/s.

Table 1 - Model Reynolds numbers for selected prototype river flows.

Prototype River Flow, ft^3/s	1500	3000	6000	10000	14000
Model Reynolds Number	3368	6518	11850	18720	24200

Sediment Modeling - Modeling sediment movement adds complexity to the modeling process and often requires distortion of some model and sediment properties. The riverbed slope, sediment size and specific gravity may require distortion to achieve similarity of sediment transport. Analytic techniques for estimating sediment transport were used to determine distortion ratios and appropriate modeling methods. To achieve similarity of bed load transport between model and prototype the difference of the Shields parameter to the critical Shields parameter should be the same in the model and prototype, (1,5). The Shields parameter, $\tau_o/(\gamma_s-\gamma)D_s$, is the ratio of bed shear force to gravity forces (τ_o = shear stress, (γ_s - γ) = submerged specific weight of sediment, D_s = particle diameter). The critical Shields parameter, $\tau_c/(\gamma_s-\gamma)D_s$, defines the point of incipient motion of bed material. Sediment scaling can be expressed on a Shield's diagram by plotting dimensionless shear versus the particle Reynolds number for model and prototype material (figure 5). The plot presents bed material scaling for a given particle size covering a range of hydraulic radii typical of the river channel. Similarity of sediment movement is achieved when $\Delta\tau$ (Tau) is similar for model and prototype. Similarity of sediment deposition is achieved by similarity of particle settling velocity (1,5). Settling velocity is a function of both particle diameter and density.

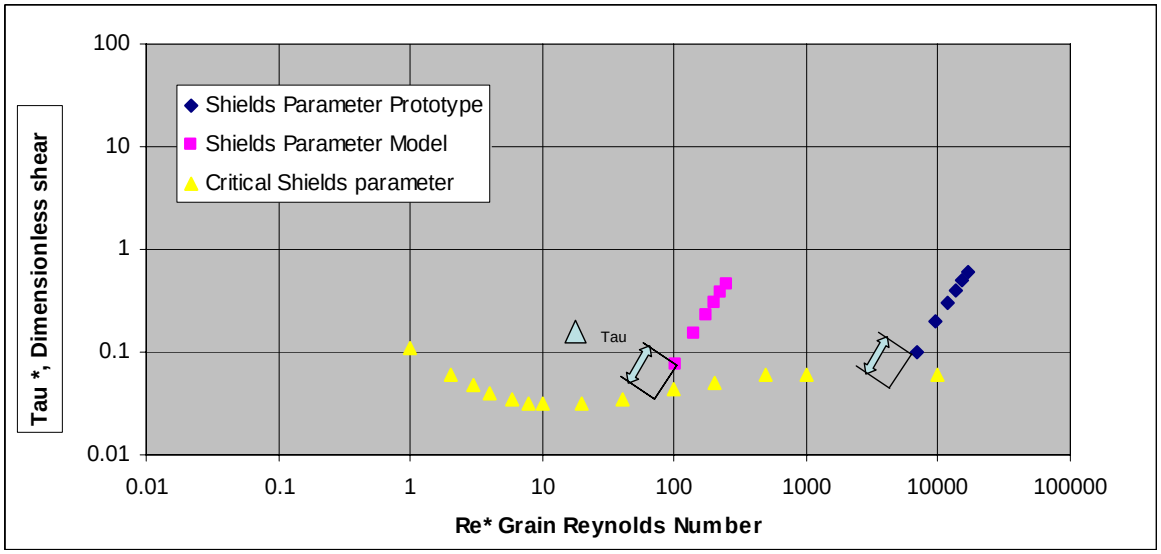

Figure 5 – Model and prototype critical shear relationship for sediment.

For granitic sand, settling velocity of particles greater than about 1 mm diameter is related to the $D_s^{1/2}$ (figure 6). Therefore, scaling of particle settling velocity in the model follows velocity scaling for prototype particles that scale greater than 1mm diameter.

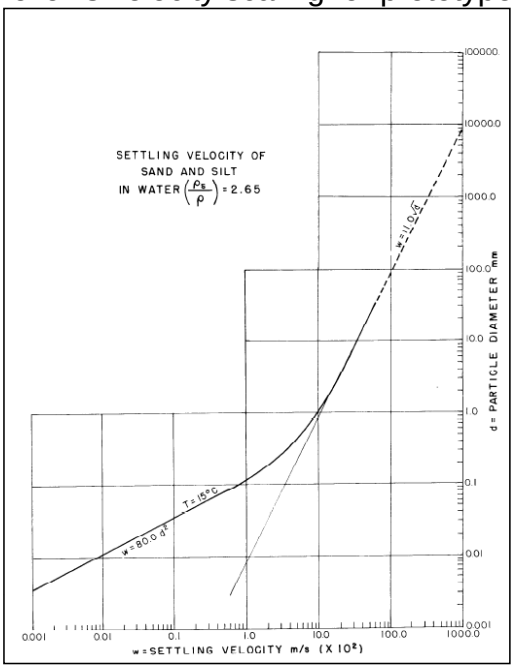

Figure 6 - Settling velocity for sand particles in water.

Similarity of sediment transport cannot be achieved at every point in a complex natural stream. Therefore, sediment transport is modeled based on similarity of average hydraulic conditions. A standard technique for calibrating sediment models is the comparison of prototype and model results where field data of flow and sediment is available (3). Limited pre-dam-removal field sediment data and post-dam-removal numerical modeling results were available for the site, however post-dam removal sediment load predictions can very widely depending on final sediment stabilization methods used, river flow history and reservoir sediment headcutting and bank failure assumptions. For the model investigation, it was assumed that bed load transport at the upstream end of the model was not limited by supply. Bed load sediment was supplied to the model at the maximum transport capacity of the river at the upstream extent of the model, RM14.17 (2). This was determined in the model by frequent adjustment of supply rate such that the bed elevation at RM 14.17 remained nearly constant during testing.

River Sediment - The type of material used in the model to represent prototype sediment depends on model scale, hydraulic characteristics of the channel reach and the type and gradation of sediment found in the river. Estimates of the reservoir sediment supply and gradation are given in the Matilija Dam Removal Appraisal Report (4). Sediment sampling of reservoir deposits found approximately 57 percent of the sediments are sand and 13 percent of the sediments are gravels and cobbles. The remaining 30 percent is silt and clay that will be largely carried in suspension. Silt and clay material was not represented in the model. The sediment size gradation used for the prototype is given in figure 7.

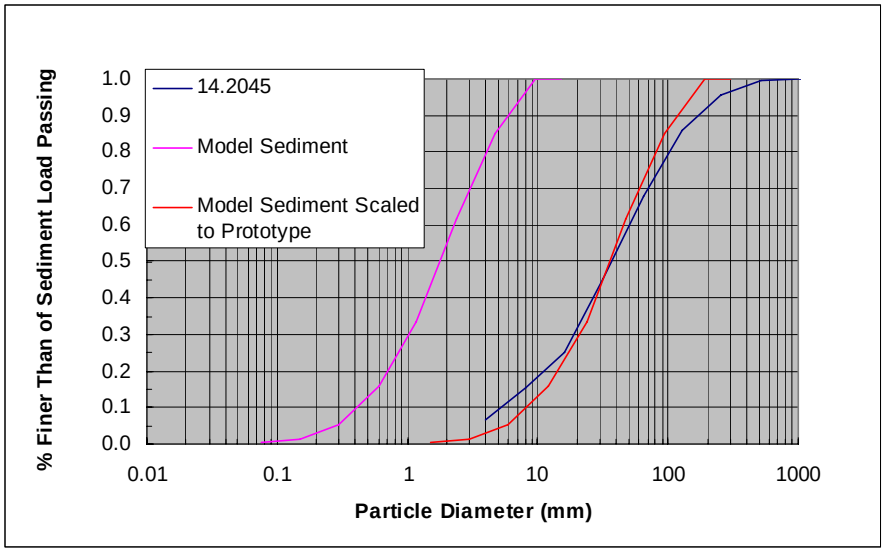

Figure 7 - Comparison of model and prototype bed material gradation.

Model Sediment – A mix of small granitic gravels and coarse and medium sands were used to represent bed sediments in the model. The density of model sediment was 2.63. Prototype material larger than about 20.0 mm diameter scales approximately by $L_{p/m}$ = 20 with no distortion of energy slope. The settling velocity relationship of prototype particles smaller than 20.0 mm will be slower in the model than in the prototype.

Bed Load Rate – Shen (6) recommends scaling bed load rate for sand and gravel dominated systems using the Meyer-Peter and Mueller (1948) bed load equation. The bed load per second per unit width is expressed as;

$$b_l = 8\left(\frac{\tau - \tau_c}{(\gamma_s - \gamma)k}\right)^{3/2}(\gamma_s - \gamma)^{3/2} k^{3/2} \frac{g^{1/2}}{\gamma^{1/2}} \qquad (1)$$

where b_l *=bed load, k=grain diameter and g* = acceleration of gravity

The ratio of bed load rate between prototype and model can then be expressed as,

$$\frac{b_{l\ p}}{b_{l\ m}} = \frac{(T - T_c)_p^{3/2}}{(T - T_c)_m^{3/2}} \frac{(\gamma_s - \gamma)_p^{3/2}}{(\gamma_s - \gamma)_m^{3/2}} \frac{k_p^{3/2}}{k_m^{3/2}} \qquad (2)$$

where, $T - T_c$ = Shields parameter – critical Shields parameter

Given the p/m ratio of $T - T_c$ and specific weights are one and a particle geometric scale ratio of 20, bed load transport rate per unit width scales by the factor,

$$\left[\frac{bed\ load}{unit\ width}\right]_{\frac{p}{m}} = 20^{3/2} = 89.4 \qquad (3)$$

Time Scale for Sedimentation Process – Based on Froude scale, time scales by the square root of the length scale. This time scale is applicable to the sedimentation process

when sediment can be modeled undistorted. This can be shown by applying similarity of bed load transport. For modeling sands and gravels, Shen proposes using a time scale based on; $T = \frac{a}{b_l/(\lambda_s - \lambda)}$ *(4)*

where, *T* = characteristic time, *a*= channel cross sectional area and b_l = bed load based on Meyer-Peter and Mueller
Equation 4 written in terms of scale ratios equals,

$$T_{\frac{p}{m}} = L_{\frac{p}{m}}^{2} (T - T_c)_{\frac{p}{m}}^{-3/2} (\gamma_s - \gamma)_{\frac{p}{m}}^{-1/2} k_{\frac{p}{m}}^{-3/2} \quad (5)$$

where: *p/m* = prototype to model scale ratio.

When $(T - T_c)_{\frac{p}{m}}$ and $(\gamma_s - \gamma)_{\frac{p}{m}}$ =1 and particle size scales geometrically,

$$T_{\frac{p}{m}} = 20^{1/2} \quad (6)$$

Hydraulic Structures

The existing diversion facility includes canal headworks, invert elevation 762.75, with three-10-ft-wide bays controlled by 8-ft-high radial gates. A gated spillway is located adjacent and to the left of the canal headworks. The spillway referred to herein as the service spillway, has one 10-ft-wide bay and three, 16-ft-wide bays controlled by 10-ft-high radial gates. The upstream apron of the service spillway is set 5 ft lower than the canal upstream apron to facilitate sluicing sediment away from the canal entrance. An incised channel extends downstream of the spillway approximately 1,000 ft before merging with the natural channel. A fishway entrance is located on the right bank near the toe of the spillway apron. The downstream spillway channel contains several rock weirs that provide improved flow conditions for upstream migrating fish. The diversion dam is an ungrouted rock structure with a wooden center cutoff wall. River flows greater than about 6,000 ft^3/s exceed the spillway capacity and overtop the rock dam. Significant overtopping has historically resulted in erosion of the downstream dam slope and downstream channel. The canal headworks, spillway, downstream spillway channel and diversion dam were included in the physical model (figure 8). Fish screen facilities and fishway are located off channel and were not included in this study. The diversion dam was modeled as a fixed, non-erodible structure.

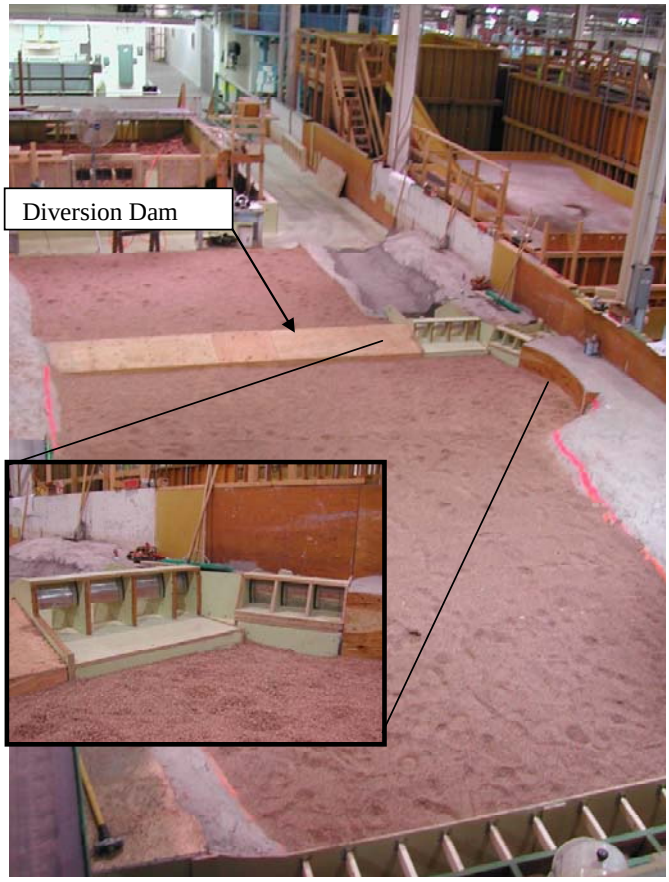

Figure 8 - View of the service spillway and canal headworks looking downstream.

View looking upstream at service spillway discharge channel.

Model Operation

Flow was provided to the model from a permanent laboratory pump and water measurement facility. Model discharge was measured using laboratory venturi meters. At the head of the model, flow entered a model headbox where it passed through a gravel baffle diffuser and over a fixed weir, (figure 4 - section). Flow distribution across the upstream weir was checked against velocity distributions from 2-dimensional numerical modeling results that included the influence of upstream channel geometry,(7). Model velocity measurements were obtained using a 2-directional acoustic velocity current meter manufactured by Sontek Corporation. Sediment was added to the flow downstream of the headbox using two 8-ft-long sand augers with 0.75- inch-high horizontal paddles for sediment injection. A gear motor was connected to the axle of each hopper to control the feed rate. Sediment added at the upstream end of the model either deposited within the model topography or moved through the model and was trapped in a downstream settling basin. Approximately six cubic yards of sediment was processed for each model test to obtain a particle gradation that scaled similar to the prototype. After each test, material deposited in the model and in the settling basin was collected and reused in subsequent tests. Prior to each test baseline topography within the channel upstream of the diversion dam was re-established. A straight screed was used to achieve a constant slope from the upstream weir (~elevation 770) to elevation 755.5 at the upstream toe of the diversion dam (figure 9). Water-surface elevations were measured using surface-mounted point gages located near the existing fishway exit, upstream and adjacent to the to the dam left of the spillway, 200 ft (prototype) downstream of the dam axis in the spillway channel and in the diversion canal. Additional tailwater control above that provided by downstream model topography was not necessary due to the steep gradient of the channel.

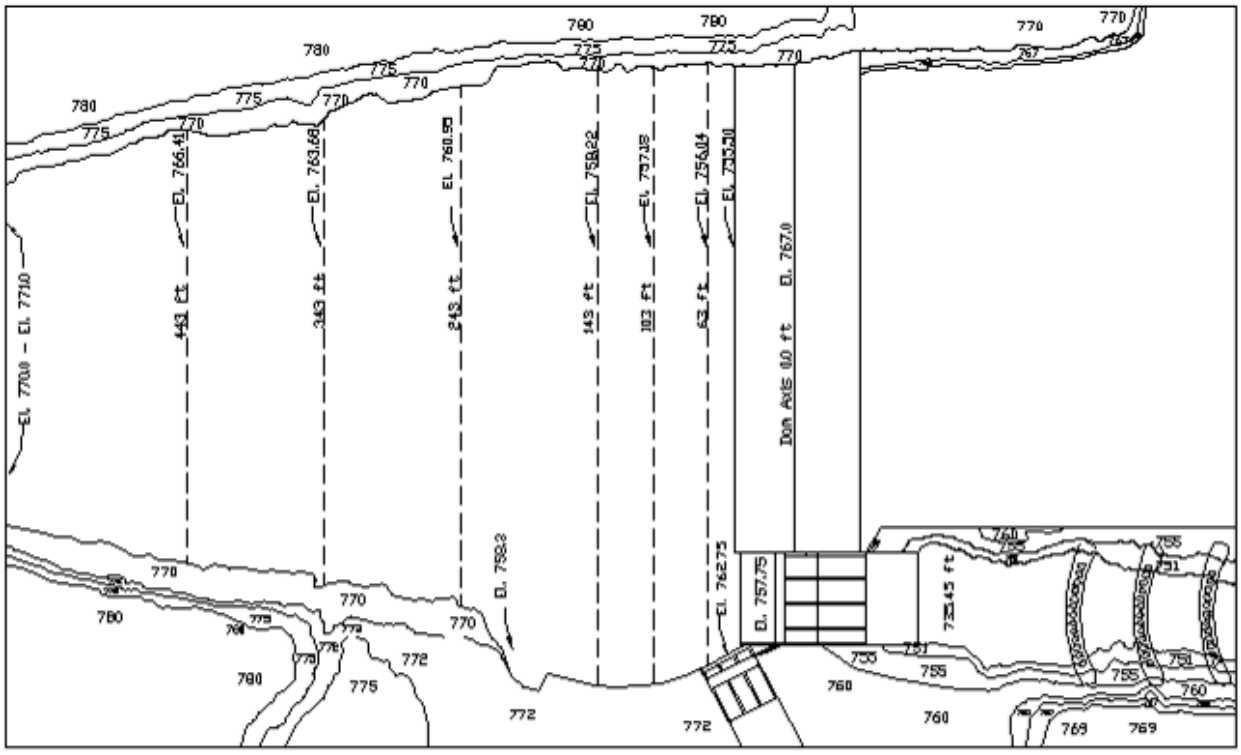

Figure 9 - Pretest channel bed topography.

Simulated Flood Hydrographs - Tests were conducted to evaluate sediment movement and canal entrainment for simulated flood hydrographs with peak discharges of 6,000 ft^3/s and 14,000 ft^3/s. A 6,000 ft^3/s peak flow is approximately a two-year return flood and a 14,000 ft^3/s peak approximately a ten-year return flood. Hydrographs were developed for each flow by using historic events of similar peak flow from average daily flow records. Prototype hydrographs were scaled to model flow and duration, (figures 10 and 11). Discharge values corresponding to one-half-hour time increments model were then selected from model hydrographs and used during testing. In the physical model, prototype hydrographs were truncated at a flow of about 2000 ft^3/s, below which numerical sediment routing analysis predicts relatively small bed load transport (4).

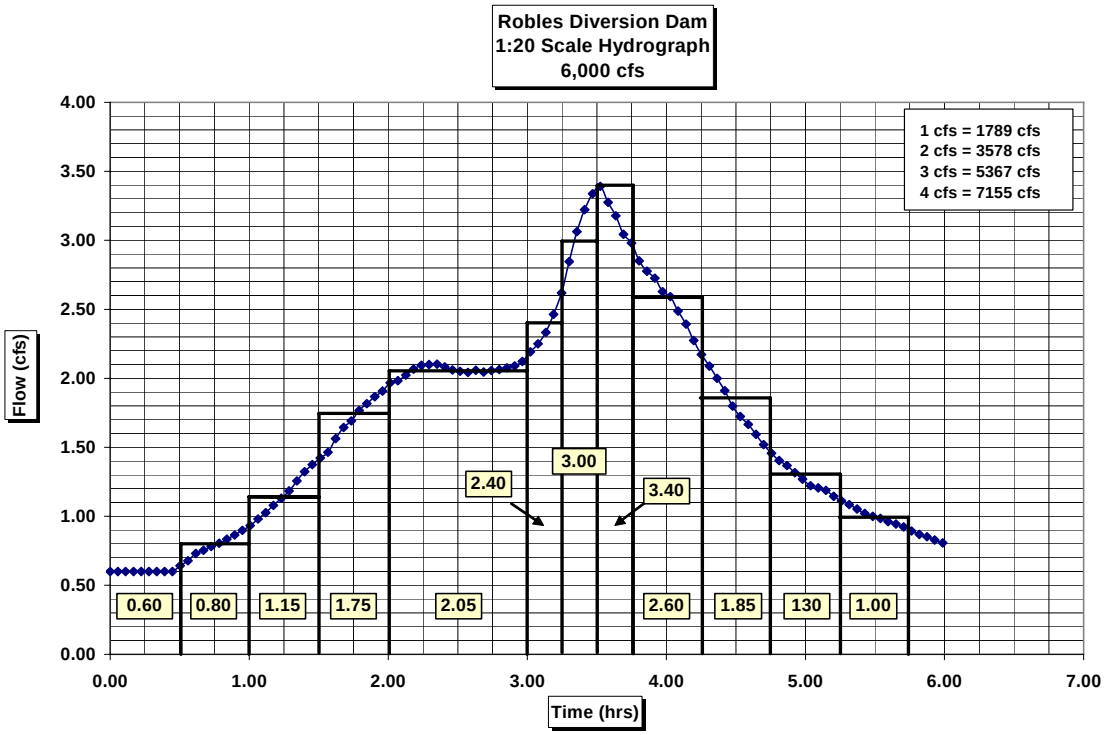

Figure 10 - Scaled 6,000 ft^3/s peak-flow hydrograph.

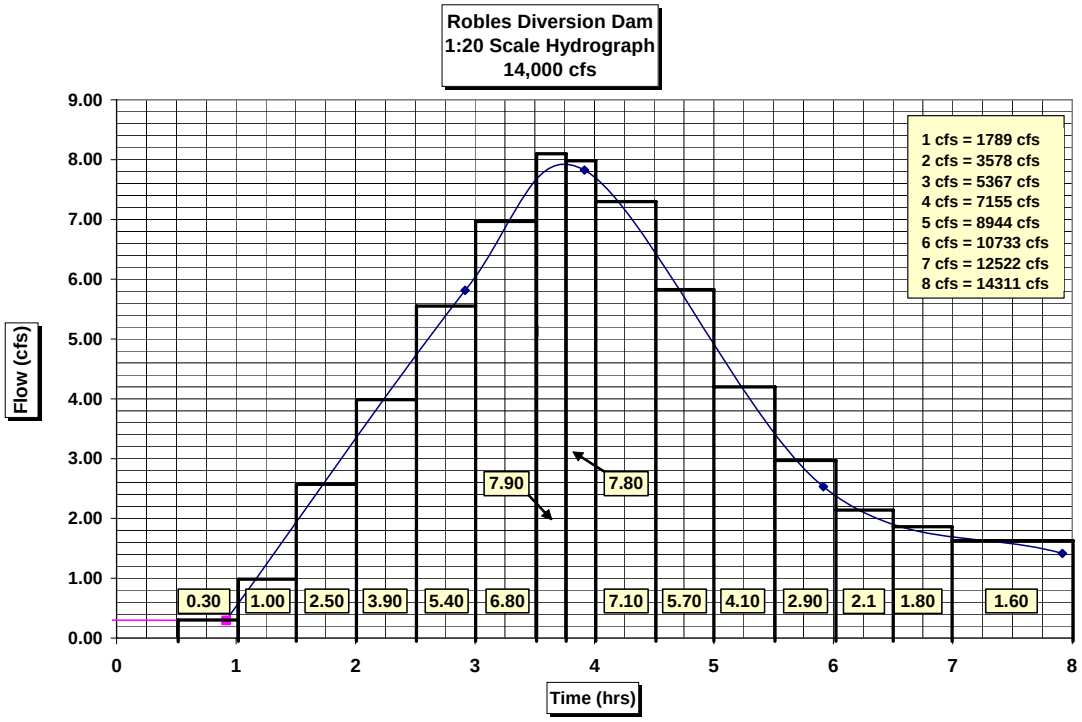

Figure 11 - Scaled 14,000 ft^3/s peak-flow hydrograph.

Model Tests

Tests were conducted for the two-year and ten-year flow hydrographs. The spillway gates were operated to maintain a pool elevation upstream of the diversion dam of 767.0 until flow exceeded the control capacity of the spillway above which the diversion dam was allowed to overtop. The canal gates were operated to limit flow diversion to the canal to a maximum of 500 ft^3/s. Gate operation (gate selection and gate opening) was varied during the study to broadly investigate the relation of gate location on sediment sluicing performance. For the study, spillway gates were referred to in increasing order from right to left looking downstream, figure 12. Individual canal gates are not referenced as they were opened uniformly during the study. Sediment was fed to the flow as required to control bed scour or bed load deposition in the channel at RM 14.27 to within +/- 1.0 ft prototype of the initial bed elevation. All tests were conducted for a post-dam-removal sediment load.

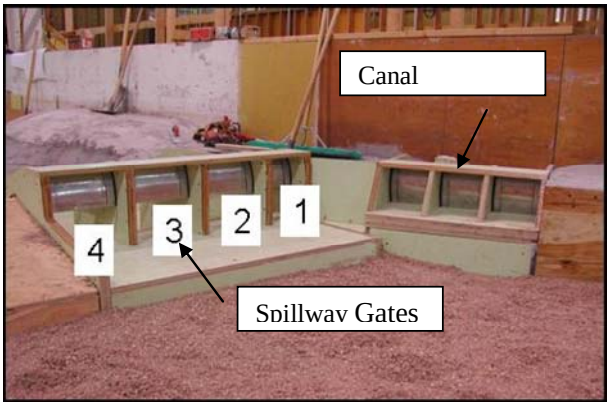

Figure 12 - Photograph of the model showing canal and service spillway.

Data Collection - Prior to and following tests, digital photographs were taken of the model from approximately twelve locations around the periphery of the model. Photographs were used to develop close range photogrammetric contour maps of the channel surface. The leading edge of the sediment delta upstream of the dam was also surveyed following each test as a check of the photogrammetric contours. During the tests, water surfaces were measured at all point gauges following flow changes. At the peak of the hydrograph, mid-depth velocity measurements were taken at 50-ft-intervals (prototype) across the channel 63 ft upstream of the dam axis. Total sediment volumes added during each test were recorded. Continuous measurement of the sediment load provided to the model was not attempted due to the difficulty of maintaining a calibrated delivery system for the large volume of sediment supplied during each test. Additional site specific velocity measurements were made during selected tests to document flow conditions for fish passage.

Test Results

Six moveable bed sediment tests were conducted to investigate spillway location. The canal headgates were operated to pass 500 ft^3/s for all tests. The model tests are referenced in the report based on the spillway options tested.

The nomenclature used to reference the six tests is listed below.

Flood Peak	Service Spillway	HFB Spillway added near Left Bank	HFB Spillway added near Right Bank
6,000 ft^3/s	Ss6000	HFB-L6000	HFB-R6000
14,000 ft^3/s	Ss14000	HFB-L14000	HFB-R14000

Two-year Flood with Post-Dam-Removal Sediment Loading, Test Ss6000 – Spillway gates were opened starting with Bay 1 followed by progressively opening bays 2-4 to maintain the pool elevation as flow increased. During the falling limb of the hydrograph, gates were closed starting with gate four and finishing with gate one. River flows and diversion pool elevation for each time step are given in table 2.

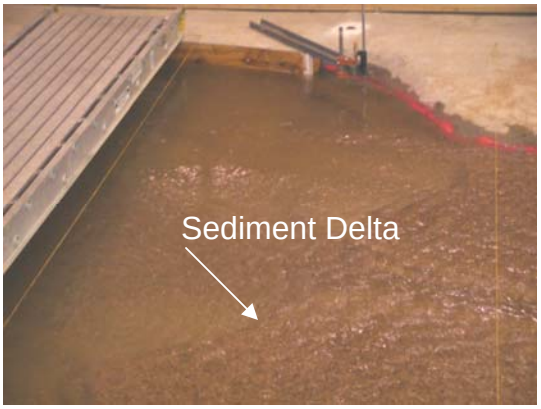

Figure 13 – Photograph of sediment delta building toward the service spillway.

Significant bed load transport started at flows between 2500 ft^3/s and 3000 ft^3/s. Bed load deposition within the diversion pool occurred largely in the form of a sediment delta that progressively worked downstream (figure 13). The delta progressed downstream faster near the left and right banks than mid-channel. This was likely due to higher flows entering the model near the left bank due to channel topography and the downstream right bank flow release through the spillway. A noticeable acceleration in the growth of the delta near the right bank was noted as the delta approached the zone upstream of the spillway where flow velocities rapidly accelerated. Upstream of the sediment delta, flow was generally shallow and swift. In the model, flow moving along the dam axis caused a strong flow contraction off the left upstream wall of bay 4 with a lesser contraction in bay 3. The contraction appeared to significantly reduce the flow capacity of bays 4 and 3 during high flows, however, no attempt was made in the study to measure the flow capacity of individual spillway bays. At the hydrograph peak the sediment delta had inundated the fishway exit (figure 14) and had reached to within about 50 ft of the spillway apron. The sediment delta reached the spillway apron after about 17 hrs (prototype) and started sluicing downstream. Flow velocity above the sediment delta was generally too shallow to measure in the model. Mid-depth flow velocities measured downstream of the sediment delta during the flood peak show a strong directional velocity component along the dam axis toward the spillway (figure 15). During the declining limb of the hydrograph, the sediment delta continued to spread laterally along the dam. Some bed sediments were entrained into the canal during the final one-third of the hydrograph as deposition in front of the canal headworks reached the canal sill elevation. Post-test channel bed elevations upstream of the dam are shown in figure 16. Photographs of the deposition pattern in the diversion pool and downstream spillway channel are shown in figure 17. Sediment deposition upstream of the delta front was fairly uniform across the channel with only minor channelization evident. The lack of channelization of the delta sediment likely resulted from the pool water surface in

Figure 14 – Sediment delta encroaching on the fishway exit at the peak of the Ss6000 test.

the model being held nearly constant until the test was terminated. This was necessary to evaluate and compare diversion pool deposition patterns as a function of spillway flow routing. The model was not operated to evaluate post-flood sediment sluicing effectiveness. Following the test, surface sediment samples were taken at a cross section 63 ft upstream of the dam axis. The gradation analysis of all samples is given in figure 18. The samples show coarser material located near the center of the channel and finer material near both banks.

Table 2 - Flow and water-surface elevations measured during test Ss6000.

Hydrograph Duration, hr	Qprototype (cfs)	Elevation (ft) Dam	Elevation (ft) Fishway Exit	Elevation (ft) Spillway Channel
0	1234			744.50
2.23	1420		766.84	n/a
4.47	2057	767.44	767.50	745.25
6.71	3130	767.27	767.19	746.60
8.94	3667	766.84	767.01	747.91
13.4	4293	766.54	766.68	747.94
14.53	5367	767.14	767.25	748.88
15.65	6082	767.24	766.94	749.35
17.14	4651	766.74	766.35	748.96
19.36	3309	766.54	766.38	747.06
21.6	2326	766.94	766.94	745.87
23.84	1789			

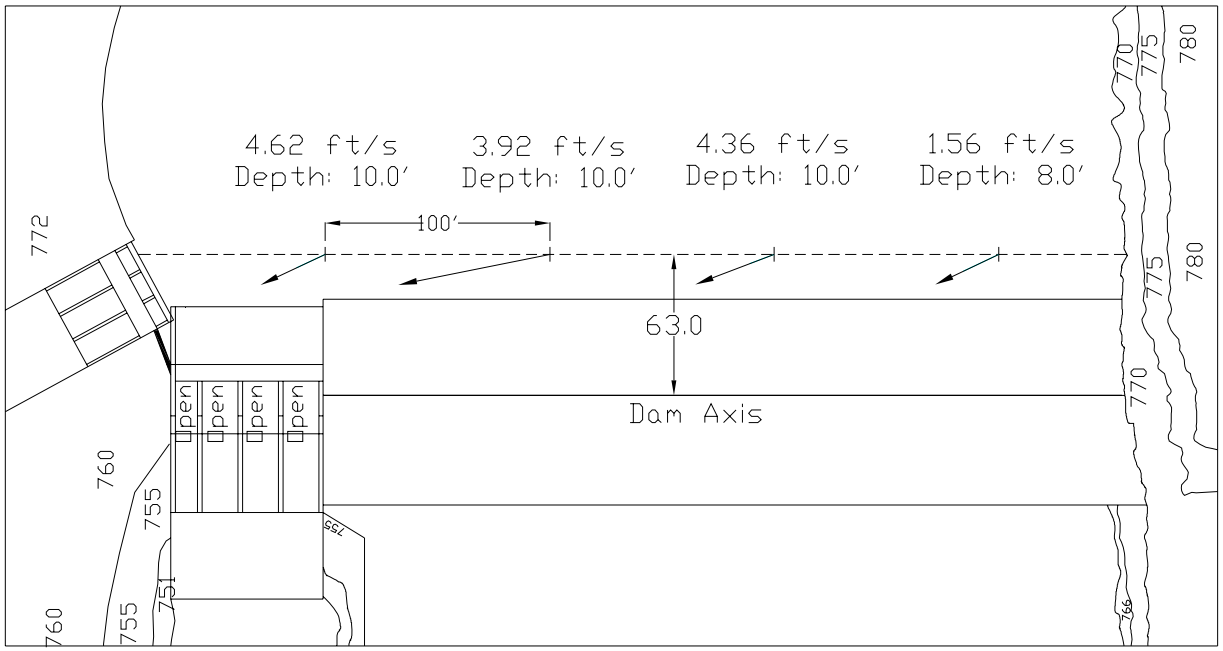

Figure 15 - Flow velocities measured during peak flow, test Ss6000.

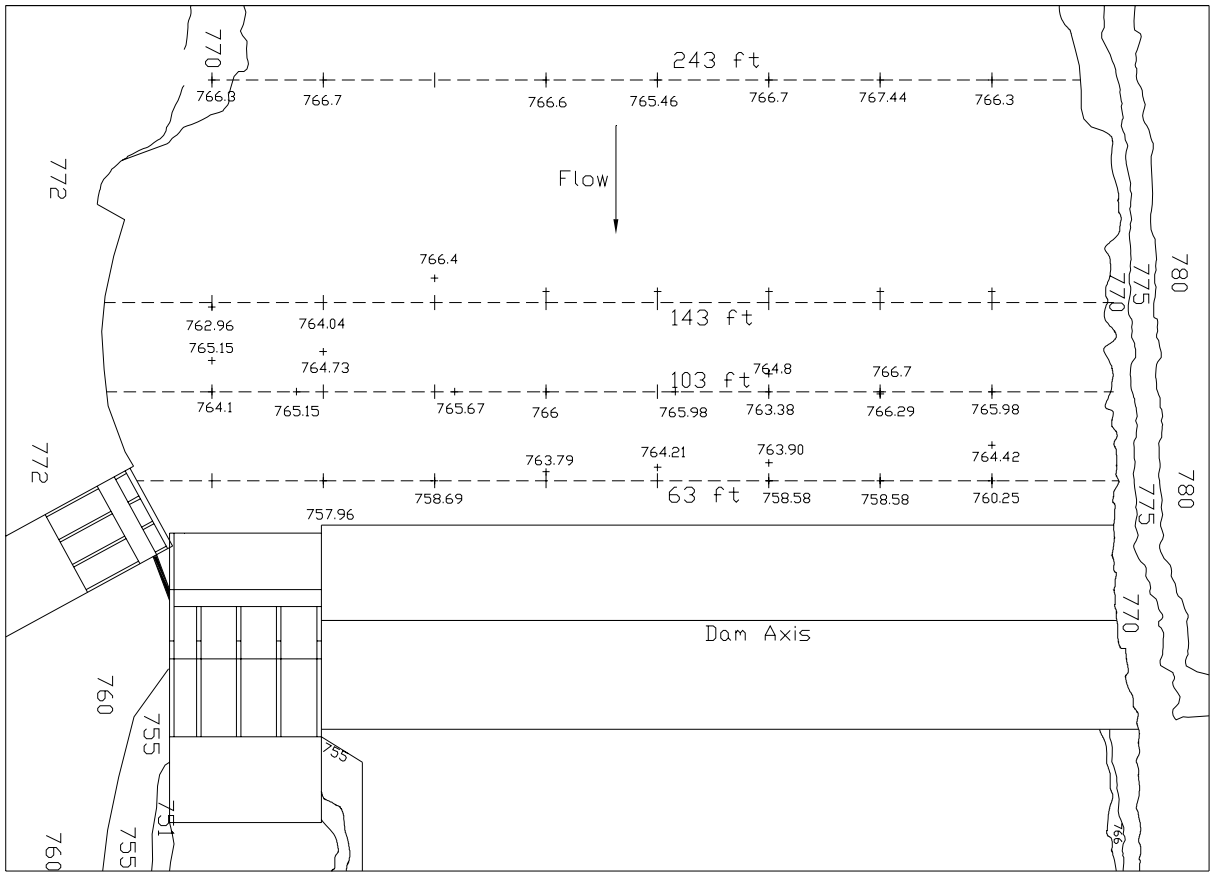

Figure 16 – Post-test Ss6000 diversion pool bed elevations upstream of diversion dam.

Diversion Pool

Upstream of Diversion Canal

Upstream Fishway Exit

Upstream of Service Spillway
Gate Structure

River Channel Downstream
of Service Spillway

Figure 17 - Post-test sediment deposition photographs for test Ss6000.

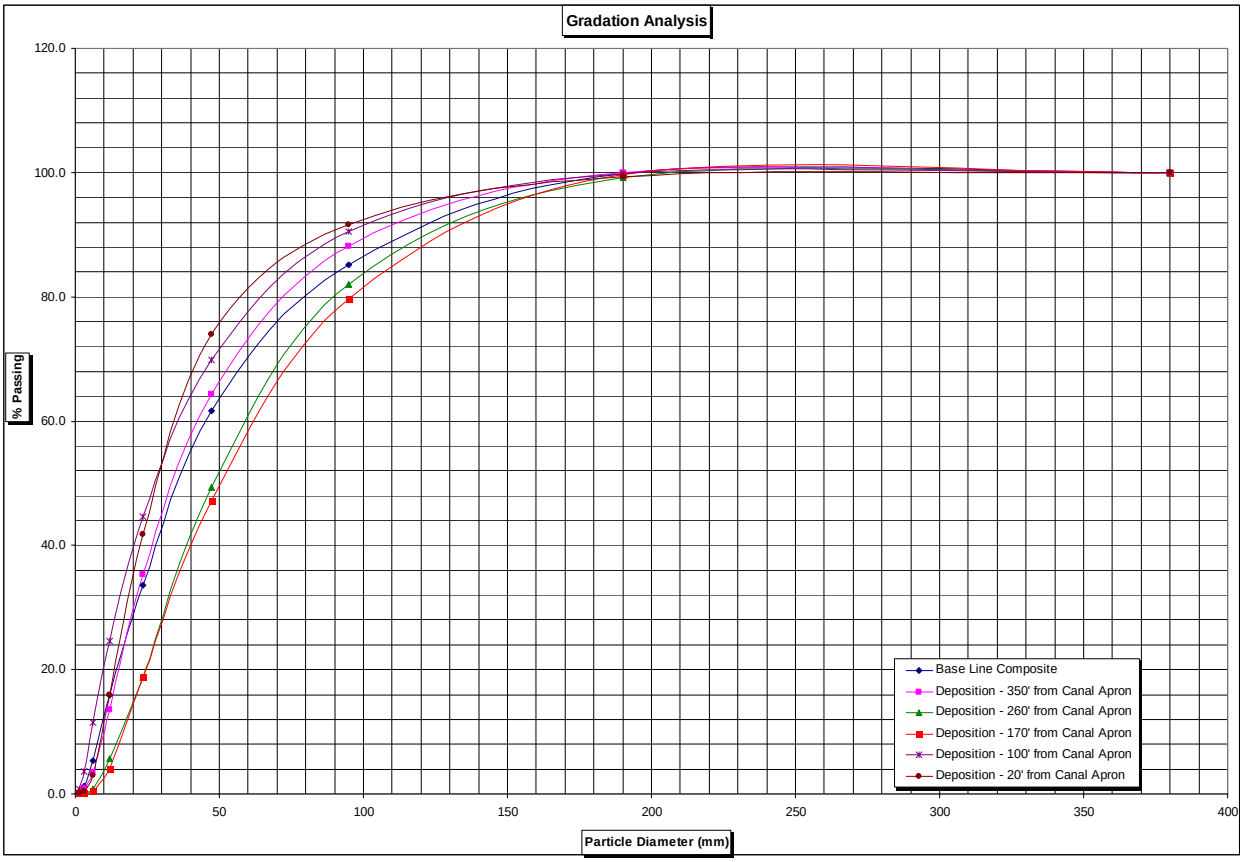

Figure 18 – Gradation of surface sediment samples taken at a cross section 63 ft upstream of the dam axis following test Ss6000.

Ten-Year Flood with Post-Dam-Removal Sediment Loading, Test Ss14000 -

The test was run for 6.0 hours in the model representing about 26.5 hours prototype. The test was terminated prior to the end of the hydrograph because sediment deposition upstream of the dam reached a steady state condition with bed load passing through the diversion pool to the spillway. Spillway gates were opened starting with Bay 1 followed by opening Bays 2-4 as required to prevent dam overtopping. The capacity of the spillway prior to dam overtopping was about 5,600 ft^3/s. Water-surface elevations measured during the test are given in table 3. Some variability in water surface elevation occurred during the testing due to the diversion pool response time and frequent gate adjustments required to maintain a nearly constant pool elevation until all spillway gates were full open.

The sediment delta extended downstream to the fishway exit after about 6.7 hrs (prototype). The delta reached the spillway apron and sediment started passing through the spillway after approximately 11 hrs (prototype) at a flow of 12,100 ft^3/s. At the flood peak, the sediment delta extended onto the canal apron initiating entrainment of bed sediment into the canal. Large quantities of sediment were entrained by the spillway into the downstream channel. Surveys of the spillway channel invert elevation during the test revealed the area between rock weirs filled with sediment changing the channel invert to a plain bed. In the model, sediment near the head of the spillway channel deposited to about elevation 750 partially covering the baffled apron and the fishway entrance. Fishway flow exiting the fishway was not modeled and therefore the model may not correctly represent local flushing of sediment near the fishway entrance. At about 17 hrs (prototype, flow = 10,000 ft^3/s) the sediment delta built to the crest of the dam and bed sediment began passing over the crest. During much of the declining limb of the hydrograph sediment depositions in the canal restricted the diversion capacity of the canal to less than full capacity. Near-dam velocities measured during the rising limb of the flow hydrograph at a flow of 6,977 ft^3/s are shown in figure 19. Upstream of the sediment delta's downstream leading edge flow depths were too shallow to measure flow velocity in the model. Near the fishway exit, greater than 11 ft of deposition occurred during the test (figure 20). In front of the canal headworks, sediment deposits reached higher than elevation 763. Post-test sediment deposition within diversion pool bed, canal and downstream channel is shown in figure 21. A general pattern within the basin of sediment movement toward the spillway and canal headworks is evident.

Table 3 - Flow and water-surface elevations measured during test Ss14000.

Hydrograph Duration, hr	Qprototype (cfs)	Elevation (ft) Dam Crest	Elevation (ft) Upstream	Elevation (ft) Spillway
0	536.66	n/a	764.46	n/a
2.23	1788.85	766.84	766.71	744.78
4.47	4472.14	766.64	766.39	748.20
6.7	6976.53	769.64	768.89	749.78
8.93	9659.81	770.37	769.95	750.82
11.16	12164.21	770.84	769.94	751.09
13.39	14131.95	771.44	769.67	751.06
14.86	13953.06	771.34	769.90	750.96
16.34	12700.87	771.44	770.07	749.91
17.82	10196.47	771.34	770.07	749.98
20.05	7334.30	770.34	n/a	749.25
21.17	5187.68	768.14	n/a	748.04
21.69	4472.14	767.24	n/a	747.71
22.21	3756.59	766.84	n/a	747.22
23.32	3219.94	766.84	n/a	747.48
24.45	2862.17	766.84	n/a	746.69

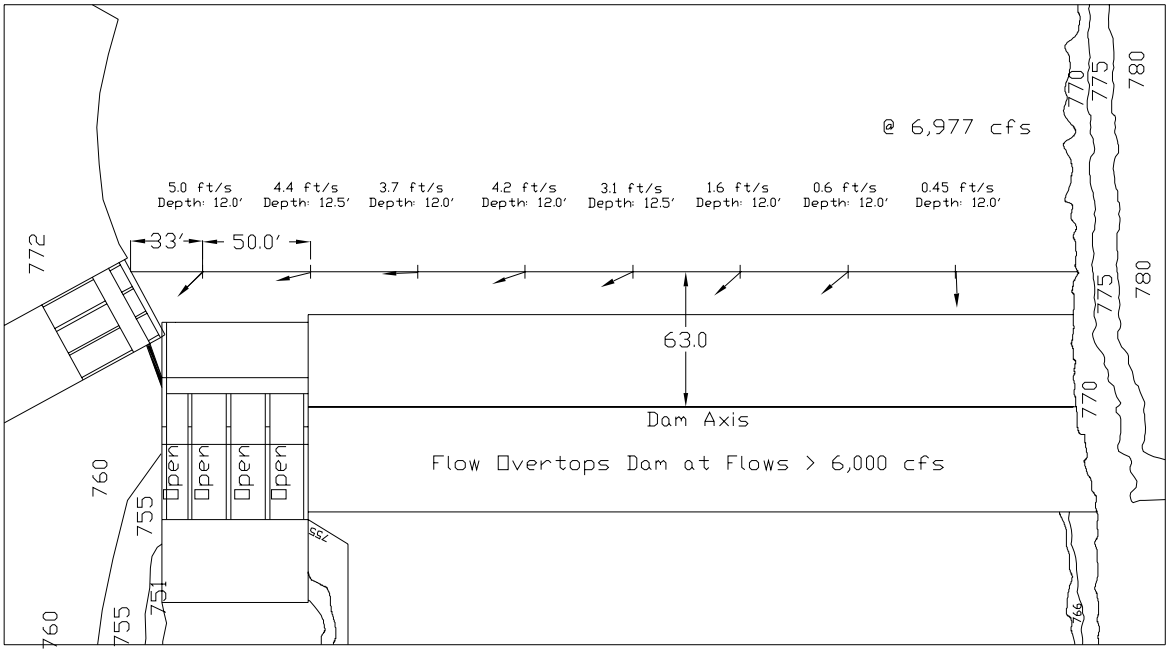

Figure 19 – Flow velocities measured during peak flow, test Ss14000.

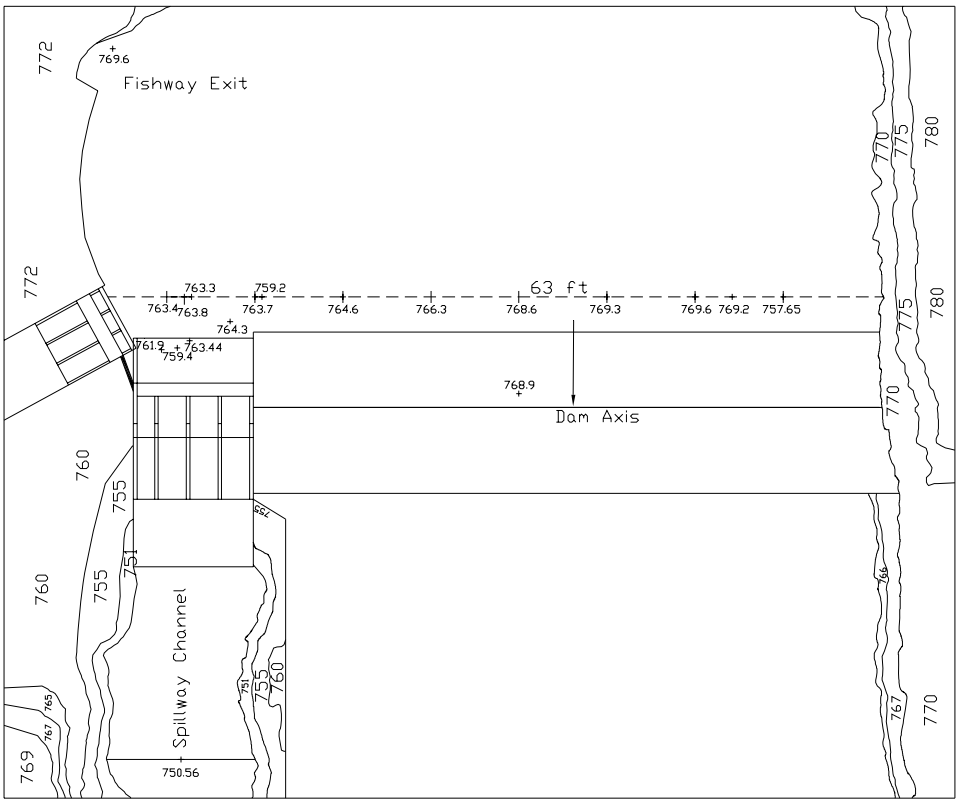

Figure 20 - Post-test Ss14000 diversion pool bed elevations upstream of diversion dam.

View looking Downstream

Downstream of Diversion Canal

Upstream Fishway Exit

River Channel Downstream of Service Spillway

Upstream of Sluice Radial Gate Structure & Dam Crest

Figure 21 - Post-test sediment deposition photographs for test Ss14000.

High Flow Bypass Spillway

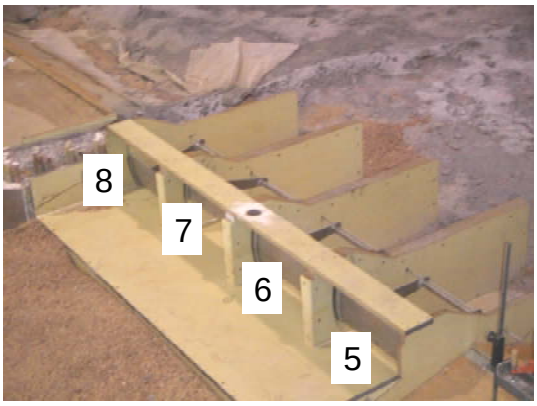

Figure 22 View of HFB spillway bay numbering scheme used in the model.

The high flow bypass spillway was designed to increase the spillway capacity of the diversion dam from about 6,000 ft^3/s to about 14,000 ft^3/s. Increased spillway diversion capacity will be needed following removal of Matillia Dam to expand the water districts ability to sluice increased bed load through the diversion pool during major flood events. The proposed HFB spillway had four 30-ft-wide radial gate spillway bays, (figure 22). In the model study, the HFB gates are referenced from right to left as spillway gates 5 through 8. The upstream sill elevation of the HFB spillway apron was set similar to the

service spillway at elevation 757.75, (figure 23). Flow from the gates entered a 51.4-ft-long Reclamation Type I stilling basin. Downstream of the HFB spillway stilling basin, the channel was sloped upward at a 1V:4H slope to elevation 757.0 followed by a rock ramp sloping downward at approximately 2.5 percent. The downstream rock ramp was designed to provide flow conditions suitable for upstream passage of adult steelhead. The service spillway channel and the HFB spillway channel were separated by a rock berm for a distance of about 900 ft downstream.

Two series of tests were conducted to evaluate sediment deposition in the diversion pool based on HFB spillway location. The first location tested was on the dam 187 ft left of the service spillway near the left bank, figure 24. This location was chosen to evaluate diversion pool sediment movement and deposition when high flows were released downstream adjacent to the bank opposite the diversion. The second HFB location tested was 30 ft to the left of the existing spillway. This location provided more of a river center release and was desirable as it provided for access to all facilitates from the right bank and allowed for easier management of spills for fish passage. Sediment movement and deposition patterns within the diversion pool were documented for both HFB positions.

Model Test Results for Left Bank HFB Spillway

HFB-L6000 Test Results – The test was run for about 5 hours in the model representing about 22 hours prototype, table 4. Spillway gate 1 was maintained at a 5 ft opening throughout the test. Gates 2-4 of the existing spillway were not opened during the test. HFB spillway gates 6 and 7 were progressively opened as needed to maintain the diversion pool and prevent dam overtopping. Near the hydrograph peak, gates 5 and 8 were opened 2 ft. Gates 5 and 8 were subsequently the first gates closed as the flows declined. The sediment delta advanced through the upper one-half of the diversion pool fairly even across the channel. As the delta moved to within about 200 ft of the spillway, the influence of the strong flow movement toward the HFB spillway accelerated the building of the delta in the direction of the HFB. The sediment delta advanced at a slower rate on the right side of the channel. The sediment delta advanced downstream to the HFB after about 10 hrs (prototype). On the right bank the delta had advanced downstream to about the fishway exit. At the flood peak, the sediment delta extended onto the HFB apron and significant bed load was continuously moving through the spillway, (figure 25). The sediment delta near the right bank had advanced to within approximately 150 ft of the dam axis inundating the fishway exit. Flow velocities measured upstream of the dam during the flow peak are shown in figure 26. During the declining limb of the hydrograph heavy sediment loads continued to pass through the HFB spillway. The progression of the sediment delta toward the service spillway and canal diversion slowed as much of the sediment was drawn toward the HFB. No bed sediments were entrained into the canal during the test.

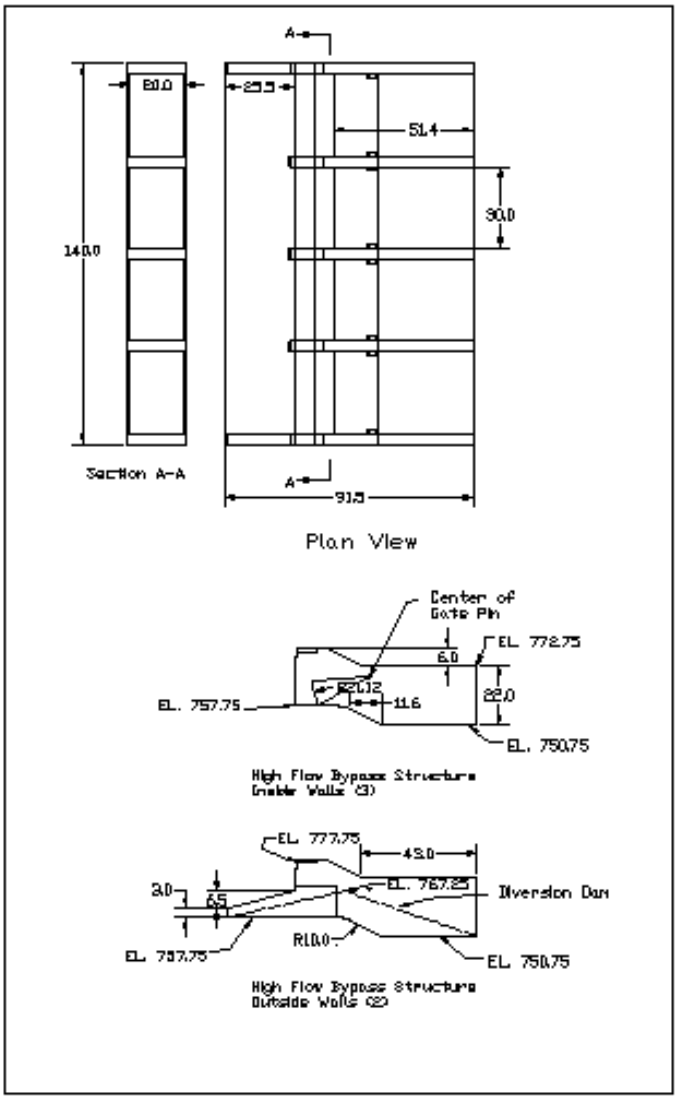

Figure 23 – HFB spillway plan and sections.

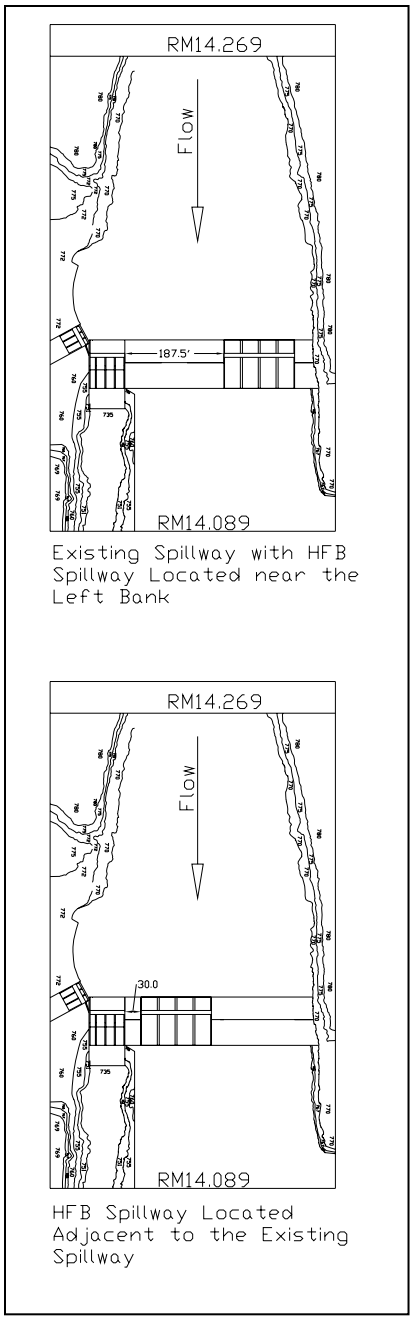

Figure 24 - HFB spillway locations tested in the model

Figure 25 - Sediment passing through the HFB spillway during the flood peak.

A small amount bed material passed downstream through gate 1 into the spillway channel. Survey bed elevations of the post-test sediment deposition in the diversion pool are given in figure 27. Photographic records of the post-test sediment deposition are given in figure 28. A close range photogrammetric survey of the post-test diversion pool bed is shown in figure 29. At the end of the test flood, the leading edge of the sediment delta near the right bank was located about 100 ft upstream of the canal diversion thus allowing the canal to be operated at capacity during the entire flood. Surface sediment gradation samples of the post-test bed near the dam do not indicate a significant change in bed material gradation occurred in the diversion pool, (figure 30). The data does show slightly finer material deposited adjacent to the channel boundaries.

Table 4 - Flow and water-surface elevations measured during test HFB-L6000.

Hydrograph Duration, hr	Qprototype (cfs)	Elevation (ft) Dam	Elevation (ft) Fishway Exit	Elevation (ft) Spillway Channel	Spillway Gate Operation
0	1431	766.54	766.30	742.10	3 canal gates open; Gate 1 @ 5'
2.23	2057	766.84	766.82	744.30	Gate 1 @ 5' & Gate 6 @ 2.5'
4.47	3130	766.44	766.43	744.43	Gate 1 @ 5' & Gate 6 @ 4.0'
6.7	3667	765.14	765.18	744.73	Gate 1 @ 5' & Gate 6&7 @ 4.5'
8.94	4293	765.64	765.61	744.79	Gate 1 @ 5' & Gate 6&7 @ 5.0'
10.06	5367	766.44	766.49	744.89	Gate 1 @ 5' & Gate 6&7 @ 6.5'
11.17	6082	766.44	765.84	745.81	Gate 1 @ 5' & Gate 6&7 @ 10.0' & Gates 5&8@2.0'
12.89	4651	766.24	765.90	745.35	Gate 1 @ 5' ; Gates 6,7 @ 5'
15.12	3309	766.54	766.43	744.89	Gate 1 @ 5' ; Gate 6 @ 5'
17.35	2326	765.94	765.77	744.66	Gate 1 @ 5' ; Gate 6 @ 2'
19.58	1789	766.74	765.44	744.73	Gate 1 @ 5' ; Gate 6 @ 1'

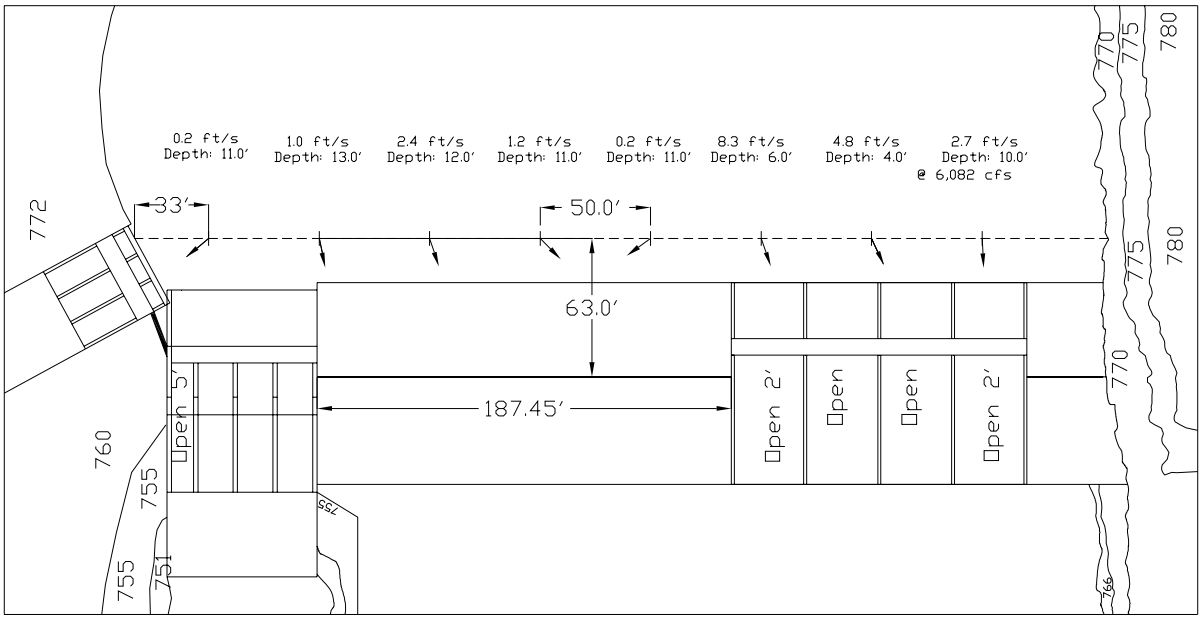

Figure 26 - Flow velocities measured during peak flow, test HFB-L6000.

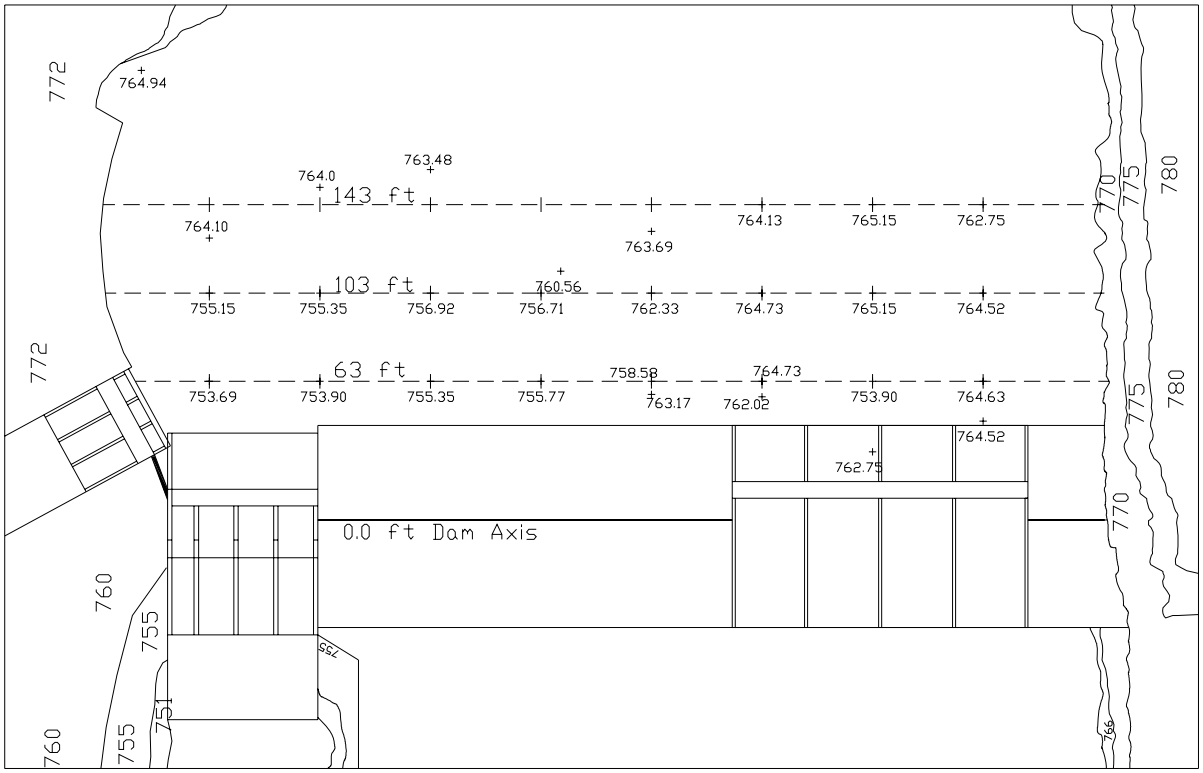

Figure 27 – Post-test HFB-L6000 diversion pool bed elevations upstream of diversion dam.

Three views of Sediment in Diversion Pool with Left Bank HFB Spillway

View of sediment deposition at fishway exit

View looking upstream at left bank rock ramp

View of Spillway Channel

Figure 28 – Post-test sediment deposition photographs for test HFB-L6000.

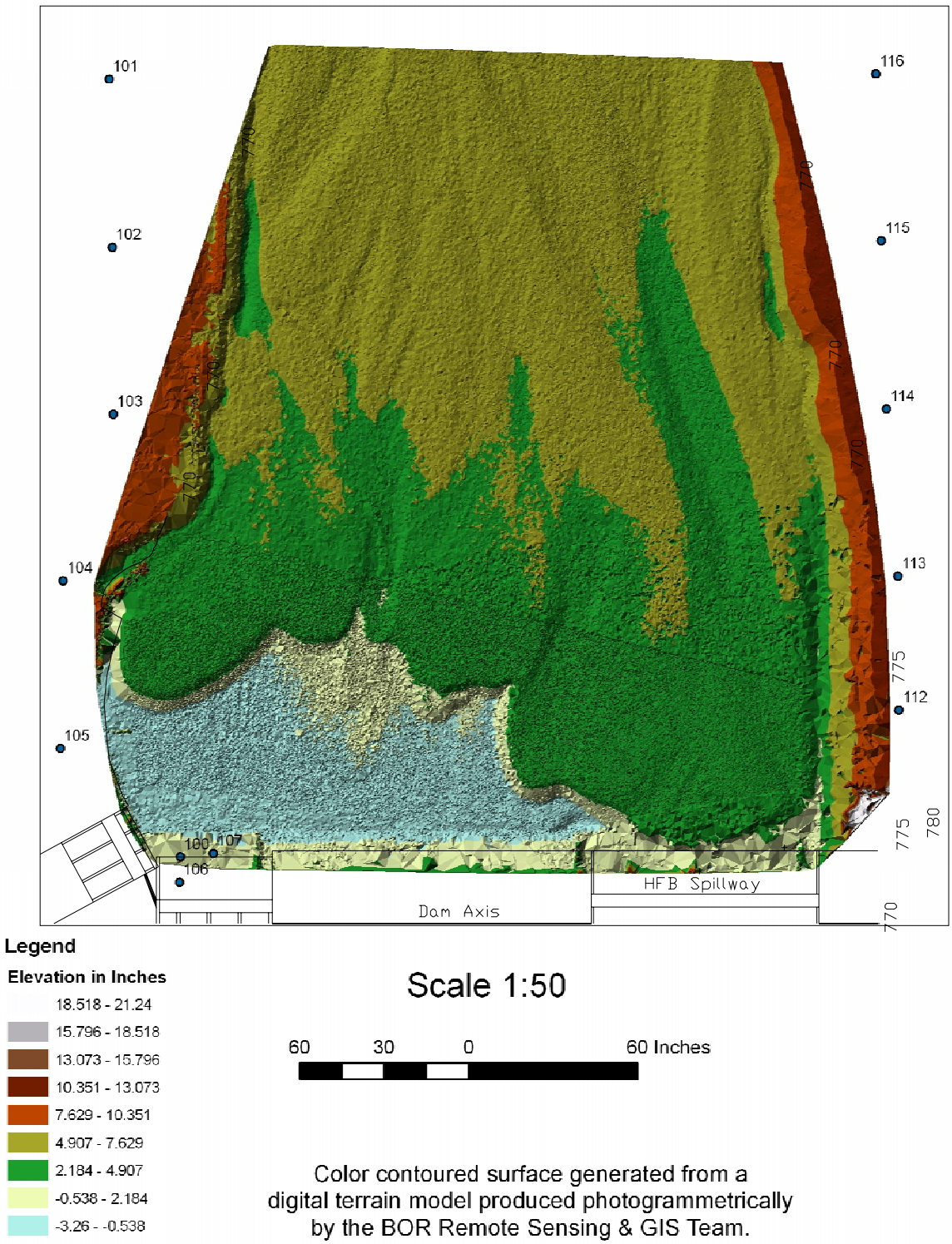

Figure 29 – Close range photogrammetry-generated plot of final channel elevations for test HFB-L6000. Elevations shown are model referenced to a zero datum at elevation 757.75.

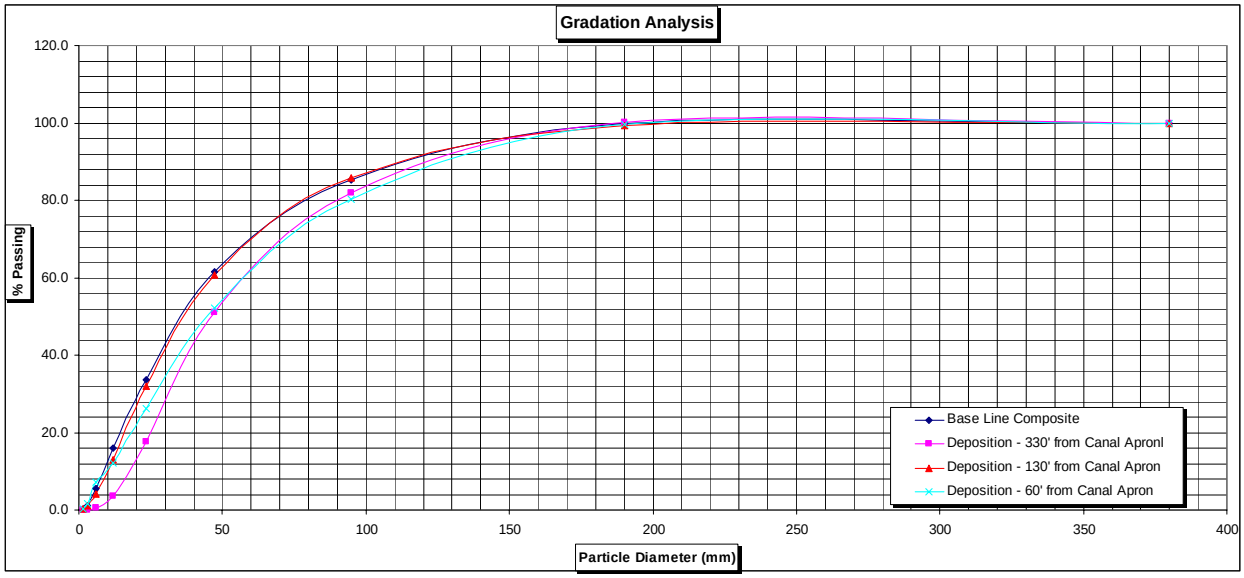

Figure 30 – HFB-L6000 surface sediment gradation sampled along a cross section located 63 ft upstream of the dam axis.

HFB-L14000 Test Results – The test was run for 7.0 hours in the model representing about 31 hours prototype, (table 5). Spillway gates were opened starting with gate 1 at a 5 ft opening followed by gates 6 and 7. When the river flow reached 7,000 ft^3/s gates 5 and 8 were partially opened. At a flow of about 10,000 ft^3/s gates 5-8 were fully open. At the flow peak all gates were fully open and the dam was overtopping by about 0.75 ft. Strong flow contractions off the upstream guide walls were visible on bays 4, 5 and 8 reducing flow capacity through those bays. The sediment delta extended downstream to the HFB spillway and started passing through the spillway after about 6.7 hrs (prototype). Eleven hours into the flood (prototype) the sediment delta moving down the right bank inundated the fishway exit. After 15 hrs (prototype) the sediment delta reached the service spillway and was passing down the spillway channel. The spillway channel rapidly filled with sediment behind the rock weirs until the channel was flowing over a smooth bed of sediment. The large amount of bed material passing through the HFB resulted in the stilling basins downstream of gates 6 and 7 and to a lesser degree gates 5 and 8 filling with sediment when the gates were fully open, figure 31. The strong flow contraction through Bays 5 and 8 tended to sluice these basins along the inside walls where flow concentration was highest. As in previous tests, some variation in water surface elevation occurred

Figure 31 - View of sediment filling the HFB stilling basin.

during the testing due to the diversion pool response time and frequent gate adjustments required to maintain a nearly constant pool elevation until all spillway gates were full open. Near-dam velocities measured at the peak discharge are shown in figure 32. A flow stagnation point is evident located about one third the dam width from the right side. This location also was found to have the greatest sediment deposition following completion of the test, (figure 33). Small amounts of bed sediment were drawn into the canal during the test. Deposition in front of the canal apron reached approximately elevation 762. During the test 6.5 yds^3 model (52,000 yds^3 prototype) of sediment were fed into the model. Photographs of the post-test channel bed and a photogrammetric-generated channel surface are given in figures 34 and 35, respectively. Gradations of surface sediments deposited along a cross section 63 ft upstream of the dam axis are given in figure 36. Sediment gradations were similar with generally finer material deposited closer to the channel banks.

Table 5 - Flow and water-surface elevations measured during test HFB-L14000.

Hydrograph Duration, hr	Qprototype (cfs)	Elevation (ft) Dam	Elevation (ft) Fishway	Elevation (ft) Spillway Channel	Spillway Gate Operation
0.00	894	766.04	766.23	742.46	3 canal gates open (only)
2.23	1789	767.04	765.90	744.59	Gate 1 @ 5' ; Gate 6 @ 1.5'
4.47	4472	766.24	766.17	744.96	Gate 1 @ 5' ; Gate 6,7 @ 3.5'
6.70	6977	765.24	765.05	745.02	Gate 1 @ 5' ; Gates 6,7 @ 10'; Gates 5,8 @ 2'
8.93	9660	766.54	765.84	749.61	Gate 1 @ 5' ; Gates 6,7 @ 10'; Gates 5,8 @ 4'
11.16	12164	766.94	765.71	749.94	All gates full open
13.39	14132	767.64	766.33	751.16	All gates full open
14.50	13953	768.04	766.69	751.19	All gates full open
15.63	12701	768.04	766.56	749.75	All gates full open
17.80	10196	766.94	766.69	749.42	Closing sequence not reported
20.00	7334	766.44		748.56	Closing sequence not reported
22.31	5188	766.44		747.12	Closing sequence not reported
24.50	3757	765.94		746.60	Closing sequence not reported
26.77	3220	766.04		746.89	Closing sequence not reported
29.00	2862				

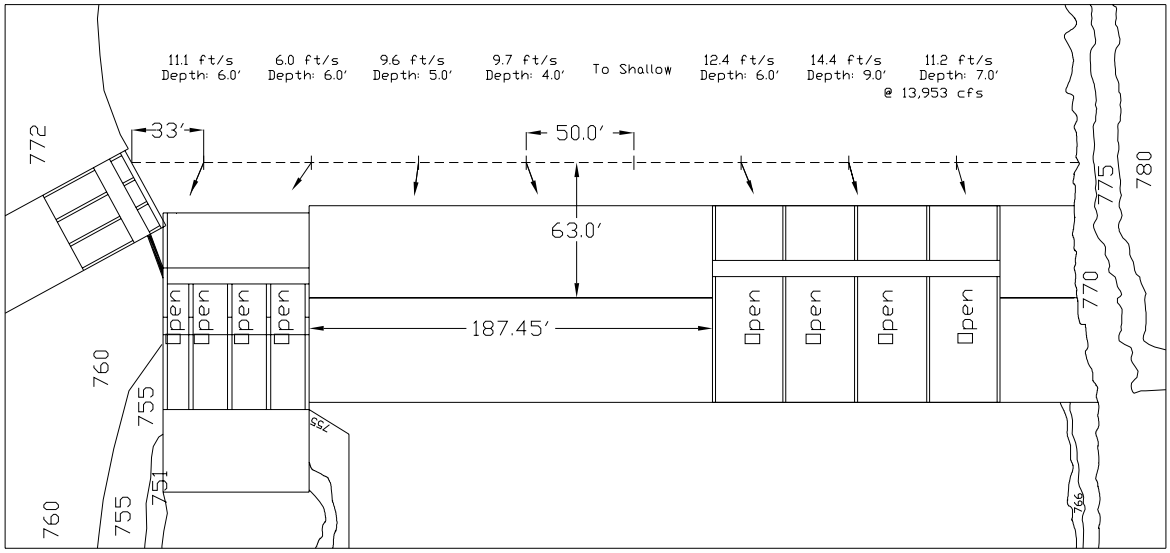

Figure 32 - Flow velocities measured during peak flow, test HFB-L14000.

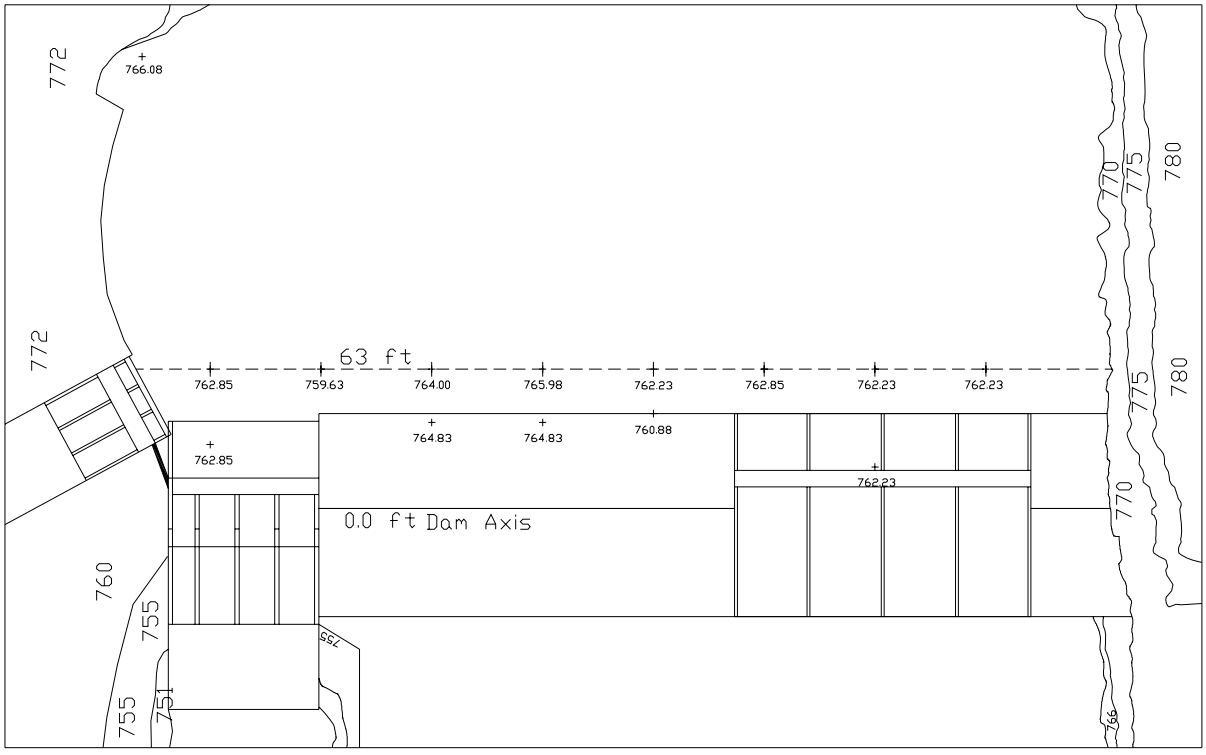

Figure 33 - Post-test HFB-L14000 diversion pool bed elevations upstream of diversion dam.

Three views of Sediment in Diversion Pool with Left Bank HFB Spillway

View looking downstream at rock ramp

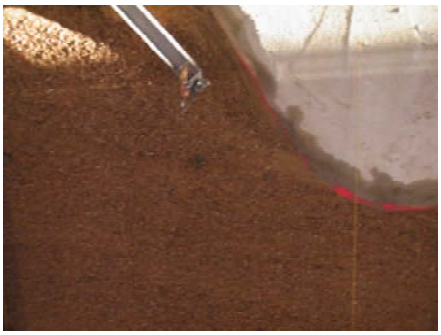

View of sediment deposition at fishway exit

Figure 34 - Post-test sediment deposition photographs for test HFB-L14000.

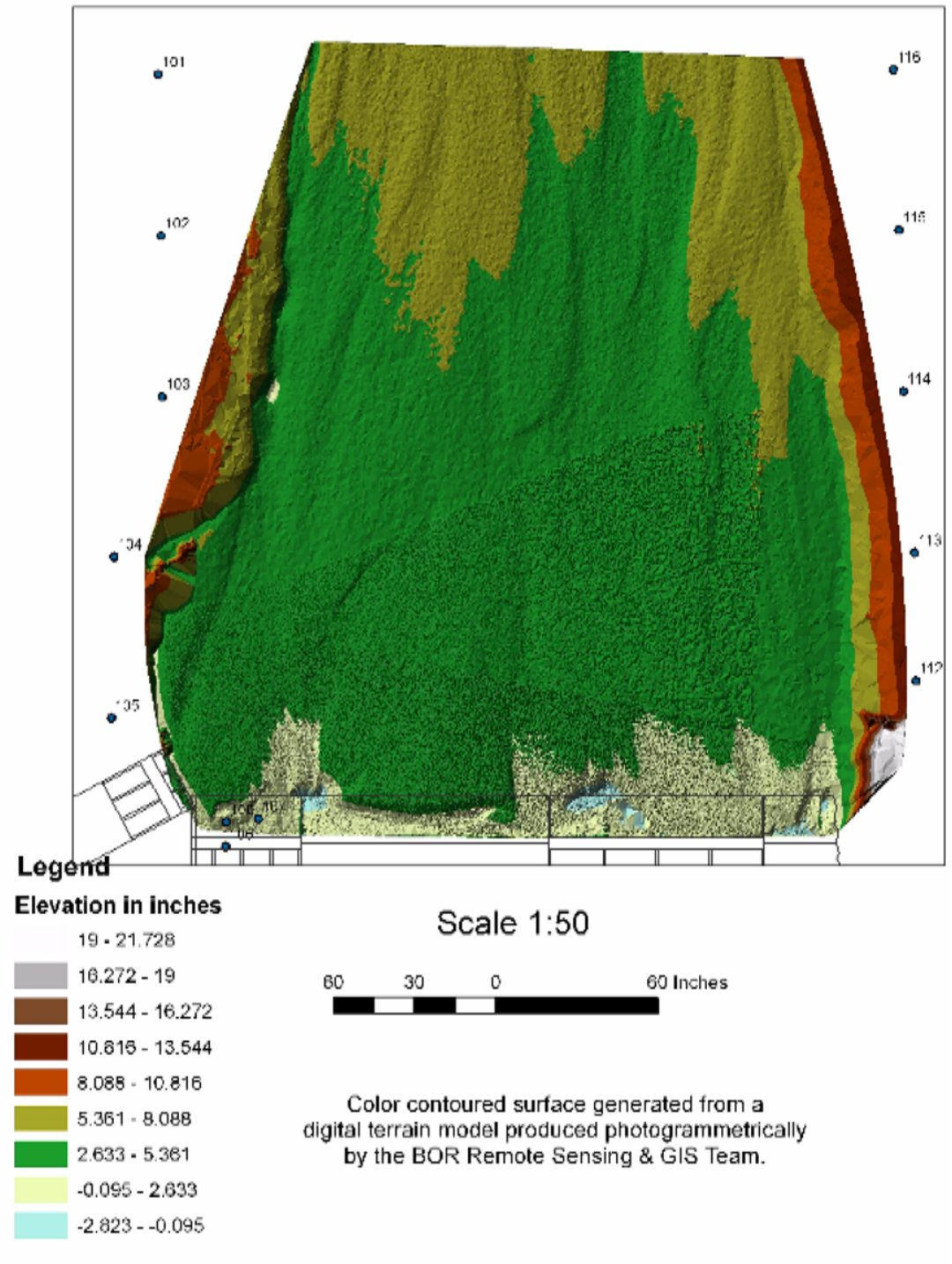

Figure 35 - Close range photogrammetry-generated plot of final channel elevations for test HFB-L14000. Elevations shown are model referenced to a zero datum at elevation 757.75.

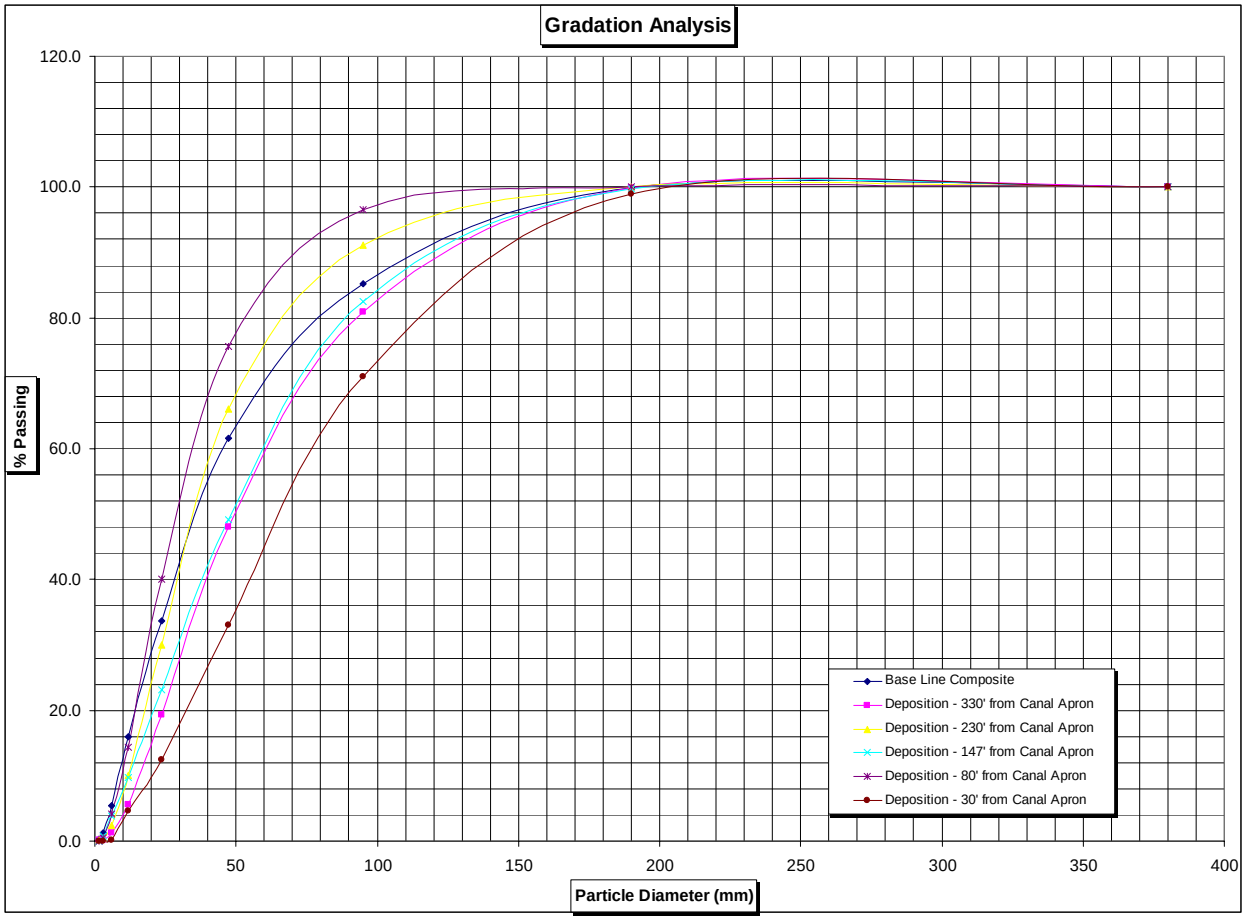

Figure 36 - HFB-L14000 surface sediment gradation sampled along a cross section located 63 ft upstream of the dam axis

Model Test Results for HFB Spillway Located Adjacent to the Service Spillway near the Right Bank

The HFB spillway was moved to a location 30 ft to the left of the service spillway and tests of 6,000 ft^3/s and 14,000 ft^3/s peak flow hydrographs repeated. Within this document the location is referred to as the right bank location. Thirty foot separation from the service spillway was chosen to provide reasonable separation of structures for construction of the prototype. The location resulted in the center of Bay 8 of the HFB spillway being approximately centered in the river channel,(figure 24).

HFB-R6000 Test Results – The test was run for about 6 hrs in the model representing about 27 hrs prototype, table 6. Service spillway gates were closed during the entire test. Primarily HFB gates 6 and 7 were operated during the tests. Gates 5 and 8 were opened 1 ft during the flood peak. During the initial eight hours (prototype) of the flood, the sediment delta built downstream fairly even across the channel to within about 160 ft of the dam axis. As the delta moved closer to the dam, the leading edge built more rapidly toward the HFB and at a slower rate along both channel banks. The delta front upstream of the HFB spillway built to within 80 ft of the dam after 14 hrs (prototype) and reached the HFB spillway 15.5 hrs (prototype) (figure 37). At the peak of the flood, sediment deposition along the right bank reached elevation 762 in front of the fishway exit with the sediment delta front located approximately 100 ft upstream of the dam axis. Flow velocities measured upstream of the dam during the flow peak are shown in figure 38. During the declining limb of the hydrograph heavy sediment loads continued to pass through the HFB spillway. The progression of the sediment delta toward the service spillway and canal diversion slowed as much of the sediment was drawn toward the HFB. No bed sediments were entrained into the canal during the test. Survey bed elevations of the post-test sediment deposition in the lower diversion pool are given in figure 39. Photographic records of the post-test sediment deposition are given in figure 40 and a close range photogrammetric survey of the post-test diversion pool bed is shown in figure 41. At the end of the test flood, the leading edge of the sediment delta near the right bank was located about 40 ft upstream of the canal diversion, thus allowing the canal to be operated at capacity during the entire flood. Surface sediment gradation samples of the post-test bed near the dam do not indicate a significant change in bed material gradation occurred in the diversion pool, figure 42. The data does show slightly coarser material deposited near the left channel bank. Gradation data was not available for the right bank.

Figure 37 -View of sediment delta reaching the HFB spillway after 15.5 hrs

Table 6 - Flow and water-surface elevations measured during test HFB-R6000.

Hydrograph Duration, hr	Qprototype (cfs)	Elevation (ft) Dam Crest	Elevation (ft) Upstream	Elevation (ft) Spillway	Spillway Gate Openings
0	1073	765.64	765.51	741.54	3 canal gates open (only)
2.23	1431	766.24	765.97	742.27	Gate 6,7 @ 0.5'
4.47	2057	766.64	766.56	742.46	Gate 6,7 @ 1'
7.45	3130	766.24	766.17	741.94	Gates 6,7 @ 3'
9.68	3667	766.74	766.59	742.04	Gates 6,7 @ 3.5'
14.15	4293	766.14	765.90	742.30	Gates 6,7 @ 5'
15.27	5367	765.74	765.57	742.56	Gates 6,7 @ 7'; Gates 5,8 @ 1'
16.38	6082	767.14	767.05	743.22	Gates 6,7 @ 7'; Gates 5,8 @ 1'
17.86	4651	767.04	766.69	742.40	Gates 6,7 @ 6'
20.09	3309	766.64	766.66	742.27	Gates 6,7 @ 3'
22.32	2326	766.24	766.46	742.23	Gates 6,7 @ 2'
24.55	1789	766.24	Sediment	742.20	Gates 6,7 @ 2'
26.78	1789				

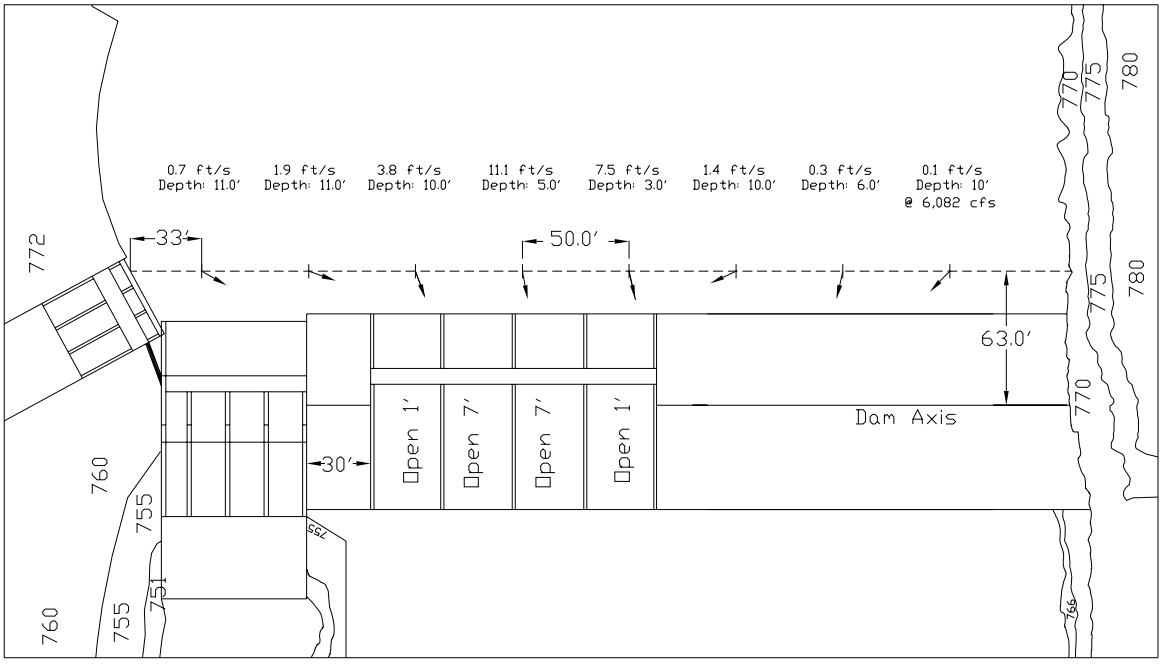

Figure 38 - Flow velocities measured during peak flow, test HFB-R6000.

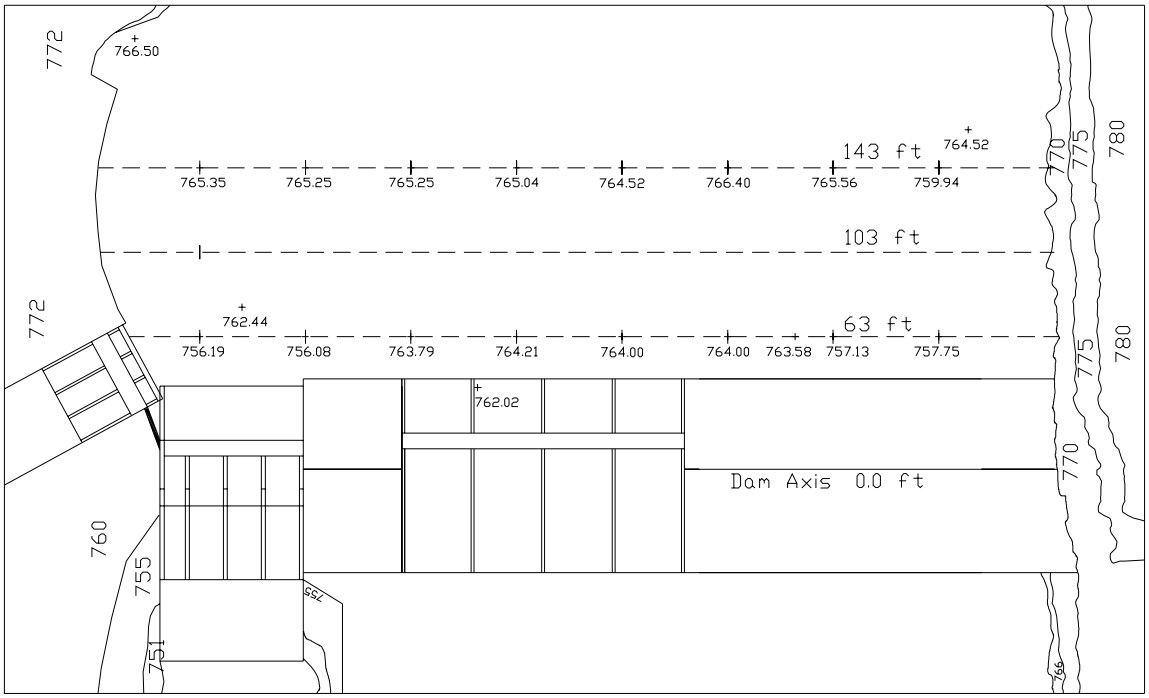

Figure 39 - Post-test HFB-R6000 diversion pool bed elevations upstream of diversion dam.

Views of the Sediment Delta In the Diversion Pool

Looking Upstream at HFB Spillway

Looking Upstream at Service Spillway Stilling Basin

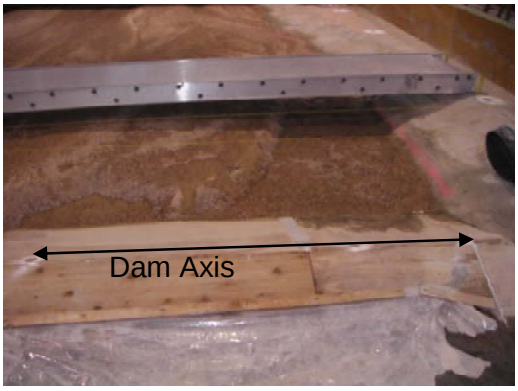

Looking Upstream from the Left Bank

Figure 40 - Post-test sediment deposition photographs for test HFB-R6000.

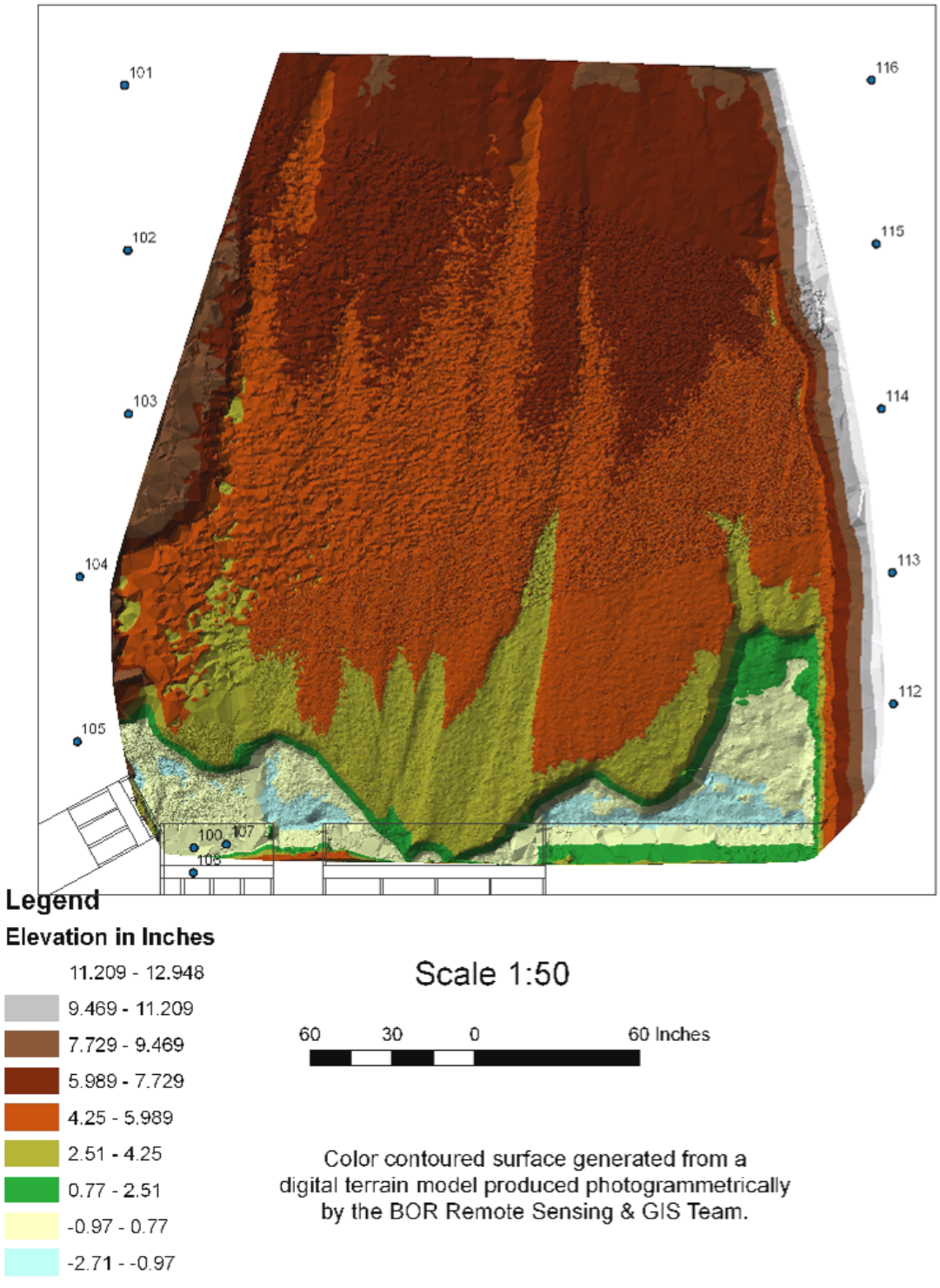

Figure 41 - Close range photogrammetry-generated plot of final channel elevations for test HFB-R6000. Elevations shown are model referenced to a zero datum at elevation 757.75

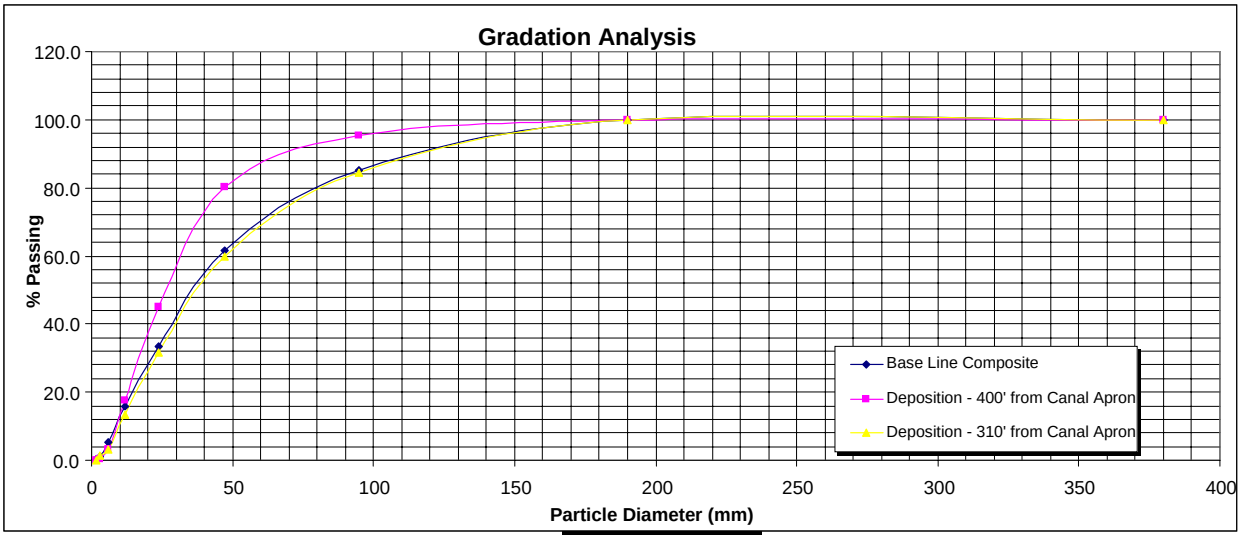

Figure 42 - HFB-R6000 surface sediment gradation sampled along a cross section located 63 ft upstream of the dam axis.

HFB-R14000 Test Results – The test was run for 6.8 hours in the model representing about 30.5 hours prototype, table 7. The HFB spillway was operated during the flood with the objective of minimizing use of the service spillway. Gate 1 was opened 5 ft during the initial stage of the flood then closed and HFB gates 6 and 7 partially opened. When the river flow reached 7,000 ft^3/s gates 6 and 7 were fully opened and gates 5 and 8 were partially opened. At a flow of about 10,000 ft^3/s gates 5-8 were fully open and gates 2, 3 and 4 were partially open. All gates were fully open for flows above12,000 ft^3/s. At the flow peak all gates were fully open and the dam was overtopping by about 0.2 ft. Strong flow contractions off the upstream guidewalls were visible on bays 4 and 5 and to a lesser degree on bay 8. The sediment delta extended downstream to the HFB spillway and started passing through the spillway after about 8 hrs (prototype). Ten hours into the flood (prototype) the sediment delta moving down the right bank inundated the fishway exit. After 12 hrs (prototype) the sediment delta reached the service spillway and was moving along the canal apron wall and passing through the spillway (figure 43). As observed in previous tests, sediment passing through the service spillway deposited in the downstream channel forming a plain bed above the rock weirs. Similar to Test 5, the HFB stilling basins partially filled with sediment with the gates fully open. The basins self cleaned as the gates were partially closed during the recession of the flood. Near-dam velocities measured at the peak discharge are shown in figure 44. Flow velocities from 10 ft/s to 15 ft/s were measured upstream of the

Figure 43 – Sediment delta passing in front of the canal entrance and flushing through the service spillway.

spillways and low velocity flow on the left half of the channel. The sediment delta in front of the canal apron reached about elevation 762.0 during the declining limb of the flood resulting in small amounts of bed sediment being entrained into the canal. During the test 6.0 yds^3 model (48,000 yds^3 prototype) of sediment were fed into the model. Post-test bed elevations, photographs of the post-test channel bed and a photogrammetric-generated map of the post-test diversion pool bed, are given in figures 45, 46, and 47, respectively. Gradations of surface sediments deposited at cross section 63 ft upstream of the dam axis are given in figure 48. Sediment gradations were similar with generally finer material deposited close to the right bank.

Table 7 - Flow and water-surface elevations measured during test HFB-R14000.

Hydrograph Duration, hr	Qprototype (cfs)	Elevation (ft) Dam	Elevation (ft) Fishway Exit	Elevation (ft) Spillway Channel	Spillway Gate Operation
0	894	764.74	764.69	742.66	3 canal gates open (only)
2.23	1789	766.54	766.46	743.02	Gate 1 @ 5'
4.47	4472	766.44	766.23	744.56	Gate 1 closed; Gate 6,7 @ 5'
6.7	6977	766.14	765.64	746.01	Gates 6,7 @ 10'; Gates 5,8 @ 4'
8.94	9660	766.54	765.64	748.11	Gates 5-8 @ 10'; Gate 2 @ 7'; Gate 3,4 @ 5'
11.17	12164	766.64	765.61	749.55	All gates full open
13.4	14132	767.34	765.57	750.20	All gates full open
14.52	13953	767.14	765.80	751.52	All gates full open
16.38	12701	767.04	765.57	751.42	All gates full open
18.61	10196	765.44	Sediment	751.55	Gates 1 and 2 closed
20.84	7334	766.34	Sediment	749.91	Gates 1,2,4 and 8 Closed
23.07	5188	765.44	Sediment	749.61	Gates 1,2,4, 7and 8 Closed
25.3	3757	764.84	Sediment	748.96	Gates 1,2,4 and 7,8 Closed
27.53	3220	766.24	Sediment	749.38	Gates 1,2,3 & 4 open
29.76	2862				

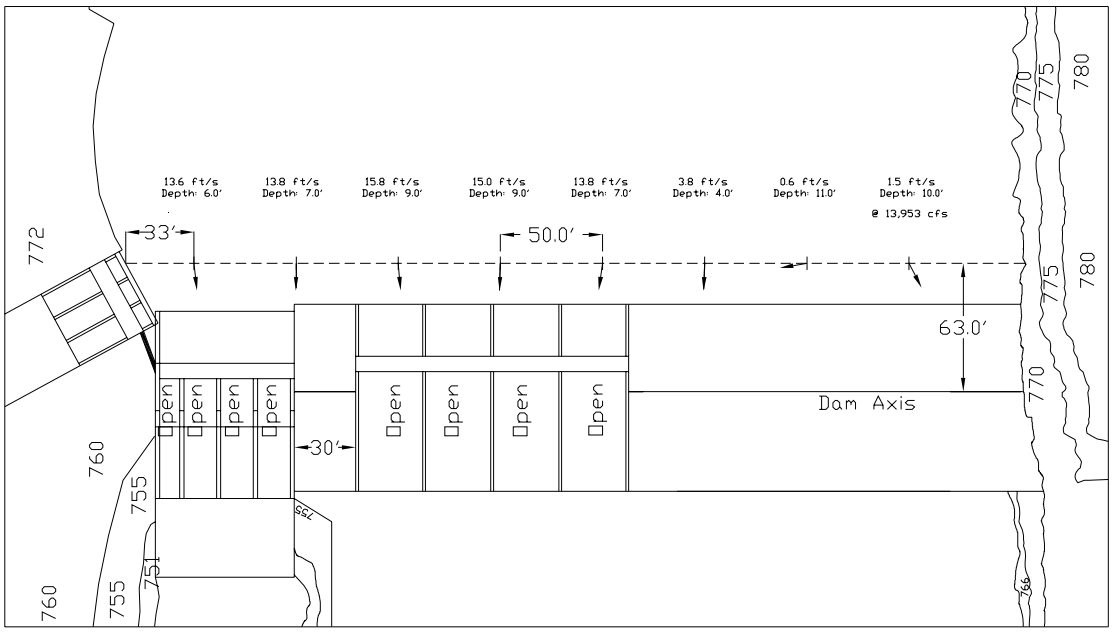

Figure 44 - Flow velocities measured during peak flow, test HFB-R14000.

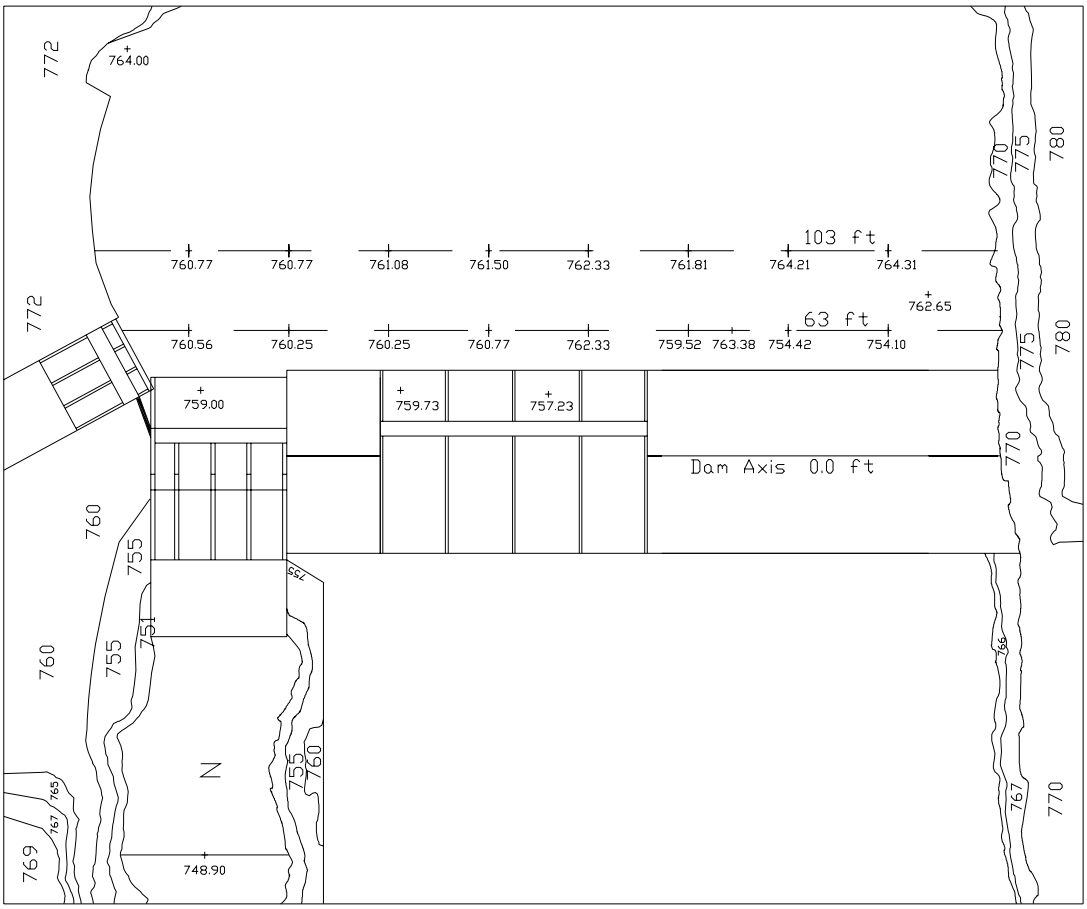

Figure 45 - Post-test HFB-R14000 diversion pool bed elevations upstream of diversion dam.

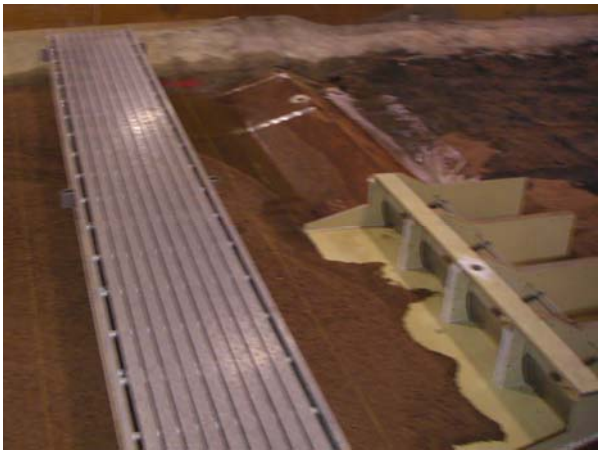

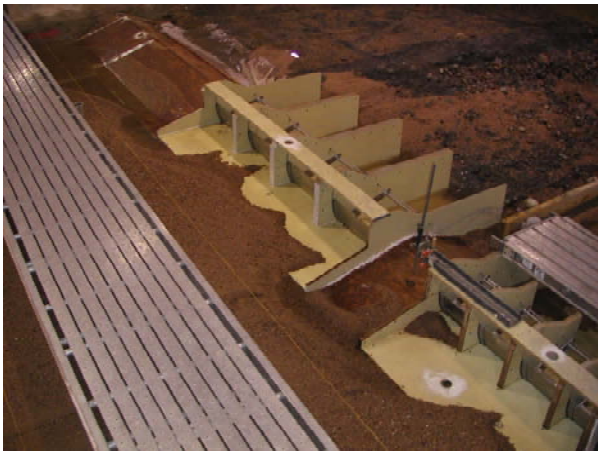

Views of Sediment Deposition Upstream of the Spillways

Diversion pool upstream of Dam

Sediment Deposition near Fishway Exit

Sediment Deposition in Spillway Channel

Figure 46 - Post-test sediment deposition photographs for test HFB-R14000.

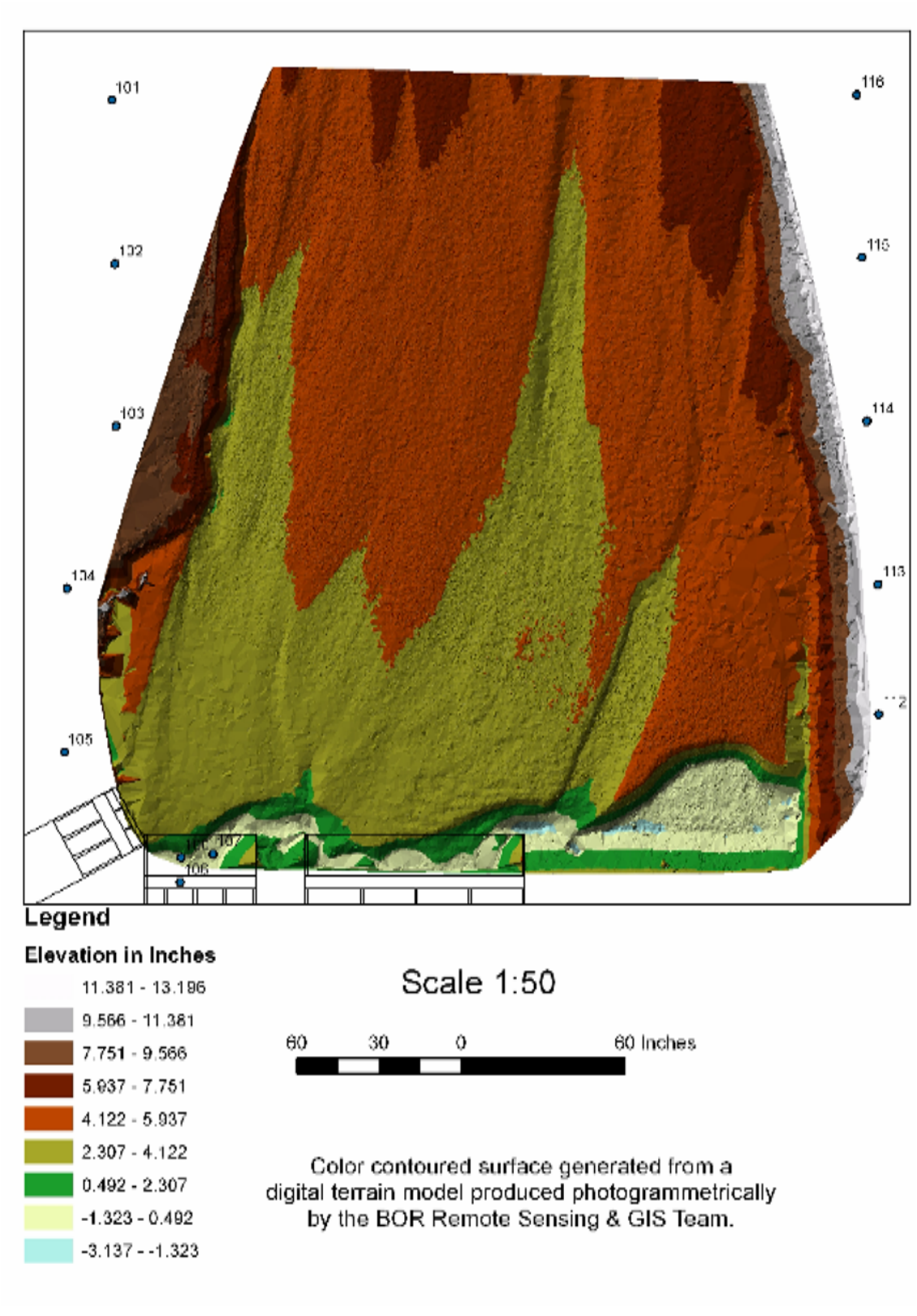

Figure 47 - Close range photogrammetry-generated plot of final channel elevations for test HFB-R14000. Elevations shown are model referenced to a zero datum at elevation 757.75

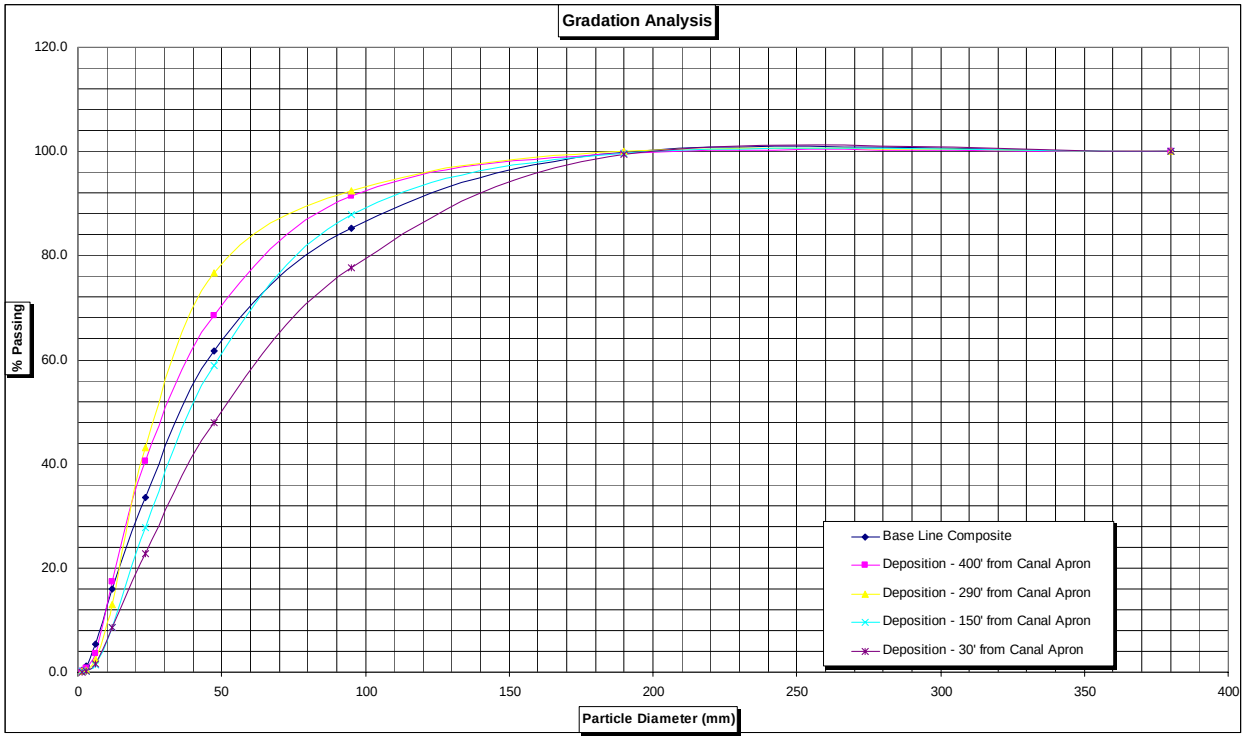

Figure 48 - HFB-R14000 surface sediment gradation sampled along a cross section located 63 ft upstream of the dam axis.

Guide Wall Modifications to the Spillway

Guide walls were added to reduce the flow contraction that occurred on the outside walls of service spillway bay 4 and HFB spillway bays 5 and 8. A strong flow contraction occurred off the left wall of bay 4 and to a lesser extent bay 3 of the service spillway. Flow velocities measured upstream of the dam in tests Ss6000 and Ss14000 show flow approaches the service spillway entrance at an angle. Adding a curved upstream guide wall extending about 21 ft into the diversion pool was found to effectively guide flow into the spillway. Figure 49 shows the guide wall arrangement tested for the service spillway with the right bank HFB spillway option. The discharge capacity of the service spillway with the guide wall extension on bay 4 was 5,800 ft^3/s at pool elevation 767.1. Strong flow contraction occurred off the outer walls of HFB bays 5 and 8 for both spillway locations tested. Entrance conditions to the spillway were improved by adding curved guide walls extended into the diversion pool similar to the service spillway guide wall. Guide walls tested for the near right bank HFB spillway location are also shown in figure 49. Although not tested in the model, similar guide walls could be applied to the left bank HFB spillway location to improve entrance conditions. For the right bank HFB location shown, guide walls between bays 4 and 5 were tested as a single pier that improved flow into both bays. The discharge capacity of the HFB spillway with upstream guide walls was 9,900 ft^3/s flow at pool elevation 767.1 (test conducted without sediment transport through the spillway).

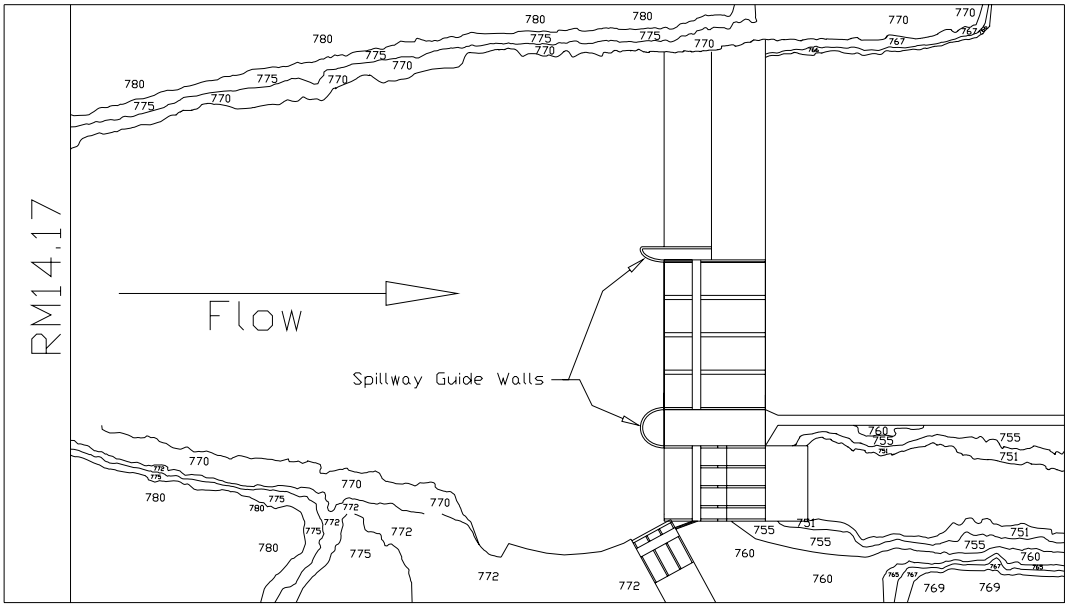

Figure 49 – Plan view of spillway guide walls tested in the model.

Fish Passage

The fish exit of the existing upstream fish passage was inundated by sediment in the diversion pool in all tests conducted. HFB spillway location and gate operation were ineffective at preventing the sediment delta from building in front of the exit. Flow through the fishway was not modeled, however, flow passing through the fishway with the sediment deposition observed would likely entrain large amounts of sediment resulting in plugging of the fishway. Based on the test results the fishway exit gates would likely be closed prior to a large flood. Fish would then have to exit through the canal headworks structure and swim past the service spillway to pass upstream. This raises the potential for fish to be re-entrained downstream through the service spillway when it is operating. To evaluate the re-entrainment potential, flow velocities were measured on a grid covering the area in front of the canal and spillway entrances for three spillway gate operations. Velocities were measured at 0.2 and 0.6 times the depth below the surface for a river flow of 5,800 ft^3/s and diversion pool elevation of about 767.0. Flow velocity was generally less than 6 ft/s for all conditions tested (figure 50). Measurements were not made with all service spillway gates open as flow depth and velocity varied substantially when the sediment delta previously discussed fully developed in front of the canal intake. Flow velocities measured during test Ss14000 indicates flow velocity could reach 15 ft/s with all gates open and shallow flow over sediment deposits.

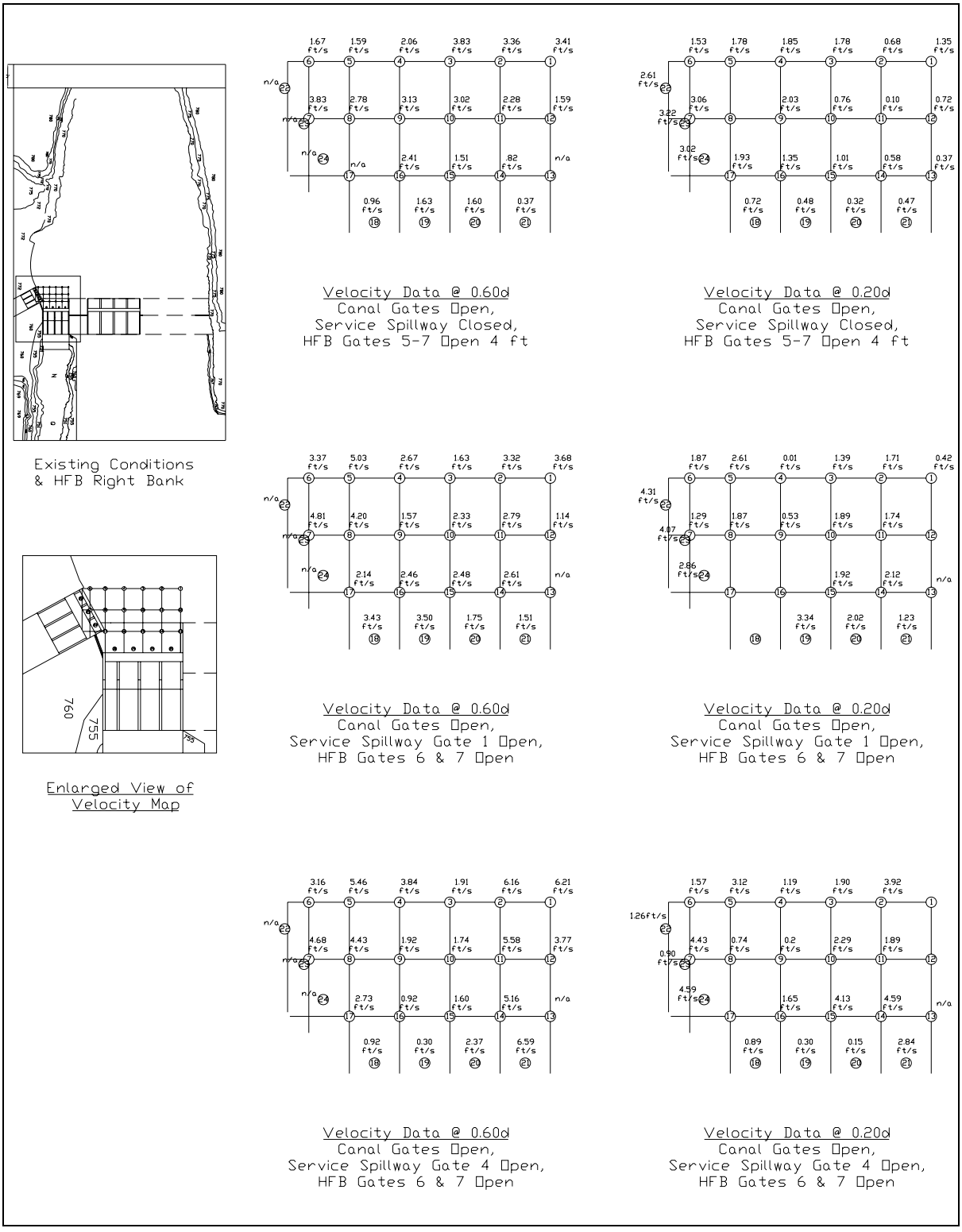

Figure 50 - Flow velocities measured in front of canal entrance.

Model tests of the HFB spillway conducted to evaluate spillway location included the existing channel topography downstream of the service spillway and a separate channel downstream of the HFB spillway. The two channels were separated by a rock berm that extended downstream about 900 ft. Several problems with the downstream channel configuration were identified during the model tests. The test results indicated the entrance to the fishway (figure 51) could be impacted by sediment deposition if the service spillway gates were used to pass significant flood flows. Sediment deposited to about elevation 750 in the fishway entrance pool and filled in the pools between rock weirs in the downstream channel. However, fishway flow was not modeled in the initial tests and therefore sediment deposition near the fishway entrances may not have been fully represented in those tests. Concerns were also expressed by fishery agencies over the length of the channel separation downstream of the spillways. Separate spillway channels would restrict the movement of fish between spillway flows and could increase the risk of fish stranding following HFB operation.

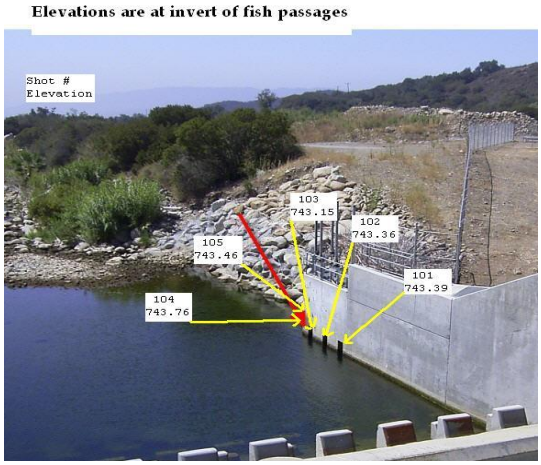

Figure 51 - Photograph of fishway entrances below Robles Diversion Dam service spillway (Casitas Irrigation District).

Stilling Pool Modifications - Previous model simulations of the ten-year flood resulted in substantial sediment deposition in the right bank fishway entrance pool when the service spillway was operated. Attempts to sluice sediment from the pool in the model were largely unsuccessful. To reduce sediment deposition in the pool and improve post-flood sluicing effectiveness, the floor of the fishway entrance pool was raised 2.75 ft to elevation 745.0. The fishway entrance slots were also raised to the new invert. The floor of the fishway entrance was left at elevation 742.25 to maintain sufficient depth on the fishway baffles. In the model, fishway flow was supplied to the fishway entrance structure to better evaluate sediment deposition near the structure.

A single stilling pool concept was tested in the model as an alternative to the initial separate channel design. A single stilling pool would allow fish during HFB operation to move across the channel, providing better access to the fishway, figures 52 and 53. For the single pool concept, the HFB stilling pool and the downstream river channel were set higher than the river downstream of the service spillway to avoid a stagnate pool from forming downstream of the HFB during flow releases less than about 1,000 ft^3/s. Tests of the single pool option identified several conditions that were undesirable. Most significantly, HFB spillway flow transported large amounts of sediment into the service spillway fishway entrance pool through the intertie between the pools. This eliminated the ability to control sediment deposition in the fishway entrance pool by adjusting spillway operation. Additionally, poor flow conditions for fish occurred during operation of the service spillway at flows above about 1,000 ft^3/s with the HFB spillway closed. This type of operation resulted in flow moving into the HFB stilling basin and then flowing downstream as a wide shallow flow over the full width of the HFB end sill.

Tailwater elevations measured in the model for service spillway operation (HFB closed) are shown in figure 54. Both sediment and flow conditions were improved by extending the length of the HFB stilling basin 11.7 ft (basin floor length of 46.7 ft) and extending the right wall of bay 5 to the downstream end of the stilling pool, figures 55 and 56. A sluice gate was placed in the wall separating the service spillway and HFB spillway stilling pools to allow controlled movement of water between the stilling pools. Tests of the downstream wall extension resulted in no discernable movement of HFB sediment into the fishway entrance pool. The wall extension also prevented flow from the service spillway into the HFB spillway when the sluice gate was closed. The sluice gate allowed for draining the HFB basin into the lower service spillway pool following HFB operation. Operation of the service spillway during the ten-year flood resulted in about 2 to 3 ft of sediment in the fishway entrance pool following a ten-year flood simulation, figure 57. Following the flood, the service spillway was operated at 2,500 ft^3/s for about eight hours prototype in an attempt to sluice material out of the fishway entrance pool. The sluicing exercise resulted in only localized scouring of material located near the base of the baffled apron, figure 58. The top three rows of baffles on the baffled apron energy dissipater were then removed in the model to determine if sluicing of the fishway entrance pool could be improved. The service spillway was again operated at full pool for eight hours prototype at 2,500 ft^3/s at full pool. Removing the baffles showed improved sluicing of sediment with material being removed from the upstream one-half of the pool, figure 59.

Left Bank Fishway - To further improve fish passage during HFB operation, a new fishway was proposed adjacent to the left wall of the HFB spillway and the dam crest was raised approximately 1.5 ft to elevation 768.75 (figure 60). During the model testing it was evident that operation of the HFB spillway, new fishway, and diversion would all benefit from having a greater range of diversion pool elevation prior to overtopping the dam. For the final model tests the crest of the dam was raised and the full diversion pool elevation was set at 768.0.

The left side fishway would only operate during HFB spillway operation. The fishway exit is shown integrated with the guide wall upstream of spillway bay eight. The maximum head drop across the fishway is about 12 ft assuming a minimum flow release of 2,500 ft^3/s from the HFB spillway. Tailwater elevations measured in the model HFB stilling basin are shown in figure 61. The fishway was designed to pass about 170 ft^3/s at pool elevation 768.0. The fishway exit was modeled as a 20 ft long sill with a crest elevation of 766.0. An overshot gate was proposed for the sill to close off the fishway when the HFB spillway was not operating. The gate was not represented in the model. The fishway modeled was 32 ft wide with 12 baffles spaced at 12.2 ft centers at an invert slope of 8.2 percent. Fishway entrance and exit flow conditions were investigated in the model. Fishway baffles were installed in the model fishway, however flow conditions within the fishway were not investigated due to the small size of the fishway in the model. Two types of fishway baffles are offered herein for consideration. First is a modified Ice Harbor weir and orifice style baffle, figure 62. Each baffle is 8 ft high with 4-2 ft square orifices located flush with the bottom and two 11 ft long weirs adjacent to the outer walls. In the center of the baffle is a 10-ft-long non-overflow wall. The pools would have an energy dissipation factor (EDF) of 3.5 ft-lbs/s/ft^3 at 170 ft^3/s flow.

The second proposed baffle design is a multiple slot roughened channel design developed by the author to mimic several important attributes of flow in a natural stream, figure 63. The baffles cause a pool and drop pattern and direct the flow toward the center of the channel creating the highest velocity in the center with lower velocity near channel edges. The rock-lined trapezoid channel produces great variability of flow depth and velocity from deep higher-velocity flow in the channel center to shallower near-bank flow with low velocity. The baffles can be designed to control flow over a wide range of head change by extending all baffles to the maximum water surface design height, or baffles near the center of the channel can be shorter and allowed to overtop as the upstream water level rises during a flood. Using shorter baffles in the center of the fishway that become submerged results in rapid increases in flow passing down the center of the fishway channel. This has proven desirable where a rapid rise in through-fishway flow is needed to produce good attraction during high river flows while providing passage conditions near the channel boundaries. The HFB fishway shown herein designed on the streaming flow concept would be a 32-ft-wide rock-lined trapezoidal channel with a 10-ft-wide bottom and 3H:1V side slopes. Typical baffles for this style fishway are composed of individual rock boulders or concrete columns set in an upstream-aligned chevron shape and spaced about 1.0 to 1.5 ft apart, depending on design flow. Boulders are typically used on lower gradient fishways with pool lengths of greater than 15 ft and a flow depth under normal conditions of less than 4 ft. Concrete columns have the advantage that they can be constructed to any height and diameter. Therefore, when strong control of the fishway flow is desired and flow depths exceed about 4 ft, columns are recommended. This design has been used for numerous non-salmonid fishways at slopes up to 5 percent, and the fishway design has proven to work well where large flows are passed through the fishway.

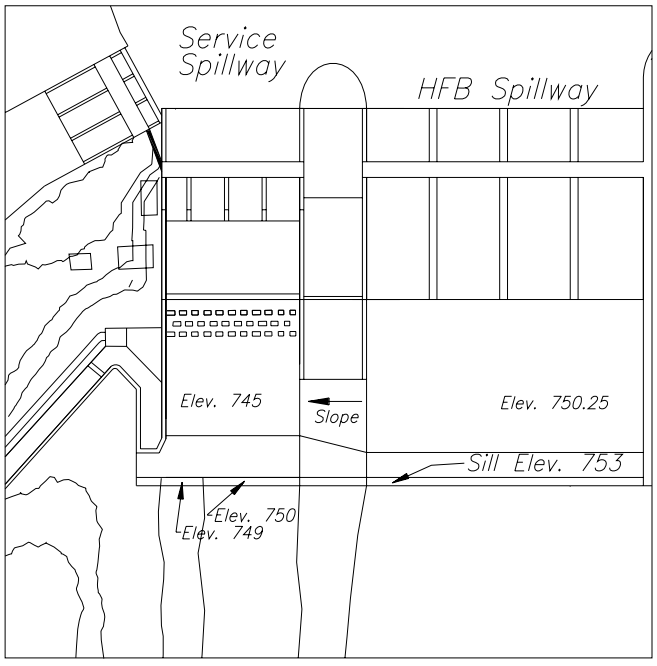

Figure 52 – Illustration of single spillway pool concept.

Figure 53 – Single pool concept shown with service spillway releases of 1,000 ft^3/s.

Downstream Channel - Downstream of the two spillways the channels merge into a common channel with a low flow channel along the right bank. The rock berm previously separating the channels was removed and the channel shape modified to gradually merge HFB flow with the service spillway flow. The channel downstream of the service spillway was modeled with a 20-ft-wide low flow channel at elevation 750.0. To the left of the low flow channel, the channel sloped up at 1 on 5 to elevation 751 and then at approximately 1 percent to the left side of the service spillway channel. The invert elevation of the low flow channel at the downstreamend of the fishway pool was held similar to existing to maintain the required tailwater on the fishway. The low flow channel was sloped at 1.5 percent until intersecting the existing channel elevation, a distance of about 400 ft. The invert elevation of the channel downstream of the HFB stilling pool was set at 753.25. The channel was sloped downstream at 2.0 percent and 0.25 percent normal to the downstream direction until intersecting the low flow channel. The left bank of the HFB channel was converged toward the low flow channel as shown in figure 60. Combined spillway operation and right and left bank fishway operation are shown in figure 64. Several photographs show dye streaks to highlight the direction of flow movement. The channel flowing at 2,500 ft^3/s released from the service spillway following a ten year flood simulation is shown in figure 65.

Service Spillway Modifications

Increasing the diversion pool by about 1 ft requires several modifications to the existing spillway. The top of the existing service spillway gates is 767.25. A 1 ft pool raise would also require the top of the gates be raised approximately 1 foot. The model also showed the hydraulic jump in the service spillway stilling basin could sweep out of the basin under the higher diversion pool. To hold the jump in the basin, the endsill was raised 1.5 ft.

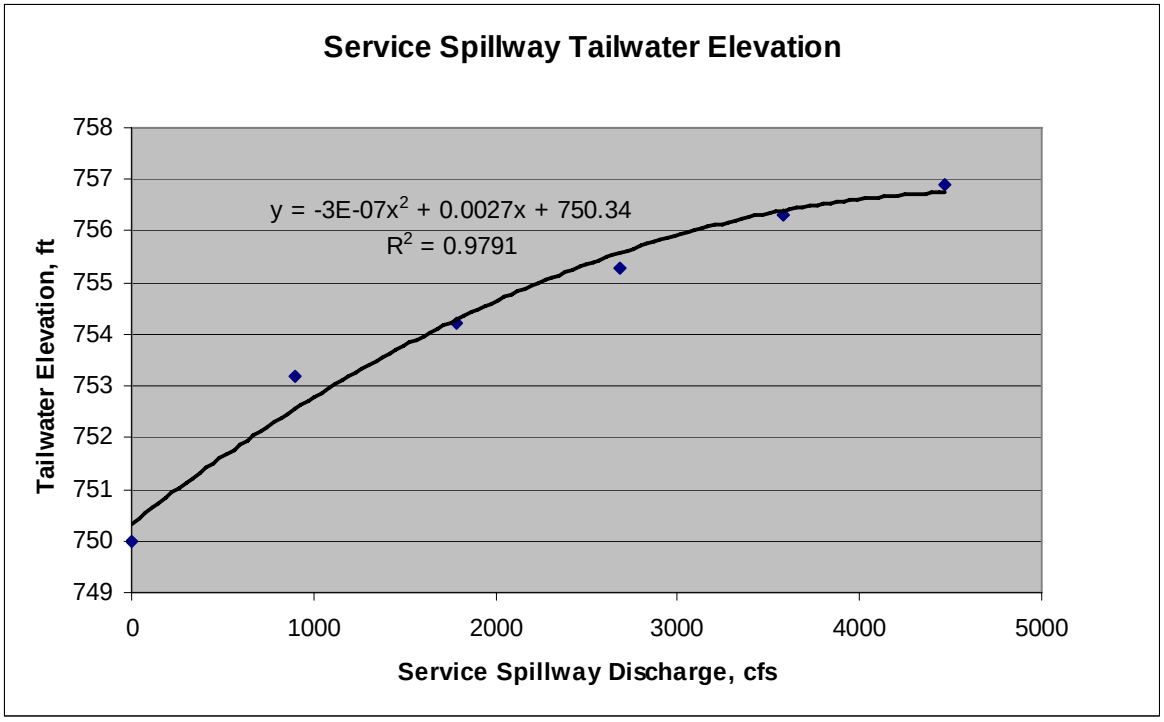

Figure 54 –Water surface elevation measured in right bank fishway entrance pool.

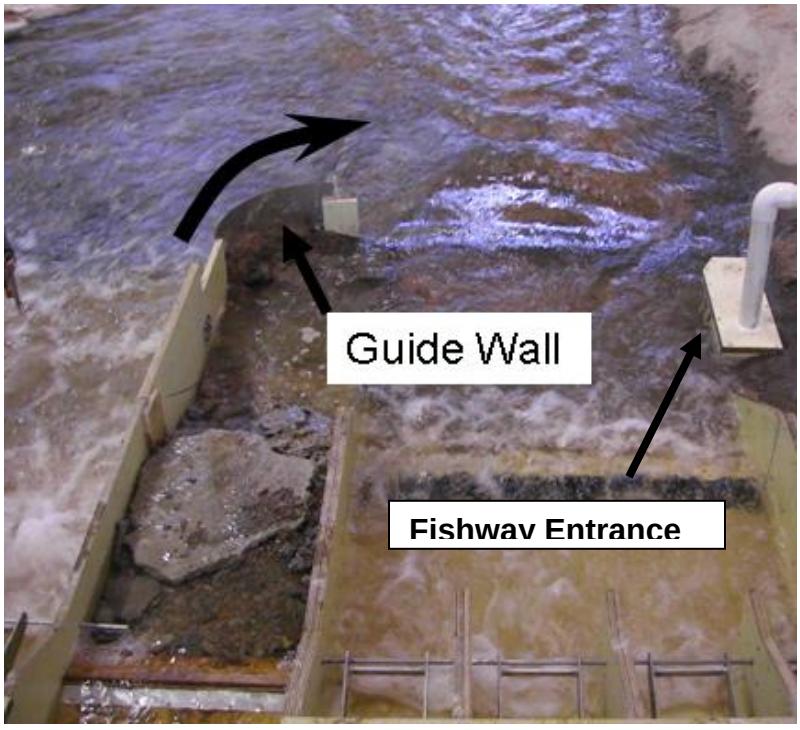

Figure 55 – View of stilling pool guide wall extension added to prevent sediment from being pulled into the right bank fishway entrance pool.

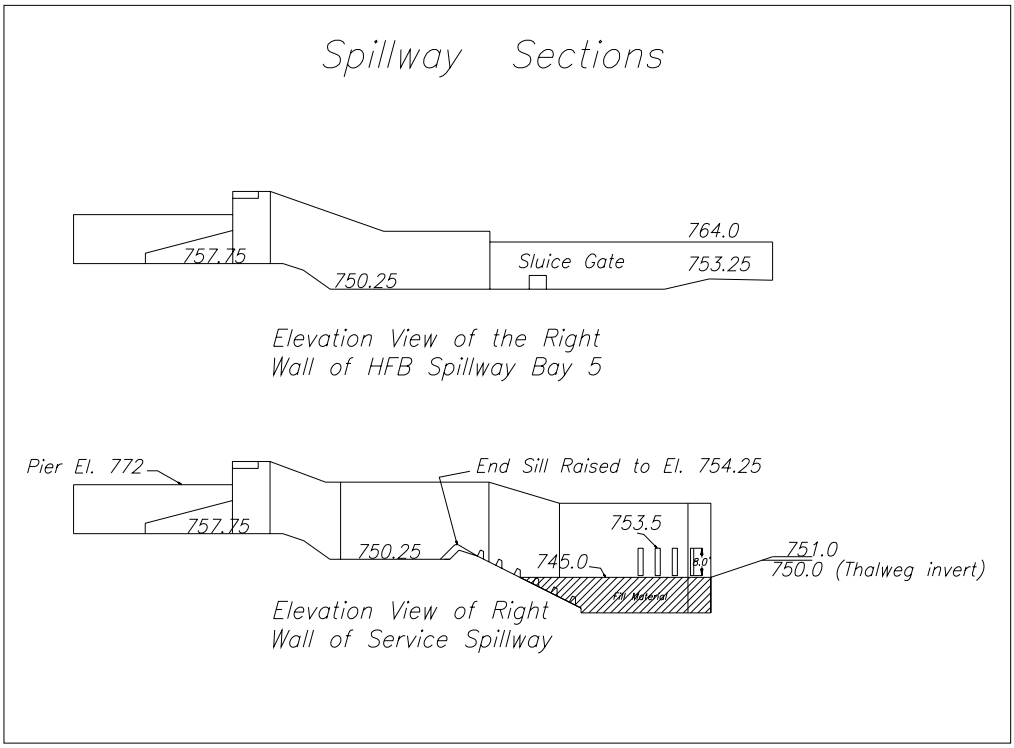

Figure 56 - Sections through the HFB spillway and service spillway.

Figure 57 - Sediment deposition in the right bank fishway attraction pool following a ten year flood simulation.

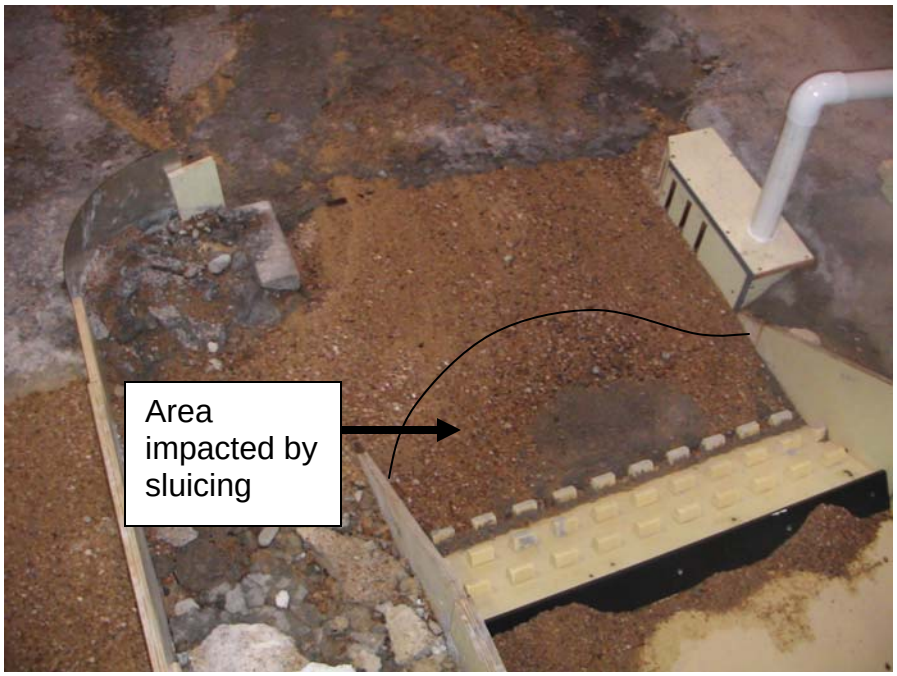

Figure 58 - Local scouring following eight hours prototype of the service spillway operating at 1500 ft^3/s.

Figure 59 - Local scouring following eight hours prototype operation of the service spillway after removal of baffles on apron. Figure 56 shows pre-sluicing condition.

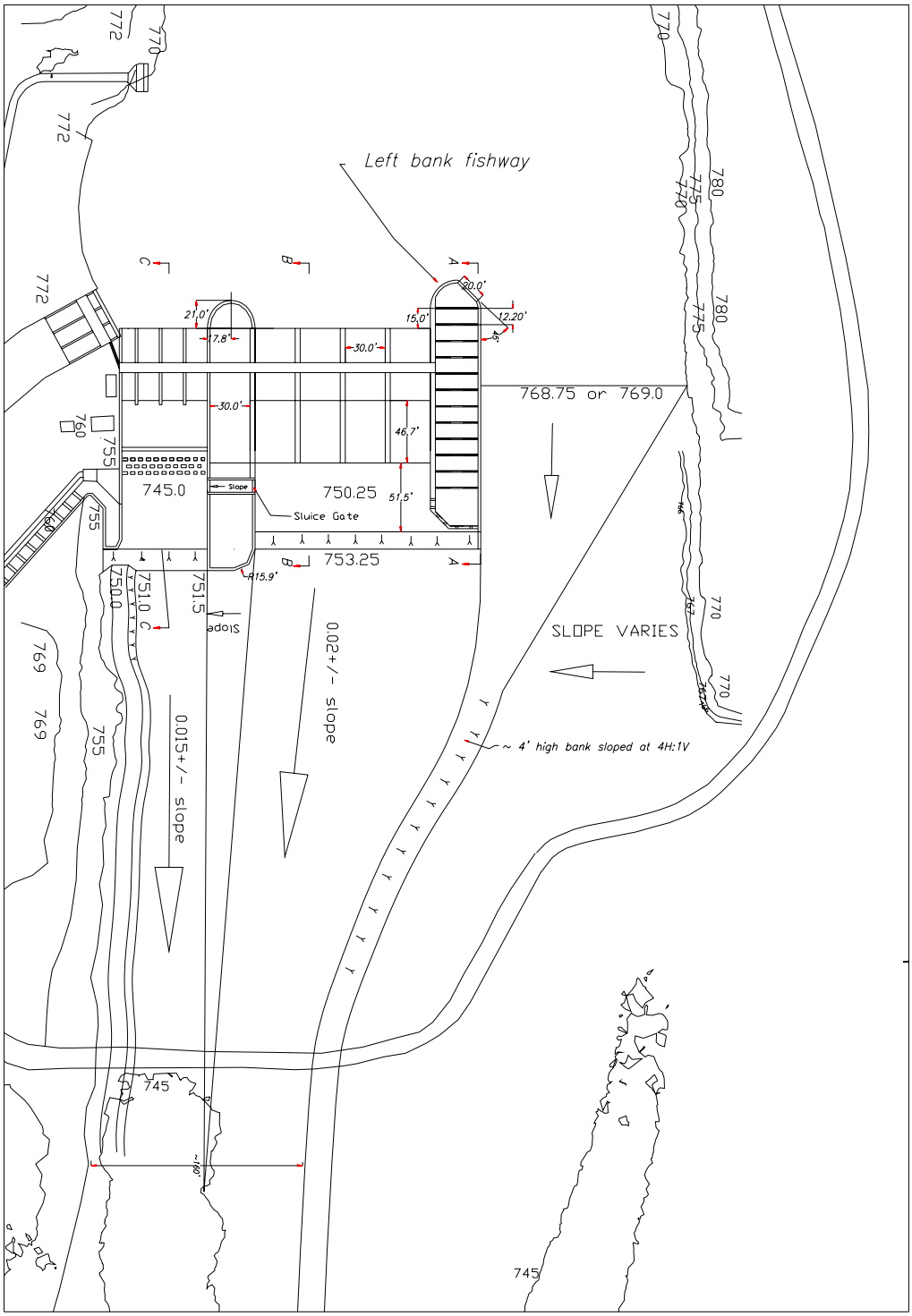

Figure 60 – Final configuration of HFB spillway with left side fishway and common downstream channel.

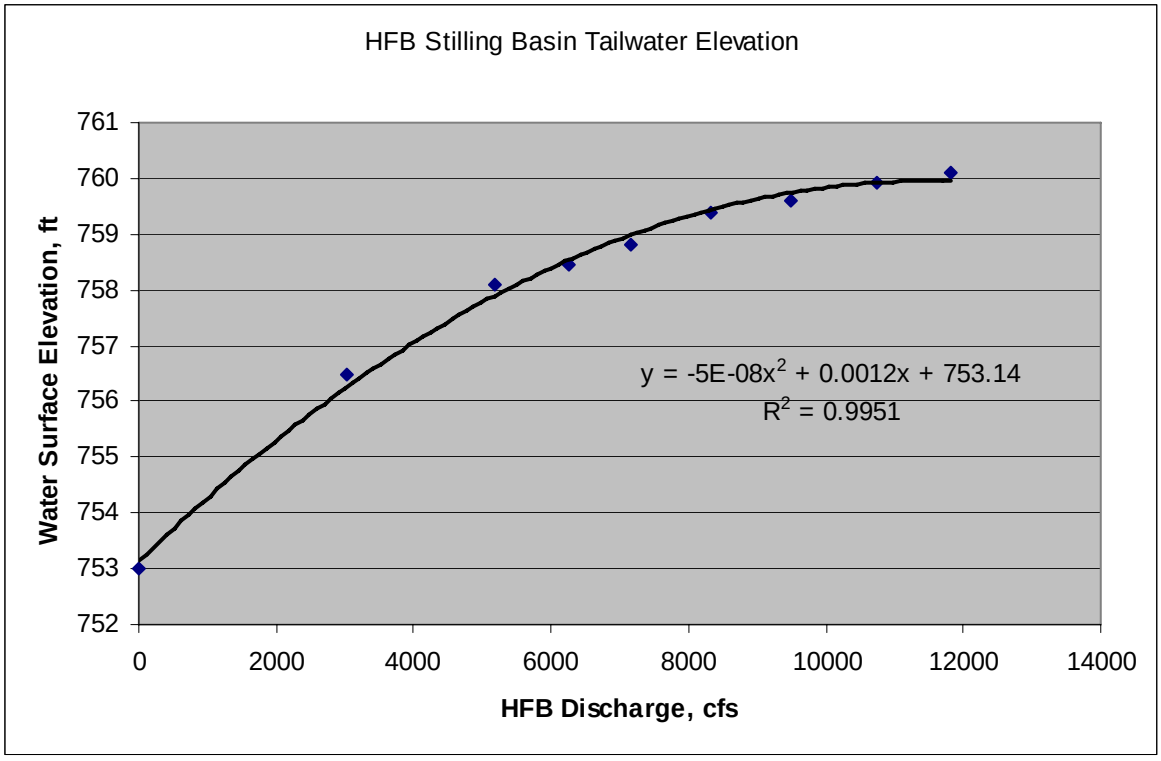

Figure 61 - Tailwater elevation measured in the HFB spillway stilling basin.

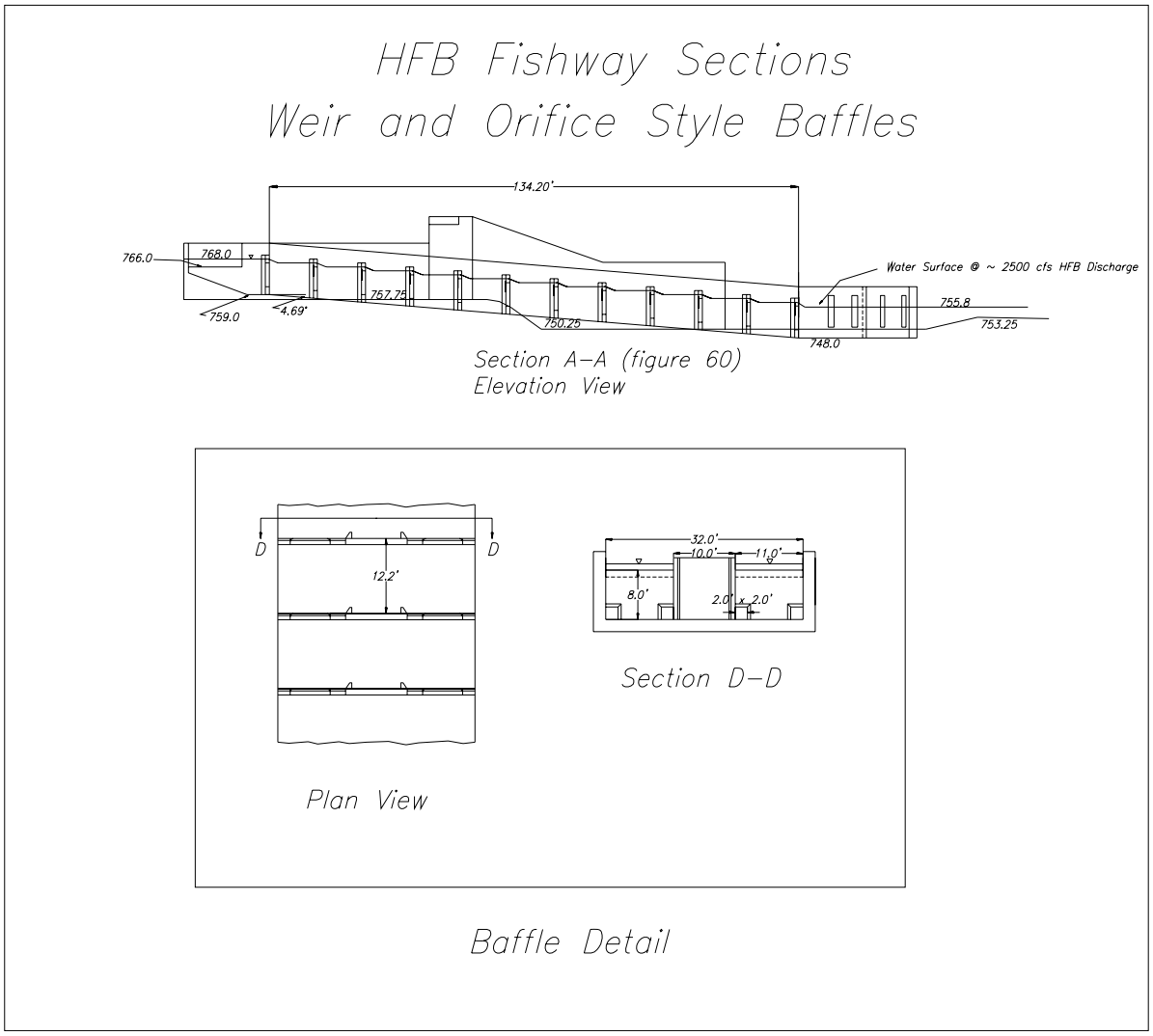

Figure 62 - HFB spillway left side fishway shown with weir and orifice baffles. (Baffle dimensions shown are preliminary.)

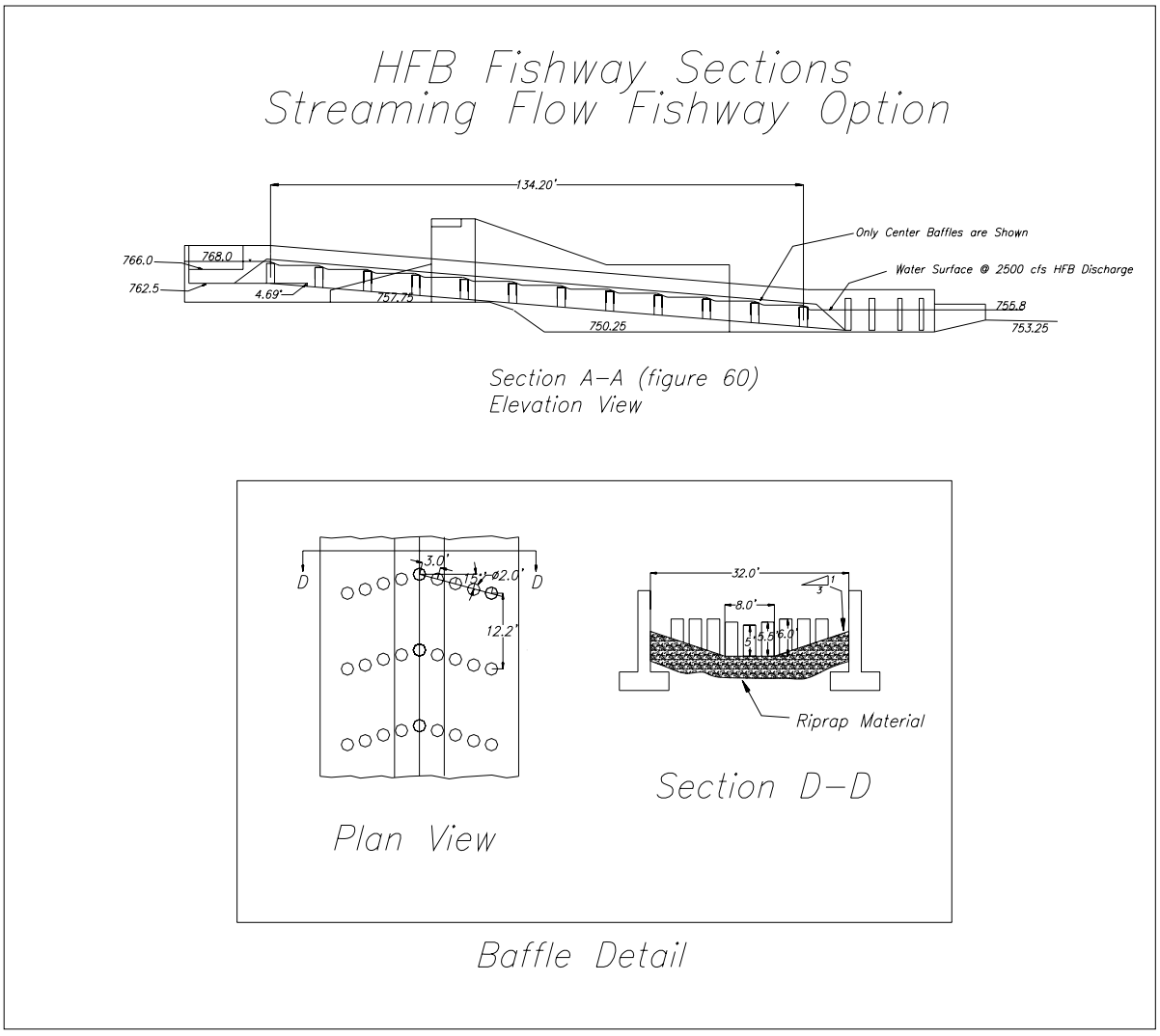

Figure 63 - Left side fishway shown with streaming flow style baffles. (Baffle dimensions shown are preliminary.)

Figure 64 – Model tests showing dye injected in the right bank fishway (top), in HFB bays 5 and 6 (middle) and in bay 8 and the left bank fishway (bottom). Spillway flows are 1,300 ft^3/s service spillway and 6,900 ft^3/s HFB spillway.

Figure 65 – Photograph of 2,500 ft^3/s released from the service spillway gates flowing down the final downstream channel geometry during the declining limb of a ten year flood simulation. HFB spillway gates are closed.

References

1. Dodge R. A. 1988. *Overtopping Flow on Low Embankment Dams – Summary Report of Model Tests.* US Bureau of Reclamation Hydraulics Laboratory. Report No. REC-ERC 88-3.

2. Dodge R.A. 1954. *Milburn Diversion Dam Model Study Missouri River Basin Project, Nebraska, Progress Report No. 4. General Studies of Headworks and Sluiceway Structures.* U.S. Bureau of Reclamation Hydraulics Laboratory. Report No. Hyd-385.

3. Franco J. J., 1978. *Guidlelines for the Design, Adjustment and Operation of Models for the Study of River Sedimentation Problems.* U.S. Army Corps of Engineers, Waterways Experiment Station.Vicksburg, Mississippi.

4. Hall E., et al. 2000, *Matilija Dam Removal Apprasial Report*, Bureau of Reclamation, Technical Service Center, Denver, Colorado.

5. Pugh A. C. 1985. *Hydraulic Model Studies of Fuse Plug Embankments.* U.S. Bureau of Reclamation Hydraulics Laboratory. Report No. REC-ERC 85-7.

6. Shen, W. Hsiew, 1971. River Mechanics Vol. II. Chapter 21, *Modeling of Fluvial Processes*, Colorado State University, Fort Collins, Colorado

7. Y.G. Lai and B.P. Greimann, 2008. "*Two-Dimensional Numerical Model Study of Sediment Movement at the Robles Diversion Dam on the Ventura River, Californi*a", Sedimentation and Rivers Group, Bureau of Reclamation, Denver Technical Center, Denver Colorado.

RECLAMATION
Managing Water in the West

DRAFT (Not Peer Reviewed)

Hydraulic Laboratory Report HL-20xx-xx

Robles Diversion Dam - Left Bank Fishway

High Flow Bypass Spillway Structure
Ventura River, California

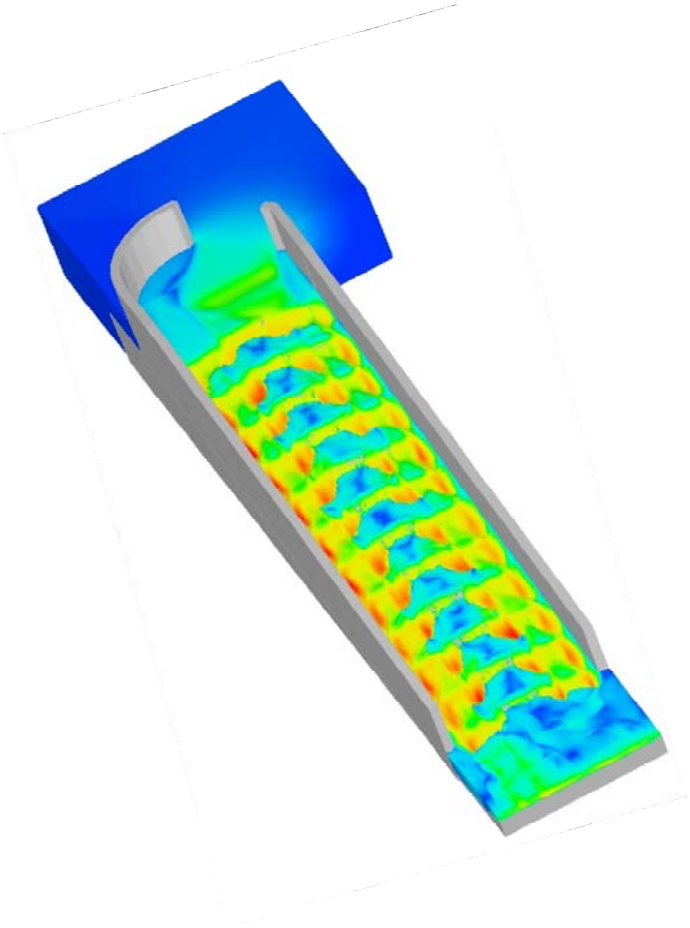

U.S. Department of the Interior
Bureau of Reclamation
Technical Service Center
Hydraulic Investigations and Laboratory Services Group
Denver, Colorado

June 2010

REPORT DOCUMENTATION PAGE

Form Approved
OMB No. 0704-0188

PLEASE DO NOT RETURN YOUR FORM TO THE ABOVE ADDRESS.

1. REPORT DATE *(DD-MM-YYYY)*	**2. REPORT TYPE**	**3. DATES COVERED** *(From - To)*
22-06-10	HL	

4. TITLE AND SUBTITLE
Robles Diversion Dam - Left Bank Fishway

High Flow Bypass Spillway Structure
Ventura River, California

5a. CONTRACT NUMBER

5b. GRANT NUMBER

5c. PROGRAM ELEMENT NUMBER

6. AUTHOR(S)
Brent Mefford

5d. PROJECT NUMBER

5e. TASK NUMBER

5f. WORK UNIT NUMBER

7. PERFORMING ORGANIZATION NAME(S) AND ADDRESS(ES)

Hydraulic Investigations and Laboratory Services

8. PERFORMING ORGANIZATION REPORT NUMBER

9. SPONSORING/MONITORING AGENCY NAME(S) AND ADDRESS(ES)
Bureau of Reclamation

10. SPONSOR/MONITOR'S ACRONYM(S)

11. SPONSOR/MONITOR'S REPORT NUMBER(S)

12. DISTRIBUTION/AVAILABILITY STATEMENT

13. SUPPLEMENTARY NOTES

14. ABSTRACT

This report presents the results of a Bureau of Reclamation study to develop the design of a fishway providing passage during operation of the proposed high-flow bypass (HFB) spillway at Robles Diversion Dam. The HFB spillway and fishway are designed as auxiliary facilities that will only operate during floods in excess of about the two-year event. The primary species of concern requiring passage is southern California steelhead, (*Oncorhynhus mykiss*). The fishway design was developed through a combination of three dimensional computational fluid dynamics (CFD) modeling and a 1:10 Froude-scale physical model. The study focused on development and evaluation of a fishway design providing effective fish passage during flood events that convey significant debris and sediment.

15. SUBJECT TERMS

16. SECURITY CLASSIFICATION OF:			**17. LIMITATION OF ABSTRACT**	**18. NUMBER OF PAGES**	**19a. NAME OF RESPONSIBLE PERSON**
					Robert F. Einhellig
a. REPORT	**b. ABSTRACT**	**a. THIS PAGE**			**19b. TELEPHONE NUMBER** *(Include area code)*
					303-445-2142

DRAFT (Not Peer Reviewed)

Hydraulic Laboratory Report HL-20xx-xx

Robles Diversion Dam - Left Bank Fishway

High Flow Bypass Spillway Structure
Ventura River, California

Prepared: Brent Mefford, P.E.
Hydraulic Research Engineer, Hydraulic Investigations and Laboratory Services Group, 86-68460

Technical Approval: Robert F. Einhellig, P.E.
Manager, Hydraulic Investigations and Laboratory Services Group, 86-68460

Peer Review: Brian Hiener
Hydraulic Engineer, Hydraulic Investigations and Laboratory Services Group, 86-68460

Date June 22, 2010

U.S. Department of the Interior
Bureau of Reclamation
Technical Service Center
Hydraulic Investigations and Laboratory Services Group
Denver, Colorado

June 2010

Mission Statements

The mission of the Department of the Interior is to protect and provide access to our Nation's natural and cultural heritage and honor our trust responsibilities to Indian Tribes and our commitments to island communities.

The mission of the Bureau of Reclamation is to manage, develop, and protect water and related resources in an environmentally and economically sound manner in the interest of the American public.

Acknowledgments

The Corps of Engineers Los Angeles District sponsored this study. The overall project lead for Reclamation was Blair Greimann, P.E., Sedimentation and River Mechanics Group (D68-68240). Jim Higgs, P.E. (D68-68460) conducted the numerical simulations for the fishway project. Rudy Campbell (D68-68460) provided AutoCAD drawings and model construction oversight.

Hydraulic Laboratory Reports

The Hydraulic Laboratory Report series is produced by the Bureau of Reclamation's Hydraulic Investigations and Laboratory Services Group (Mail Code 86-68460), PO Box 25007, Denver, Colorado 80225-0007. At the time of publication, this report was also made available online at **http://www.usbr.gov/pmts/hydraulics_lab/pubs/**.

Disclaimer

The information provided in this report is believed to be appropriate and accurate for the specific purposes described herein, but users bear all responsibility for exercising sound engineering judgment in its application, especially to situations different from those studied. References to commercial products do not imply endorsement by the Bureau of Reclamation and may not be used for advertising or promotional purposes.

CONTENTS

FIGURES

Executive Summary

This report presents the results of a Bureau of Reclamation study to develop the design of a fishway providing passage during operation of the proposed high-flow bypass (HFB) spillway at Robles Diversion Dam. Robles Diversion Dam is located in southern California on the Ventura River approximately 14 river miles from the ocean and approximately two miles downstream of Matilija Dam. The HFB spillway and fishway are designed as auxiliary facilities that will only operate during floods in excess of about the two-year event. The primary species of concern requiring passage is southern California steelhead, (*Oncorhynhus mykiss*). The fishway design was developed through a combination of three dimensional computational fluid dynamics (CFD) modeling and a 1:10 Froude-scale physical model. The study focused on development and evaluation of a fishway design providing effective fish passage during flood events that convey significant debris and sediment. Fishway designs were tested to investigate flow conditions in the fishway, determine fishway discharge rating and evaluate debris passage characteristics of the design. A preferred baffle design was developed for the fishway based on the study. All dimensions presented in the study are in English units.

Background

Figure 1 – Areal view of Robles Diversion Dam

Robles Diversion Dam is located on the Ventura River near Ventura, California at approximately river mile (RM) 14.16 (Figure 1). The diversion supplies water to Lake Casitas by canal. The normal maximum diversion is approximately 500 ft^3/s. The existing diversion dam is a low rock weir with a gated spillway, canal diversion headworks and a fish pass located on the right abutment. The diversion weir has a hydraulic height of 13 feet.

Two miles upstream of Robles Diversion Dam is Matilija Dam, a 160 ft high (originally 190 ft high) concrete arch dam that is scheduled to be removed to restore access to the upper watershed for southern California steelhead (*Oncorhynhus mykiss*). Removal will release large volumes of sediments to the lower river impacting operation of Robles Diversion Dam. Mitigation of impacts prompted the design of a new auxiliary spillway at Robles Diversion Dam designed specifically to pass large flood flows and sediment loads through the dam. The new auxiliary spillway at Robles, referred to as the high-flow bypass

(HFB) spillway, will be located to the left of the existing spillway. The spillway was the focus of a model study in 2008, (Mefford et. al. 2008). During the 2008 study, concerns were raised over the adequacy of the existing right bank fishway to attract upstream migrating fish during HFB releases. These concerns resulted in a second study to investigate the design of a left bank auxiliary fishway designed to operate in conjunction with the HFB spillway. The 2008 study recommended a HFB fishway be located adjacent to the left spillway abutment as shown in Figure 2.

This report covers physical and numerical modeling of the fishway conducted at the Bureau of Reclamation's Hydraulics Laboratory in Denver, Colorado. The model study provided design support to the Army Corps of Engineers, Los Angles District, the principle designer for the project.

Study Objectives

The primary objectives of the model study were to develop a fishway design based on the following performance objectives:

1. Fishway flow conditions shall encourage upstream passage of adult steelhead. Steelhead are strong swimmers. Several researchers have reported swimming speeds and recommended velocities for upstream passage of adult steelhead trout (McEwan 2001, Bell, 1991, Bjornn and Reiser, 1991 reported in Levy and Slaney, 1993). McEwan suggests passage should not require fish to exceed swimming at 10.0 ft/sec for more than 5 seconds while Bell; and Bjornn and Reiser suggest steelhead are capable of sustained swim speeds in access of 10 ft/s and darting speeds in excess of 15 ft/s. Thompson, 1972 (reported in Barnhart, 1986) reported upstream migration of steelhead is not impaired at depths greater than 0.6 ft, however, deeper depths are recommended for passage. Based on the cited studies, a flow velocity objective for the HFB fishway of 10 ft/s with frequent resting pools was adopted. The objectives for fishway flow depth were set as follows; pool depth = 3 to 4 ft and passage depth = 1.0 to 3 ft.
2. The fishway will only be operated during flow releases through the HFB spillway. The fishway may operate several times a year for a typical duration of one day to five days.
3. Due to anticipated high debris loads during operation, auxiliary attraction flow requiring a grated intake is not acceptable. Attraction to the fishway entrance is to be achieved by flow conveyed through the fishway channel.
4. Fishway flow will likely contain high amounts of brush, willows and other types of small woody debris dislodged during strong storm events. To the degree possible, fishway operation should not be impaired by debris entrained with fishway flow. As a flood-only-operated fishway, the fishway will draw water from high in the diversion pool at all times, thus primarily entraining floating debris.

5. The fishway entrance must be located within the HFB stilling basin pool thus allowing fish within the HFB spillway stilling basin to access the fishway.
6. Stranding of fish within the fishway is a concern during fishway shutdown. Minimizing the opportunity for fish stranding requires controlling flows during facility shutdown. The fishway should provide for a gradual reduction in fishway flows combined with a gradual concentration of flow during shutdown. Fish accustom to the rapid decline of flows that occur in desert streams will likely respond to declining flow and flow depth signals by moving out of the fishway either upstream or returning downstream to the stilling basin pool. Water and fish in the stilling basin pool following closure of the HFB spillway will be passed into the river channel immediately downstream of the service spillway where upstream passage can occur through the existing fishway (Mefford et. al., 2008).
7. The fishway exit shall be gated to prevent flow entering the fishway during non- HFB spillway operation. The release of any flow (including gate leakage) thought the left bank fishway during non-HFB spillway operation is highly undesirable due to the value of the water.

Study Approach

The 2008 HFB spillway study produced a preliminary fishway design based on a hydraulic drop of 12.3 ft and a fishway length of about 150 feet or a fishway slope of about eight percent. The present study evaluated the preliminary fishway design against fishway performance objectives and implemented a series of modifications to the design to improve fishway performance. The fishway study objectives supported the development of a HFB fishway with similar characteristics to many roughened channel style fishways successfully used by Reclamation at slopes of generally less than five percent, Mefford, 2009. Two principle characteristics of many Reclamation roughened channel fishways desirable in the Robles HFB fishway are:

- A wide trapezoidal channel designed to pass large flows through the fishway, thus avoiding the need for auxiliary attraction flow. The trapezoid channel provides diversity of flow depth and velocity within the channel cross section.

- Multiple slot baffles designed to pass floating debris. Flow baffles are composed of a series of concrete piles or rock boulders placed across the fishway. Baffle segments referred to as piles are designed to be submerged during large flow events. Overtopping a segment of the baffles promotes debris passage and produces a rapid increase in fishway flow at the onset of overtopping enhancing fish attraction as river stage rises.

The study is designed to investigate the hydraulic characteristics of minimally baffled fishways at a slope of about 8 percent. The unique operating requirements

of the Robles HFB fishway resulted in a study implementing both three dimensional numerical modeling and a physical model.

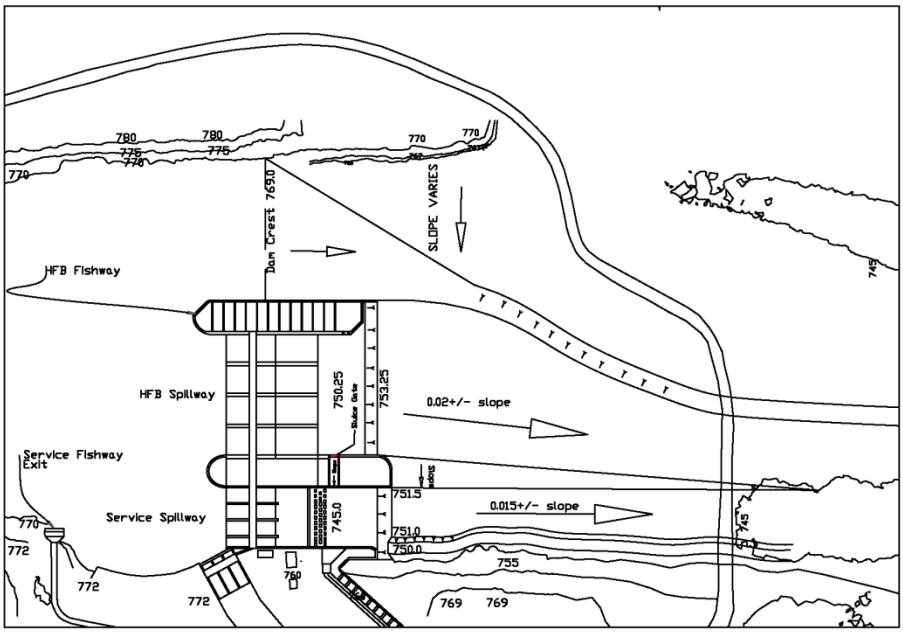

Figure 2 – Plan view of proposed HFB spillway and new HFB fishway, (Mefford et.al., 2008).

Fishway Baffle Development

3-Dimensional Computational Fluid Dynamics (CFD) Modeling

A three dimensional CFD model of an eight percent slope roughened channel fishway with baffles composed of cylindrical piles was developed to investigate fishway flow conditions. The CFD model included approximately 100 ft of the upstream diversion pool, fishway exit structure, baffles and entrance. Simulations of four baffle designs were conducted (labeled A to D in Figure 3). These models allowed investigators to determine how fishway designs successfully used at lower slopes would operate at an eight percent slope. Cylindrical shaped pile baffles were used for ease of modeling. Piles were arranged in an upstream pointing chevron shape similar to other Reclamation roughened channel fishways.

The chevron baffle pattern is used to concentrate flow toward the center of the fishway channel and provide greater variability of passage flow conditions (Mefford, 2009). To promote flushing of floating debris through the fishway, the height of the three center piles were set lower than piles located to the outside of the channel. A 20 ft wide weir with a crest elevation of 766.0 was modeled across the fishway exit. The weir was proposed during the HFB spillway design to restrict fishway operation to diversion pool elevations above the elevation required for full diversion. The invert elevation of the fishway entrance was set at 750.25, equal to the invert elevation of the stilling basin floor.

A trapezoidal fishway channel 32.0 ft wide at the top with a 8 ft wide bottom and 3H:1V side slopes was modeled for all simulations, Figure 3. The channel invert was assumed to be riprap lined and was represented by a 0.5 ft uniform channel roughness height. All baffle configurations were modeled as groups of piles set in a chevron shape with an internal angle of 150 degrees. Twelve baffles consisting of nine piles each were spaced at 14.6 ft center to center along the fishway. The baffle spacing yields a step-pool style fishway with approximately 1.1 ft water surface drop between pools. All simulations were modeled using a fishway flow of 200 ft^3/s which corresponded to the predicted maximum flow that could be passed over the fishway exit weir at diversion pool elevation 768.0.

Baffle A (see Figure 4) consisted of nine 2-ft diameter piles spaced on 3.5 ft centers with 1.5 ft clear opening between piles. The height of the piles relative to the top of riprap in the center of the channel starting with the center pile and moving outward were 4.0 ft, 4.5 ft, 5.0 ft, 5.0 ft and 5.0 ft, respectively. Fishway surface flow velocities (not depth averaged) from the simulation are shown in Figure 5. Surface velocity between piles located in the center of the channel is 10 ft/s to 12 ft/s. Flow velocity between piles located closer to the channel fringes reduces to about 6 ft/s to 8 ft/s. Pool velocity ranges from about 2 ft/s to 4 ft/s. Corresponding flow depths predicted from the simulation are shown in Figure 6. A fishway flow of 200 ft^3/s resulted in a depth in the center of the channel of about 4.3 ft producing shallow overtopping of the center pile. All piles located off centerline extended above the flow. Flow conditions within the fishway at 200 ft^3/s were considered acceptable for passage of adult steelhead however, submergence of the center piles was felt to be insufficient to achieve flushing of floating debris through the fishway.

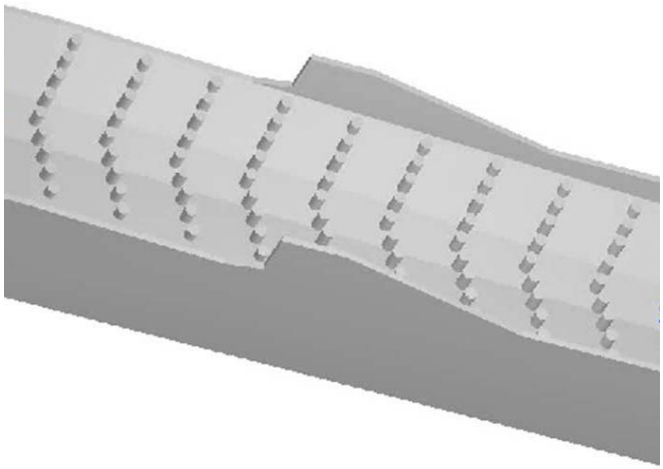

Figure 3 – Isometric view showing a section of the trapezoidal fishway channel with cylindrical pile baffles modeled in Flow3D.

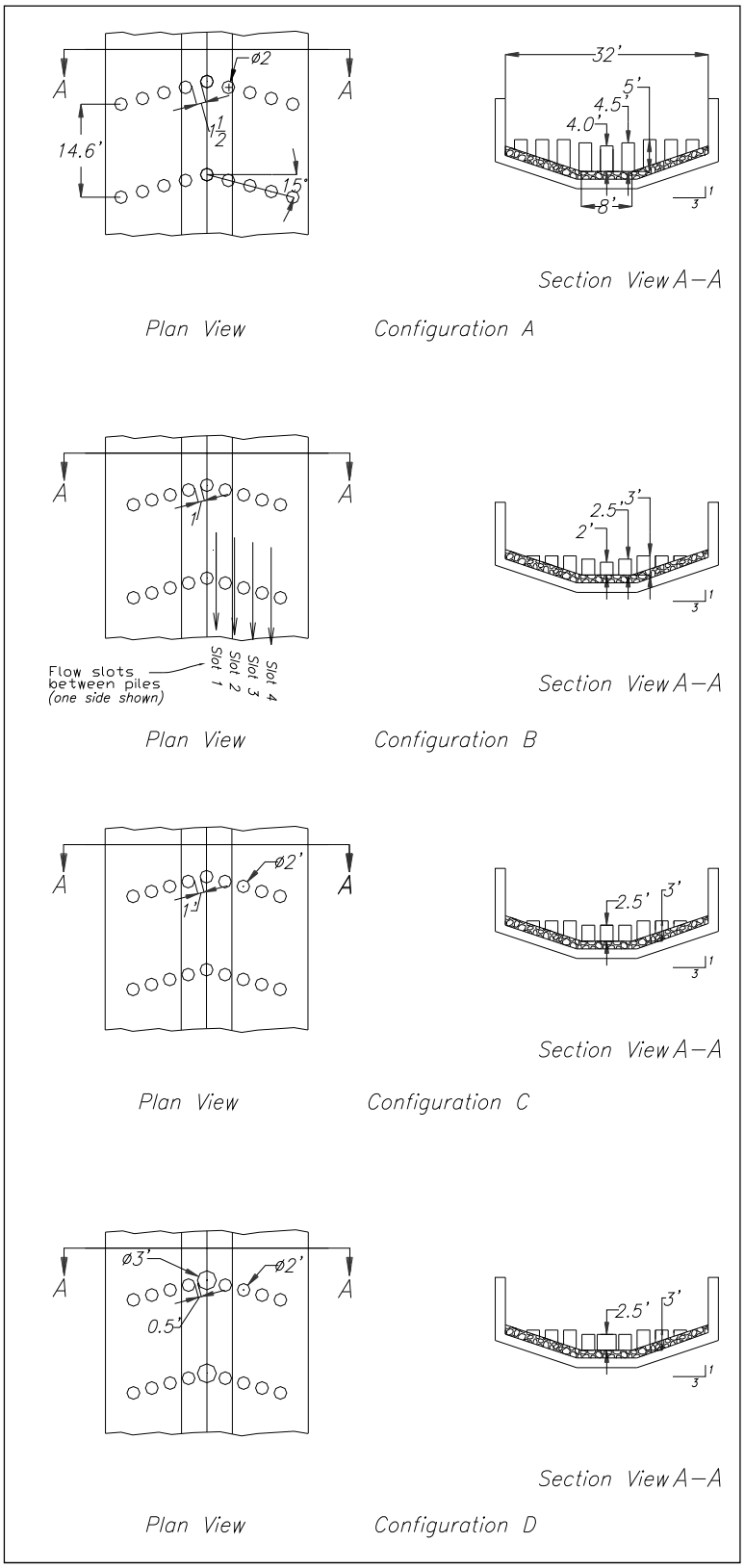

Figure 4 – Fishway baffle designs modeled using the numerical model Flow3D.

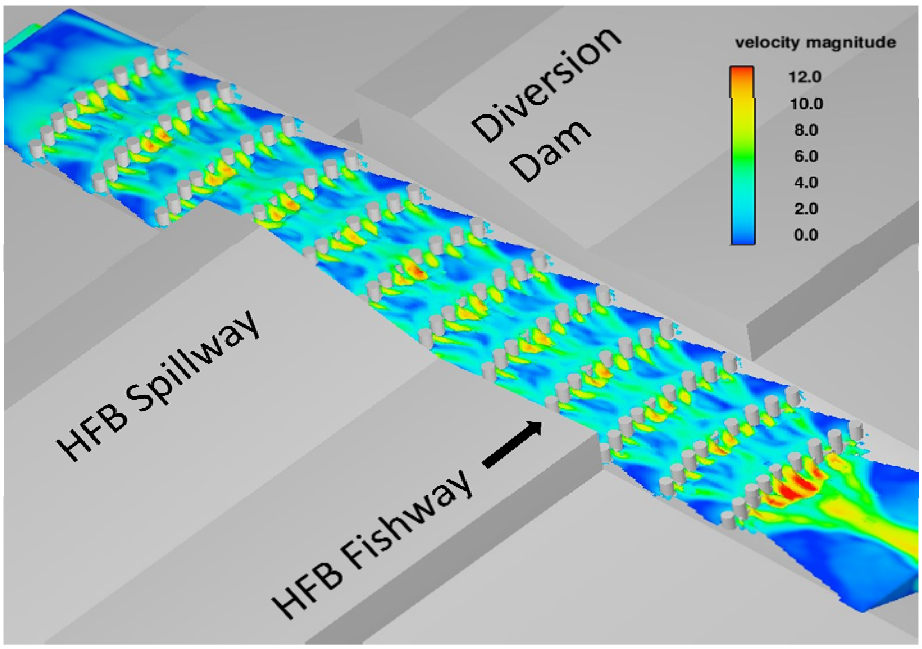

Figure 5 – Isometric view of fishway showing surface flow velocity in ft/s for Baffle A at 200 ft^3/s.

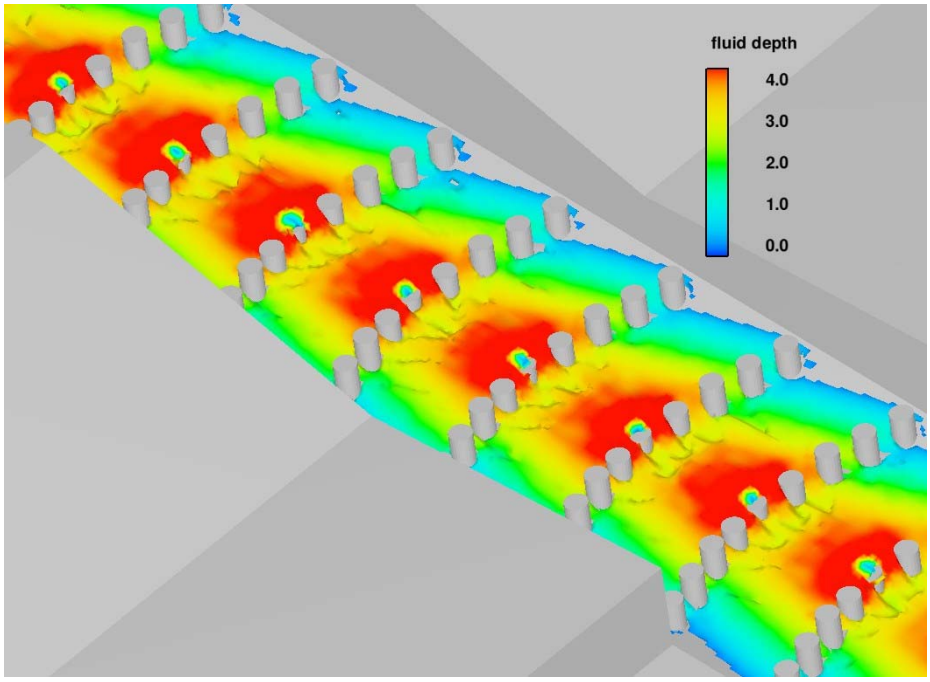

Figure 6 - Fishway flow depth in feet at 200 ft^3/s flow for Baffle A.

A second simulation was conducted of a modified baffle with shorter piles designed to increase the amount of unobstructed near-surface flow in the center of the fishway. Baffle B (see Figure 4) consisted of nine 2.5-ft-diameter piles spaced on 3.0 ft centers with a 1.0 ft clear opening between piles. The spacing between piles was decreased to maintain approximately a 4 ft flow depth in the fishway. The height of the piles relative to the top of riprap in the center of the channel starting with the center pile and moving outward were 2.0 ft, 2.5 ft, 3.0 ft, 3.0 ft and 3.0 ft, respectively. Figures 7 shows fishway surface flow velocity for Baffle B. A strong centered flow is evident with velocity reaching 14 ft/s downstream of the center piles and generally less than 10 ft/s to either side. Vertical velocity contours cut along the fishway passing between piles (see Figure 7 are given in Figures 8, 9 and 10. Figure 8 shows flow velocity and depth along slot line 1 shown in Figure 7. Flow is dominated by standing waves formed by the baffles followed by deep toughs in the pool area between baffles. Flow velocities generally exceed 10 ft/s in the toughs between waves. A similar plot along slot line 2 (Figure 9) shows less wave action and generally lower velocity. Flow velocity along the second slot line is about 8 ft/s to 10 ft/s through the slots with pool velocities less than about 6 ft/s. Closer to the bank, flow velocity and depth decrease further as shown in Figure 10. A plan view showing flow depth at a flow of 200 ft^3/s is given in Figure 11. The center three piles are overtopped by about 1 ft by the standing waves atop each baffle. The scalloped depth pattern in the center of the channel shows the extent of the strong wave action noted.

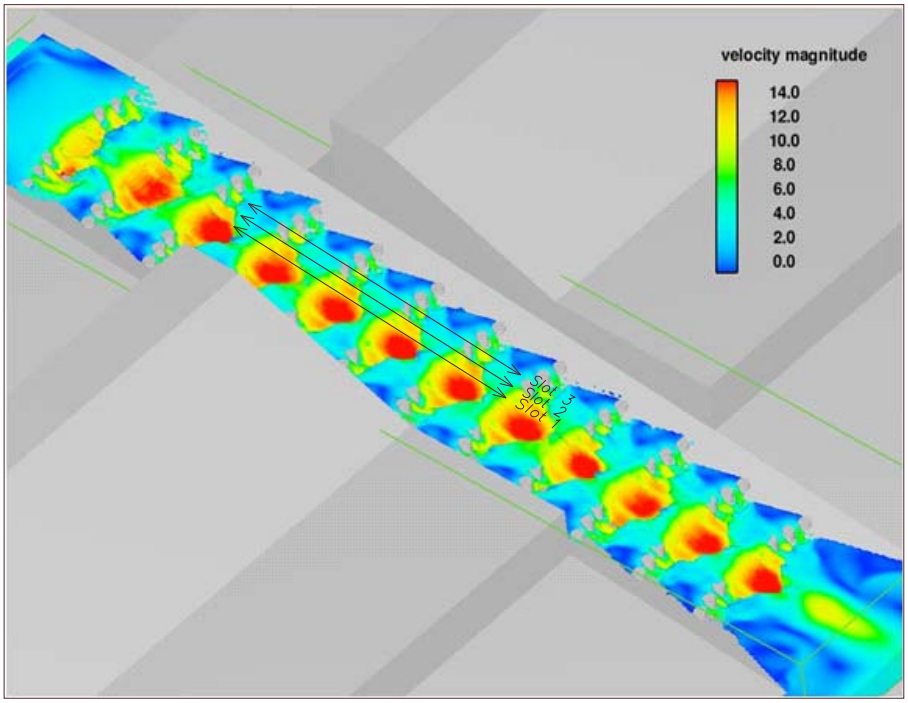

Figure 7 - Surface flow velocity in ft/s for Baffle B at 200 ft^3/s fishway flow.

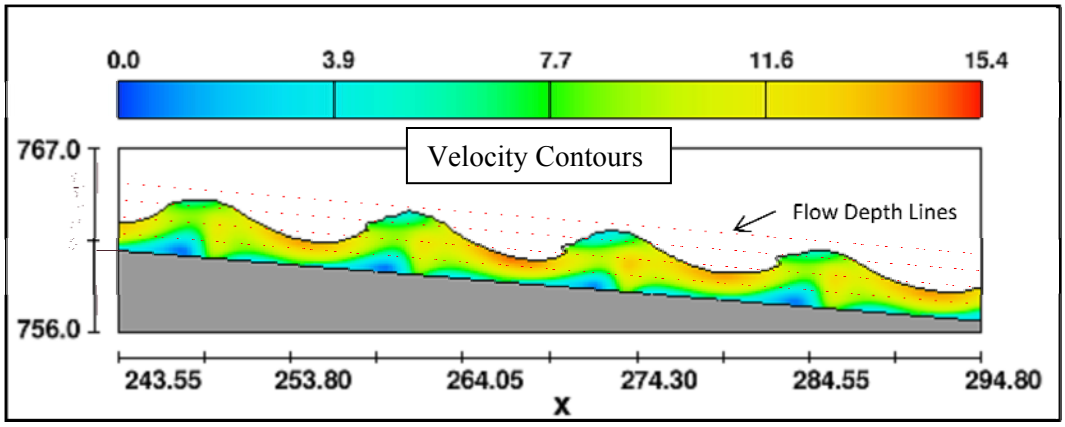

Figure 8 - Baffle B, XZ Section cut through slot 1, see Figure 7.

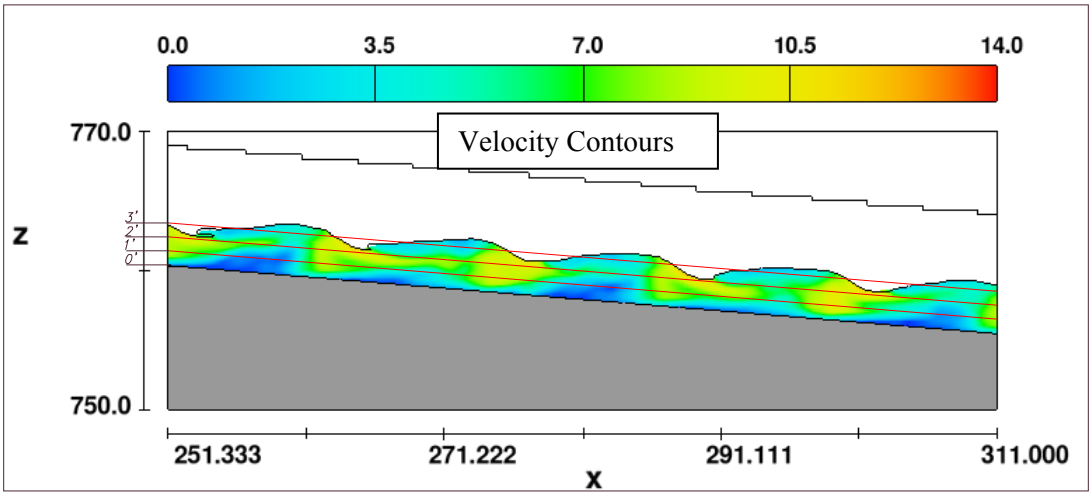

Figure 9 - Baffle B, XZ Section cut through slot 2, see Figure 7.

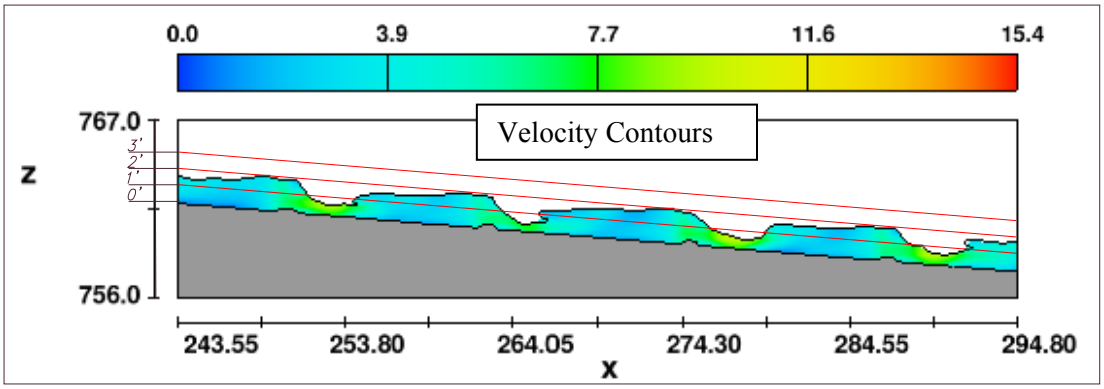

Figure 10 - Baffle B, XZ Section cut through slot 3, see Figure 7.

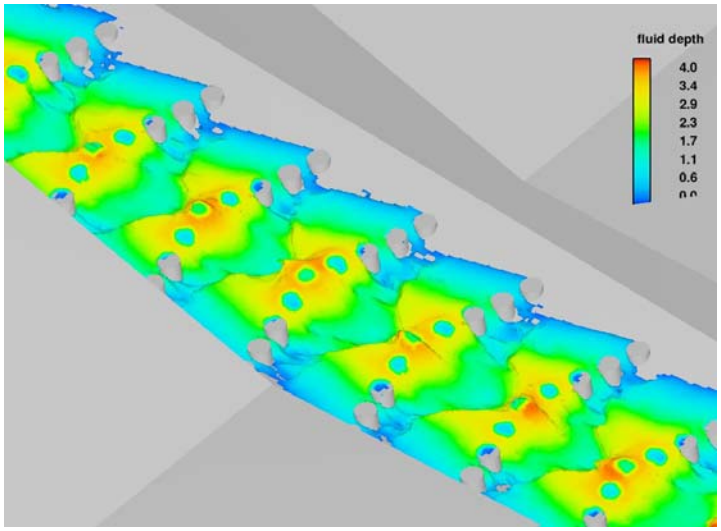

Figure 11 - Fishway flow depth (ft) at 200 ft^3/s flow for Baffle B.

A third simulation was conducted of the fishway with the baffle center pile raised 0.5 ft (see Figure 4, Baffle C). The center pile was raised in an attempt to increase baffle control and dampen the strong wave action noted for Baffle B. A plot of surface velocity is shown in Figure 12. Fishway flow using Baffle C shows a reduction in the highest velocity regions downstream of each baffle compared to Baffle B (Figure 7). This is also shown by comparing vertical sections along slot line 1 in Figures 13 and 8. Comparing flow conditions along adjacent slot lines (Figures 13 and 14), indicate using piles of similar height in the center of the channel yields better uniformity of flow conditions when piles are submerged. Flow depth within the fishway at a flow of 200 ft^3/s is shown in Figure 15. Depth near the center of the fishway is about 3.5 ft. Flow overtops the center three piles from 1.0 ft to 1.3 feet.

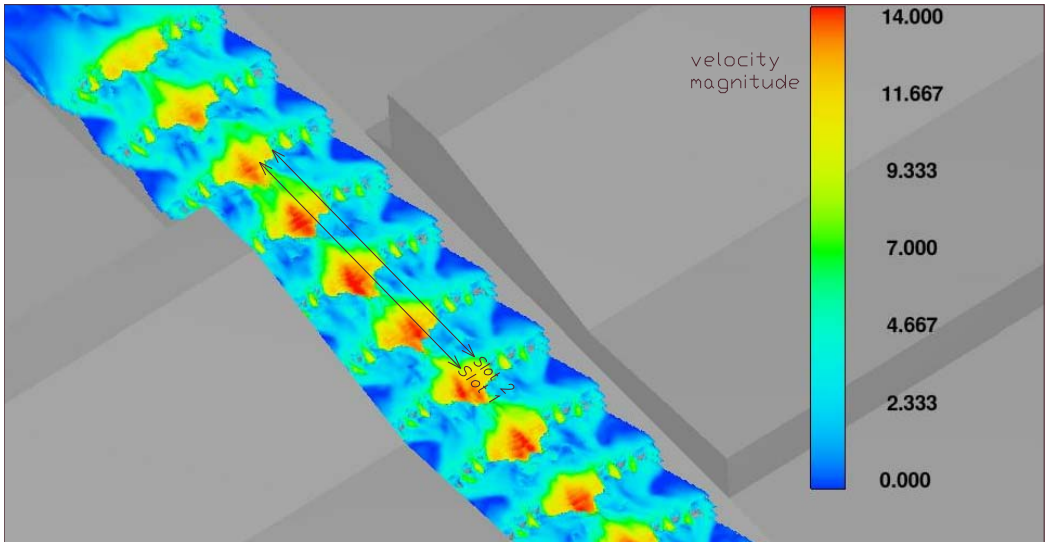

Figure 12 - Surface flow velocity in ft/s for Baffle C at 200 ft^3/s fishway flow.

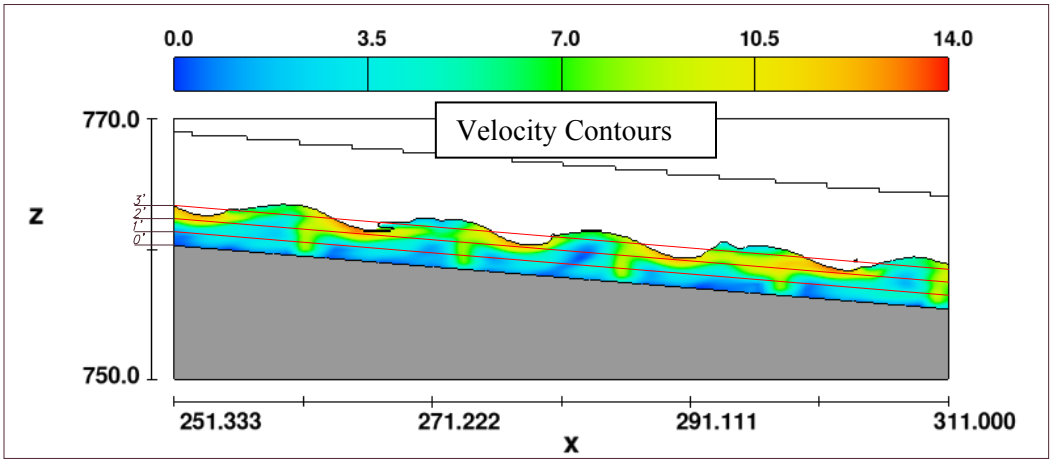

Figure 13 - Baffle C. XZ Section cut through slot 1, see Figure 12.

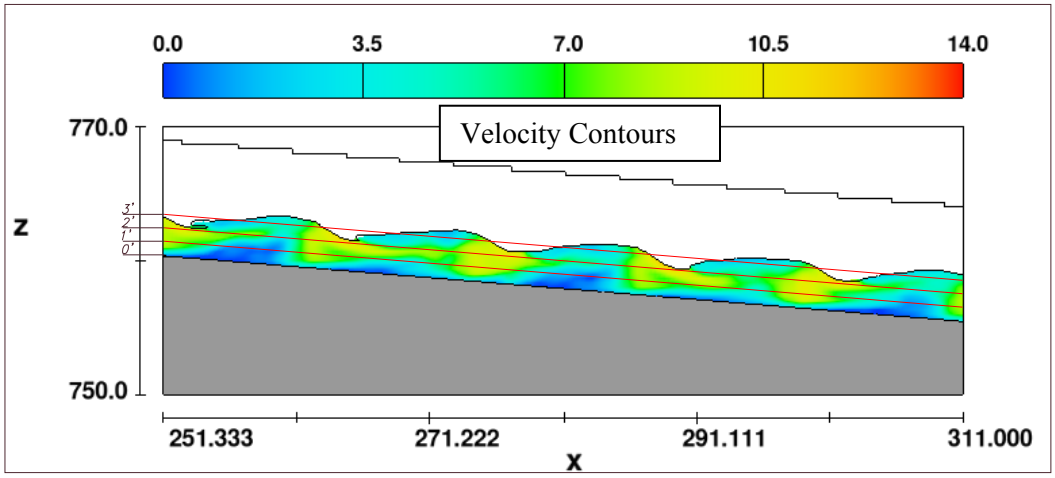

Figure 14 - Baffle C. XZ Section cut through slot 2, see Figure 12.

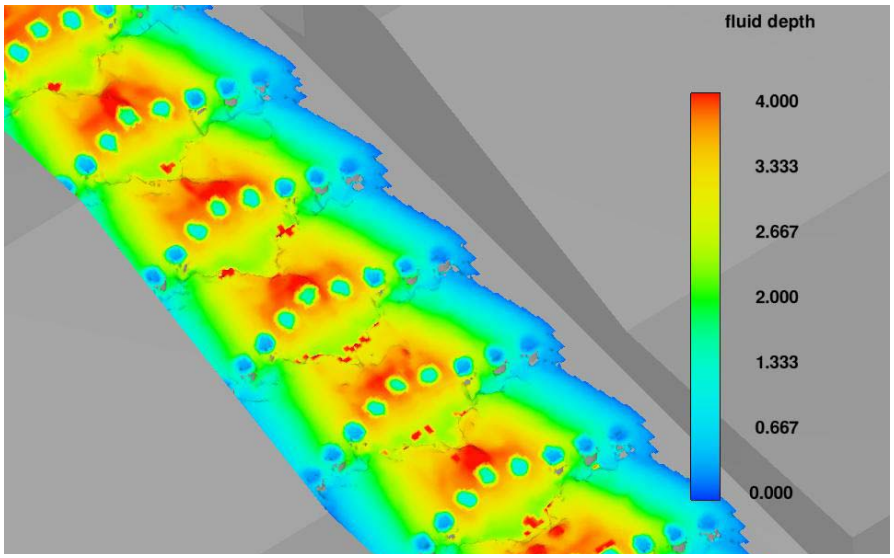

Figure 15 - Fishway flow depth (ft) at 200 ft^3/s flow for Baffle C.

A fourth baffle design labeled Baffle D, was modeled with the slot area on both sides of the center pile reduced from 1 ft to 0.5 ft, (see Figure 4). This simulation was conducted to investigate velocity and depth changes associated with a further reduction of slot flow in the center of the fishway. The slot area was reduced by increasing the diameter of the center pile to 3.0 ft. Surface velocities are shown in Figure 16 and vertical velocity contours along slot lines 1 to 3 (Figure 16) are given in Figures 17 to 19. The change in slot area was small compared to the total flow area; therefore the flow field for baffles "C" and "D" are fairly similar. The most apparent difference in the flow fields is an expansion of low velocity area downstream of each baffle along slot line one, Figure 17.

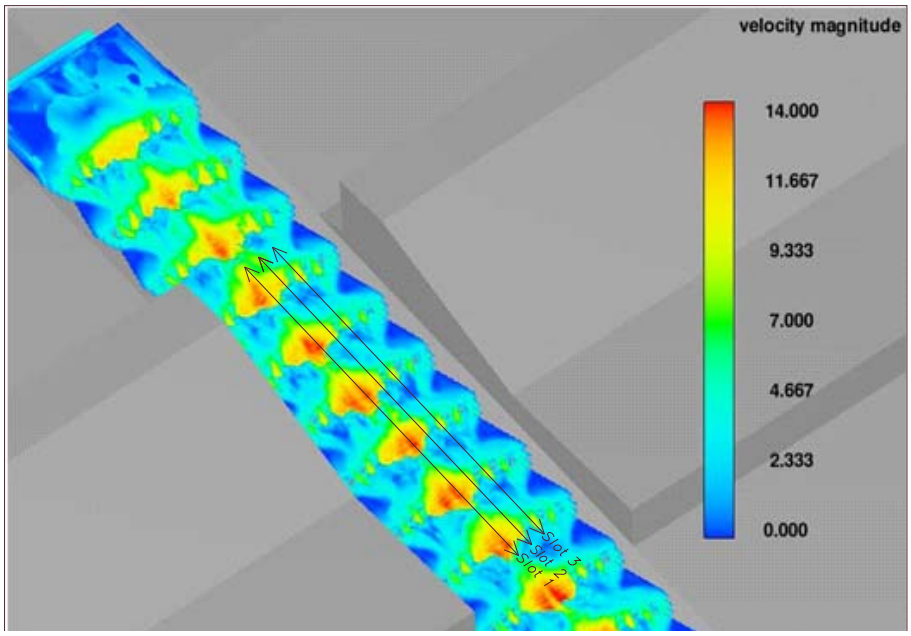

Figure 16- Surface flow velocity in ft/s for Baffle D at 200 ft^3/s fishway flow.

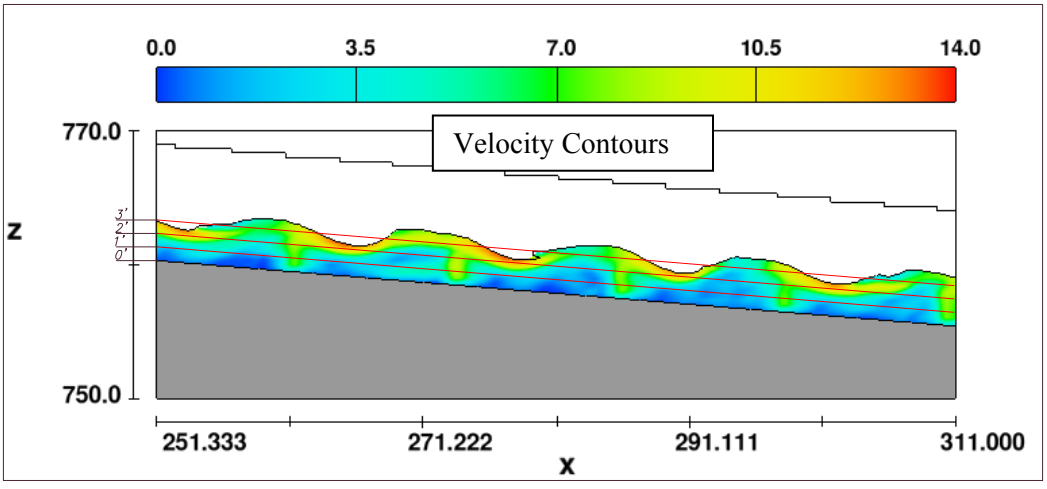

Figure 17- Baffle D, XZ Section cut through slot 1, see Figure 16.

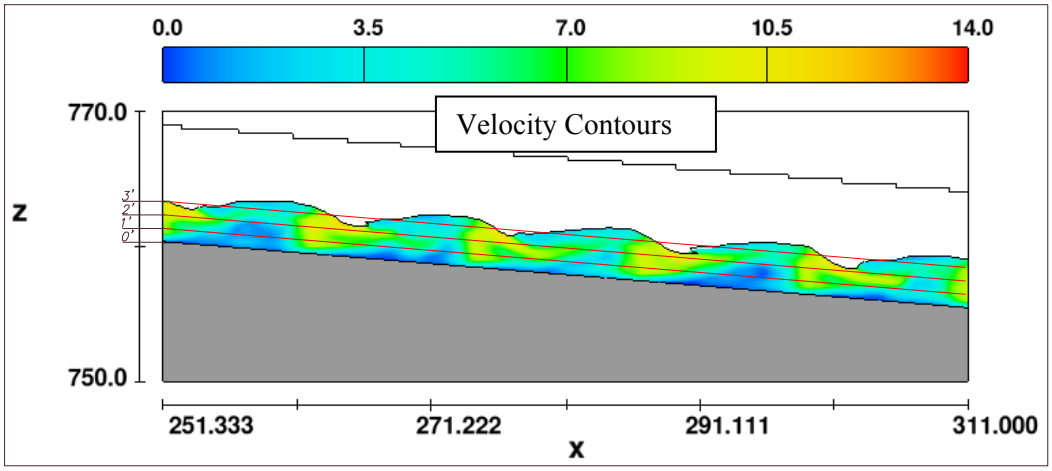

Figure 18 - Baffle D, XZ Section cut through slot 2, see Figure 16.

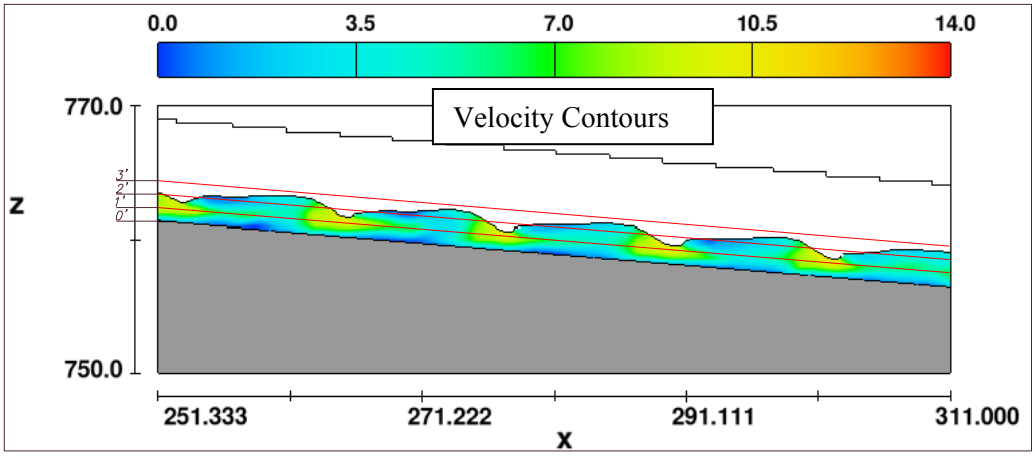

Figure 19 - Baffle D, XZ Section cut through slot 3, see Figure 16.

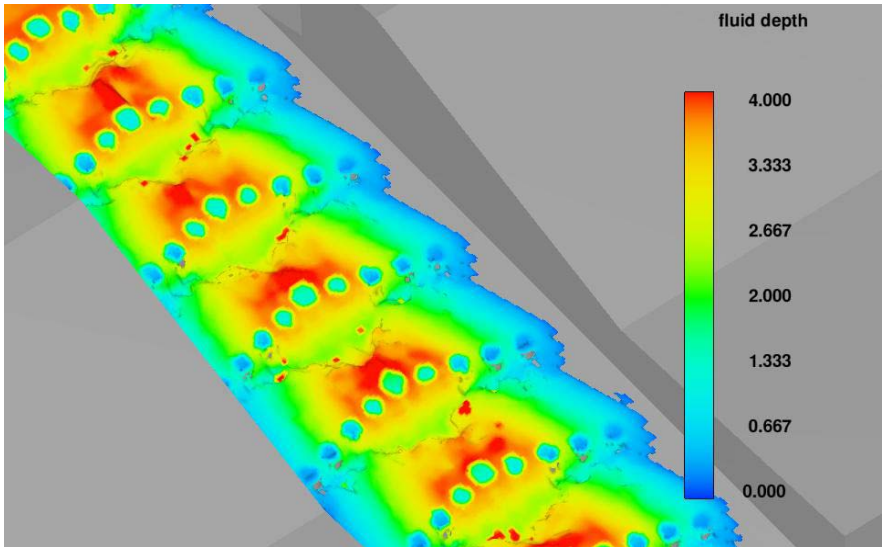

Figure 20- Fishway flow depth (ft) at 200 ft^3/s flow for Baffle D.

Physical Model

A 1:10 Froude-scale physical model of the fishway and a portion of the HFB spillway was constructed at the WRRL (Figure 21). The model included a portion of Robles Diversion Dam, the left most HFB spillway bay, fishway, downstream stilling basin and a section of the rock ramp. A partial width of the HFB spillway was included in the model to simulate tailwater conditions and merging of fishway and spillway flow. The fishway was located similar to the proposed design developed in the HFB spillway study. The entrance is located upstream of the HFB stilling basin endsill on the left side of the leftmost HFB spillway gate. The fishway exit is located on the backside (leftside) of the left spillway gate. Flow enters the fishway through a 20-ft-wide opening with an invert elevation of 766.0. The invert elevation of the fishway exit was fixed at 765.0 to prevent loss of water down the fishway during non-flood conditions. The fishway exit will be gated to allow the diversion pool to rise to elevation 768.0 without release of flow through the fishway. The gate structure was not included in the model as the gate will only be operated in a full open or closed position. The fishway channel was modeled as a riprap-lined trapezoidal channel with an eight-ft-wide bottom and 3:1 side slopes. The downstream rock ramp was also modeled using the similar riprap material as used in the fishway. The HFB spillway gate was modeled as a simple vertical sluice gate.

Physical Model Scaling

Physical model scaling is used to create similitude between model and prototype of major forces controlling the physical processes being studied. Not all forces can be properly scaled simultaneously. Generally, open channel flow problems are modeled based on a Froude scaling relationship. The Froude number relates inertia and gravity forces expressed as, $F_r = v/\sqrt{gd}$ (*v = flow velocity, g = acceleration of gravity and d = flow depth)*. Similitude between model and prototype is achieved when the Froude number in the model and prototype are the same. Using Froude scaling the following relationships apply to the 1:10 geometric scale chosen:

$$L_{p/m} = 10$$

$$V_{p/m} = \sqrt{10} = 3.16$$

$$q_{p/m} = 10^{1.5} = 31.6$$

$$Q_{p/m} = 10^{2.5} = 316.2$$

where: L is length or depth, V is velocity, q is discharge per unit width, Q is discharge and p/m refers to a ratio of prototype to model

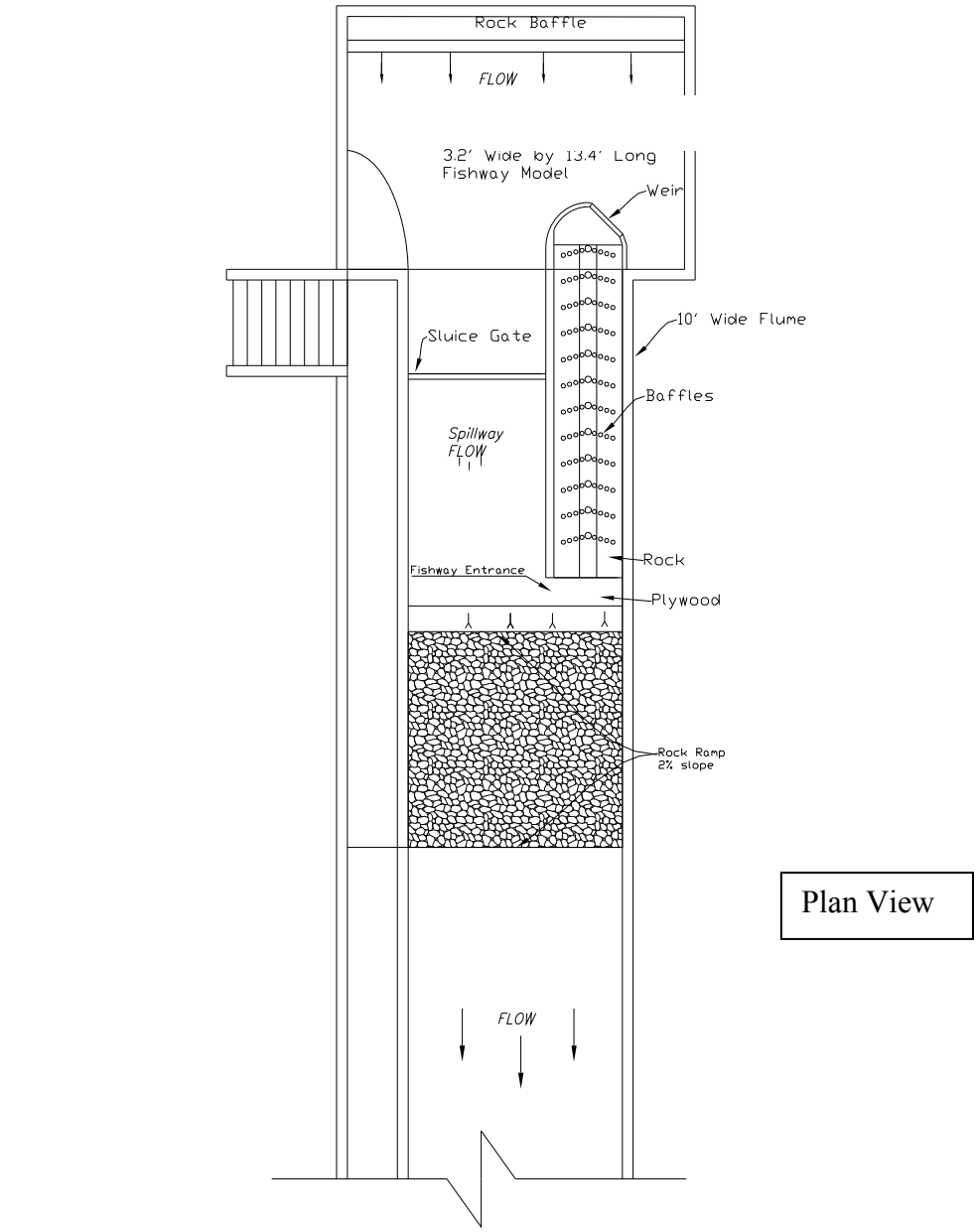

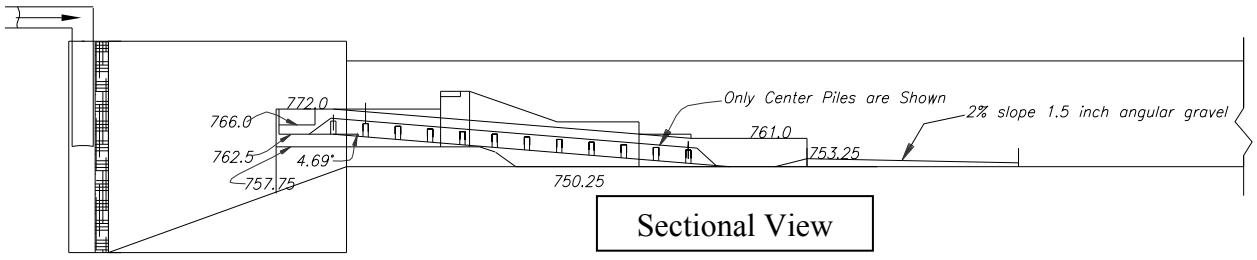

Figure 21 – Plan and sectional view of 1:10 scale physical model.

Fishway Baffle Tests

Baffle configuration "D" was initially installed in the physical model. The model was operated at diversion elevation 768.0 which produced a fishway flow of 160 ft^3/s. Observations of flow conditions in the fishway indicated flow was not sufficient to achieve the desired overtopping of the center piles. The elevation of the exit weir was then lowered to 765.4 which increased fishway flow to about 250 ft^3/s. At the lower exit weir elevation strong skimming flow occurred down the center of the fishway channel. The multiple slot design with overtopping of the three center piles produced a good variety of flow conditions with mid-depth slot velocities measuring about 8 ft/s and lower velocities through the outer slots. An evaluation of debris passage through the fishway was performed by dropping wood material simulating approximately 3 to 5 ft long by 0.25 ft diameter woody debris into the diversion pool. The majority of this material was trapped by the fishway baffles. About 25 percent of the material was carried entirely through the fishway by the flow skimming over the piles in the center of the channel. Although the results of the debris tests were considered as antidotal information, the results clearly indicated narrow slots even with one to two feet of flow overtopping would likely plug during a storm event. A series of quick modifications to the baffle design were then made to investigate possible improvements for debris passage.

The baffle design was changed from ten narrow slots to four wide slots per baffle. This was accomplished in the model by removing the third pile either side of center and then closing several slots to form wider piles. To maintain flow depth, the number of slots was reduced to four. Slots between the center pile and adjacent piles and the slots between the fourth and fifth piles on each side were closed using tape, Figure 22. This resulted in four approximately four-foot-wide (prototype) slots per baffle, one each side of the center pile and one between the outer pile and fishway wall on each side. Limited testing of the modified baffle configuration revealed a significant loss of flow depth and improved debris passage compared to Baffle D. At diversion pool elevation 768.0, the maximum depth in the fishway pools between baffles was about 2.75 ft resulting in little overtopping of the center baffle. Tests of buoyant debris indicated about 60 to 70 percent of the floating material entering the fishway flushed entirely through the fishway. Trapped debris lodged largely against upstream baffle faces near the flow surface and along the channel edges where flow depths were shallow. Some bridging of the 4 ft wide slots by debris was noted as was debris being dislodged by flow after being trapped for a period of time. Major disruption of flow through a slot by debris was not noted in any trials. Observations and water surface measurements revealed the exit weir caused a 15 inch (prototype) drop in the water surface across the weir and a horizontally skewed flow distribution downstream of the weir. The angled exit weir forced significantly more flow to the right side of the fishway resulting in higher flow on the right side than the left for about the upper five baffles. The poor flow distribution was improved by inserting a shallow curved guide wall between the exit weir and the first baffle, Figure 23.

Figure 22 – View looking down the fishway showing flow through the modified baffles. to three piles with four 4-ft-wide flow slots.

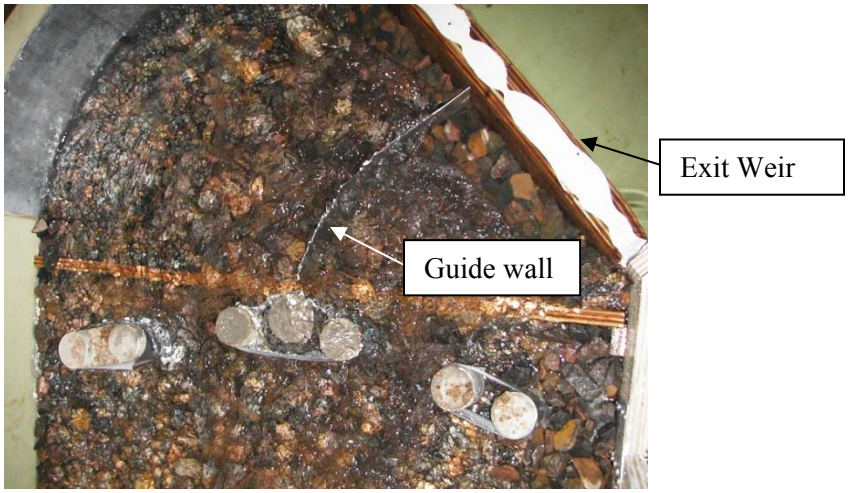

Figure 23 - View of the guidewall installed between the exit weir and upstream baffle.

Modified Fishway Design

Following modification testing the model fishway was rebuilt to implement changes identified during testing. The exit of the fishway was changed to increase fishway flow and reduce the flow skewness created by the exit weir. The crest elevation of the exit weir was lowered to elevation 763.5 and a horizontal weir was installed to elevation 765.2 across the fishway at the start (looking

downstream) of the straight chute, Figure 24. Several baffle heights and a center baffle with a shallow "V" notched crest were investigated with the objectives of maximizing debris passage while providing a minimum flow depth of about 3.5 feet in the center of the fishway and an average flow velocity through the slots of about 10 ft/s. The "V" shaped crest was tested to evaluate potential passage and debris flushing benefits of concentrating flow passing over the center baffle. A schematic of the center pile V crest is given in Figure 25. To facilitate ease of investigating baffle height, model baffles were mounted on guide rods set at each baffle location, Figure 26. The height of baffles positioned on each set of rods were then adjusted by adding or removing sections of piles. The cylindrical piles used in the previous tests were replaced by elongated piles with rounded ends. Model piles were milled from high density urethane foam. Figure 27 shows the new baffle arrangement mounted in the model with 3.0 ft high center piles and 3.8 ft high outer piles (referenced to the channel center elevation).

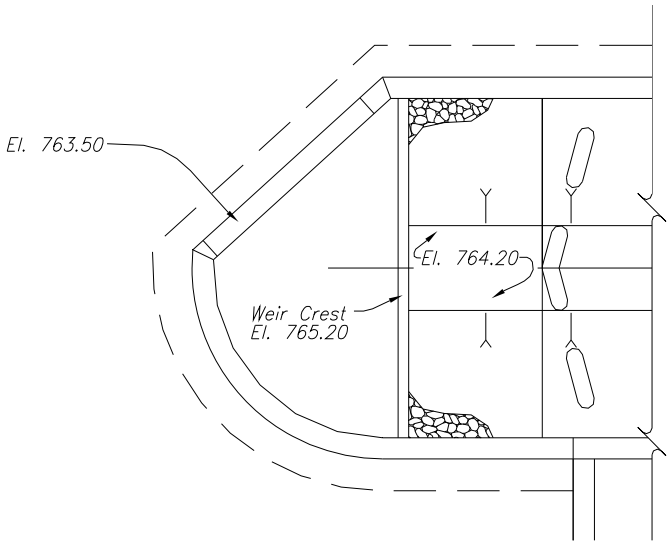

Figure 24 – Plan view showing fishway exit weir and weir added at upstream end of fishway chute.

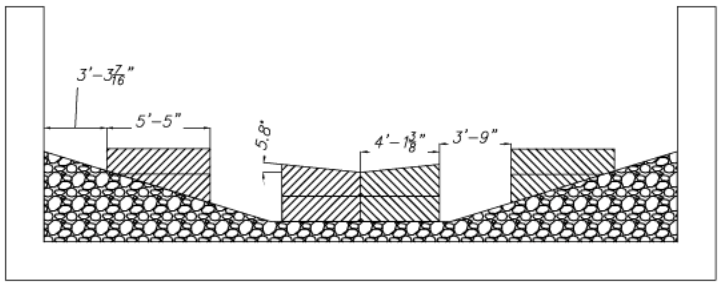

Figure 25 - Sectional view cut along baffle centerline of initial four-slot baffle design.

Figure 26 – Baffle mounting rods used to position fishway baffles in the model.

Figure 27 – Photograph of reconstructed fishway baffles.

Changes to the fishway exit resulted in fishway flow increasing to about 305 ft^3/s at diversion pool elevation 768.0. Flow control shifted from the exit weir to the fishway baffles. With the new fishway weir crest aligned straight with the fishway, the horizontal uniformity of flow approaching the fishway baffles was improved allowing the upstream guidewall to be removed. The model was operated at pool elevation 768.0 while observing fishway flow conditions and debris flushing characteristics. Flow depth through the outer slots was generally less than 1.0 ft which was considered too shallow for effective passage of adult steelhead trout.

The channel shape and baffle design were again modified with the objective of increasing the flow depth through the outer slots. The outer edges of the channel were cut away to create 8.0 ft wide benches on the outer edges of the fishway. The benches set 1.15 ft above the channel thalweg. The outer slot width was reduced to 2.9 ft (34.8 in) by increasing the length of the outer piles. Flow conditions in the revised fishway channel were evaluated for center baffle heights between 2 ft and 4 ft and outer baffle heights between 0 ft and 2 feet. These tests indicated baffles composed of a center pile with the V notched crest set at a notch height 2.4 ft above the channel center and outer piles of height 1.5 ft above the outer bench provided the best flow conditions for achieving fish passage and debris flushing objectives. Plan and centerline profile of the final fishway design are shown on Figure 28. Details of the baffle layout are presented on Figures 29 and 30.

Flow velocity measurements for the final fishway design are presented in Figure 31. Velocity was measured in the model using a 2-D Acoustic Doppler Velocity Meter mounted on an overhead trolley. Shallow flow depths in the physical model limited the locations at which flow velocity could be measured. Velocity measurements were attempted at 0.6 tenths of flow depth. Determining the velocity measurement depth was difficult due to the highly variable water surface, shallow flow depths and large bed roughness. Therefore, the 0.6 tenths depth location reported for velocity measurements is considered to be approximate. Slot velocity was highest downstream of the slot openings in the trough between standing waves created by the baffles. Time-averaged velocity ranged between 6 ft/s and 7 ft/s. Peak instantaneous velocities measured were as high as twice the time-averaged values.

Fishway water surface and depth were measured using a trolley mounted point gage. Water surface profiles were measured along the centerline of the channel and the centerline of the inner and outer slots. The changes to the channel and baffles resulted in flow depth through the outer slots of between 1.5 ft and 2 ft at pool elevation 768.0, (305 ft^3/s fishway flow), Figure 31. Flow depth along a path passing through the center of the inner slots and channel centerline varied between 3 ft and 4.5 ft. Photographs of the model fishway final geometry operating at pool elevation 768.0 are given in Figures 33, 34 and 35.

The fishway will be slowly shutdown following closure of the HFB spillway to encourage fish to move out of the fishway. Fishway flows will decline during the shutdown process by either drawdown of the diversion pool or closure of the isolation gate located atop the exit weir. Model data relating fishway flow depth and diversion pool elevation is given in Figure 36. The data shows all fishway flow will pass through the inner slots (fishway bench areas are dry) when the diversion pool elevation falls below 766.0 ft. The fishway isolation gate was not included in the model and therefore closure simulations based on exit gate operation were not conducted. Development of procedures and duration for shutting down the fishway were not studied in the model and are best accomplished during commissioning of the prototype structure.

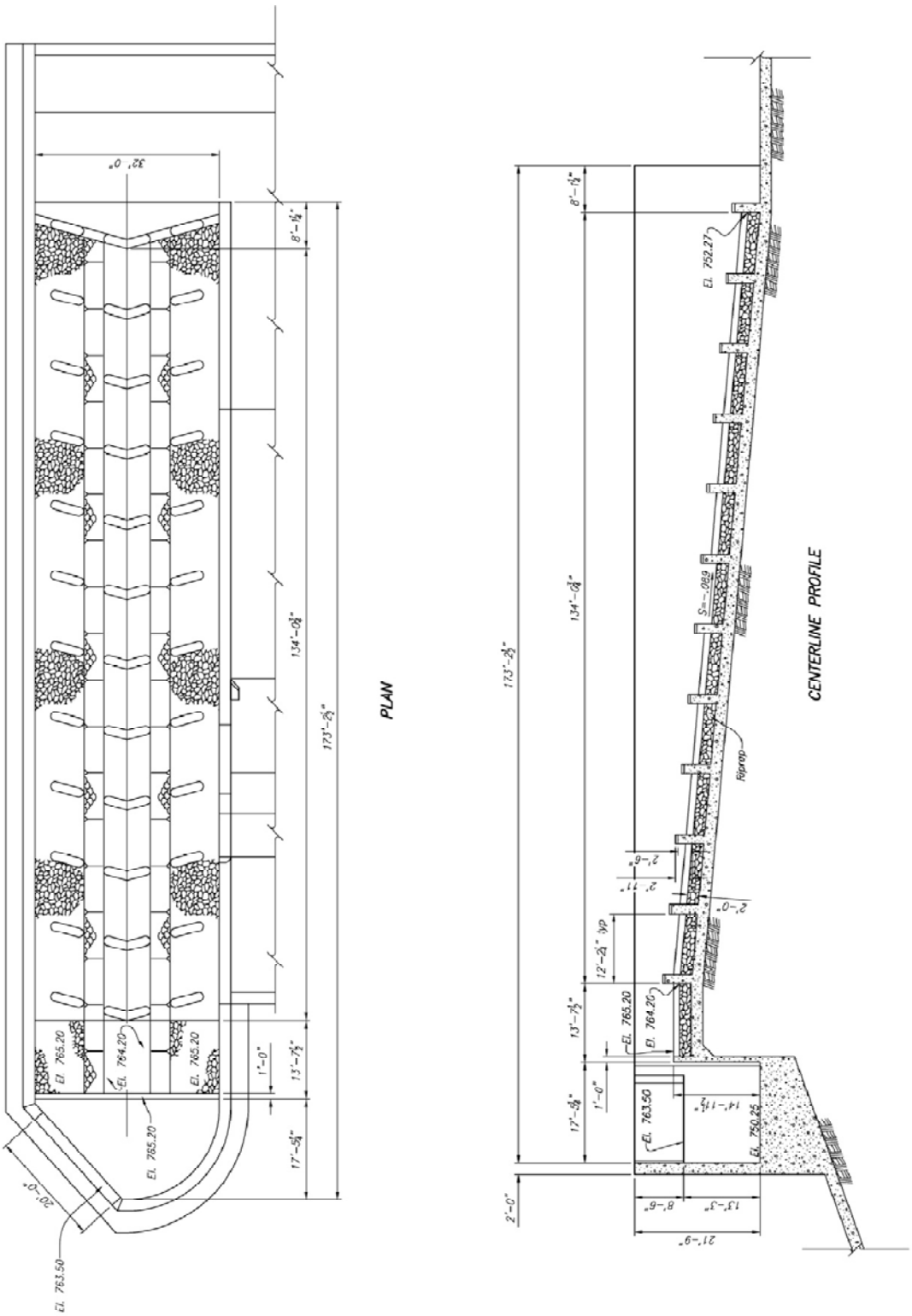

Figure 28 – Plan and centerline profile section of the final fishway design.

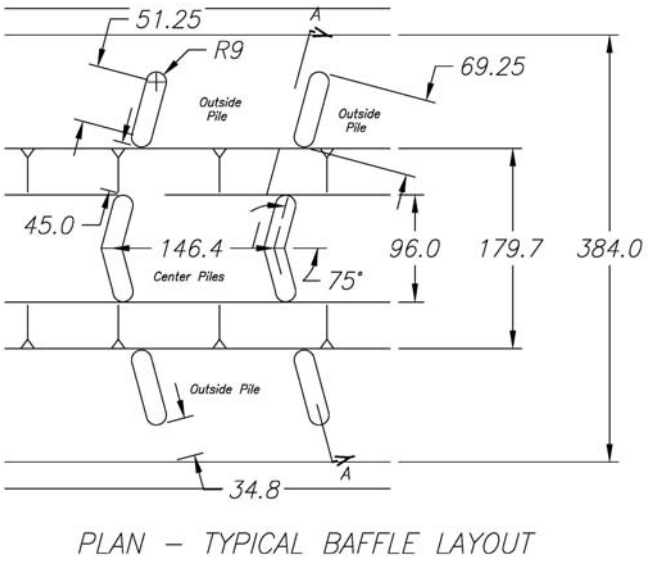

Figure 29– Layout of final fishway baffle design. Dimensions are shown in inches prototype.

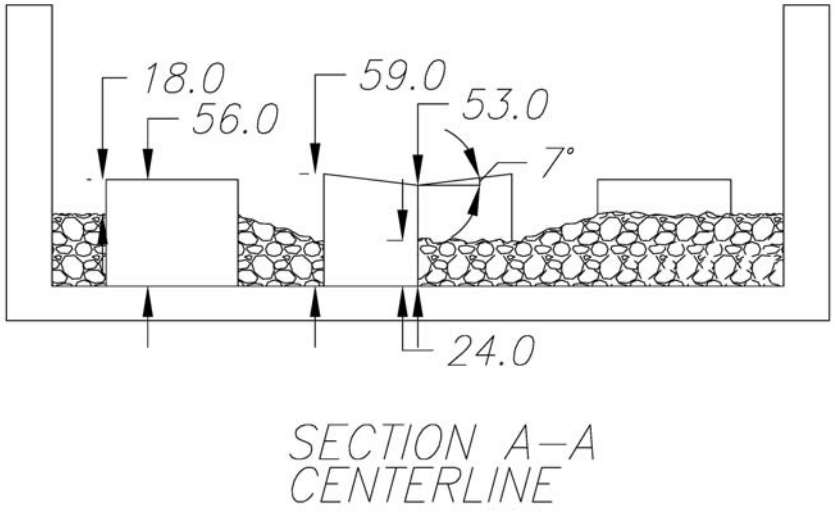

Figure 30 - Sectional view of final fishway baffle design. Refer to Figure 29 for section location. Dimensions are shown in inches prototype.

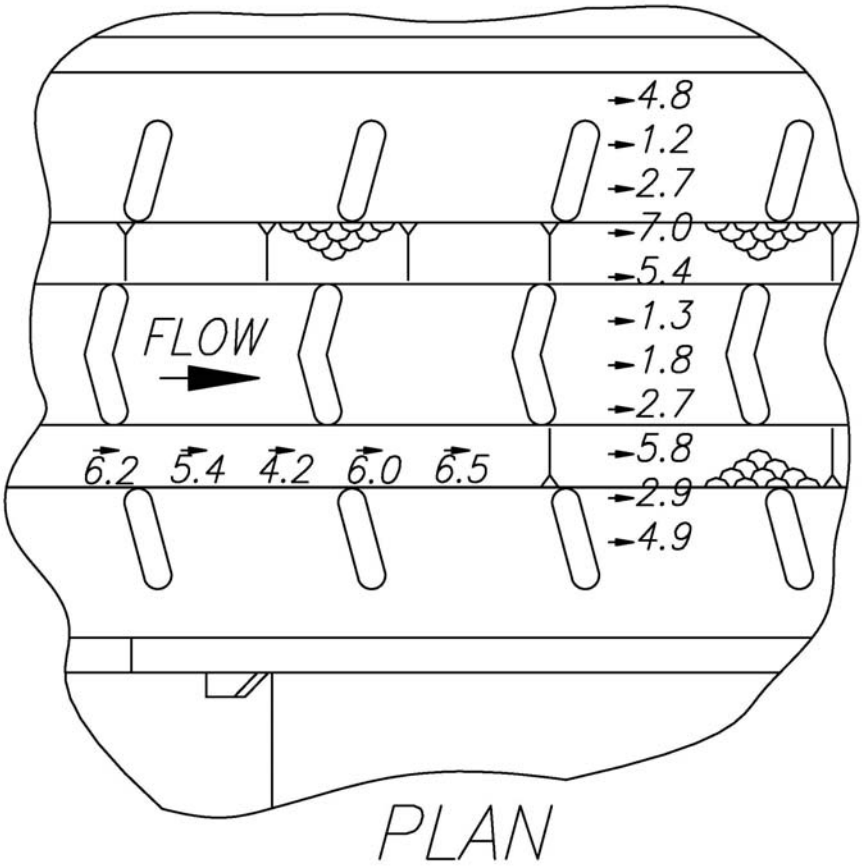

Figure 31 – Plan view of fishway showing location and magnitude of measured flow velocities in ft/s prototype operating at diversion pool elevation 768.0. Velocities were measured at approximately 0.6 tenths depth.

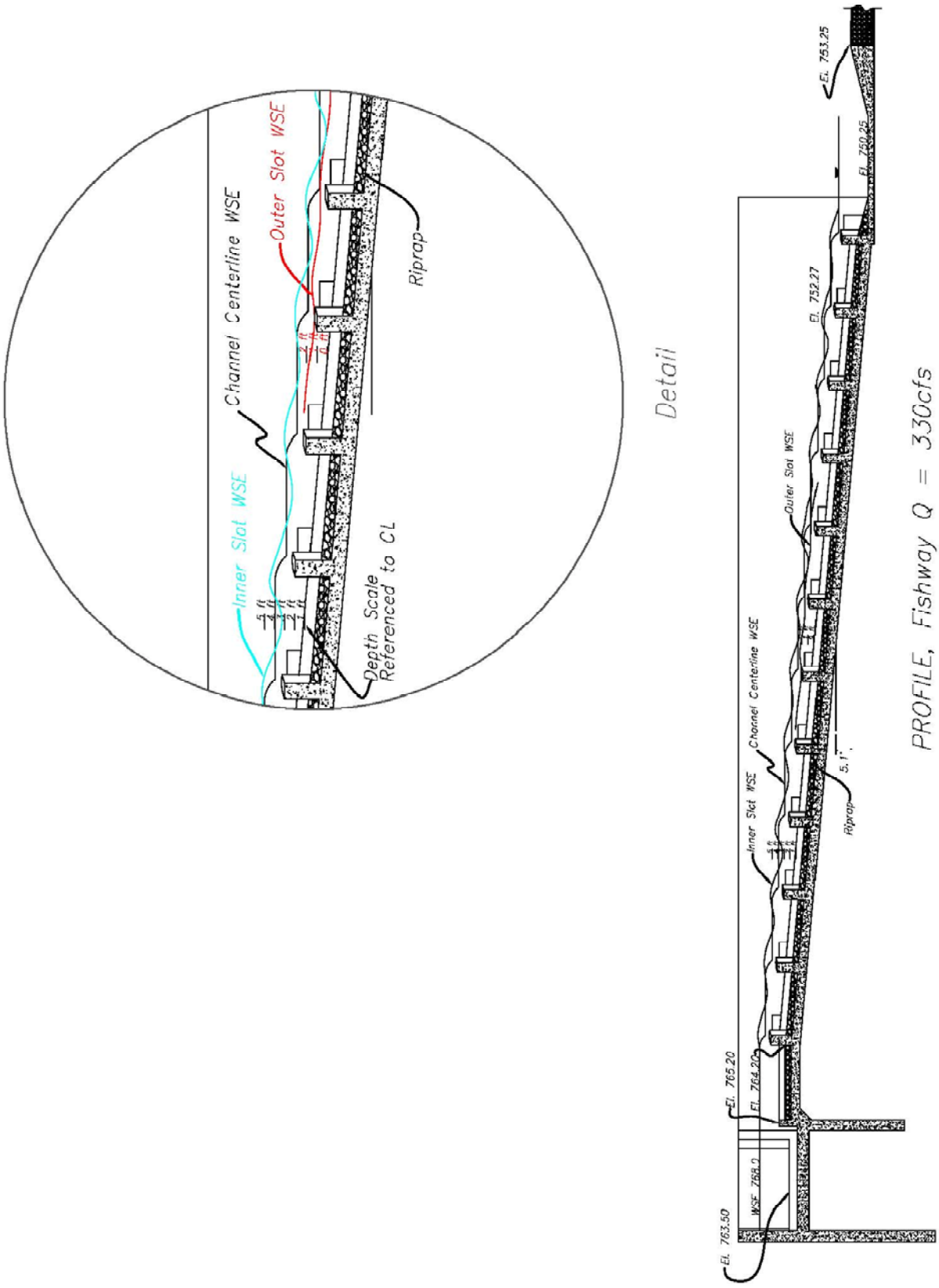

Figure 32 – Section view showing water surface elevations measured in the physical model at the center of the channel, center of the inner baffle slot and center of the outer baffle slot for diversion pool elevation 768.0.

Figure 33– Photograph of the final fishway design showing the fishway exit sill and the fishway weir located at the upstream end of the straight chute. The diversion pool is elevation 768.0.

Figure 34- Photograph of the final fishway design looking upstream toward the fishway exit.

Figure 35– Close-up surface view of flow passing through the recommended fishway baffle arrangement.

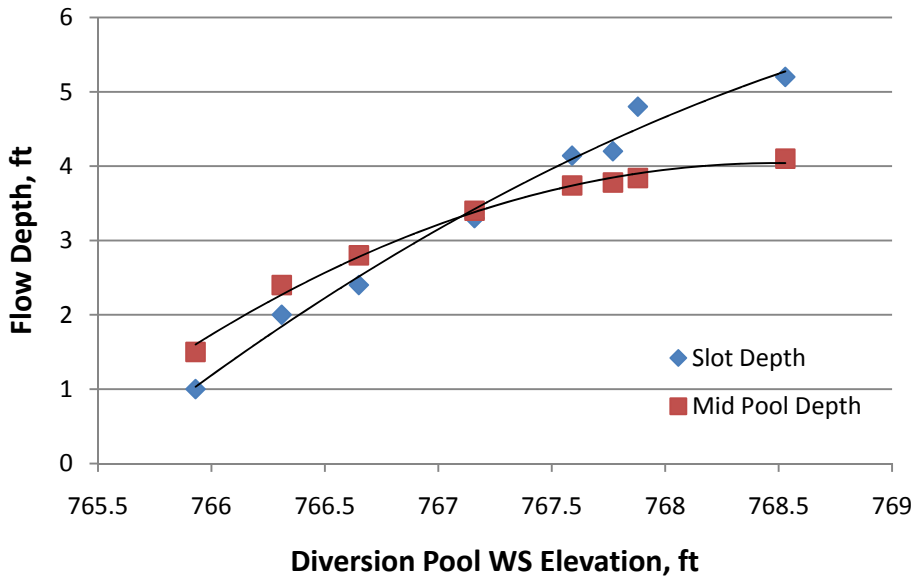

Figure 36 - Fishway flow depth for diversion pool elevations below design.

Numerical Modeling of Fishway Final Geometry

The final fishway design determined from the physical model was numerically modeled using FLOW3D to better document flow velocity and depth conditions beyond what was possible to measure in the physical model. Numerical simulations of the fishway operating at normal diversion pool (El. 768.0) and at high pool (El. 768.5) were conducted. The fishway riprap invert was modeled using a bed roughness of 0.25 ft. The roughness was chosen to represent riprap material ($D_{50} \approx 1.25$ ft) with intestinal voids choked using a graded cobble/gravel/sand material. Choking the riprap matrix in the fishway is recommended to fill large voids. The choke material reduces interstitial flow through the riprap and eliminates large surface depressions that could strand fish during shutdown of the fishway. The X and Y model coordinates referenced in the model output plots is given in Figure 37.

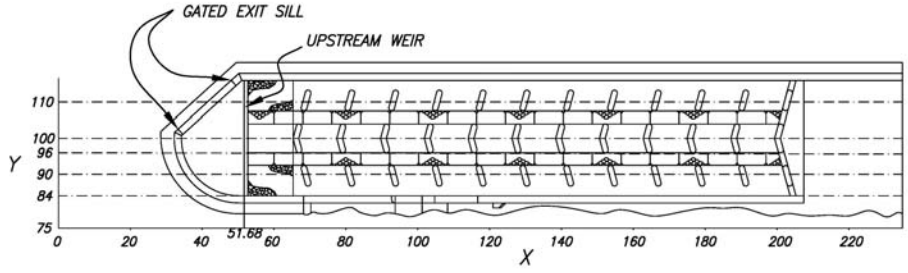

Figure 37 – Plan view showing numerical model X and Y coordinates.

Figures 38 through 42 present flow velocities predicted by Flow3D for the final fishway geometry with the upstream diversion pool water surface set at elevation 768.0. The simulation predicts a flow of 295 ft^3/s through the fishway. Figure 38 presents a plan view of depth average velocity contours within the fishway and downstream basin. Predicted velocities through the baffle slots are higher than the averaged point velocities presented in Figure 31 for the physical model. Peak velocities reported from the physical model more closely compare with numerically predicted velocities. Due to the difficult measurement conditions in the physical model previously discussed, the higher velocities predicted by the numerical simulations are thought to better represent actual flow conditions. Vertical velocity contours through the baffle's inner slot are presented in Figure 39. The sectional view shows flow moves down the fishway inner slots at a velocity of about 10 ft/s. Highest flow velocity (10 ft/s to 13 ft/s) occur in the wave trough downstream of each baffle. Vertical sections showing flow velocities adjacent to the slots are shown in Figures 40 and 41. Flow overtops the fishway baffles by about 1 ft creating three lines of step-pool-cascades. Flow velocity in the pools between baffles is generally less than 4 ft/s with large areas

less than 2.5 ft/s. Flow depth between baffles in the center of the fishway (Y=100, Figure 37) is about 3.5 ft. Depth in the outer pools (Y=86, Figure 37) is about 2 ft. A profile of flow velocity through the outer slots is given in Figure 42. Flow velocities are similar to the inner slot with velocities ranging from about 8 to 12 ft/s. Flow depth along the outer slot averages about 1.5 ft. Minimum depth in the wave troughs is about 1.0 ft. Flow depths for the entire fishway are given in Figure 43.

Similar plots of flow velocity and depth for the fishway operating at diversion pool elevation 768.5 are given in Figures 44 through 49 for comparison. The simulation predicts an increase in fishway flow to 385 ft^3/s at pool elevation 768.5. The simulations show fishway flow velocities are similar between normal and high pool operation with fishway flow depth increasing about 0.2-0.3 ft. at high pool.

Conclusions and Recommendations

A minimally baffled fishway was developed for Robles Diversion Dam to provide passage for adult steelhead trout. The fishway is designed to operate as an auxiliary fishway during flood events in excess of about a two year event. An engineered roughened-channel-fishway design is recommended for the project. This type of fishway was selected because large flows needed for fish attraction could be passed directly through the fishway, thus eliminating the need for auxiliary attraction flow facilities. The fishway is designed to convey 300 ft^3/s flow at normal diversion pool (el. 768.0 ft) with flow increasing to about 400 ft^3/s at maximum pool (el.768.5 ft). Key features developed for the design in an effort to provide unimpeded fish passage during debris-laden flood flows are:

- Baffles designed to reduce the probability of debris jams totally blocking passage by incorporating multiple passage routes across each baffle.
- Baffles with wide passage openings (slots) reducing the risk of small woody debris bridging across slots.
- Baffle slots aligned along the fishway creating flow chutes that convey debris straight through the fishway.
- Baffles designed to be overtopped under normal fishway flow facilitating flushing of floating debris.

The recommended fishway design is shown in Figures 28, 29 and 30. The fishway functions as a step-pool type fishway with resting areas located on the periphery of the main flow. Therefore, pools do not serve to dissipate the energy of the main flow. Channel slope, bed roughness and the energy loss due to flow expansion and contraction passing between baffles are the primary controls on passage velocity. Model data predicts average velocity in the passage chutes of about 10 ft/s. Resting pools are spaced at 12.2 ft on center. Fish moving from pool to pool through the baffle slots will encounter 10 ft/s flow for distances less than 10 ft. Passage is also possible for fish passing from pool to pool by jumping

or swimming over the baffles. The 8.9 percent slope of the fishway was chosen based on fitting the fishway into the proposed HFB spillway while meeting fish passage flow requirements. The proposed fishway meets passage objectives as set for this study, however during design, opportunities that allow the fishway slope to be reduced should be considered.

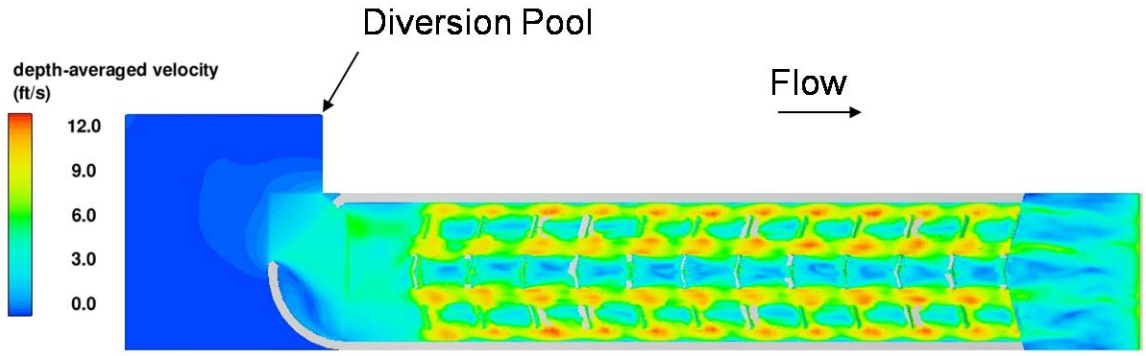

Figure 38 – Plan view showing depth average velocity contours of flow through the final fishway geometry at diversion pool elevation 768.0. Predicted fishway flow is 295 ft^3/s.

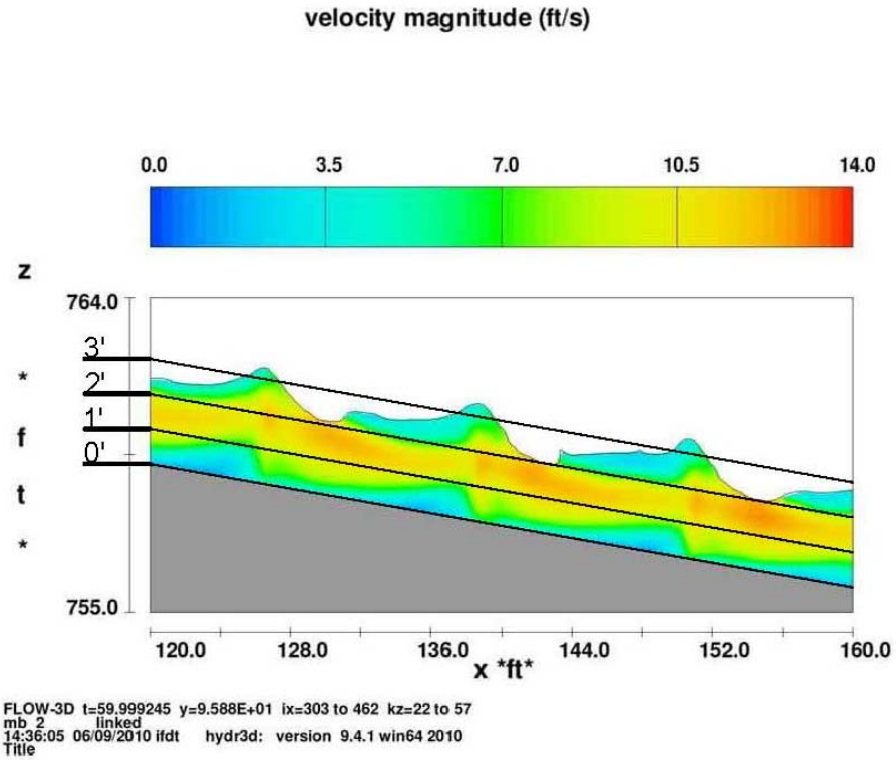

Figure 39 - Elevation sectional view showing flow velocity through the inner slots (see Figure 36 reference location Y=96 ft) at diversion pool elevation 768.0. Flow depth and elevation are shown on the vertical axis.

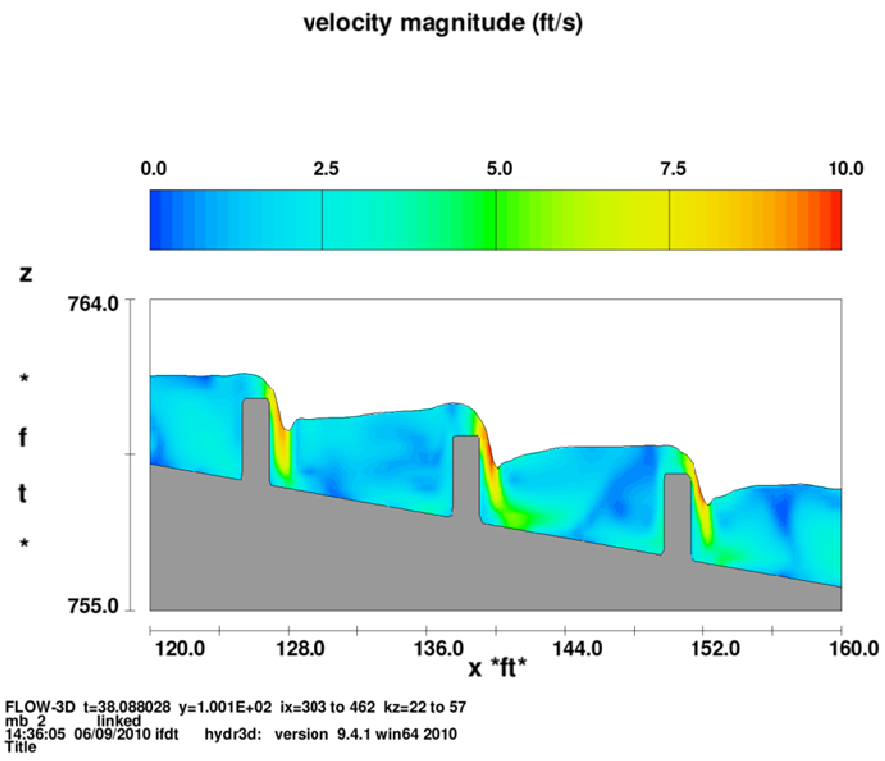

Figure - 40 Elevation sectional view showing flow velocity along the fishway centerline (see Figure 36 reference location Y=100 ft) at diversion pool elevation 768.0.

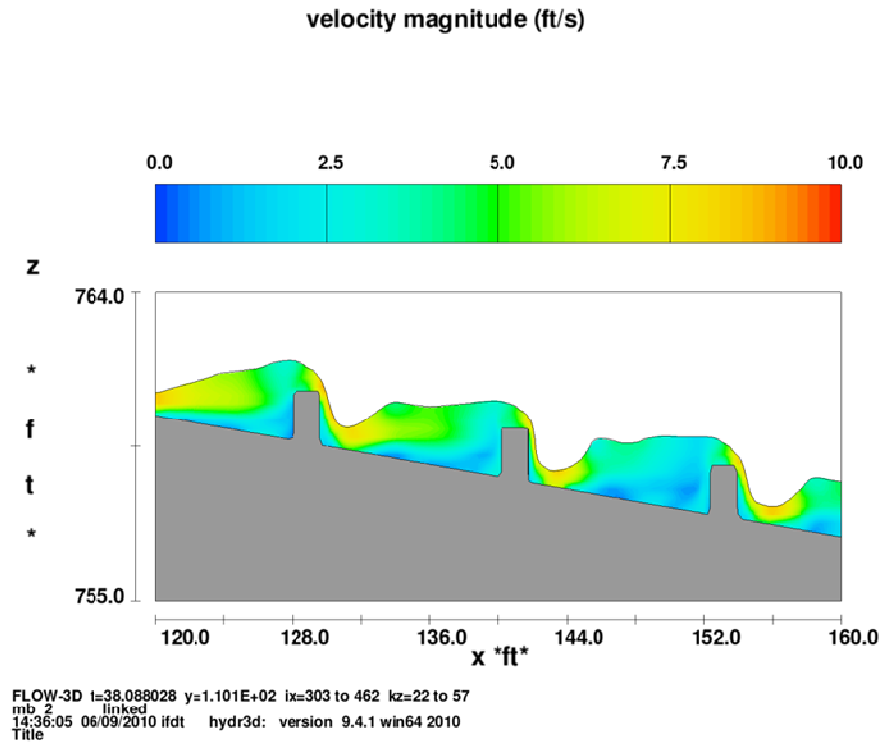

Figure 41 – Elevation sectional view showing flow velocity along the centerline of the outer pile (see Figure 36 reference location Y=110 ft) at diversion pool elevation 768.0.

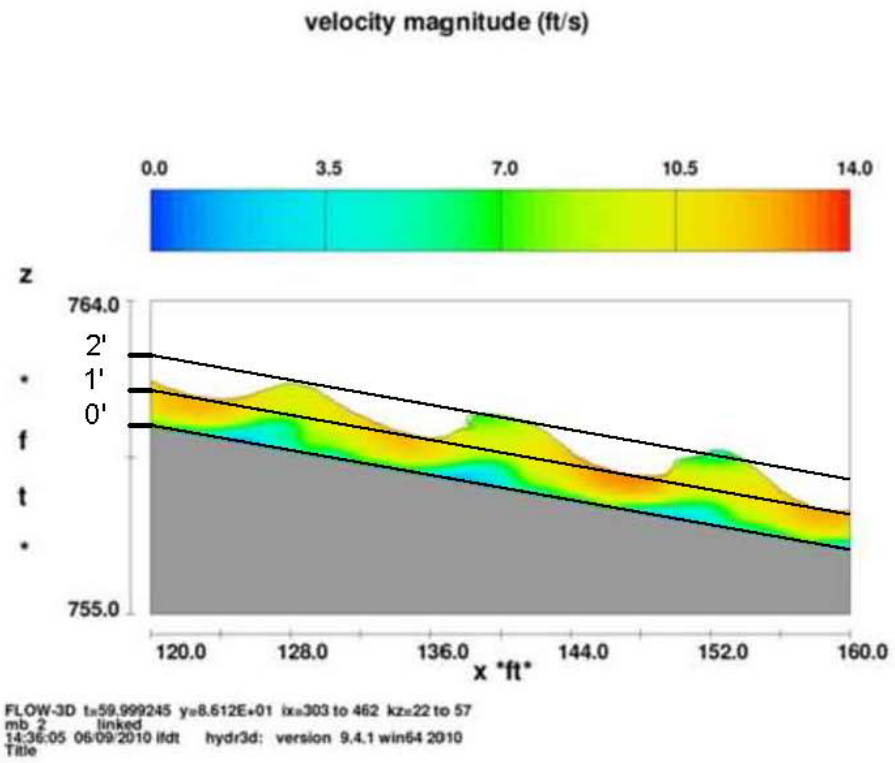

Figure 42 - Elevation sectional view showing flow velocity along the centerline of the outer slot (see Figure 36 reference location Y= 86 ft) at diversion pool elevation 768.0.

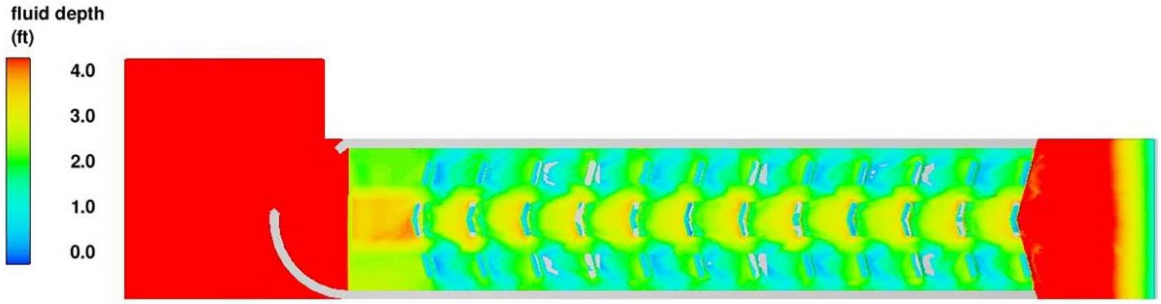

Figure 43 – Plan view showing fishway flow depth predicted by the numerical simulation for reservoir pool elevation 768.0. Fishway flow is 295 ft^3/s.

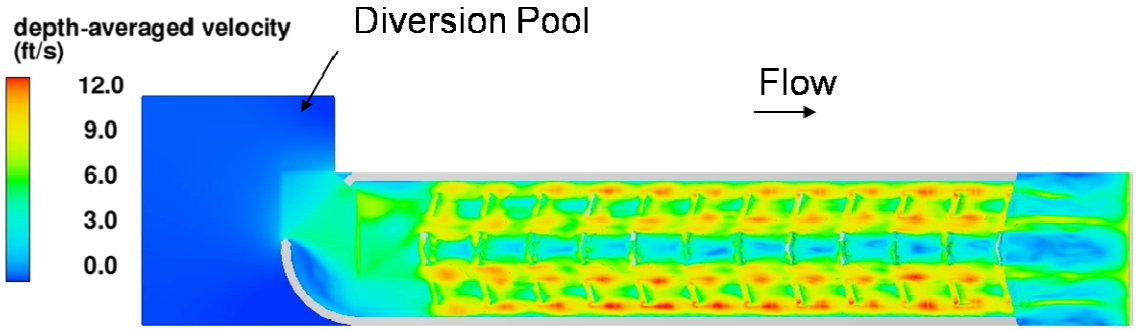

Figure 44– Plan view showing depth average velocity contours of flow through the final fishway geometry at diversion pool elevation 768.5. Predicted fishway flow is 385 ft^3/s.

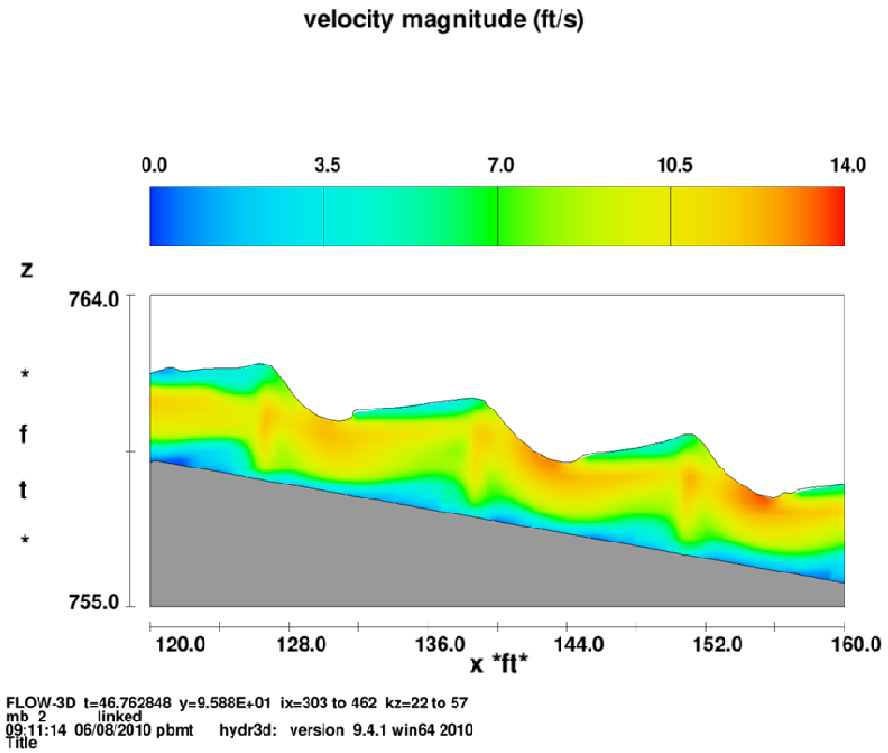

Figure 45 - - Elevation sectional view showing flow velocity through the inner slots (see Figure 36 reference location Y=96 ft) at diversion pool elevation 768.5.

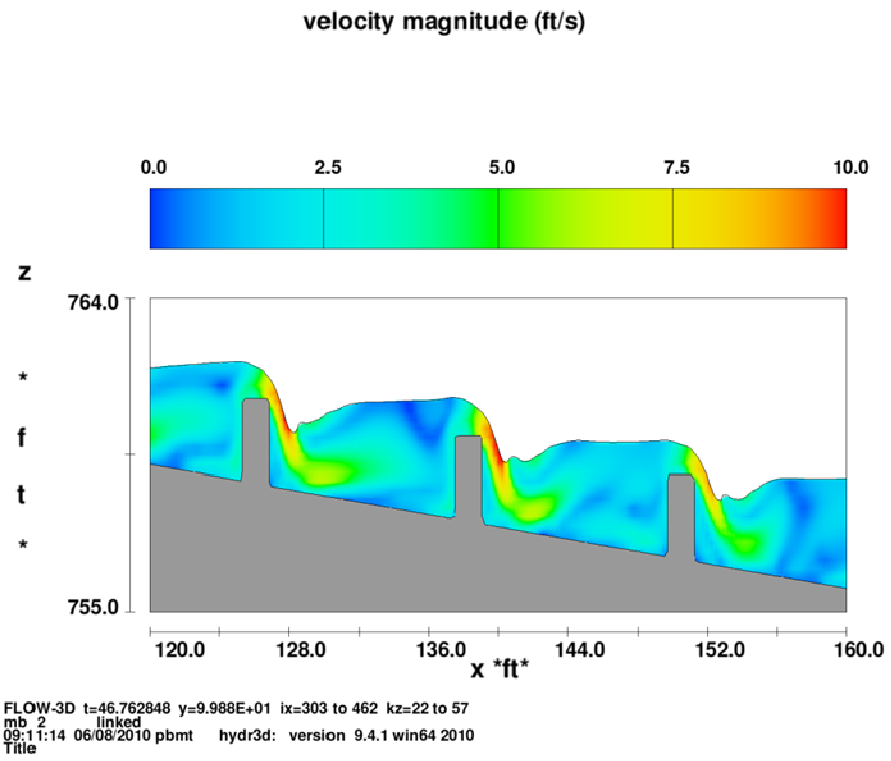

Figure 46 - Elevation sectional view showing flow velocity along the fishway centerline (see Figure 36 reference location Y=100 ft) at diversion pool elevation 768.5.

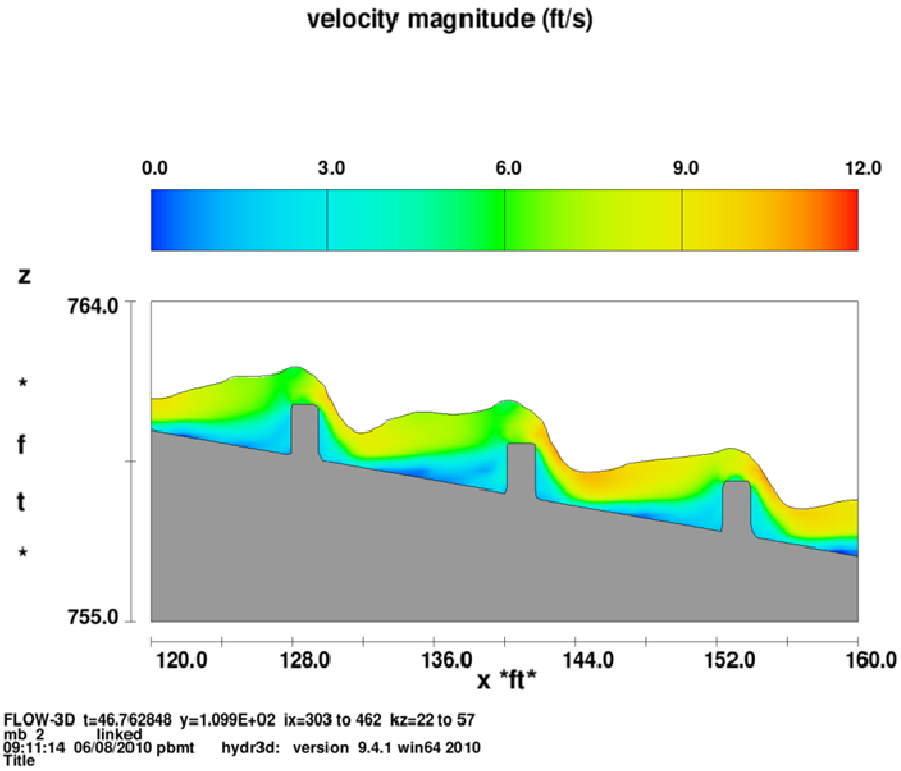

Figure 47– Elevation sectional view showing flow velocity along the centerline of the outer pile (see Figure 36 reference location Y=110 ft) at diversion pool elevation 768.5.

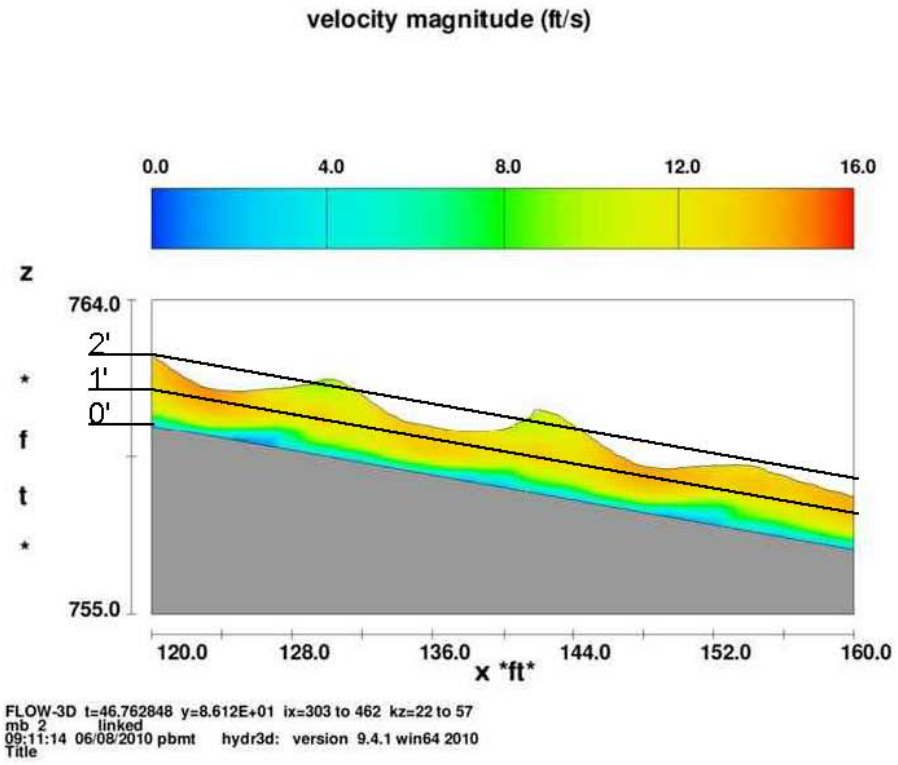

Figure 48 - Elevation sectional view showing flow velocity along the centerline of the outer slot (see Figure 36 reference location Y=86 ft) at diversion pool elevation 768.5.

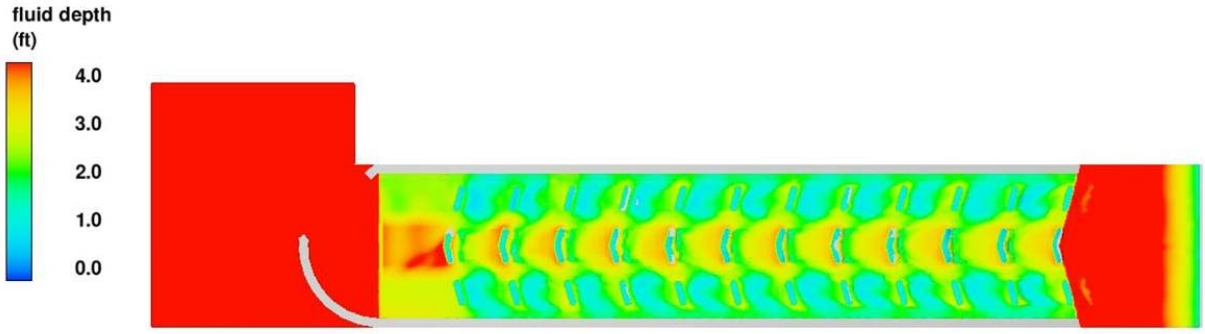

Figure 49– Plan view showing fishway flow depth predicted by the numerical simulation for reservoir pool elevation 768.5. Fishway flow is 385 ft^3/s.

References

Bell, Milo, “Fisheries Handbook of Engineering Requirements and Biological Criteria”, Fish passage development and evaluation program, USACE, North Pacific Division, 1991.

Mefford, B. 2009, “USBR Experience with Multiple-Slot-Baffled Fishways”, 33rd IAHR Congress, Vancouver, British Columbia, CANADA, August 9-14, 2009.

Mefford, B., Stowell, H. and Heinje, C., “Robles Diversion Dam High Flow and Sediment Bypass Structure, Venture, California,” Hydraulic Laboratory Report HL-2008-7, USBR Hydraulics Laboratory, Denver Co., 2008.

David A. Levy and Tim L. Slaney, “A Review of Habitat Capacity for Salmon Spawning and Rearing,” B.C. Resources Inventory Committee (RIC), Dept. of Fisheries and Oceans,Vancouver, B.C.,1993.